Clinical Imaging of SPINAL TRAUMA

A Case-Based Approach

EDITED BY Zoran Rumboldt

CAMBRIDGE Medicine

Clinical Imaging of Spinal Trauma

Clinical Imaging of Spinal Trauma

A Case-Based Approach

Edited by
Zoran Rumboldt
University of Rijeka
Medical University of South Carolina
Telemedicine Clinic

CAMBRIDGE
UNIVERSITY PRESS

CAMBRIDGE
UNIVERSITY PRESS

University Printing House, Cambridge CB2 8BS, United Kingdom

One Liberty Plaza, 20th Floor, New York, NY 10006, USA

477 Williamstown Road, Port Melbourne, VIC 3207, Australia

314–321, 3rd Floor, Plot 3, Splendor Forum, Jasola District Centre, New Delhi – 110025, India

79 Anson Road, #06–04/06, Singapore 079906

Cambridge University Press is part of the University of Cambridge.

It furthers the University's mission by disseminating knowledge in the pursuit of education, learning and research at the highest international levels of excellence.

www.cambridge.org
Information on this title: www.cambridge.org/9781107427471
DOI: 10.1017/9781139871372

First published 2018

Printed in the United Kingdom by TJ International Ltd. Padstow Cornwall

A catalogue record for this publication is available from the British Library

Library of Congress Cataloging-in-Publication data
Names: Rumboldt, Zoran, editor.
Title: Clinical imaging of spinal trauma : a case-based approach / edited by Zoran Rumboldt.
Description: Cambridge ; New York, NY : Cambridge University Press, 2018. | Includes bibliographical references and index.
Identifiers: LCCN 2017042438 | ISBN 9781107427471 (pbk. : alk. paper)
Subjects: | MESH: Spinal Injuries–diagnostic imaging | Tomography, X-Ray Computed | Magnetic Resonance Imaging | Case Reports
Classification: LCC RD768 | NLM WE 737 | DDC 617.4/820757–dc23 LC record available at https://lccn.loc.gov/2017042438

ISBN 978-1-107-42747-1 Paperback

Contents

Contributors

Vikas Agarwal, MD
Department of Radiology,
University of Pittsburgh Medical Center,
PA, USA

Russel Chapin, MD
Department of Radiology, MUSC, Charleston, SC, USA

Alessandro Cianfoni, MD
Department of Neuroadiology, Neurocenter, Lugano, Switzerland

Orrie Close, MD
Department of Radiology, University of Pittsburgh Medical Center, PA, USA

Daniela Distefano, MD
Department of Neuroradiology, Neurocenter, Lugano, Switzerland

Doris Dodig, MD
Department of Radiology, University of Rijeka, Croatia

Stephen P. Kalhorn, MD
Department of Neurosurgery, MUSC, Charleston, SC, USA

Stephen R. Love, MD
Department of Neurosurgery, MUSC, Charleston, SC, USA

Emanuele Pravatà, MD
Department of Neuroradiology Neurocenter, Lugano, Switzerland

Eytan Raz, MD
Department of Radiology, NYU Langone Medical Center, New York City, NY, USA

Zoran Rumboldt MD, PhD
Department of Radiology, University of Rijeka, Croatia; MUSC, Charleston, SC, USA; Telemedicine Clinic, Barcelona, Spain, and Sydney, Australia

Alisa Sumkin
Department of Radiology, University of Pittsburgh Medical Center, PA, USA

Abhay Varma, MD
Department of Neurosurgery, MUSC, Charleston, SC, USA

Hrvoje Vavro, MD
Department of Radiology, Dubrava University Hospital, University of Zagreb, Croatia; Telemedicine Clinic, Barcelona, Spain, and Sydney, Australia

Gregory A. Vorona, MD
Children's Hospital of Richmond, Virginia Commonwealth University, VA, USA

Michael Paul Yannes, MD
Department of Radiology, University of Pittsburgh Medical Center, PA, USA

Giulio Zuccoli, MD
Neuroradiology Section, Children's Hospital, University of Pittsburgh Medical Center, PA, USA

Acknowledgments

This book was made possible through the help and support of my family, colleagues and friends. I would like to thank all the authors for their contributions, and would especially like to express my gratitude to Alessandro Cianfoni and Abhay Varma who have not just written their chapters, but also assisted me in the editing of the book by engaging other contributors, reading and offering comments, and allowing me to quote their remarks.

SECTION **1**

Normal Variants and Mimickers

Cases

(1A)

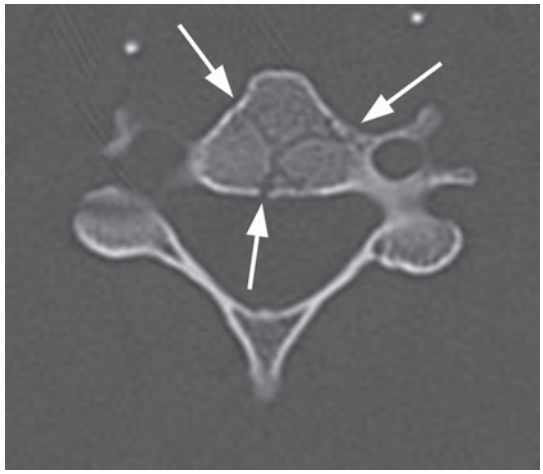

(1B)

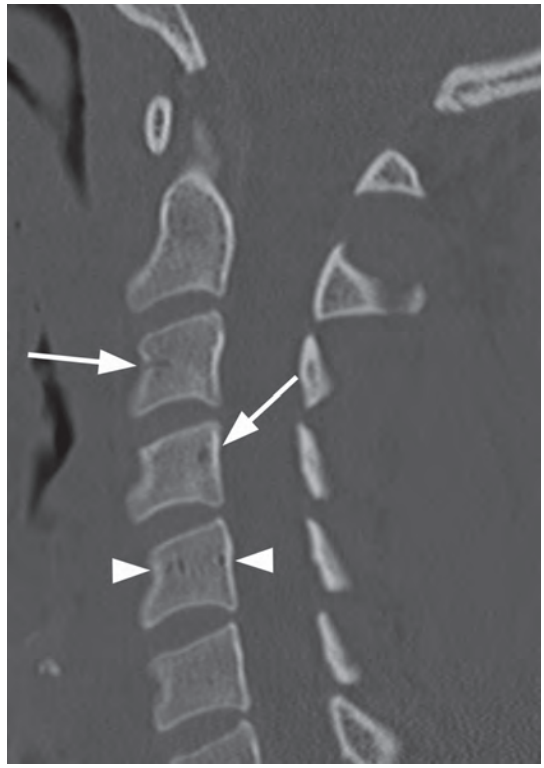

Figure 1.1 **A)** Axial CT image shows branching linear lucencies (arrows) at C5 vertebral body, which may potentially be concerning for fractures, although the curvilinear course is very typical for vascular channels. There is also a suggestion of sclerotic margins of the lucencies. **B)** Reconstructed sagittal CT shows the C4 vascular channels as oval structures with well-corticated margins (arrowheads). Additional vascular channnels are present at C3 and C4 vertebral bodies (arrows).

(2A)

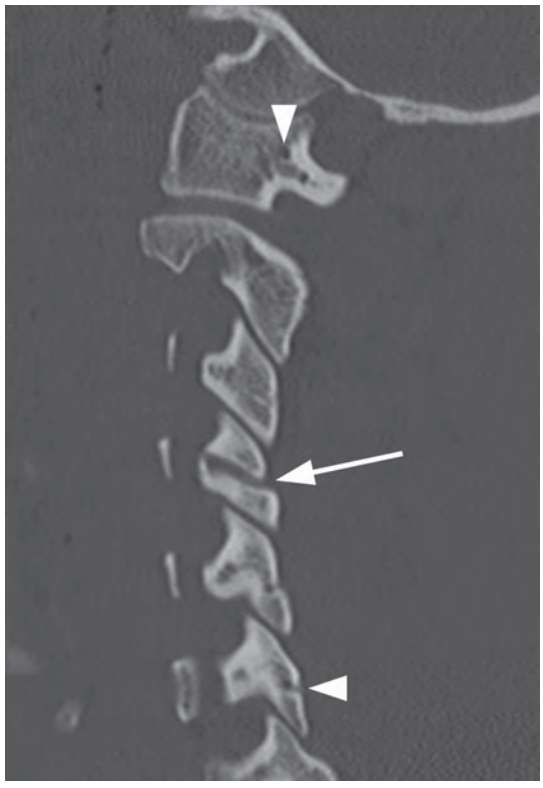

(2B)

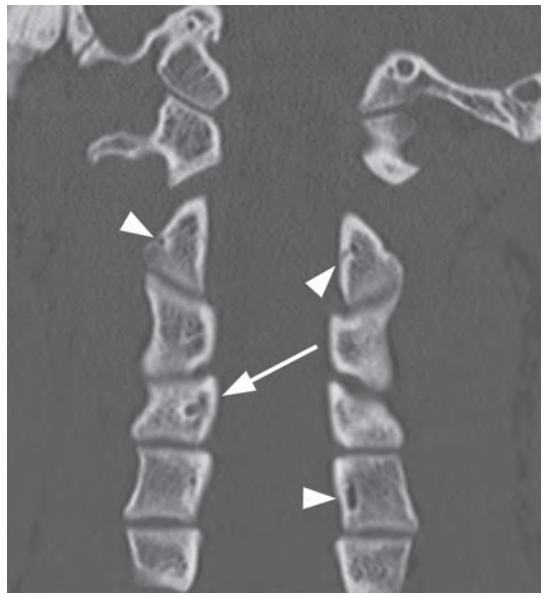

Figure 1.2 **A)** Sagittal CT image shows a probable vascular channel at C4 articular pillar (arrow). Note additional vascular grooves (arrowheads on some). **B)** Coronal CT confirms sclerotic margins of the right C4 channel (arrow); multiple other grooves (arrowheads on some).

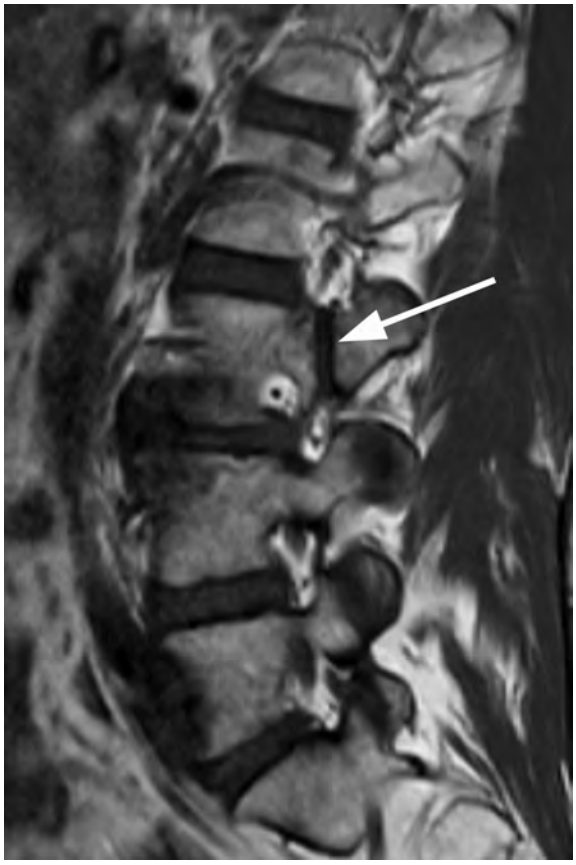

Figure 1.3 Sagittal T1-weighted MRI reveals a linear corticated defect (arrow) at L3 pedicle, consistent with a retrosomatic cleft.

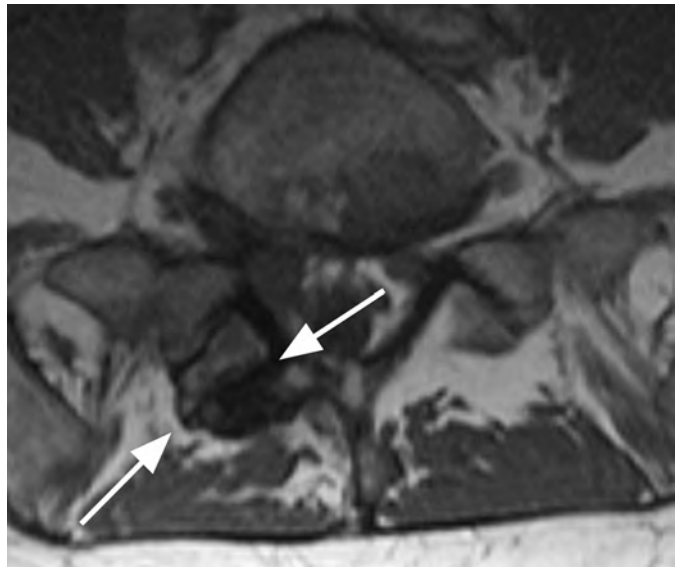

Figure 1.4 Axial T1-weighted MRI in a different patient shows a linear defect of the right lamina (arrows) with some bony overgrowth – a retroisthmic cleft.

Figure 1.5 Coronal CT image demonstrates bilateral indentations (arrowheads) at the base of the axis, on either side of the dens with well-corticated margins. The findigs are consistents with bilateral clefts, a developmental variant.

Figure 1.6 Coronal CT image in another patient shows shallow bilateral clefts along the superior aspect of C2 body; the one on the left extends through the body in a curvilinear fashion (arrow), consistent with a vascular channel.

CASE 1 Vascular Channels (Grooves) and Normal Clefts

Zoran Rumboldt

Imaging Findings

Modern multidetector CT scanners frequently reveal the vertebral vasculature perforating through the cortical surface of the vertebral body and other parts of the vertebrae. These vascular (also known as nutritive) channels may simulate fracture lines, with which they may occasionally be confused. Careful review of images reconstructed in different planes typically allows identification of their characteristic vascular course, round to oval appearance on images that are perpendicular to their long axis, and their sclerotic margins.

Clefts at the base of the dens, which are remnants of a synchondrosis, may have similar appearance. They are commonly bilateral, but may also be unilateral, potentially simulating a fracture.

Clefts may occur at several locations within the more inferior vertebrae, most commonly through the spinous process (spina bifida occulta), resulting from failed osseous fusion of the posterior synchondrosis. A cleft may also occur within the pars interarticularis (spondylolysis), pedicle (retrosomatic cleft), or lamina (retroisthmic cleft). The characteristic location, sclerotic margins, and associated degenerative changes are typical features that allow distinction from acute fractures.

Differential Diagnosis

Acute Nondisplaced Fracture

Straight, sometimes irregular lucent lines, without sclerotic margins, typically extending through the entire bone, without rounded appearance on images perpendicular to their long axis.

Chronic Fracture

Typically straight lines with corticated margins, usually extending through the entire bone, without rounded appearance on images perpendicular to their long axis.

Clinical Findings, Implications, and Treatment

Vascular channels are normal findings and therefore do not require any treatment. Their identification may at times be difficult, typically due to presence motion or streak artifacts. In these cases, repeat focused CT of the area in question, possibly with a different technique (removal of any metallic foreign bodies, lower positioning of the shoulders/arms down, increased kVp), may be needed. Absence of bone marrow edema on MRI is also reassuring.

Additional Information

Increasing quality and decreasing slice thickness of CT scans over time has led to improved identification of anatomic details, including normal variants, especially with high-resolution isotropic images reconstructed in three or more planes. As with other anatomical structures and clinical settings, this allows for better detection of pathological processes but, at the same time, may also be responsible for an increase in false-positive findings, since various anatomic variants are now visualized more and more frequently.

Retrosomatic and retroisthmic clefts are far less common than spondylolysis (pars interarticularis defect). The cause of these clefts is unclear; they may be associated with repetitive stress and should be differentiated from acute fractures.

References

1 Daffner RH. *Imaging of vertebral trauma*. Cambridge University Press, 3rd edition, 2011.

2 Carr RB, Fink KR, Gross JA. Imaging of trauma: part 1, pseudotrauma of the spine – osseous variants that may simulate injury. *AJR Am J Roentgenol* 2012;199: 1200–1206. doi: 10.2214/AJR.12.9083.

3 Keats TE, Anderson MW. *Atlas of normal roentgen variants that may simulate disease*. Saunders, 9th edition, 2013.

(1A)

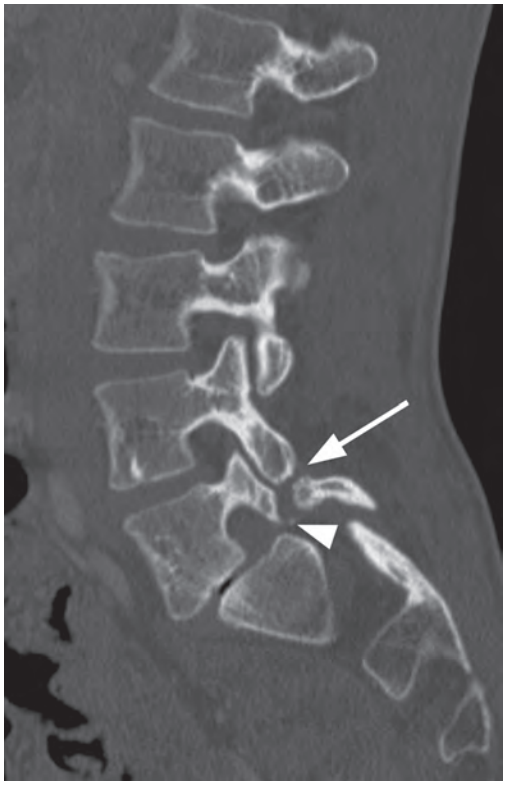

(1B)

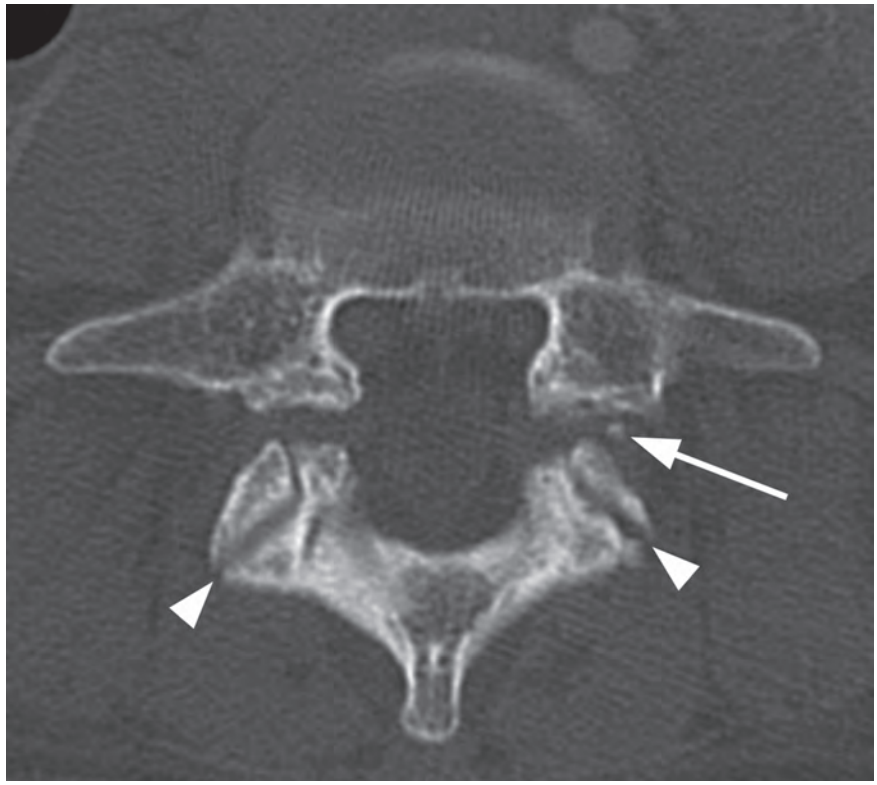

Figure 2.1 **A)** Sagittal CT image shows spondylolisthesis of L5 with pars interarticularis defect (arrow). A bony element is filling the pars defect (Gill's nodule, arrowhead). **B)** On the axial CT image the bilateral pars defects can be differentiated from the adjacent facet joints (arrowheads) by the more anterior location, more irregular contours, and sclerotic margins. A Gill's nodule is well seen (arrow).

(2A)

(2B)

Figure 2.2 **A)** Sagittal T1-weighted image demonstrates a defect of the pars interarticularis involving L3 vertebra with sclerotic margins. **B)** STIR image reveals that the L3 pars defect is filled high signal intensity (arrow), consistent with fluid/inflammatory tissue.

Figure 2.3 Sagittal T1-weighted VIBE images clearly demonstrate the pars interarticularis defect (arrows). This fat suppressed T1-weighted sequence has a higher sensitivity for spondylolysis. (Courtesy of Tommaso Bartalena, MD, Imola.)

CASE 2

Pars Defects

Eytan Raz and Zoran Rumboldt

Imaging Findings

Spondylolysis refers to the radiolucent defect in the pars interarticularis. Multiple signs of spondylolysis have been described on radiographs, including lateral deviation of the spinous process, sclerosis of the contralateral pedicle, and the lucency at the neck of the "Scotty dog" on the oblique views. On axial CT scans at the level of the pedicles, discontinuity of the neural arch indicates a pars defect ("incomplete ring sign"). Pars defects are differentiated from the adjacent facet joints by their more irregular contours and sclerotic margins. If spondylolisthesis coexists, the axial scan also depicts the widened sagittal diameter of the spinal canal. In spondylolytic spondylolisthesis, the spinous process step-off is at the level above the pars defect on the sagittal images, in contrast to degenerative spondylolisthesis in which forward displacement of the vertebra is at the same level with the spinous process, with associated narrowing of the spinal canal. Sagittal CT images are also the most accurate in showing fractures, even incomplete, usually located in the infero-medial cortex of the pars. CT may depict bony elements in or adjacent to the fibrous or fibrocartilaginous tissue filling the pars defect (Gill's nodules). Axial CT and MRI images also show "continuous" or "endless" appearance of the facet joints when scrolling through the adjacent levels, without presence of intact laminae in between the joints.

On MRI, the pars defect appears as an interruption of the cortex and marrow through the pars, best seen on T1-weighted images. If there is also a gap at the site of the lysis, the signal intensity of the tissue filling the defect varies: low on T1- and T2-weighted images when composed of fibrous tissue, or high on T2-weighted sequences due to the presence of inflammatory tissue or fluid. Recognition of an incomplete fracture and of spondylosis without spondylolisthesis is the main challenge for MRI; ancillary findings may help the diagnosis, such as the widened sagittal diameter of the spinal canal, wedging of the posterior aspect of the vertebral body at the level of the spondylolysis, location of the step-off, and reactive marrow changes in the pedicles adjacent to a pars defect. In case of spondylolisthesis, MRI can also demonstrate the radicular stretching linked to the displacement of the slipping vertebra and rule out other causes of nerve root compression. Fat suppressed sagittal oblique VIBE T1-weighted sequence may have higher sensitivity for the diagnosis of spondylolysis.

Differential Diagnosis

Acute Fracture

Lucent fracture line is without sclerotic margins, sometimes irregular.

Other Vertebral Clefts (Retrosomatic, Retroisthmic, Spina Bifida)

In different locations (pedicle, lamina, spinous processes), not at the pars interarticularis.

Clinical Findings, Implications, and Treatment

Most cases of spondylolysis are completely asymptomatic or characterized by notable discrepancy between clinical and radiological findings. The most common finding on physical examination is a hyperlordotic curvature. Symptomatic patients usually complain of mechanical-type low back pain, worsened by activity (particularly flexion–extension) and improved with rest. Radicular symptoms are less common, especially in young patients. The treatment for spondylolysis and spondylolisthesis is initially conservative and aims to reduce pain and facilitates healing; surgical treatment is generally reserved for patients who fail to respond to conservative management.

Additional Information

The pathogenesis remains controversial and several observations favor a hereditary predisposition. Pars defect may also be an acquired stress fracture secondary to chronic low-grade trauma, rarely following acute trauma. Developmental factors, such as posture or certain repetitive physical activities, may lead to a stress fracture of the pars interarticularis. The most probable mechanism of lumbar spondylolysis is multifactorial with a stress fracture occurring through a congenitally weak or dysplastic pars interarticularis. Pars defect almost always occurs bilaterally and involves the L5 vertebra in 95% of cases. The incidence progressively decreases in a cephalad direction.

References

1 Leone A, Cianfoni A, Cerase A, Magarelli N, Bonomo L. Lumbar spondylolysis: a review. *Skeletal Radiol* 2011;40:683–700.

2 Dunn AJ, Campbell RS, Mayor PE, Rees D. Radiological findings and healing patterns of incomplete stress fractures of the pars interarticularis. *Skeletal Radiol* 2008;37:443–450.

3 Johnson DW, Farnum GN, Latchaw RE, Erba SM. MR imaging of the pars interarticularis. *AJR Am J Roentgenol* 1989;152:327–332.

4 Ulmer JL, Elster AD, Mathews VP, King JC. Distinction between degenerative and isthmic spondylolisthesis on sagittal MR images: importance of increased anteroposterior diameter of the spinal canal ("wide canal sign"). *AJR Am J Roentgenol* 1994;163:411–416.

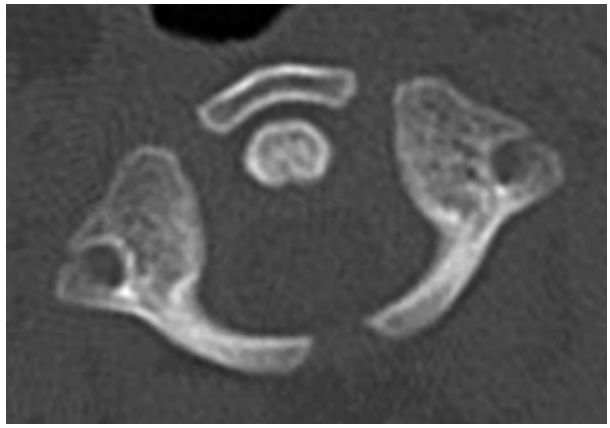

Figure 3.1 Axial CT image of C1 in a 19-month-old female shows 3 separate ossification centers of the atlas: 1 anterior central arch and 2 posterior neural arches. The posterior synchondrosis should fuse first between the ages of 3 to 5 years. The synchondroses anteriorly usually fuse between 5 and 8 years of age.

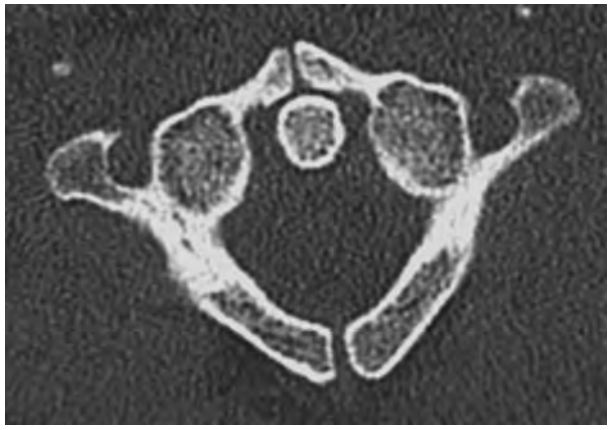

Figure 3.2 Axial CT image in an adult patient imaged for trauma. There is non-fusion at the midline of C1 anteriorly and posteriorly. Note the well-corticated margins anteriorly and posteriorly and slight hypertrophy of bone at the anterior non-fusion. The posterior midline type of non-fusion is more common.

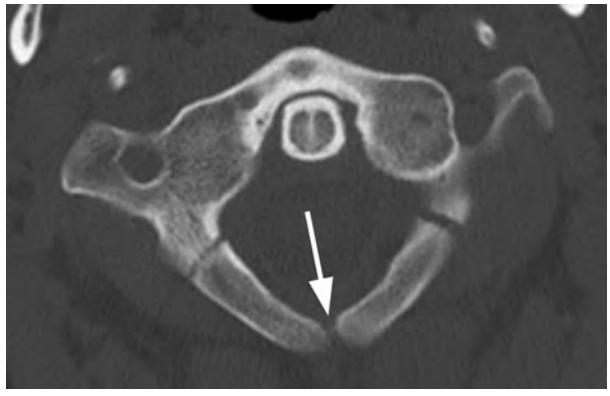

Figure 3.3 Axial CT image obtained in a 48-year-old man with neck pain and temporary loss of consciousness after an MVC. There are defects of the posterior lateral aspect of the arch of C1 bilaterally with non-corticated margins and slight widening on the left. These are bilateral posterior arch fractures of C1. Contrast these with the midline well-corticated defect (arrow), which is a typical midline non-fusion variant.

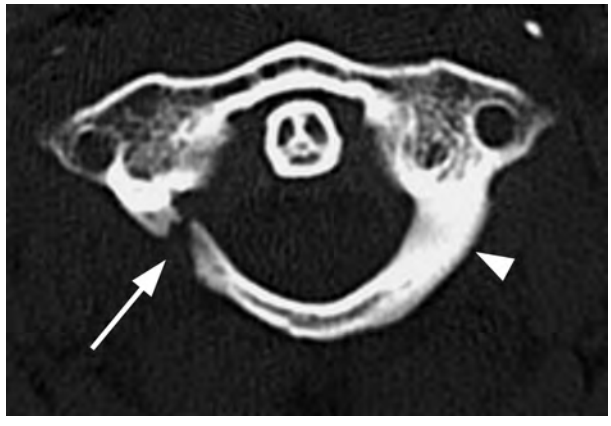

Figure 3.4 Axial CT image in a 23-year-old with altered mental status after an MVC. There is posterior lateral non-fusion of right arch of C1 with tapered apposing margins of the bone (arrow). There is mild secondary hypertrophy and sclerosis of the left posterior arch (arrowhead). This unusual variant is secondary to a dysplasia of the right posterior neural arch, which may be secondary to injury during development.

CASE 3 Unfused Arches of C1

Russel Chapin

Imaging Findings

Differentiation of a non-fusion variant of C1 from a fracture is dependent on knowledge of their occurence and recognition of their well-corticated appearance when compared to fractures. The most common site of non-fusion of C1 is at the posterior midline occuring in 3–4% of patients. Non-fused posterior clefts may also be located slightly off the midline unilaterally or bilaterally. Anterior C1 non-fusion is substantially less common than the posterior form; these clefts are typically also at or just off the midline. However, variant clefts may be found anywhere around the C1 ring. In more extreme variant forms, dysplasia of 1 of the 3 normal ossification centers may present with a wider irregular but corticated defect.

Differential Diagnosis

C1 (Jefferson) Fracture

Irregular fracture lines without corticated margins.

Post-operative Bone Defect

Bone defect with straight lines, sclerotic margins are not formed yet following recent surgery.

Clinical Findings, Implications, and Treatment

True anatomic variants are essentially always unrelated to the patient's injury or reason for CT or MR examination. However, in some cases, well-corticated defects that are secondary to old injury may be confused with normal variation. C1 fractures in skeletally immature patients may have a delayed presentation after minor injury with pain and torticollis. If missed initially, these fractures may do well with conservative or no treatment and mimic a variant on a later exam. In the uncommon situation that a variant could not be distinguished from acute fracture, MRI may show a lack of adjacent soft tissue and bone marrow edema or ligamentous injury.

There are rare case reports of instability or neurologic deficit after minor injury related to preexisting variant C1 fusion defects. Associated symptoms in these case reports have generally been transient. Evaluation in these patients would include flexion-extension radiography, when clinically appropriate. A majority of true C1 fractures are treated conservatively in a collar.

Additional Information

The atlas forms from 3 ossification centers: 1 anterior central arch and 2 posterior neural arches. The posterior synchondrosis generally fuses first between the ages of 3 and 5 years. The synchondroses anteriorly usually fuse between the ages of 5 and 8 years. At birth, the posterior arches demonstrate partial ossification, while the anterior arch is completely cartilaginous in 80% of patients. Up to 25% of 2-year-olds continue to show non-ossification of the anterior arch. There may be more than 1 ossification center of the anterior arch; one study found 2 anterior ossification centers in 18% of patients, 3 ossification centers in 5%, and 4 centers in 4%. An anterior midline/median non-fusion may occur secondary to non-union between multiple anterior arch ossification centers or due to complete absence of the anterior arch. Anterior arch defects are reported in less than 1% of skeletally mature patients.

In a recent study of CT scans and cadaveric specimens, 40 anomalies (2.95%) were found in 1,354 evaluated cases. Of the 1,104 patients in whom CT scans were acquired, 37 (3.35%) had congenital defects of the posterior arch of the atlas; only one patient (0.09%) had an anterior arch cleft.

References

1 Rao RD, Tang S, Lim C, Yoganandan N. Developmental morphology and ossification patterns of the C1 vertebra. *J Bone Joint Surg Am* 2013;95: e1241–e1247. doi: 10.2106/JBJS.L.01035.

2 Junewick JJ, Chin MS, Meesa IR, et al. Ossification patterns of the atlas vertebra. *AJR Am J Roentgenol* 2011;197:1229–1234. doi: 10.2214/AJR.10.5403.

3 Piatt JH Jr, Grissom LE. Developmental anatomy of the atlas and axis in childhood by computed tomography. *J Neurosurg Pediatr* 2011;8:235–243. doi: 10.3171/2011.6.PEDS11187.

4 Currarino G, Rollins N, Diehl JT. Congenital defects of the posterior arch of the atlas: a report of seven cases including an affected mother and son. *AJNR Am J Neuroradiol* 1994;15:249–254.

5 Senoglu M, Safavi-Abbasi S, Theodore N, etal. The frequency and clinical significance of congenital defects of the posterior and anterior arch of the atlas. *J Neurosurg Spine* 2007;7:399–402.

(1A)

(1B)

Figure 4.1 **A)** Axial CT image shows a well-corticated ossicle (arrow) at the lateral margin of the space between the right posterior arch of C1 and the adjacent occipital bone. This is consistent with an incomplete ponticulus posticus. **B)** Sagittal CT demonstrates the well-corticated ossicle (arrow), which is at the lateral margin of the posterior arch of C1. The ossicle is posterior to the junction of the lateral mass and posterior arch of C1 and posterior to the atlanto-occipital joint.

Figure 4.2 Sagittal CT in another patient shows an incomplete ring of bone (arrow) extending from the posterior arch of atlas to the posterior aspect of its lateral mass. This is an incomplete ponticulus posticus.

Figure 4.3 Sagittal CT in a 35-year-old with neck pain after an MVC. A complete ring of bone is extending from the posterior arch of C1 up to the posterior aspect of the lateral mass of C1 (arrow). This is a complete ponticulus posticus or arcuate foramen encircling the vertebral artery.

CASE 4 Ponticulus Posticus

Russel Chapin and Zoran Rumboldt

Imaging Findings

After the vertebral artery passes superiorly through the transverse foramen of C1, it must travel horizontally in a medial direction to enter the foramen magnum. There is a groove on top of the posterior arch of C1 where this horizontal portion of the vertebral artery passes. In 5–35% of individuals, there is a partial or complete sagitally oriented ring of bone forming a roof over the vertebral artery at this location. This has been given a variatety of names including the arcuate foramen, ponticulus posticus (little posterior bridge), Kimmerle anomaly, Kimmerle variant, or foramen arcuale. When incomplete, it is most important to differentiate this from a small avulsion fracture of the base of the occiput or ring of C1 on CT. Familiarity with this variant, its characteristic location superior to the vertebral artery, and its well-corticated appearance prevent these errors.

Differential Diagnosis

Occipital Condyle Avulsion Fracture

Posterior aspect of the lateral mass of C1 (surgical posterior approach).

Clinical Findings, Implications, and Treatment

This is usually an incidental finding in asymptomatic individuals. The bony arcuate foramen has been noted to compress the V3 segment of the vertebral artery. The foramen also contains the vertebral venous plexus and the sub-occipital nerve. Compression of the vertebral artery at the foramen has been hypothesized as cause for headache, vertigo, vertebral artery V3 segment injury, and vasomotor disturbances. Symptoms have been noted to improve in some patients after lysis of the ponticulus with periarterial sympathectomy.

Careful assessment via preoperative multiplanar and 3D CT should be performed prior to C1 pedicle screw fixation in patients with ponticulus posticus, to avoid mistaking the ponticulus posticus for a widened dorsal arch of the atlas, as this may result in C1 screw placement through the vertebral artery.

Additional Information

The ponticulus posticus may be complete or incomplete and present unilaterally or bilaterally. It has been proposed to represent acquired ossification in the atlanto-occipital membrane, an accessory attachment of the atlanto-occipital membrane, or an accessory transverse foramen of C1. Recent studies have estimated its prevalence at 15–17% of the general population. A meta-analysis of published radiographic and cadaver series of more than 20,000 individuals found the overall prevalence of 16.7% of the overall sample. The anomaly was identified in 18.8% of cadaver, 17.2% of CT, and 16.6% on radiographic studies. Ponticulus posticus composed a complete foramen in 9.3% of patients and was partial or incomplete in 8.7%. It was present bilaterally in 5.4% of cases and unilateral in 7.6%. There was no significant difference in prevalence between sexes.

References

1 Chen CH, Chen YK, Wang CK. Prevalence of ponticuli posticus among patients referred for dental examinations by cone-beam CT. *Spine J* 2015;15:1270–1276. doi: 10.1016/j.spinee.2015.02.031.

2 Elliott RE, Tanweer O. The prevalence of the ponticulus posticus (arcuate foramen) and its importance in the Goel-Harms procedure: meta-analysis and review of the literature. *World Neurosurg* 2014;82:e335–e343. doi: 10.1016/j.wneu.2013.09.014.

3 Tubbs RS, Johnson PC, Shoja MM, Loukas M, Oakes WJ. Foramen arcuale: anatomical study and review of the literature. *J Neurosurg Spine* 2007;6:31–34.

4 Geist JR, Geist SM, Lin LM. A cone beam CT investigation of ponticulus posticus and lateralis in children and adolescents. *Dentomaxillofac Radiol* 2014;43:20130451. doi: 10.1259/dmfr.20130451.

5 Gibelli D, Cappella A, Cerutti E, et al. Prevalence of ponticulus posticus in a Northern Italian orthodontic population: a lateral cephalometric study. *Surg Radiol Anat* 2016;38:309–312. doi: 10.1007/s00276-015-1554-0.

Figure 5.1 Sagittal CT image shows a bony gap between the superior odontoid process/dens of C2 (arrow) and the body and hypoplastic odontoid base (small arrowhead) of C2. The opposed ends of bone have well-corticated margins. The anterior portion of the C1 ring (large arrowhead) is enlarged and the space between the ossicle and C1 is narrowed with remodeling of the opposing bone surfaces.

Figure 5.2 Sagittal CT image in a different patient shows very similar findings at C1–C2 level: the superior part of the dens is separated from the rest of the odontoid process and the body of axis, with clearly corticated margins of both the os odontoideum and the odontoid base. The atlanto-dental interval is also narrowed.

(3A)

(3B)

Figure 5.3 **A)** Coronal CT image demonstrates a rounded well-corticated os odontoideum detached from the odontoid base. **B)** Sagittal CT reveals that the os odontoideum (arrow) is fused (arrowheads) to the anterior arch of the atlas.

CASE 5 Os Odontoideum

Russel Chapin and Zoran Rumboldt

Imaging Findings

An os odontoideum is a well-corticated ossicle superior to a hypoplastic (often dramatically so) odontoid base. As opposed to an os terminale, the level of separation is at or below the transverse ligament of C1. Anatomically and functionally, it is similar to a non-united type 2 dens fracture. To distinguish the os odontoideum from a chronic type 2 dens fracture, it is helpful to note that the os lacks the normal morphology of the superior dens, appearing somewhat smaller with more rounded margins. The non-ossified gap between an os odontoideum and hypoplastic dens is usually larger than the gap in a fractured dens. Adittionally, the anterior ring of C1 demonstrates compensatory enlargement in the case of an os odontoideum. While the os may be located in the normal position of the superior dens, it is often dystopically fused to the anterior ring of C1 or the basion of the occiput.

Differential Diagnosis

Dens Fracture (Type 2)

The fracture line is without corticated margins, the edges may be irregular, possible displacement.

Os Terminale

The line of separation is above the transverse ligament.

Clinical Findings, Implications, and Treatment

An os odontoideum most frequently presents with pain or myelopathy, often after a relatively minor injury. In one series, 15% of cases were considered to be incidental. CT and MRI should both be performed for detailed evaluation of bony relationships and assessment of the spinal canal and spinal cord, respectively. Additionally, flexion-extension radiography is indicated in the cooperative patient to assess for stability. Nonoperative treatment with serial follow-up is indicated in asymptomatic stable patients. Surgical treatment options include C1–C2 screw placement with posterior stabilization, transarticular screw placement, sublaminar wiring, or craniocervical fusion. Independent screw placement in the lateral mass of C1 and pedicle of C2 for posterior fusion is considered the treatment of choice. The co-occurrence of atlanto-occipital osseous abnormalities (necessitating craniocervical fusion) and vertebral artery variant anatomy with an os odontoideum should be considered in surgical planning.

Additional Information

An os odontoideum may be attributed to congenital, developmental, or traumatic causes, with most cases hypothesized to arise from trauma during childhood. This is supported by the fact that the vestigial disc between the dens and body of the axis (known as the neurocentral synchondrosis) is located slightly inferior to the superior facets of C2 while the os odotoideum and type 2 dens fracture extend above these facets. A recent case report suggests that os odontoideum forms after a fracture through the apical odontoid epipyisis, where the fractured fragment remodels and eventually assumes the classic form of an os.

References

1 Arvin B, Fournier-Gosselin MP, Fehlings MG. Os odontoideum: etiology and surgical management. *Neurosurgery* 2010;66(3 Suppl):22–31.

2 Carr RB, Fink KR, Gross JA. Imaging of trauma: part 1, pseudotrauma of the spine – osseous variants that may simulate injury. *AJR Am J Roentgenol* 2012;199:1200–1206. doi: 10.2214/AJR.12.9083.

3 Klimo P Jr, Coon V, Brockmeyer D. Incidental os odontoideum: current management strategies. *Neurosurg Focus* 2011;31:E10.

4 Zhao D, Wang S, Passias PG, Wang C. Craniocervical instability in the setting of os odontoideum: assessment of cause, presentation, and surgical outcomes in a series of 279 cases. *Neurosurgery* 2015;76:514–521.

5 White IK, Mansfield KJ, Fulkerson DH. Sequential imaging demonstrating os odontoideum formation after a fracture through the apical odontoid epiphysis: case report and review of the literature. *Childs Nerv Syst* 2013;29:2111–2115.

Figure 6.1 Sagittal CT image shows a calcification (arrow) adjacent to the anterior superior aspect of C4 vertebral body – the margins are hard to define as well corticated, given technique and mild motion artifact. However, the adjacent corner of C4 is well corticated, and the calcification is slightly smaller than the defect in the body, indicating some component of soft tissue filling this space, consistent with a limbus vertebra.

Figure 6.2 Sagittal CT image reveals a well-corticated triangular ossicle (arrow) at the anterior superior margin of L4 with a well-corticated smooth surface at the apposed corner of L4 (arrowhead) – a classic limbus vertebra. The thin soft tissue space between the limbus and vertebral body is composed of partially herniated disc material.

Figure 6.3 Sagittal CT image shows a crescent-shaped cortical fragment at the anterior aspect of C3–C4 disc space slightly displaced from the anterior inferior corner of C3. The corner of C3 shows subtle loss of cortical bone, consistent with a donor site of a small fracture. Compare this to the oblong, vertically oriented, well-corticated calcification (arrow) at C4–C5 level, which represents dystrophic calcification of the annulus fibrosus.

Figure 6.4 Sagittal CT image demonstrates a corticated ossification (arrow) and a corticated irregular margin of the adjacent anterior superior portion of L5 vertebral body (arrowhead). This represents a Schmorl's node with partial limbus formation. Further sagittal images demonstrated this calcification to be partially continuous with the vertebral body.

CASE 6 Limbus Vertebral Body

Zoran Rumboldt

Imaging Findings

A limbus vertebral body is a well-corticated ossicle at the corner of a vertebral body caused by herniation of the nucleus pulposus of the disc into the edge of the vertebral body and beneath the ring apophysis. Limbus ossicles are triangular or rounded in shape. Visualization of an intact cortex is the most helpful feature for differentiation from a fracture, which can indicate significant injury with flexion or extension ligamentous avulsion. If calcification near the anterior corner of the vertebral body has linear vertical extension, is slightly beyond the margin of the adjacent vertebral body, and is not accompanied by a corresponding defect in the vertebral body; it is best termed calcification of the annulus fibrosus.

Differential Diagnosis

Teardrop Flexion or Extension Fracture

Absence of sclerotic cortical bone at both the vertebral body donor site and the teardrop fragment, extensive associated soft tissue injury, possible additional fractures.

Posterior Limbus Fracture

The defect is located along the posterior corner of lumbar vertebral bodies, associated with disc herniation, bone fragment may not be present, typically occurs in children and adolescents.

Calcification or Ossification of the Annulus Fibrosus

Linear vertical extension, not accompanied by a corresponding defect in the vertebral body.

Clinical Findings, Implications, and Treatment

Originating from intravertebral herniation of disc material, limbus vertebral bodies are similar to Schmorl's nodes in etiology. Limbus vertebrae are asymptomatic findings requiring no treatment. While generally considered to be incidental findings, Schmorl's nodes are associated with degenerative disc findings and may be painful at the time of occurrence. In contrast, posterior limbus fractures present with acute pain or neurologic compression symptoms in adolescent patient. An acute occurrence should be considered when a vertebral limbus is discovered posteriorly.

Additional Information

The limbus vertebra was in fact first described by Schmorl in 1927. In addition to isolated Schmorl's nodes, the pathophysiology is noted to be similar to Scheuermann's disease, and an association of all of these entities with disc degeneration is noted. Limbus verterbrae are most commonly present at the anterior superior corner of vertebral bodies in the lumbar spine. However, they are also seen in the cervical and thoracic spine and can involve the anterior inferior corner of the vertebral body. In a skeletally immature patient, a developing limbus may have the appearance of isolated corner irregularity of the vertebral body without the adjacent well-corticated ossicle because of nonmineralization of the ring apophysis.

References

1 Henales V, Hervás JA, López P, et al. Intervertebral disc herniations (limbus vertebrae) in pediatric patients: report of 15 cases. *Pediatr Radiol* 1993;23:608–610.

2 Wagner AL, Murtagh FR, Arrington JA, Stallworth D. Relationship of Schmorl's nodes to vertebral body endplate fractures and acute endplate disk extrusions. *AJNR Am J Neuroradiol* 2000;21:276–281.

3 Takahashi K, Miyazaki T, Ohnari H, Takino T, Tomita K. Schmorl's nodes and low-back pain. *Eur Spine J* 1995;4:56–59.

4 Beggs I, Addison J. Posterior vertebral rim fractures. *Br J Radiol* 1998;71:567–572.

5 Kerns S, Pope TL Jr, de Lange EE, et al. Annulus fibrosus calcification in the cervical spine: radiologic-pathologic correlation. *Skeletal Radiol* 1986;15:605–609.

Figure 7.1 Sagittal CT image of the cervical spine shows a well-corticated ossification (arrow) extending longitudingally along the nuchal ligament centered posterior to the spinous process of C5. Note that there is no defect of the spinous processes. The nuchal ligament is faintly seen on this bone window as soft tissue density (arrowhead) surrounded by fat and extending to the occiput more superiorly.

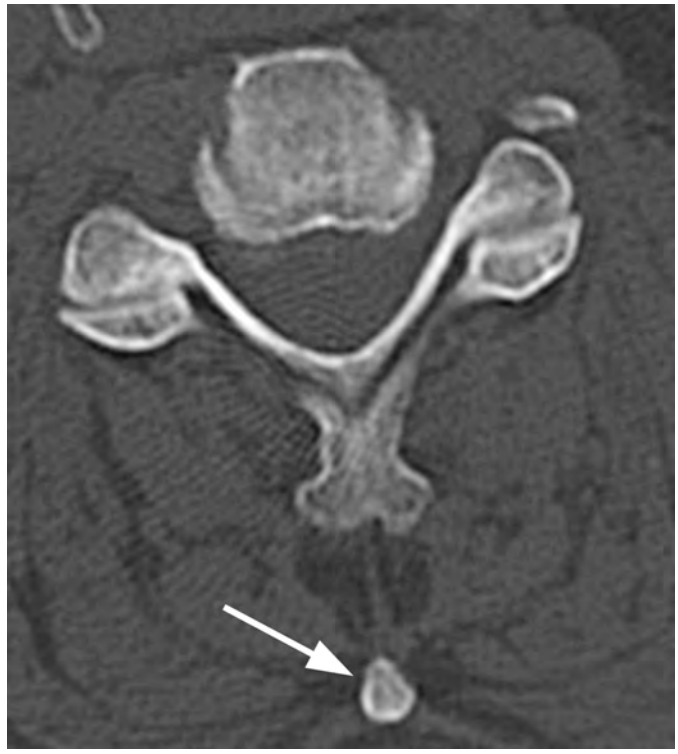

Figure 7.2 Axial CT image in a different patient also at the level of C5 shows a well-corticated round ossification in the midline (arrow) posterior to the spinous process. Once again, the adjacent spinous processes are well corticated, and the nuchal ligament ossification is signficantly posterior to the spinous processes.

Figure 7.3 Sagittal CT image demonstrates three well-corticated ossifications (arrowheads) extending along the vertical course of the nuchal ligament located a significant distance posterior to the spinous processes, consistent with nuchal ligament ossification. Note the bulky anterior paravertebral ossifications typical of DISH (diffuse idiopathic skeletal hyperostosis). Nuchal ligament ossifications have been associated with aging, DISH, and cervical spine degenerative changes.

CASE 7

Ossification of the Nuchal Ligament

Zoran Rumboldt

Imaging Findings

Well-corticated ossicles within the posterior midline soft tissues of the neck are frequently seen and known as ossification of the nuchal ligament. On CT or MRI, these can be directly visualized to lie within the nuchal ligament. With ossification of the nuchal ligament, there is no corresponding defect in the spinous processes. The margins of the ossicles are made up of compact cortical bone, and the central aspect of the ossicles is trabecular bone. As opposed to spinous process fractures, they are often widely separated from the adjecent spinous proceses, particularly when located at C5 or above. They are most typically posterior to the spinous processes of C5 and C6. Fifty to eighty percent occur at the C5–C6 and/or C6–C7, which are the levels of maximal flexible mobility in the cervical spine.

Differential Diagnosis

Clay Shoveler's Fracture

Noncorticated margins along the fracture line, the fragments are typically in a more horizontal orientation.

Calcific Tendinitis (Tendonitis)

Retropharyngeal location, longus colli involvement, frequent associated edema.

Clinical Findings, Implications, and Treatment

The estimated prevalence of nuchal ligament ossification is 4% in females and 11% in males. It is generally considered an asymptomatic incidental finding. However, an increased incidence has been noted in patients with degenerative changes of the cervical spine, and an association with prior injury is frequently postulated. Additionally, an association with aging, diffuse idiopathic skeletal hyperostosis (DISH), and ossification of the posterior longitudinal ligament has been noted. Given very similar proposed etiologies, anatomic localization, and histologic findings, nuchal ligament ossification is likely closely related to the rare entity of nuchal fibrocartilaginous pseudotumor, which undergoes surgical resection. Calcification/ossification is absent in nuchal fibrocartilaginous pseudotumors. The major differential diagnosis of a clay shoveler's fracture of the spinous process is treated in a cervical collar. Calcific tendinosis is an uncommon entity that is sometimes seen along the anterior longus colli muscles. This would be very rare in the posterior neck soft tissues and has an amorphous, nonosseous pattern of mineralization. Given the importance of the nuchal ligament for support of the cervical spine and the standard of posterior midline dissection in cervical spine surgery, abundant ossification of the nuchal ligament should be noted in preoperative patients.

Additional Information

The nuchal ligament is a midline band of fibrous tissue that extends from the external occipital protuberance to the spinous process of C7. It is contiguous with and analogous to the supraspinous ligament, which extends from the spinous process of C7 to the sacrum. Ossification of the nuchal ligament is generally thought to occur secondary to chronic repetitive mechanical irritation of the ligament against the spinous processes when the neck flexes. This low-grade irritation induces fibrocartilaginous and osseous metaplasia within the nuchal ligament.

References

1 Wang H, et al. Analysis of radiography findings of ossification of nuchal ligament of cervical spine in patients with cervical spondylosis. *Spine (Phila Pa 1976)* 2014;39:E7–E11. doi: 10.1097/BRS.0000000000000037.

2 Paraskevas GK, Raikos A, Martoglou S, Ioannidis O. Sesamoid ossicles within the nuchal ligament: a report of two cases and review of the literature. *J Radiol Case Rep* 2011;5:22–29. doi: 10.3941/jrcr.v5i8.708.

3 Takeshita K, Peterson ET, Bylski-Austrow D, Crawford AH, Nakamura K. The nuchal ligament restrains cervical spine flexion. *Spine (Phila Pa 1976)* 2004;29:E388–393.

4 O'Connell JX, Janzen DL, Hughes TR. Nuchal fibrocartilaginous pseudotumor: a distinctive soft-tissue lesion associated with prior neck injury. *Am J Surg Pathol* 1997;21:836–840.

5 Wang H, et al. The correlation between ossification of the nuchal ligament and pathological changes of the cervical spine in patients with cervical spondylosis. *Spine (Phila Pa 1976)* 2014;39(26 Suppl 1):S145–S149. doi: 10.1097/BRS.0000000000000430.

Figure 8.1 Two sagittal reformatted cervical spine CT images show diffuse motion artifacts revealed by double contours of the bony margins of the vertebral bodies, articular pillars, and laminae (arrows).

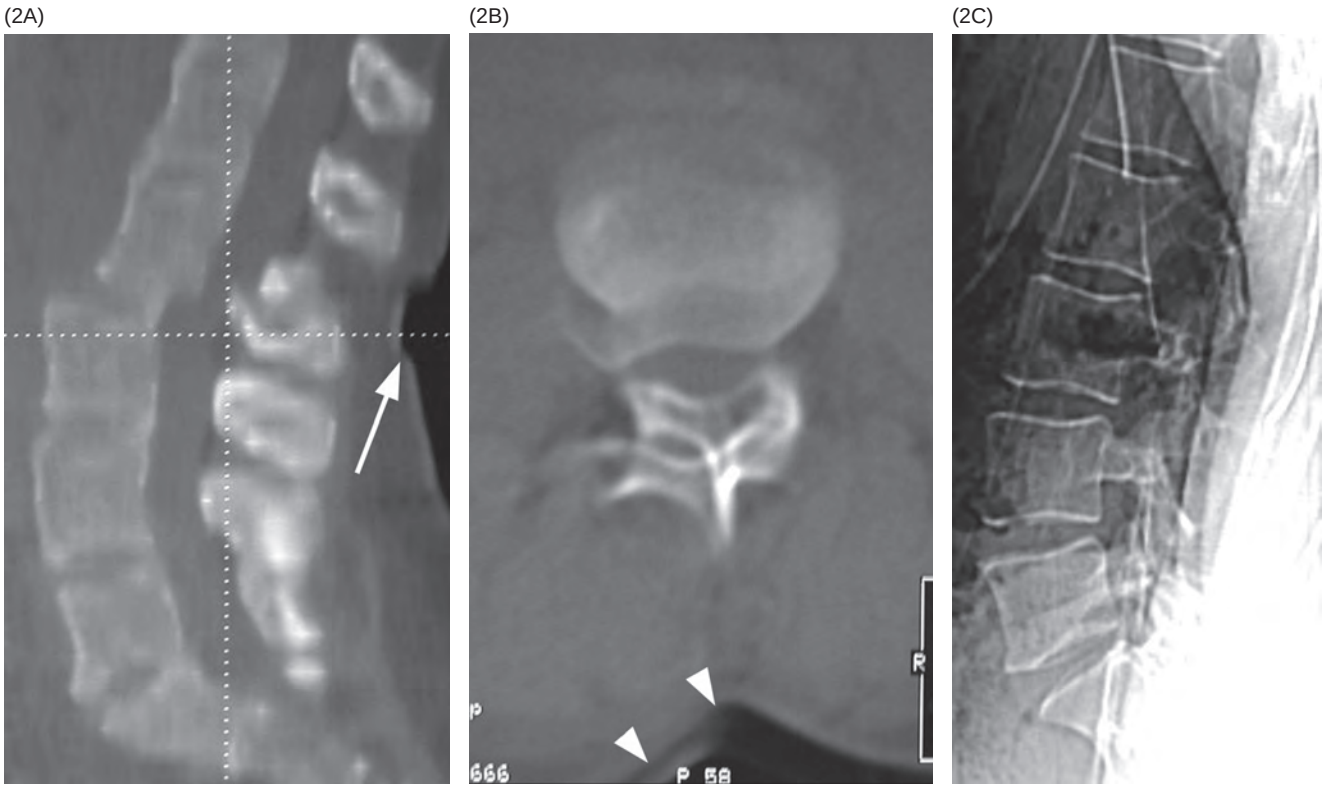

Figure 8.2 **A)** Midsagittal reformatted lumbar spine CT image in a trauma patient shows misalignment at L2–L3 level, mimicking a severe disc disruption and spine luxation. The central canal also appears narrowed at this level. The morphology of the luxation is atypical, and focal discontinuity of the skin line is noted at this level (arrow). **B)** Axial CT source image at L2–L3 reveals double contour of bony structures and of the skin (arrowheads), consistent with motion artifact. **C)** Lateral localizer CT scan confirms normal alignment of the lumbar spine.

CASE 8 CT Motion Artifacts

Alessandro Cianfoni

Imaging Findings

Motion artifacts on CT result in blurred images, with ill-defined contours of anatomical structures and significant loss of spatial resolution. Extensive patient motion during spiral CT scanning produces uninterpretable images or data of very poor diagnostic value, both on axial source images and on reformatted multiplanar images. More subtle or brief patient movement during scans, such as with coughing, swallowing, hickup, or shivering, can produce artifacts that are not easy to recognize. Motion artifacts might obscure pathological findings and/or generate false-positive findings, especially on reformatted sagittal and coronal images, mimicking fractures lines, cortical bone discontinuity, spine misalignment, and luxation. Artifactual fracture lines generally appear blurred and not sharply demarcated, which is also true for the adjacent structures with duplication of soft tissues, in contrast to the well-delineated structures cranial and caudal to the level of the artifact. A typical finding with cervical spine imaging is the ill-defined appearance of the tracheal contours at the level of the fake fracture. A double bone margin is usually visible on axial thin sections at the artifact level. Blurring of osseous or soft tissues, additional artifactual fractures lines of other bony structures, and at times discontinuity of the skin line are observed on multiplanar reformatted images at the z-axis level of the artifact in a band-like distribution, corresponding to the level at which the CT gantry was scanning when motion occurred.

Differential Diagnosis

Fractures

Usually visible as sharply demarcated cortical discontinuity, visible in one or two planes and less visible in the plane parallel to the fracture line. There are no double bony margins, and the adjacent soft tissues do not appear blurred or duplicated.

Facet Disclocation, Luxation, and Subluxation

Sharply demarcated anatomical structures with angulation of the metameric anatomy. Soft tissues and other structures at the level of the injury are well demarcated, and the skin line is continuous, without artifactual interruption on sagittal reformatted images.

Clinical Findings, Implications, and Treatment

Motion artifacts obscuring pathological findings might be responsible for unstable spinal lesions, resulting in inappropriate clearing of the spine in trauma patients, with potentially devastating consequences. These artifacts partially account for reduced sensitivity of CT imaging. On the other hand, motion artifacts mimicking fractures or subluxations reduce the specificity of the technique and may lead to unwarranted further investigation, prolonged unnecessary immobilization, and hazardous interventions. Clinical correlation should be pursued to validate imaging findings whenever possible.

Additional Information

Motion artifacts are errors of integration of axial image data during reconstruction due to the incongruous positions of moving structures at the time of image acquisition.

A negative CT scan should be assessed for technical quality, to be sure that no significant findings are missed because of artifacts, and if necessary, the exam should be repeated. A positive finding on a trauma spine CT exam should be critically reviewed to ensure it is not a motion artifact–generated image, assessing axial source images, adjacent soft tissues, and multiplanar images at the level of the finding. Review of the CT localizer scout views or plain films is helpful and in some cases may be necessary to reliably rule out the findings.

References

1 Sciubba DM, Dorsi MJ, Kretzer R, Belzberg AJ. Computed tomography reconstruction artifact suggesting cervical spine subluxation. *J Neurosurg Spine* 2008;8:84–87.

2 Mehta S, Goss B, Gibson A, et al. Computed tomographic artifact suggesting cervical facet subluxation. *Spine (Phila Pa 1976)* 2011;36: E1038–E1041.

3 Dhandapani S, Salunke P, Mukherjee KK. "Artifactual fracture-subluxation" of cervical spine in computed tomography screening sans plain radiographs. *Spine J* 2013;13:e45–e48.

4 Coats AC, Nies MS, Rispler D. Cervical spine computed tomography imaging artifact affecting clinical decision-making in the traumatized patient. *Open Orthop J* 2014;8:372–374.

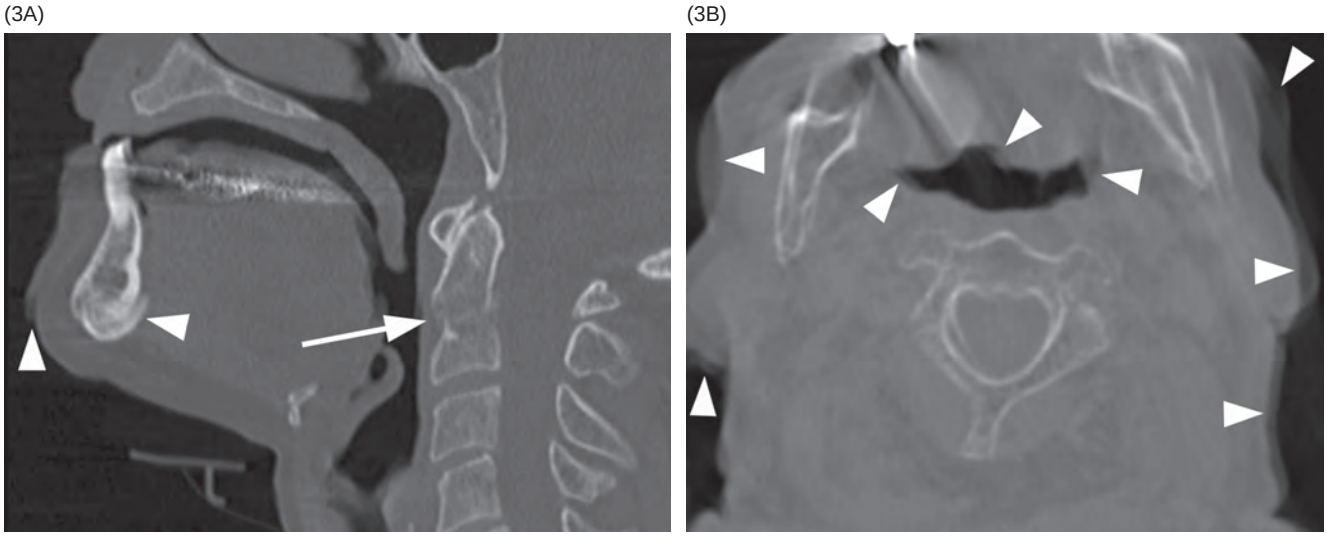

Figure 8.3 **A)** Midsagittal reformatted CT image of the upper cervical spine shows focal cortical discontinuity at the base of the dens (arrow), mimicking a type 2 odontoid fracture. At the same level, in a band-like fashion, discontinuity and double contour is noted of the skin, mandible, tongue base, and posterior pharyngeal wall (arrowheads), strongly suggesting motion artifact. **B)** Axial source image at the level of C2 confirms double bony contours and blurring of the soft tissue–air interfaces (arrowheads), confirming the artifactual nature of the abnormal finding.

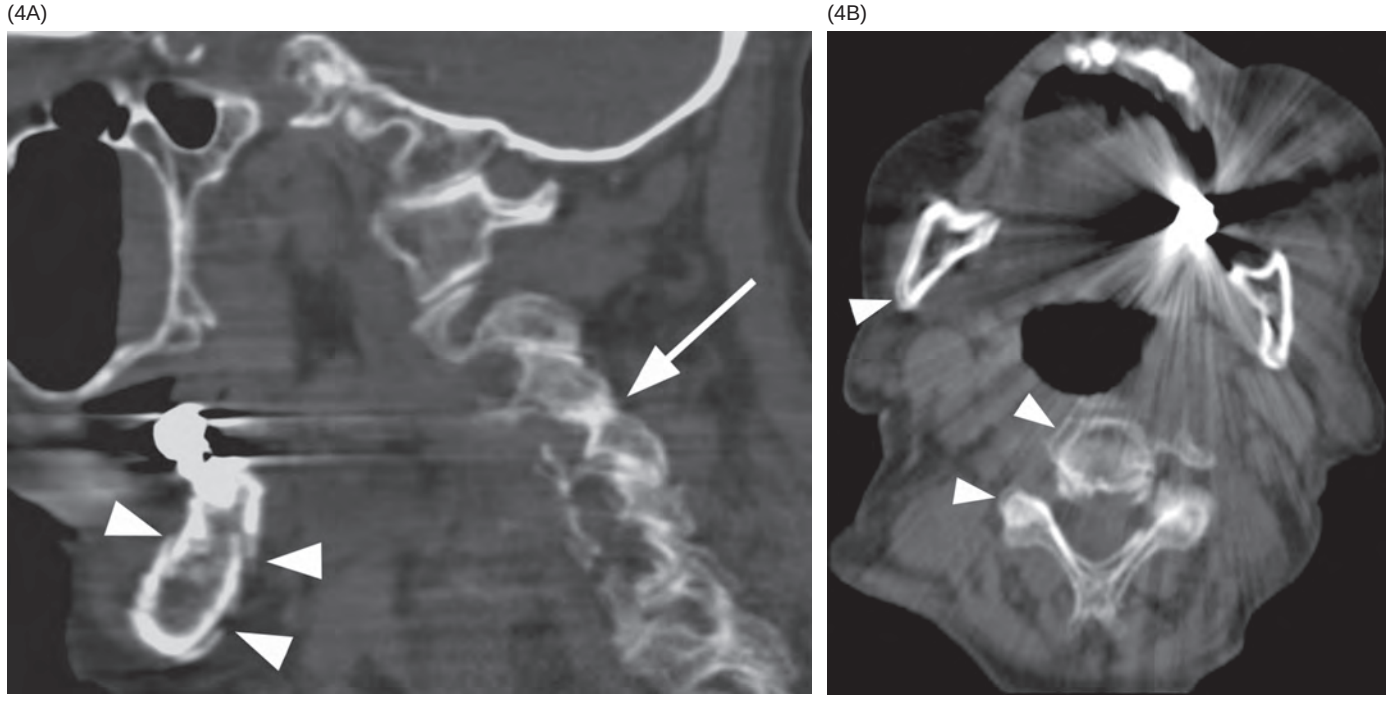

Figure 8.4 **A)** Sagittal CT image along the articular pillars demonstrates apparent subluxation at C3–C4 with perched facets (arrow). The scan is of suboptimal quality with motion artifacts, as suggested by multiple discontinuities of the mandibular bony contours (arrowheads). **B)** Axial CT source image at C3–C4 level reveals double contour of bony structures, confirming motion artifact. Repeat scan at C3–C4 showed normal alignment of the facet joints.

SECTION **2**

Recommendations, Pitfalls, and Controversies

Cases

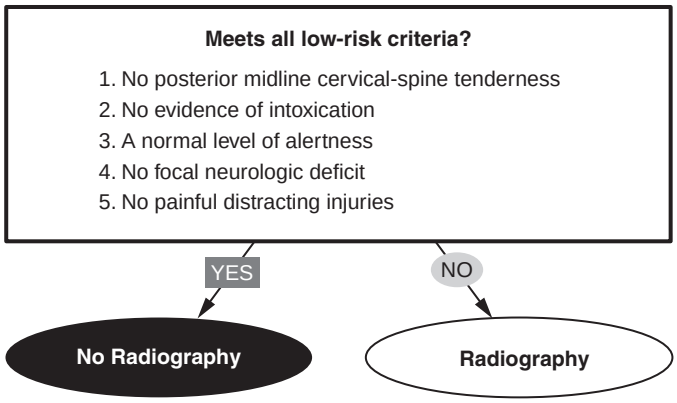

Figure 9.1 National Emergency X-Ray Utilization Study (NEXUS) Criteria.

(2A)

(2B)

Figure 9.2 **A)** Sagittal CT image shows jumped facet/severe facet dislocation injury at C5–C6. **B)** Midsagittal T2-weighted MR image reveals edema in the posterior soft tissues with disruption of the posterior ligamentous complex, disruption of the anterior and posterior longitudinal ligaments, as well as spinal cord injury centered at the C5–C6 level.

CASE 9 When and How to Scan

Vikas Agarwal

Imaging Findings

Two sets of clinical decision rules serve as guidelines for determining whether patients should have imaging of the cervical spine in the setting of trauma. NEXUS (National Emergency X-Ray Utilization Study) and the Canadian C-Spine rule identify individuals with a low probability of injury and therefore not warranting imaging. For those patients who do not meet the low-risk criteria, multidetector spiral (helical) non-contrast CT is the primary screening study. Coronal and sagittal reconstructions help improve detection of fractures and malalignment that can be difficult to visualize in the axial plane alone.

MRI allows evaluation of the spinal cord and other soft tissues, but it has a suboptimal sensitivity for fractures. With regards to spinal cord injury, MRI can offer prognostic information regarding potential recovery. Protocols should include sagittal T2w and STIR, as well as axial and/or sagittal gradient echo T2* sequences. Contrast agent is not required. While its role in the setting of acute trauma is controversial, it is the study of choice for determining the cause of neurological symptoms after a negative CT.

In contrast to the cervical spine, there are no established validated criteria for imaging the thoracolumbar spine in the setting of trauma. CT is routinely performed as first-line imaging to evaluate for acute injury. Given that trauma patients often undergo CT imaging of the chest, abdomen and pelvis, data obtained from these scans can be used to evaluate the thoracolumbar spine avoiding the need for additional scan. MRI offers the same advantages as in the cervical spine, and is valuable for scoring the thoracolumbar spine injuries, as far as ligamentous injury is concerned.

Clinical Findings, Implications, and Treatment

Patients who have experienced blunt trauma and meet all five of the NEXUS criteria are classified as having a low probability of injury. The criteria are: (1) no midline cervical tenderness; (2) no focal neurologic deficit; (3) normal alertness; (4) no intoxication; and (5) no painful, distracting injury. The Canadian C-spine rule only applies to alert and stable trauma patients where cervical spine injury is a concern, and asks the three questions: (1) Is there a high-risk factor (age $>$ 64, dangerous mechanism of injury, or paresthesia in extremities) mandating radiography? (2) Is there a low-risk factor (a simple rear-end motor vehicle collision, sitting position in Emergency Department, ambulatory since injury, delayed onset of neck pain, or absence of midline tenderness) that allows safe assessment of motion? (3) Is the patient able to actively rotate the neck 45° to the left and right? Imaging is not needed when there are no factors in question 1 present, at least one factor in question is 2 present, and the patient is able to complete the task in question 3.

Although less than 3% of blunt trauma patients have clinically important cervical spine injuries, the consequences of missed or delayed diagnosis are disastrous. Up to one-third of fractures involving the thoracolumbar spine are associated with spinal cord injury. The thoracolumbar junction (T10–L2) is especially vulnerable to injury in part related to the biomechanical transition from thoracic kyphosis to lumbar lordosis. The high sensitivity and specificity of CT warrants its use despite higher cost and radiation dose. Plain films have low accuracy and therefore should be abandoned.

Additional Information

The ACR appropriateness criteria for imaging in cervical spine trauma draw from both the NEXUS and Canadian C-spine rule. The recommendations are that no imaging is required in alert patients who have never lost consciousness, are not under the influence of drugs or alcohol, have no distracting injuries, have no cervical tenderness, and have no neurologic findings. Patients not fulfilling these criteria should proceed straight to CT.

References

1 Hoffman JR, Mower WR, Wolfson AB, et al. Validity of a set of clinical criteria to rule out injury to the cervical spine in patients with blunt trauma. National Emergency-Radiography Utilization Study Group. *N Engl J Med*. 2000;343:94–99.

2 Stiell IG, Wells GA, Vandemheen KL, et al. The Canadian C-sine rule for radiography in alert and stable trauma patients. *JAMA*. 2001;286:1841–1848.

3 Muchow RD, Resnick DK, Abdel MP, et al. Magnetic resonance imaging (MRI) in the clearance of the cervical spine in blunt trauma: a meta-analysis. *J Trauma*. 2008;64:179–189.

4 Bozzo A, Marcoux J, Radhakrishna M, et al. The role of magnetic resonance imaging in the management of acute spinal cord injury. *J Neurotrauma*. 2011;28:1401–1411.

5 Rogers LE, West OC. Thoracolumbar spine trauma. In *Imaging skeletal trauma*, 4th edition, Philadelphia: Saunders, 2014, pp. 90–127.

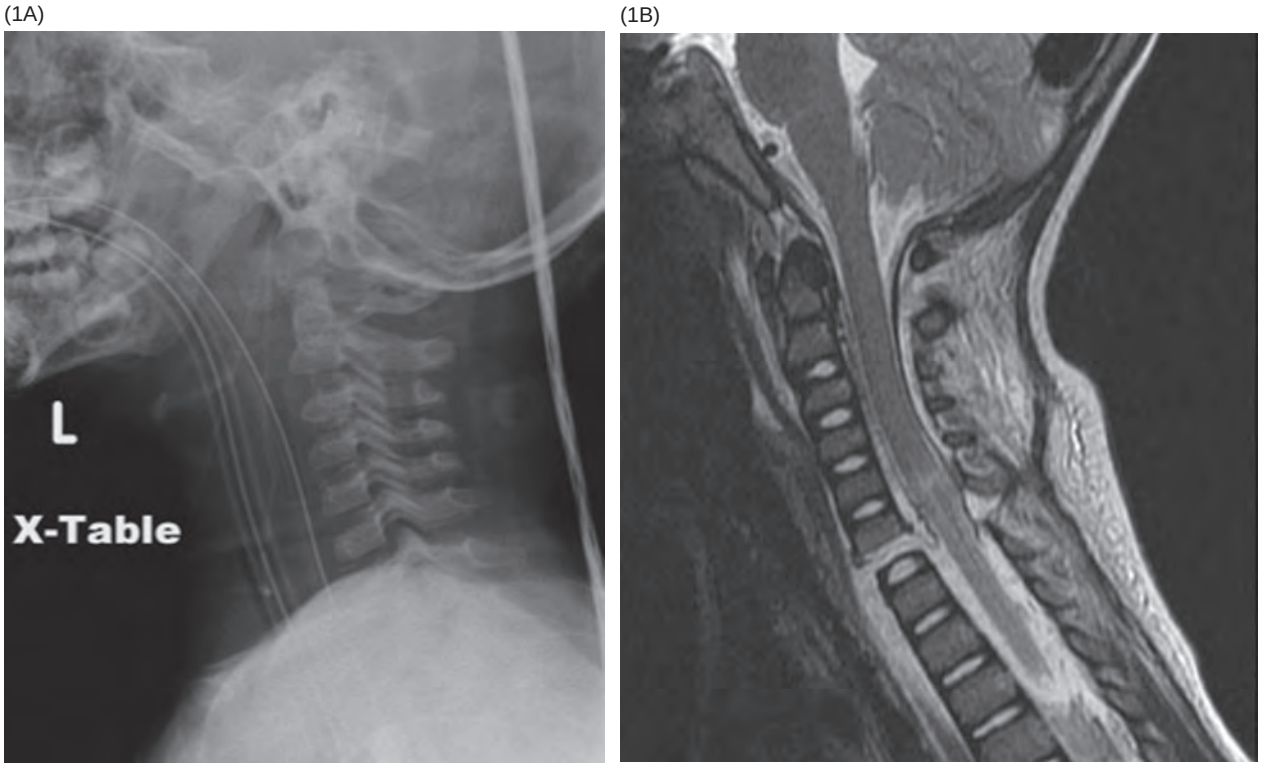

Figure 10.1 A 2-year-old patient following an MVA. **A)** Lateral view radiograph seems negative. The patient is comatose, and MRI (**B**) is then performed, demonstrating spinal cord transection (arrowheads) and disruption of the anterior and posterior longitudinal ligaments as well as posterior ligamentous complex at C6–C7 level.

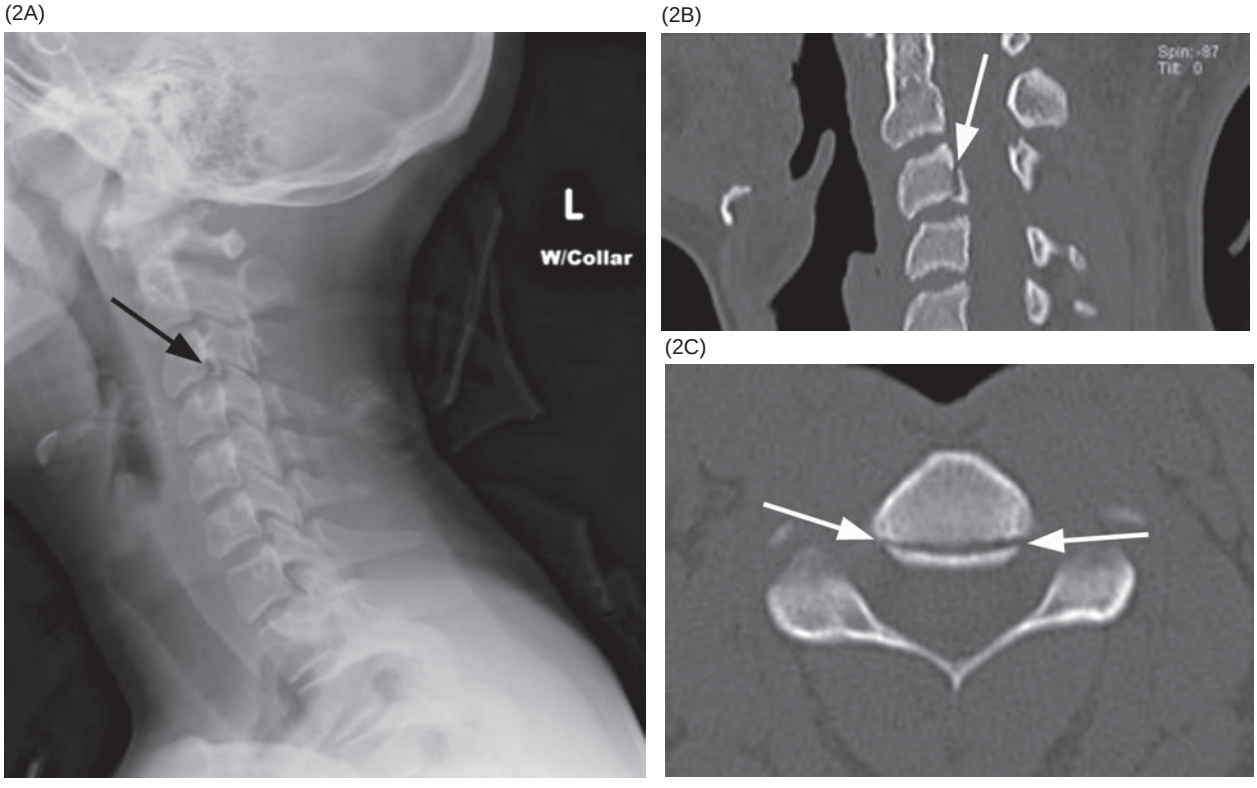

Figure 10.2 A 15-year-old boy status post diving injury. **A)** C3 fracture was suspected on lateral view x-rays (arrow). Focused CT images in the sagittal (**B**) and axial (**C**) planes confirmed the suspicion (arrows). CT was performed at only a few levels to reduce the radiation dose.

CASE 10 Role of Plain Films in Spine Trauma

Gregory A. Vorona and Eytan Raz

Adult Patients

One of the first questions when facing a patient with spinal trauma is whether the injury is stable or unstable. Stability is defined as the capacity of the spine to limit the segmental motion so as to not damage the neural structures and is provided by intact bones and ligaments. Radiographic images can answer this basic question in certain cases: plain films are a widely available, quick way to evaluate the spine. The question is: How to clear the cervical spine nowadays – with CT or plain films? Unfortunately, radiographs, even with the best possible technique, may underestimate spine injury. The main limitations of plain films are generally low sensitivity (65–85%), low accuracy for the craniovertebral junction, and poor visualization of C6 through T1 levels; also, linear or nondisplaced fractures can be difficult to detect, and fractures of the pedicle and uncinate process may not be seen. In the cervical spine, radiographs detect only 60–80% of fractures; a significant number of fractures are not visible, even when multiple views are performed. An advantage of plain films over CT or MRI is the relative ease of obtaining flexion-extension images, which can be active, when allowed by pain, or passive. Discussion over the safety and adequacy of this technique remains open.

CT has become the primary and only imaging modality in high-risk adult patients and can be simply added to the trauma CT protocol together with the evaluation of other anatomical regions.

Pediatric Patients

Plain films still play an important role for pediatric patients. There is currently insufficient data to support the routine use of NEXUS or CCR criteria in pediatric patients. It is generally agreed that imaging is necessary in symptomatic pediatric patients, but there are no current consistent guidelines on specific imaging indications or modalities. The absence of validated clearance protocols and controversy surrounding appropriate imaging result in significant variation in practice patterns. The current American Association of Neurological Surgeons consensus guidelines for symptomatic pediatric patients recommends screening radiographs followed by focused CT if abnormalities are present on the radiograph. In the setting of normal radiographs and pain with range of motion, a neurological deficit, or if the patient is intubated, an MRI of the cervical spine is usually obtained.

The largest multicenter study performed to assess sensitivity of radiographs was through the PECARN (Pediatric Emergency Care Applied Research Network), in which the radiology reports of 186 pediatric patients under the age of 16 years with known cervical spine injury were reviewed. The authors reported an overall sensitivity of 90% (95% CI 85–94%), which was lower for children 7 years of age or younger (83%, 95% CI 70–92%), compared with children between the ages of 8 and 15 years (93%, 95% CI 88–97%). Other small retrospective studies in pediatric trauma patients have reported similar sensitivities. On the other hand, there are many limitations in accurately assessing the radiation dose of a single CT examination, as well as interpreting the significance of this radiation exposure within the context of an individual patient's overall risk for developing cancer. There is evidence that the tube current and tube potential can both be substantially decreased when performing CT of the spine, without significant detrimental effect on diagnostic utility. Iterative reconstruction instead of filtered back projection image reconstruction further decreases the dose. Whatever the present risk is, it will continue to decrease as CT hardware and software continues to develop and improve.

References

1 Hoffman JR, Mower WR, Wolfson AB, Todd KH, Zucker MI. Validity of a set of clinical criteria to rule out injury to the cervical spine in patients with blunt trauma. National Emergency X-Radiography Utilization Study Group. *N Engl J Med* 2000;343:94–99.

2 Stiell IG, Wells GA, Vandemheen KL, et al. The Canadian C-spine rule for radiography in alert and stable trauma patients. *JAMA* 2001;286:1841–1848.

3 Anderson PA, Muchow RD, Munoz A, Tontz WL, Resnick DK. Clearance of the asymptomatic cervical spine: a meta-analysis. *J Orthop Trauma* 2010;24:100–106.

4 Nigrovic LE, Rogers AJ, Adelgais KM, et al. Utility of plain radiographs in detecting traumatic injuries of the cervical spine in children. *Pediatr Emerg Care* 2012;28:426–432.

5 Hernandez JA, Chupik C, Swischuk LE. Cervical spine trauma in children under 5 years: productivity of CT. *Emerg Radiol* 2004;10:176–178.

6 Pearce MS, Salotti JA, Little MP, et al. Radiation exposure from CT scans in childhood and subsequent risk of leukaemia and brain tumours: a retrospective cohort study. *Lancet* 2012;380:499–505.

7 Mulkens TH, Marchal P, Daineffe S, et al. Comparison of low-dose with standard-dose multidetector CT in cervical spine trauma. *AJNR* 2007;28:1444–1450.

8 Becce F, Ben Salah Y, Verdun FR, et al. Computed tomography of the cervical spine: comparison of image quality between a standard-dose and a low-dose protocol using filtered back-projection and iterative reconstruction. *Skeletal Radiol* 2013;42:937–945.

(1A)

(1B)

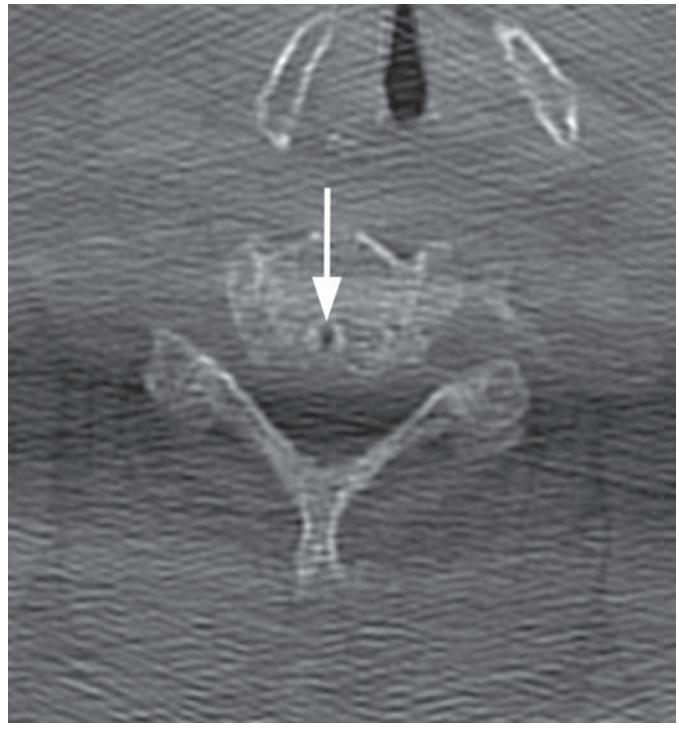

Figure 11.1 **A)** Reconstructed midsagittal CT demonstrates a substantial degradation of image quality at C4 and more inferior levels due to extensive streak artifacts from the shoulder girdle in this patient with C2 fracture and anterolisthesis. **B)** The artifact is also present on the axial CT at C5–C6; however, the image quality is significantly better, and fracture can be reliably excluded at this level. There is an incidental vascular channel (arrow).

Figure 11.2 Axial CT image at C1–C2 level shows prominent streak artifacts, representing the classic location and appearance for artifacts arising from dental fillings. This figure illustrates the notion that C2 fractures are more likely to be overlooked – subtle fractures of the axis may at times be missed due to inadequate image quality.

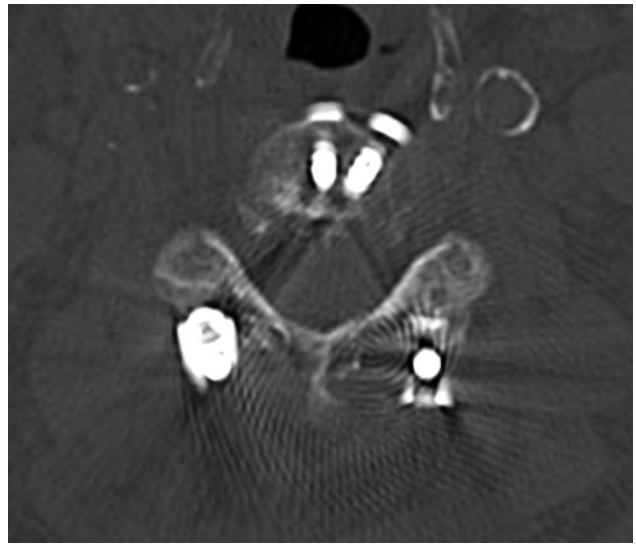

Figure 11.3 Axial CT image in a patient with anterior and posterior instrumented fusion of the cervical spine demonstrates typical artifacts, which, however, do not significantly limit the detection of possible traumatic injuries. Some implants may produce much more prominent artifacts.

CASE 11 CT Streak Artifacts

Zoran Rumboldt

Imaging Findings

CT images of cervical spine and other structures at the base of the neck are often degraded by beam-hardening streak artifact from the shoulder girdle. Although less prominent, this artifact remains an issue even with multidetector CT scanners. Optimized shoulder positioning by the patient (patients pushing their shoulders downward) improves the image quality by increasing the length of the cervical spine not superimposed by the shoulder girdle and decreasing noise. Another option is swimmer's CT position, similar to the patient positioning for the cervical spine radiographs, with one arm raised above head and the other with shoulder depressed. Swimmer's position has been found to offer both potential dose reduction and improved image quality.

Despite advances in detector technology and computer software, artifacts from metal implants can seriously degrade the quality of CT images, sometimes to the point of making them diagnostically unusable. The main sources of metallic artifact in CT imaging of the spine are dental hardware and surgical spine instrumentation. Several factors may help reduce the number and severity of these artifacts at multidetector CT, including decreasing the detector collimation and pitch, increasing the kilovolt peak and tube charge, and using appropriate reconstruction algorithms and section thickness. The image degradation is usually less prominent in the axial plane than in the reconstructed planes; all available images should be closely inspected to ensure that the artifact is not obscuring fractures, dislocations, or other abnormal findings.

Differential Diagnosis

There is really no differential diagnosis for these artifacts; the main issue is the possibility of false negative scans due to obscuration of abnormalities by the artifact.

Clinical Findings, Implications, and Treatment

Metallic hardware causes severe beam hardening and dramatically attenuates the X-ray beam, degrading image quality to the extent that the resultant image is either incomplete or is a faulty projection of the data with consequent reconstruction artifacts. Materials with lower X-ray beam attenuation coefficients (density) produce fewer artifacts (plastic < titanium < stainless steel < cobalt–chrome).

The fractures most likely to be missed in the cervical spine by CT appear to occur at C2, which is at least in part caused by dental artifacts.

Additional Information

The generation of artifacts at CT from metal hardware is related to the image reconstruction parameters, X-ray kilovolt peak, tube current, pitch, as well as hardware composition, shape, and location. Iterative reconstruction of the CT data and dual-energy CT have been proposed as means of reducing beam-hardening artifacts. The use of dual-energy scanners allows the synthesis of virtual monochromatic (monoenergetic) spectral (VMS) images. Monochromatic images depict how the imaged object would look if the X-ray source produced X-ray photons at only a single energy level. In one recent study, the magnitude of metallic artifact seen with titanium fixation rods was minimized at monoenergies of 90 keV and higher, using a collimation width of 20 mm and large field of view; the artifact with cobalt–chromium fixation rods was minimized at monoenergies of 110 keV and higher.

References

1 Stradiotti P, Curti A, Castellazzi G, Zerbi A. Metal-related artifacts in instrumented spine. Techniques for reducing artifacts in CT and MRI: state of the art. *Eur Spine J* 2009;18 Suppl 1:102–108. doi: 10.1007/s00586-009-0998-5.

2 Mueck FG, Roesch S, Geyer L, et al. Emergency CT head and neck imaging: effects of swimmer's position on dose and image quality. *Eur Radiol* 2014;24:969–979. doi: 10.1007/s00330-014-3105-1.

3 Daffner RH, Sciulli RL, Rodriguez A, Protetch J. Imaging for evaluation of suspected cervical spine trauma: a 2-year analysis. *Injury* 2006;37:652–658.

4 Komlosi P, Grady D, Smith JS, et al. Evaluation of monoenergetic imaging to reduce metallic instrumentation artifacts in computed tomography of the cervical spine. *J Neurosurg Spine* 2015;22:34–38. doi: 10.3171/2014.10.SPINE14463.

CASE 12 Utility of MRI after Negative CT

Stephen R. Love and Stephen P. Kalhorn

Background

Imaging and clearance of spinal injury remain somewhat controversial in the current literature. Most trauma protocols standardize initial imaging of the cervical spine via the National Emergency X-Ray Utilization Study (NEXUS) criteria or the Canadian C-spine rule. While this works well for asymptomatic patients, difficulties arise in the absence of abnormalities on computed tomography (CT) in symptomatic or obtunded patients. Here we describe the utility of magnetic resonance imaging (MRI) following negative CT.

Cervical Spine

In the presence of any positive condition within the criteria of NEXUS or the Canadian C-spine rule, patients are routinely immobilized in collars, and nearly all trauma algorithms suggest high-resolution CT of the cervical spine. In the absence of neurologic deficit and in awake, alert patients, the cervical spine may be cleared of the cervical collar even in the presence of cervical spine tenderness in the setting of a negative thin-cut CT. A great deal of literature exists to support clearance of cervical precautions in obtunded blunt trauma patients in the setting of a negative thin-cut CT.

A major drawback to MRI in these situations is its relatively low specificity. MRI will detect clinically insignificant soft tissue disruption, which may lead to more interventions, including unnecessary hard collar use or surgery. The literature does not support MRI as part of a further workup of the patient's neck tenderness if the patient does not have a focal neurologic deficit. Additionally, there is some evidence to support that findings seen on early MRI do not alter clinical course or management in these patients.

In awake or obtunded patients with a focal neurologic deficit, MRI of the cervical spine following a negative CT may be useful. Several studies examining the benefit of MRI in patients with unreliable or abnormal neurologic exams have found some utility to MRI examination in this cohort of patients (such as cord contusion in the setting of SCIWORA, nerve root avulsions, epidural and subdural hematomas). Additionally, Chew and colleagues noted that MRI also helped guide surgical intervention in patients with neurologic deficit and a normal CT. Certainly, in our clinical practice, we routinely investigate unexplained neurologic deficits in an aggressive manner in both awake and obtunded patients, and this includes MRI in the face of negative CT.

Thoracolumbar Spine

While ample evidence exists that MRI not only can prove useful in surgical decision-making but also change spinal fracture classification in patients with positive findings on CT, literature on utility of MRI after negative CT scan is sparse. MRI is indicated in the presence of neurological deficit.

References

1 Mavros MN, Kaafarani HM, Mejaddam AY, et al. Additional imaging in alert trauma patients with cervical spine tenderness and a negative computed tomographic scan: is it needed? *World J Surg* 2015;39:2685–2690.

2 Badhiwala JH, Lai CK, Alhazzani W, et al. Cervical spine clearance in obtunded patients after blunt traumatic injury: a systematic review. *Ann Intern Med* 2015;162:429–437.

3 Patel MB, Humble SS, Cullinane DC, et al. Cervical spine collar clearance in the obtunded adult blunt trauma patient: a systematic review and practice management guideline from the Eastern Association for the Surgery of Trauma. *J Trauma Acute Care Surg* 2015;78:430–441.

4 James IA, Moukalled A, Yu E, et al. A systematic review of the need for MRI for the clearance of cervical spine injury in obtunded blunt trauma patients after normal cervical spine CT. *J Emerg Trauma Shock* 2014;7:251–255.

5 Satahoo SS, Davis JS, Garcia GD, et al. Sticking our neck out: is magnetic resonance imaging needed to clear an obtunded patient's cervical spine? *J Surg Res* 2014;187:225–229.

6 Chew BG, Swartz C, Quigley MR, et al. Cervical spine clearance in the traumatically injured patient: is multidetector CT scanning sufficient alone? Clinical article. *J Neurosurg Spine* 2013;19:576–581.

7 Ackland HM, Cameron PA, Wolfe R, et al. Outcomes at 12 months after early magnetic resonance imaging in acute trauma patients with persistent midline cervical tenderness and negative computed tomography. *Spine* 2013;38:1068–1081.

8 Khanna P, Chau C, Dublin A, et al. The value of cervical magnetic resonance imaging in the evaluation of the obtunded or comatose patient with cervical trauma, no other abnormal neurological findings, and a normal cervical computed tomography. *J Trauma Acute Care Surg* 2012;72:699–702.

9 Panczykowski DM, Tomycz ND, Okonkwo DO. Comparative effectiveness of using computed tomography alone to exclude cervical spine injuries in obtunded or intubated patients: meta-analysis of 14,327 patients with blunt trauma. *J Neurosurg* 2011;115:541–549.

CASE 13 Stable vs. Unstable Spine Injuries

Abhay Varma and Alessandro Cianfoni

Biomechanics

Stability of spine is the ability to limit patterns of displacement under physiologic loads so as not to damage or irritate the spinal cord or nerve roots and, in addition, to prevent incapacitating deformity or pain caused by structural changes. Instability is, conversely, the inability to limit excessive or abnormal spinal displacement under physiological loading. Trauma can disrupt one or more elements responsible for maintaining stability.

Different algorithms have been described to diagnose spinal instability in the setting of a traumatic injury. Numerous classification systems have been proposed to describe injuries, predict stability, and dictate treatment, but none of them are universally accepted. Denis's model uses a 3-column system to evaluate spinal stability. The anterior column includes the anterior half of vertebral bodies, disks, and anterior longitudinal ligament; the middle column comprises of the posterior half of the vertebral bodies, disks, and posterior longitudinal ligament; and the posterior column is made up of neural arches and the posterior ligamentous complex (supraspinous ligament, interspinous ligament, ligamentum flavum, and the joint capsules). Simultaneous failure of two columns makes the spine potentially unstable. The thoracolumbar injury classification and severity score (TLICS) was designed not only to assess stability but also to determine the need for surgical intervention. TLICS takes into account the posterior ligamentous structures (posterior ligamentous complex, PLC), so that an apparently simple anterior column fracture warrants surgical stabilization if accompanied by PLC disruption. The quantification method, as used in TLICS, has been also applied to cervical spine injuries, such as with subaxial injury classification (SLIC). A note should be made that all these models apply to subaxial cervical and thoracolumbar spine (C3 and lower segments), but a much more complex set of classifications exist for injuries at C0–C2 (from the occipital condyles to the axis) levels.

Radiology

Multislice CT is the diagnostic modality of choice for detecting fractures and spatial orientation of bone fragments, and for evaluation of vertebral alignment. The specificity and sensitivity of multislice helical CT in diagnosing cervical spine injury is 99.9%, and negative predictive value of a normal CT is 100%. About 20% of thoracolumbar burst fractures are misdiagnosed as wedge compression fractures on radiographs, and CT can help in establishing the correct diagnosis by demonstrating disruption of posterior vertebral cortical lines with 100% sensitivity.

MRI is the diagnostic modality of choice for assessing changes in ligaments, spinal cord, and other soft tissues. It can be selectively used in obtunded patients, or in conscious patients with pain or tenderness along the vertebral column or neurological deficit.

Clinical Findings, Implications, and Treatment

Surgeon expertise and experience remains an important factor in determination of stability. Stable injuries are managed conservatively with pain control and temporary bracing. Injuries that appear stable, on the initial evaluation, may transition into delayed instability. Treating physician should reevaluate for instability in case of persisting pain or development of neurological symptoms or signs. Instability is associated with deformity and often neurological deficit. Deformity, even without neurological deficit, can result in debilitating pain. Unstable injury is managed with surgical stabilization with or without decompression, depending on the presence of neural compression.

References

1 Denis F. The three columns spine and its significance in the classification of acute thoracolumbar spinal injuries. *Spine* 1983;8:817–831.

2 Schroeder GD, Harrop JS, Vaccaro AR. Thoracolumbar trauma classification. *Neurosurg Clin N Am* 2017;28:23–29.

3 Stone AT, Bransford RJ, Lee MJ, et al. Reliability of classification systems for subaxial cervical injuries. *Evid Based Spine Care J* 2010; 1:19–26.

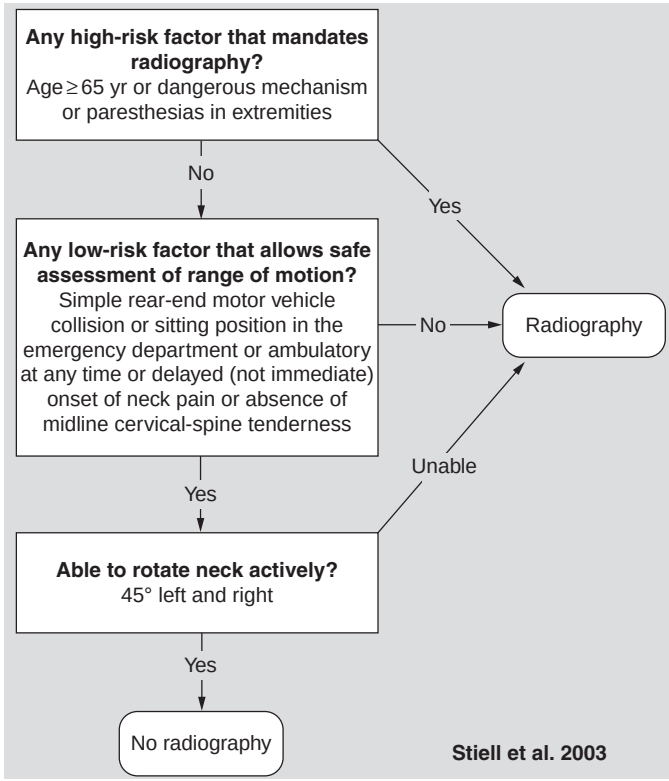

Figure 14.1 Canadian C-spine rule imaging criteria for use in alert and stable trauma patients.

CASE 14 Whiplash Injury

Abhay Varma and Stephen P. Kalhorn

Neck sprain, or "whiplash injury," most commonly seen in car impacts, has constituted a frustrating problem in clinical practice. Lack of specific clinical and radiological findings makes it difficult to understand what has been injured and why some patients do not recover. Neck sprain symptoms after trauma are not specific and can be difficult to distinguish from nontraumatic origin. Similar symptoms are seen after rear-end, frontal, and side impacts. In fact, any trauma exposing the head, neck, and trunk to noncoherent movements can cause these symptoms. The Quebec Task Force proposed that the common term "whiplash-associated disorders" be used for these conditions.

Imaging Findings

The imaging studies are generally negative, while a mild cervical kyphosis may be present. On MRI, T2 hyperintensity of various ligaments, primarily the alar and transverse ligaments, has been described in the literature; however, more recent studies have shown that these findings are present in a high percentage of normal individuals. MRI signal changes of alar and transverse ligaments therefore do not appear to be caused by whiplash injury, and MRI examination should not be used in the routine workup of these patients.

Differential Diagnosis

Whiplash Fracture

Possible neurological findings, associated vertebral body fracture, malalignment common.

Clinical Findings, Implications, and Treatment

Patients typically complain of neck pain and stiffness, shoulder pain, paresthesias and pain in upper extremities, headaches, dizziness, visual impairments, tinnitus, nausea, and cognitive function disorders. Signs typically include localized spasm and tenderness as well as limitation of neck movement. Neurological examination is normal, but it is important to perform a thorough exam to rule out more serious injury. Patients present with symptoms including pain, headaches, stiffness, numbness, weakness, and associated radicular irritation. Imaging is recommended in the presence of high-risk factors ($\geq$65 years of age, dangerous mechanism of injury, paresthesias in extremities). These injuries have significant challenges in management, with 40–60% of cases transitioning into persistent disorders. The treatment most often involves reassurance with acknowledgment that the patient is hurt and their symptoms are a normal reaction. Treatment during the initial phase following injury should focus on early resumption of normal activities, nonsteroidal anti-inflammatory drugs, and physical therapy for core strengthening and range of motion of cervical spine. Interventional therapy like epidural steroid injections, trigger point injections, facet block, botulinum injection in tender muscles, and radiofrequency (RF) ablation of facet nerve supply (medial branch of ramus dorsalis of cervical nerves) are an option in the chronic phase. Of these, evidence is strongest in support of role of RF ablation.

Focusing on improvements in function and maintaining life activities are important factors in getting better. Range-of-motion exercises and isometric exercises for the neck are recommended to restore proper muscle control. Medications should not be prescribed for neck pain alone, but NSAIDS may be used when musculoskeletal signs are present; opioids are rarely prescribed but may be used sparingly.

Additional Information

Whiplash injury of the cervical spine results from energy transfer to cervical spine from acceleration–deceleration type of mechanism. It is important to realize that the injury results from low-velocity collision, and should be differentiated from whiplash fractures resulting from accidents involving higher magnitude of energy transfer. The underlying pathology is not clear but is thought to involve injury to the soft tissues of the neck. Available evidence seems to suggest that facet joint injury (including capsular strain, joint hemorrhage) disc injury (annulus tears, disruption of nucleus) and tears in ligaments (anterior longitudinal ligament, ligaments of craniovertebral junction) contribute to conglomeration of symptoms following whiplash injury. Long-term studies have failed to establish higher incidence of degenerative changes in symptomatic patients compared with asymptomatic patients, following whiplash injury.

Constellation of symptoms following an acceleration-deceleration type injury is referred to as whiplash-associated disorder (WAD). Acute phase of WAD lasts first 3 weeks following injury, followed by subacute stage that lasts up to 3 months, and WAD is labeled chronic if symptoms persist beyond 3 months. Approximately 85% patients recover sufficiently within 6 months to resume their regular activities, while 15–30% develop chronic symptoms. Greater initial neck pain severity after accident, prior history of neck pain, frequent and early health care use, post-injury psychological distress and passive type of coping, compensation, and legal factors predispose to chronicity.

References

1 Gwendolen J, Kenardy J, Hendrikz J, et al. Management of acute whiplash: a randomized controlled trial of multidisciplinary stratified treatments. *J Pain* 2014;154:1798–1806.

2 Lamb SE, Gates S, Williams MA, et al. Emergency department treatments and physiotherapy for acute whiplash: a pragmatic, two-step, randomized controlled trial. *Lancet* 2013;381:546–556.

3 Gross A, Forget M, St George K, et al. Patient education for neck pain. *Cochrane Database Syst Rev* 2012; 3:CD005106. doi: 10.1002/14651858. CD005106.pub4.

4 Carroll LJ, Holm LW, Hogg-Johnson S, et al. Course and prognostic factors for neck pain in whiplash-associated disorders (WAD): results of the Bone and Joint Decade 2000–2010 Task Force on Neck Pain and Its Associated Disorders. *Spine (Phila Pa 1976)* 2008; 33(4 Suppl): S83–S92.

5 Stiell IG, Clement CM, McKnight RD, et al. The Canadian C-spine rule versus the NEXUS low-risk criteria in patients with trauma. *N Engl J Med* 2003;349:2510–2518.

6 Freeman MD, Croft AC, Rossignol AM. "Whiplash associated disorders: redefining whiplash and its management" by the Quebec Task Force. A critical evaluation. *Spine* 1998;23:1043–1049.

7 Li Q, Shen H, Li M. Magnetic resonance imaging signal changes of alar and transverse ligaments not correlated with whiplash-associated disorders: a meta-analysis of case-control studies. *Eur Spine J* 2013;22:14–20.

8 Anderson SE, Boesch C, Zimmermann H, et al. Are there cervical spine findings at MR imaging that are specific to acute symptomatic whiplash injury? A prospective controlled study with four experienced blinded readers. *Radiology* 2012;262:567–575.

9 Vetti N, Kråkenes J, Ask T, et al. Follow-up MR imaging of the alar and transverse ligaments after whiplash injury: a prospective controlled study. *AJNR Am J Neuroradiol* 2011;32:1836–1841.

10 Dullerud R, Gjertsen O, Server A. Magnetic resonance imaging of ligaments and membranes in the craniocervical junction in whiplash-associated injury and in healthy control subjects. *Acta Radiol* 2010;51:207–212.

CASE 15 Findings Likely to Be Missed

Zoran Rumboldt

Imaging Findings

A recent study evaluated the effectiveness of second-opinion radiology consultations at a referral center to reassess the cervical spine CT scans of the trauma patients and found that in 92% of patients, the first-read and the over-read reports had consistent radiologic findings. False positive diagnosis was cleared in 3%, while a missed diagnosis was detected in 5%. The most common missed radiologic findings were transverse and spinous process fractures, followed by dens and lamina fractures; the most common misdiagnoses were dens fractures.

Although vertebral fractures represent frequent incidental findings on multidetector CT scans of the chest and/or abdomen and may be easily identified on sagittal reformats, they are often underreported by radiologists, most likely because of unawareness of their clinical importance – around 85% of the thoracolumbar spine fractures were missed in one study.

There is a substantial variability in the presence or degree of marrow edema on MRI scans following injury, primarily depending on the fracture type. Only vertebral body compression fractures reliably generate marrow edema, while fractures without compression and/or fractures with distraction may not generate marrow edema and can lead to a false negative MRI.

Clinical Findings, Implications, and Treatment

In addition to the dens, transverse processes, spinous processes, and laminae may require special attention in order to avoid missed fractures on CT scans in trauma patients.

CT is the modality of choice for evaluation of suspected spine injury, which may be supplemented by MRI in selected cases, but MRI should not be used as the only imaging modality, as it is has poor sensitivity for fractures.

Obtaining a second opinion from the radiologists in a tertiary care hospital provides reassurance and confirms the findings, or demonstrates misdiagnoses or missed findings, thereby improving diagnostic accuracy and benefiting patient care.

Additional Information

A number of studies have compared MRI to intraoperative findings of soft tissue injuries in patients with spine trauma. The published results for most ligamentous structures are somewhat conflicting: both high and low sensitivity as well as specificity have been found. Disruption of the hypointense band, especially on T1-weighted images, is a very specific sign of ligamentous injury, essentially without false positive findings. Hyperintensity on T2-weighted images with fat suppression (STIR or fat saturated T2w) is, on the other hand, very sensitive but with low specificity and therefore frequently overestimates injury to the ligaments of the spine.

References

1 Khalilzadeh O, Rahimian M, Batchu V, et al. Effectiveness of second-opinion radiology consultations to reassess the cervical spine CT scans: a study on trauma patients referred to a tertiary-care hospital. *Diagn Interv Radiol* 2015;21:423–427. doi: 10.5152/dir.2015.15003.

2 Bartalena T, Giannelli G, Rinaldi MF, et al. Prevalence of thoracolumbar vertebral fractures on multidetector CT: underreporting by radiologists. *Eur J Radiol* 2009;69:555–559. doi: 10.1016/j.ejrad.2007.11.036.

3 Brinckman MA, Chau C, Ross JS. Marrow edema variability in acute spine fractures. *Spine J* 2015;15:454–460. doi: 10.1016/j.spinee.2014.09.032.

4 Haris AM, Vasu C, Kanthila M, et al. Assessment of MRI as a modality for evaluation of soft tissue injuries of the spine as compared to intraoperative assessment. *J Clin Diagn Res* 2016;10:TC01–TC05. doi: 10.7860/JCDR/2016/17427.7377.

5 Goradia D, Linnau KF, Cohen WA, et al. Correlation of MR imaging findings with intraoperative findings after cervical spine trauma. *AJNR Am J Neuroradiol* 2007;28:209–215.

SECTION **3**

Trauma to Uncompromised Spine

Cases

Figure 16.1 Sagittal CT image shows mild impaction of the anterior superior T1 vertebral body endplate with anterior buckling (arrow). Note intact posterior cortex (arrowhead).

Figure 16.2 Midsagittal CT image shows compression fracture of the anteror superior L2 endplate. Note the horizontal sclerotic band at the upper vertebral body representing trabecular impaction (arrowhead).

(3A)

(3B)

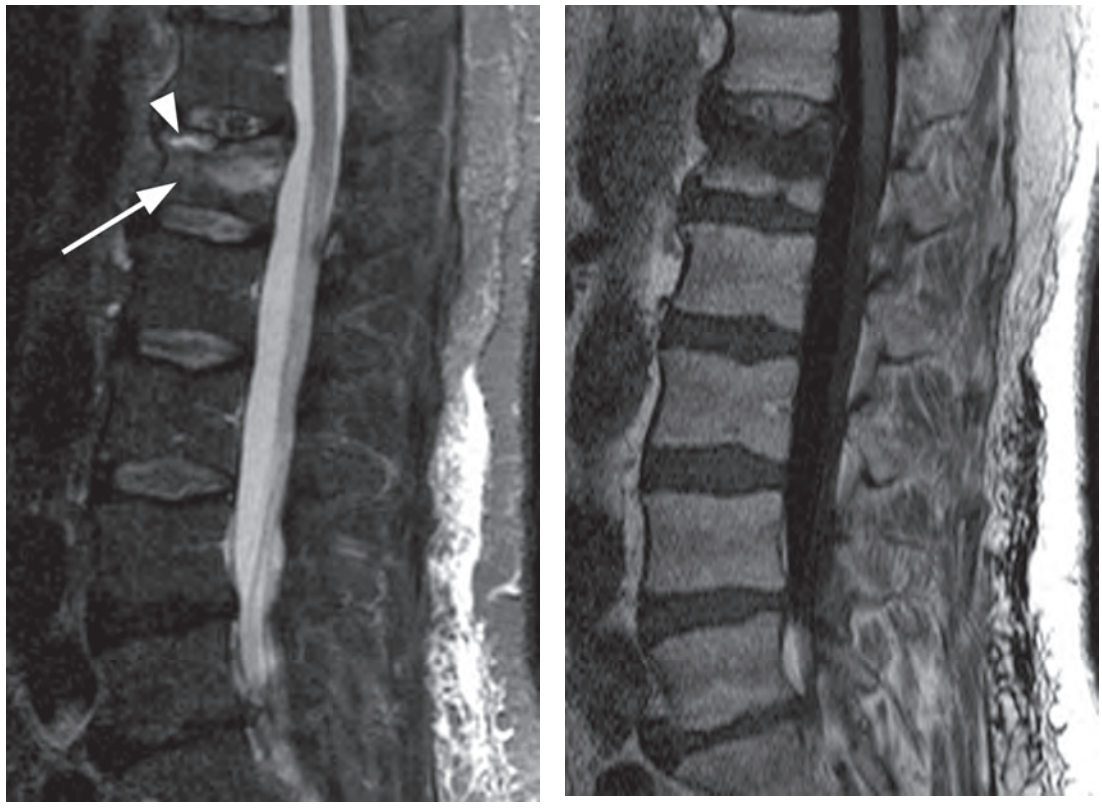

Figure 16.3 Midsagittal STIR MR image (**A**) reveals L1 superior endplate depression and underlying bone marrow edema consistent with a recent fracture (arrow). Note a small amount of fluid signal (arrowhead). The edematous bone marrow is hypointense on corresponding T1-weighted MR image (**B**). No retropulsion into the spinal canal.

CASE 16 Simple Compression Fracture

Hrvoje Vavro

Imaging Findings

Imaging reveals reduction of the anterior height and buckling of the superior-anterior part of the vertebral body due to impaction and cortical disruption of the anterior part of the superior endplate. There is often a horizontal sclerotic band in the upper vertebral body, reflecting trabecular impaction. Inferior endplate is affected less frequently. Posterior cortex is normal, as only the anterior column is involved. Most of the wedge fractures are symmetric, but in 8–14% of cases there is left–right asymmetry (lateral wedge fracture). There is focal kyphosis at the level of injury. MR imaging additionally shows marrow edema of the superior part of the vertebral body (T2-weighted sequences with fat suppression – T2 FS or STIR), possibly with fluid signal within the fracture. There is no anterior or posterior translation of the vertebral bodies. Underlying metastases or other neoplasm and osteomyelitis may be DWI hyperintense and without fluid signal on STIR images.

Differential Diagnosis

Unstable Wedge Fracture

Trauma to the anterior column and the posterior column, including posterior ligamentous complex – signs of posterior column disruption on CT and MRI.

Burst Fracture

Compression of whole vertebral body with posterior cortex involvement, often with sagittal fracture lines and fragmentation with posterior fragment dislocation – consider if loss of vertebral body height is more than 40%.

Chronic Wedge Fracture

An old fracture will have a certain degree of remodeling and smoothing of the cortical edges, without a clearly visible fracture line. Recently fractured cortex of the vertebral body is sharply marginated and often angulated. No bone marrow edema on MRI.

Scheuermann's Disease

Most frequent thoracic (type I), followed by thoracolumbar (type II) – anterior wedging of at least three contiguous vertebral bodies; endplate irregularities are always present; no anterior vertebral body buckling.

Clinical Findings, Implications, and Treatment

The main symptom is pain; in osteoporotic fractures the onset may be insidious and the pain may be mild. As this type of fracture does not involve retropulsion of bone fragments into the spinal canal, neurologic symptoms are rarely present.

Stable wedge fractures make up for 50% of all traumatic thoracolumbar fractures, most commonly occurring at levels T12–L2. In the setting of osteoporosis insufficiency, compression fractures can occur at any level, most frequently in mid-thoracic spine. Nonoperative treatment is the standard: it includes pain medication and brief rest. Early mobilisation is recommended, using hyperextension braces for 6–12 weeks. Vertebroplasty or kyphoplasty is considered, especially in patients with long-standing pain or severe kyphotic deformity.

Additional Information

The presence of injury to the anterior longitudinal ligament, superior endplate and disc, or a high level of bone edema appear to be the critical factors that determine progression of kyphotic deformity following conservatively treated stable thoracolumbar compression fractures. The intraosseus fluid sign on CT can be seen in acute (as well as chronic) fractures and seems to predict greater height loss and kyphotic angulation.

References

1 Lenchik L, Rogers LF, Delmas PD, Genant HK. Diagnosis of osteoporotic vertebral fractures: importance of recognition and description by radiologists. *AJR Am J Roentgenol* 2004;183:949–958.

2 Parizel PM, van der Zijden T, Gaudino S, et al. Trauma of the spine and spinal cord: imaging strategies. *Eur Spine J* 2010;19(Suppl 1):8–17. doi:10.1007/s00586-009-1123-5.

3 Alexandru D, So W. Evaluation and management of vertebral compression fractures. *Perm J* 2012;16:46–51.

4 Jun DS, Shin WJ, An BK, Paik JW, Park MH. The relationship between the progression of kyphosis in stable thoracolumbar fractures and magnetic resonance imaging findings. *Asian Splin J* 2015;9:170–177.

5 Hutchins TA, Wiggins RH, Stein JM, Shah LM. Acute traumatic intraosseus fluid sign predisposes to dynamic fracture mobility. *Emerg Radiol* 2017;24:149–155.

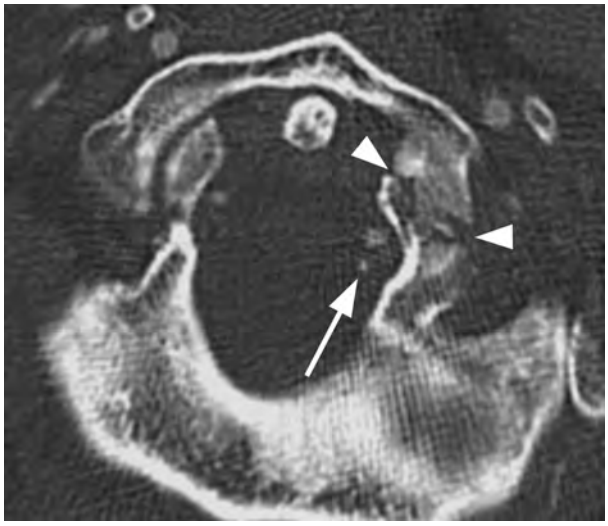

Figure 17.1 Axial CT image of the atlanto-occipital junction shows a comminuted fracture of the left occipital condyle with several directions of fracture line (arrowheads) and small separated fragments (arrow), consistent with an Anderson Type I fracture.

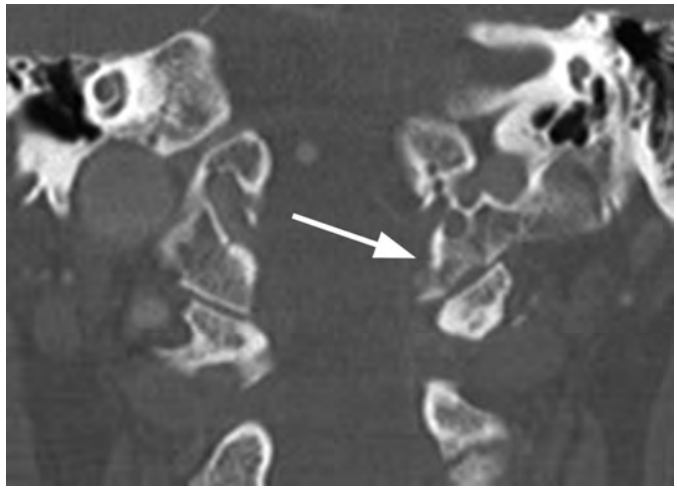

Figure 17.2 Coronal CT image in a different patient shows a fracture of the left occipital condyle (arrow) with several fracture lines and a small area of depression of the occipital condylar surface. This is an Anderson Type I fracture as well.

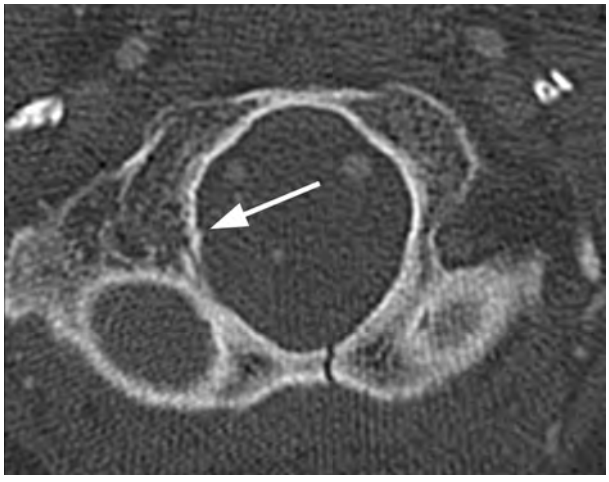

Figure 17.3 Axial CT shows an antero-posteriorly directed fracture of the posterior inferior occiput extending into the foramen magnum. There is a subtle fracture line of the right occiput (arrow) with vertical extension more inferiorly into the right occipital condyle. This is Anderson Type II occipital condyle fracture.

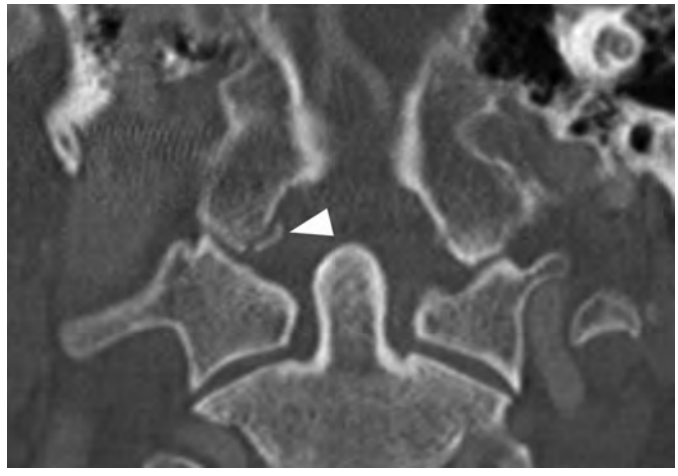

Figure 17.4 Coronal CT image shows an avulsion fracture of the inferior medial aspect of the right occipital condyle (arrow) at the insertion site of the right alar ligament. This is an Anderson Type III fracture, the least stable of the condyle fractures, but is generally treated conservatively as well. Note that there is no widening of the atlanto-occipital joint.

(5A)

(5B)

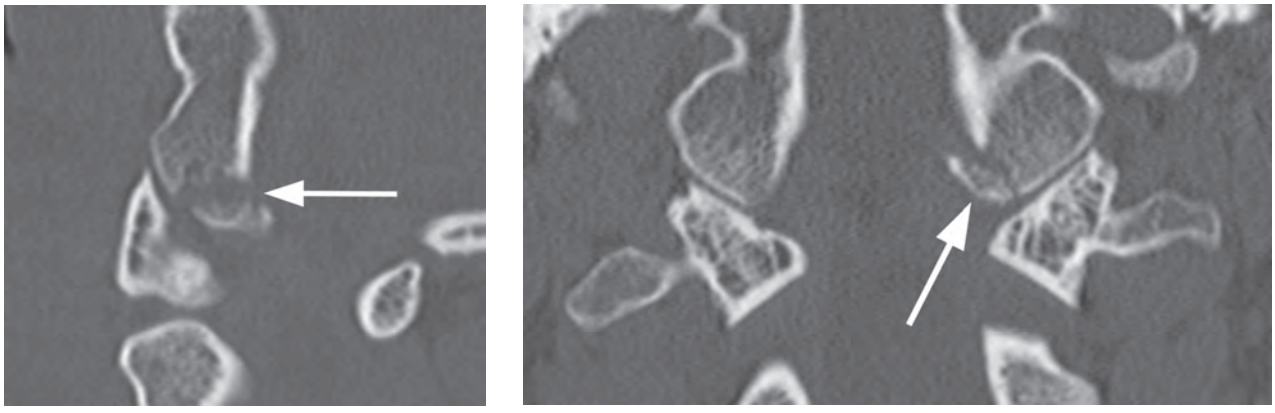

Figure 17.5 Sagittal (**A**) and coronal (**B**) CT images show another Anderson Type III fracture – an avulsion fracture of the left occipital condyle (arrows).

CASE 17 Occipital Condyle Fractures

Russel Chapin and Hrvoje Vavro

Imaging Findings

Occipital condyle fractures need to be evaluated with multiplanar CT, as they may at times be clearly seen in a single plane only. These fractures are classified into three types by the Anderson and Montesano scheme: Type I – comminuted and nondisplaced secondary to axial loading; Type II – extend into the condyle from a linear fracture in the remainder of the skull base (generally involve the base of the occipital condyle without complete separation of the condyle from the skull); Type III – avulsion fractures of the occipital condyle. Tuli et al. proposed a classification scheme consisting of type 1 (nondisplaced), type 2a (displaced stable), and type 2b (displaced unstable) fractures. This group suggested that more than 8 degrees of rotation or 1 mm of translation of the occiput relative to C1, direct evidence of alar ligament avulsion, or MRI evidence of atlanto-axial disruption is consistent with instability. Anderson classification is more widely accepted.

The role of MRI for direct inspection of the alar ligaments and tectorial membrane is questionable. More important is careful inspection of CT images for additional injuries of the skull, atlas, and axis because of the significant forces involved and anatomic proximity of critical structures.

Differential Diagnosis

Ponticulus Posticus

Vascular Channel

Dystropic Calcification/Ossification Adjacent to the Odontoid Process

- Sclerotic margins, contiguous with/intact adjacent occipital condyle.

Clinical Findings, Implications, and Treatment

Because of the associated high-energy mechanism of injury, patients with occipital condyle fractures frequently are obtunded at presentation; otherwise, pain is the predominant complaint. Lower cranial nerve palsies are present in one-third of patients and may present in a delayed fashion. Criteria for the stability of occipital condyle fractures are not universally defined. A study by Maserati et al. on 100 patients (25% of whom were lost to follow-up) treated patients with occipital condyle fractures and less than 2 mm of atlanto-occipital (AO) joint offset conservatively with good outcomes. The 2013 meta-analysis by Theodore et al. focused on 415 reported cases and concluded that nearly all occipital condyle fractures can be managed nonsurgically. Surgical treatment is indicated for patients with AO offset (>2 mm) or evidence of significant neural compression and may be with occipito-cervical fusion or halo placement. Conservative management consists of rigid collar placement with 6-week follow-up dynamic radiographs.

Additional Information

The ligamentous junction of the occiput and superior cervical spine includes the synovial articular capsules, anterior atlantooccipital membrane, apical ligament of the dens, superior crus of the transverse ligament, paired alar ligaments, transverse ligament, tectorial membrane, and posterior atlantooccipial membrane. The alar ligaments extend from the medial inferior aspect of the occipital condyles to the superior lateral tip of the dens bilaterally and they limit contraolateral AO rotation. The tectorial membrane is contiguous with the posterior longitudinal ligament and is posterior to the apical and alar ligaments. Finally, the posterior atlanto-occipital membrane connects the posterior arch of the atlas to the posterior and lateral foramen magnum.

References

1 Maserati MB, Stephens B, Zohny Z, et al. Occipital condyle fractures: clinical decision rule and surgical management. *J Neurosurg Spine* 2009;11:388–395.

2 Hanson JA, Deliganis AV, Baxter AB, et al. Radiologic and clinical spectrum of occipital condyle fractures: retrospective review of 107 consecutive fractures in 95 patients. *AJR Am J Roentgenol* 2002;178:1261–1268.

3 Karam YR, Traynelis VC. Occipital condyle fractures. *Neurosurgery* 2010;66 (3 Suppl):56–59.

4 Theodore N, Aarabi B, Dhall SS, et al. Occipital condyle fractures. *Neurosurgery* 2013;72(2 Suppl):106–113.

5 Leone A, Cerase A, Colosimo C, et al. Occipital condylar fractures: a review. *Radiology* 2000;216:635–644.

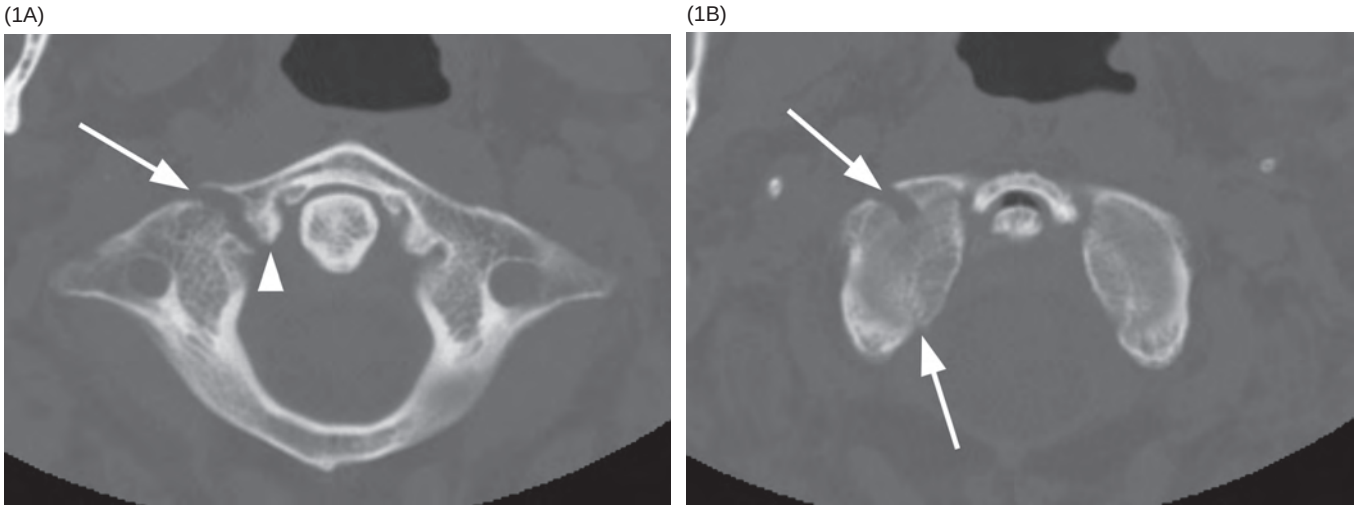

Figure 18.1 Axial CT images (**A**, **B**) show a fracture of the right lateral mass of C1 (arrows) without comminution. The fracture line is just lateral to the tubercle (arrowhead) where the transverse ligament attaches. There were no additional fractures. Slightly increased atlanto-dental interval.

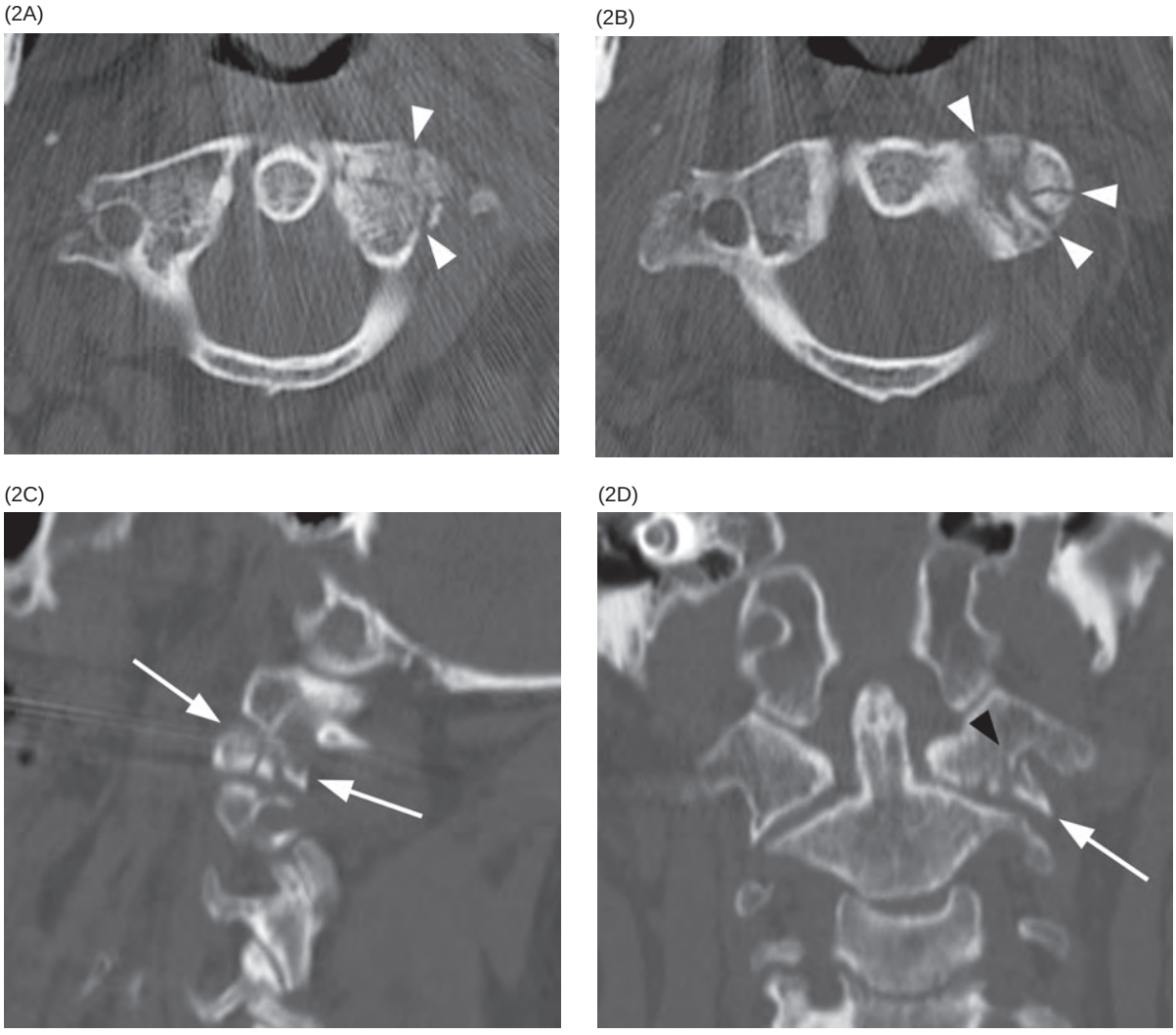

Figure 18.2 Axial (**A, B**) CT images show a comminuted fracture (arrowheads) of the left lateral mass of the atlas, also seen in the sagittal plane (**C**). **D** In addition to fracture lines (arrowhead), coronal CT demonstrates mild outward displacement of the left C1 lateral mass (arrow).

CASE 18 C1 Lateral Mass Fracture

Doris Dodig

Imaging Findings

Lucent line through the C1 lateral mass or avulsed bone fragment from the medial portion of the lateral mass, which is best appreciated on an open mouth radiograph and especially CT images, indicate C1 lateral mass fracture. Additional signs are unilateral atlanto-axial displacement or diminished lateral mass height. C1 lateral mass fractures should be fully assessed by CT imaging, where transverse ligament avulsion fracture, intra-articular, or fracture through the transverse foramen should be scrutinized for on coronal and axial images. The fractures may be simple or comminuted and are considered type III atlas fractures.

Differential Diagnosis

Rotational Malalignment

The lateral mass of C1 is displaced medially on C2, by less than 2 mm.

Congenital Clefts of C1 Arches

Well-corticated margins; unilateral or bilateral atlanto-axial offset less than 3 mm.

Clinical Findings, Implications, and Treatment

Integrity of the transverse ligament determines the stability of C1 lateral mass fracture and guides further imaging and treatment. Atlanto-axial lateral displacement greater than 7 mm and atlanto-dental interval greater than 3 mm are indirect signs of transverse ligament rupture recognized on open-mouth and lateral radiographs. Assessed on CT imaging, avulsion at the transverse ligament insertion at the medial part of C1 lateral mass and comminuted lateral mass fracture indicate Dickman type II transverse ligament lesion. Transverse ligament rupture can be well appreciated on axial T1 and T2 MR images as hypointense ligament band disruption. Furthermore, MR is crucial in assessing possible spinal cord injuries by dislocated bone fragments, and is indicated in patients with neurologic deficit. Stable fractures can be treated with rigid cervical collar for 8–12 weeks, while comminuted or unstable fractures are treated either with a rigid cervical orthosis or a halo vest.

Additional Information

Fractures of C1 lateral masses are the least common of all atlas fractures, and occur in flexion injuries with asymmetric axial loading. Fracture extending through transverse foramen should prompt further evaluation of vertebral artery injury, which can cause ischemic events of the posterior circulation and, in more serious cases, occlusion of the basilar artery with death and locked-in syndrome. A unilateral sagittal split subtype of the lateral mass fracture is a rare condition that can cause a subluxation of the occipital condyle into the fracture gap, resulting in late deformity and pain. This type of unusual fracture requires surgical treatment in spite of intact transverse ligament. Intra-articular lateral mass fracture can be the cause of posttraumatic arthritis, associated with chronic occipital neck pain and stiffness as well as neuralgia from intraforaminal compression of C2 nerve.

References

1 Mead LB 2nd, Millhouse PW, Krystal J, Vaccaro AR. C1 fractures: a review of diagnoses, management options, and outcomes. *Curr Rev Musculoskelet Med* 2016;9:255–262.

2 Babak KS. Fractures of the C1 and C2 vertebrae. *Seminars in Spine Surgery* 2013;25:23–35.

3 Seo SJ, Kim HR, Choi EJ, et al. Unrecognized C1 lateral mass fracture without instability: the origin of posterior neck pain. *Korean J Pain* 2012;25:258–261.

4 Kaiser DR, Ciarpaglini R, Maestretti G. An uncommon C1 fracture with longitudinal split of the transverse ligament. *Eur Spine J* 2012;21: S471–S474.

5 Bransford R, Falicov A, Nguyen Q, et al. Unilateral C-1 lateral mass sagittal split fracture: an unstable Jefferson fracture variant. *JNS* 2009;10:466–473.

(1A)

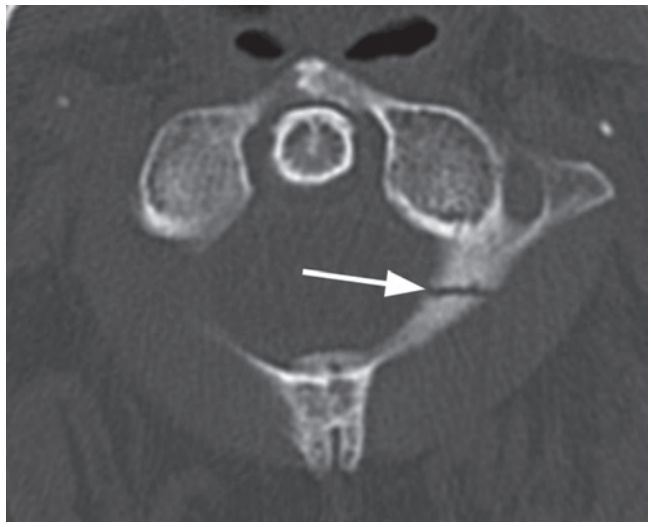

(1B)

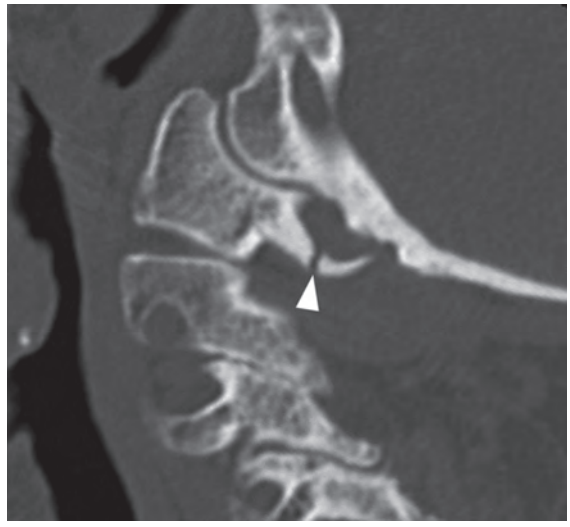

Figure 19.1 A) Axial CT image shows a nondisplaced fracture (arrow) through the posterior arch of C1 on the left. There may be slight sclerosis along the irregular fracture edges, suggesting that the injury may be subacute. **B)** Sagittal CT image also demonstrates the nondisplaced fracture line. The ring of the atlas was otherwise intact, without additinal fractures.

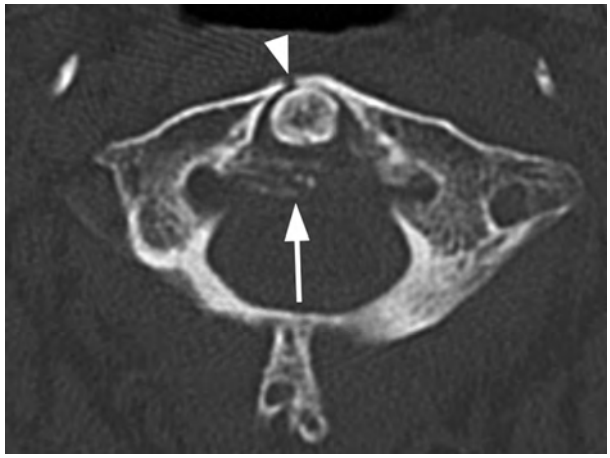

Figure 19.2 Axial CT image in an 82-year-old patient presenting with neck pain following trauma demonstrates an isolated fracture (arrowhead) through the anterior arch of the atlas. Note the otherwise intact ring of C1 and degenerative changes, with calcifications along the transverse ligament (arrow).

(3A)

(3B)

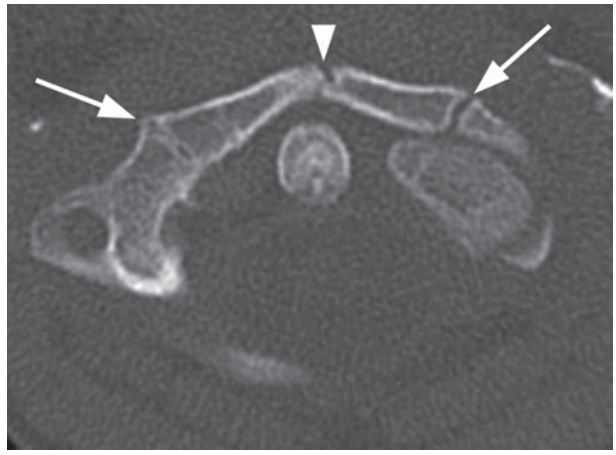

Figure 19.3 A) and **B)** Axial CT images in young child reveal a vertical fracture through the anterior arch of the atlas (arrowheads). Note bilateral open synchondroses (arrows) with smooth, well-corticated edges in this skeletally immature patient.

CASE 19 Isolated Fracture of the Anterior or Posterior Arch of Atlas

Doris Dodig and Zoran Rumboldt

Imaging Findings

These injuries are classified as Type I fractures of the atlas. Fracture of the posterior arch is seen on lateral radiographs as a lucent, noncorticated line through the posterior element. It occurs most often near the junction with lateral masses, and is best appreciated on axial CT images due to its most common vertical orientation. Horizontal fracture of the anterior arch is detected on lateral radiograph as a lucent, irregular, noncorticated line and is best appreciated on sagittal CT images. Vertical anterior arch fracture or a "plough fracture" can be occult on radiography, and the comminuted, anteriorly displaced bone fragments are best seen on axial CT images. Retropharyngeal space width of more than 5 mm at the level of C3 body is the indirect sign of anterior arch fracture on lateral radiographs. CT is necessary for complete assessment of these injuries, especially in young children, as atlas may not be visualized on radiographs. Possible associated fractures, primarily of the odontoid process, need to be excluded.

Differential Diagnosis

Jefferson Fracture

More than one fracture of the C1 arches.

Posterior Arch Cleft

Sclerotic margins of the bone defect, commonly in the midline.

Anterior Arch Non-United Secondary Ossification Center or Calcification of the Longus Colli Muscle

Well-delineated bone fragment adjacent to the lower pole of the anterior arch without prevertebral tissue swelling.

Clinical Findings, Implications, and Treatment

Isolated fractures of the atlas arches are stable, presenting with minor symptoms such as neck pain and stiffness, dizziness, or headache. However, they are often associated with other cervical spine fractures. Integrity of the transverse ligament is the most important determinant of fracture stability that guides further imaging and treatment. Atlanto-axial offset greater than 7 mm evaluated on open-mouth radiographs and coronal CT images, and atlanto-dental interval (ADI) greater than 3 mm, measured on lateral radiographs and sagittal CT reconstructions, indicate transverse ligament rupture. Ligament injury can be visualized on axial T1- and T2-weighted MR images as a disruption of the hypointense band of the transverse ligament. Stable fractures are treated with rigid collar immobilization for 8–12 weeks, while unstable fractures require either a halo vest or definitive surgical treatment.

Additional Information

Posterior arch fracture occurs during hyperextension, when the junction with lateral masses is compressed between the occiput and the spinous process of C2. Horizontal anterior arch fracture is an avulsion fracture at the insertion of the longus colli muscle or anterior atlanto-dental ligament. "Plough fracture" is a serious, although extremely rare, condition, occurring during hyperextension, when the anterior arch is shorn off, anteriorly displaced, and fragmented by the odontoid process. It is unstable and can be accompanied by atlanto-occipital dissociation and posterior displacement of the cranium relative to the cervical spine.

References

1 Babak KS. Fractures of the C1 and C2 vertebrae. *Semin Spine Surg* 2013;25:23–35.

2 Pratt H, Davies E, King L. Traumatic injuries of the C1/C2 complex: computed tomographic imaging appearances. *Curr Probl Diagn Radiol* 2008;37:26–38.

3 Mead LB 2nd, Millhouse PW, Krystal J, Vaccaro AR. C1 fractures: a review of diagnoses, management options, and outcomes. *Curr Rev Musculoskelet Med* 2016;9:255–262.

4 Sasaka KK, Decker GT, El-Khoury GY. Horizontal fracture of the anterior arch of the atlas associated with a congenital cleft of the anterior arch. *Emer Radiol* 2006;12:130–132.

5 Mohit AA, Schuster JA, Mirza SK, et al. "Plough" fracture: shear fracture of the anterior arch of the atlas. *AJR* 2003;181:770.

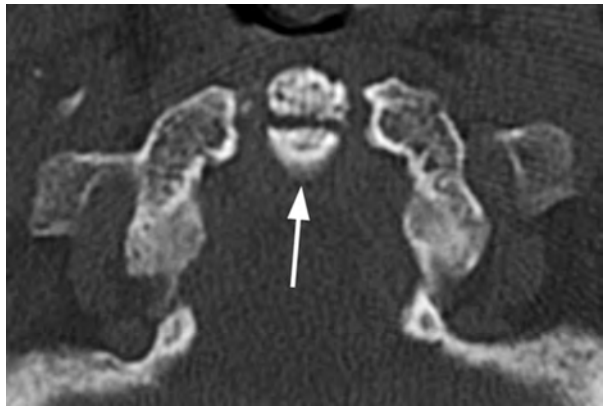

Figure 20.1 Axial CT image demonstrates a fracture of the odontoid tip (arrow) with mild displacement, consistent with type 1 fracture of the odontoid.

(2A)

(2B)

Figure 20.2 Dentocentral synchondrosis remnant is a landmark for odontoid types 2 and 3 fracture differentiation. It is seen as a horizontal line (arrows), hypointense on sagittal T2w MRI (**A**) and partially sclerotic on sagittal CT image (**B**).

Figure 20.3 Midsagittal CT image shows a type 3 odontoid fracture. An oblique fracture line (arrow) is extending through the body of the axis with anterior displacement of the dens.

(4A)

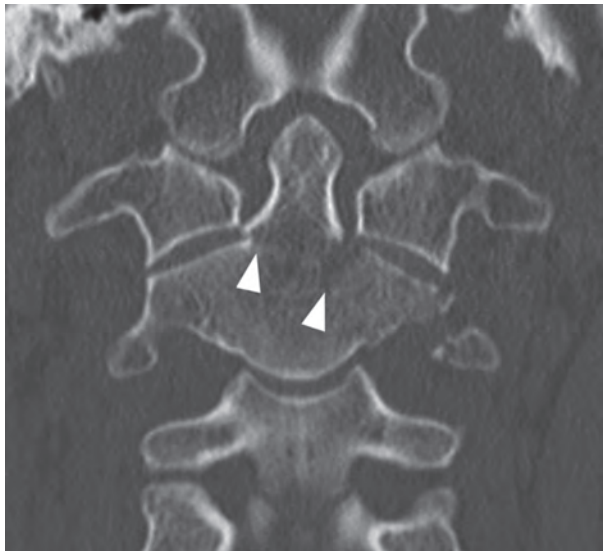

(4B)

Figure 20.4 CT of an unstable type 3 odontoid fracture in a different patient following a fall. The fracture lines (arrowheads) are extending into the body of C2 and left lateral mass with fragment displacement on coronal (**A**) and 3D volume rendered (**B**) images.

CASE 20 Odontoid Fractures Types 1 and 3

Doris Dodig and Abhay Varma

Imaging Findings

Odontoid fracture type 1 is an avulsion fracture of the odontoid tip. It is recognized as a very small bony fragment with irregular and noncorticated margins avulsed from the lateral side of the odontoid tip at the alar ligament attachment. Type 3 odontoid fracture extends from the dens through the body and/or lateral masses of C2 vertebra. Widened prevertebral tissue (>6 mm at C2 level) and disruption of the axis or "Harris" ring on lateral radiographs are the signs of type 3 fracture. Dentocentral synchondrosis remnant is an important anatomical landmark for distinguishing type 2 from type 3 odontoid fractures. It represents the border between the base of the odontoid process and the body of C2 vertebra and is situated below the superior border of C2 lateral masses. It can be seen in the majority of patients as a hypodense horizontal line on sagittal T1- and T2-weighted images, or less commonly as a sclerotic line on sagittal CT images. Fracture orientation angle, fragment dislocation, angulation and comminution, as well as possible additional craniocervical junction injuries should be searched for and evaluated on reformatted CT images to assess fracture stability. Injury to the alar and transverse ligaments, tectal membrane, prevertebral tissues, presence of epidural hematoma, pseudomeningocele, and spinal cord injury are assessed on MRI.

Differential Diagnosis

Persistent Ossiculum Terminale

Nonfused secondary ossification center along the tip of the odontoid process, small bone fragment with smooth corticated margins of disproportionate shape and size to the V-shaped cartilaginous cleft along the subjacent superior margin of the odontoid process.

Os Odontoideum

Well-corticated bone fragment along the superior margin of the odontoid process accompanied by a foreshortened base of the dens and hypertrophied anterior C1 arch.

Clinical Findings, Implications, and Treatment

Odontoid fractures result from both hyperflexion and hyperextension injuries to the cervical spine. They typically occur in young patients involved in a high-energy trauma. In the elderly with osteopenic bone, even a low-energy trauma can fracture the odontoid. Cervical spine CT is recommended as the initial imaging modality due to low sensitivity and specificity of radiography and often very subtle clinical findings. MRI is indicated in patients whose neurological status cannot be assessed and in those with suspected spinal cord or nerve root injury. Type 1 fractures are avulsion fractures involving the apical and alar ligaments. These fractures are stable when at least one alar and the transverse ligament are intact. Most type 1 odontoid fractures are stable and heal well with cervical immobilization. In extreme cases with bilateral alar ligament injury, type 1 odontoid fracture may be associated with atlanto-occipital instability that requires occipitocervical fusion. Type 3 odontoid fractures heal well with cervical immobilization because of large bony contact area and adequate vascular supply. In nondisplaced type 3 fractures, rate of healing, with cervical immobilization, is close to 95%. Risk factors for non-union include fractures that involve the waist of the dens or when there is anterior or posterior displacement. Vertically displaced type 3 fractures are extremely unstable and associated with brainstem and spinal cord injury. Anterior fixation may render best results in younger patients, while posterior spinal fusion may be the treatment of choice in the elderly.

Additional Information

Odontoid fractures in the elderly deserve separate mention because of higher associated mortality and morbidity. Reasons include higher incidence of osteopenia, associated comorbidities, and poor rehabilitation potential. In-hospital mortality can be close to 35% in patients aged >70 years. These patients also tolerate halo-vest immobilization poorly because of impaired cardiopulmonary reserve. Hence many surgeons recommend early surgical treatment of odontoid fractures in the elderly when there is significant risk of non-union.

References

1 O'Brien WT, Shen P, Lee P. The dens: normal development, developmental variants and anomalies, and traumatic injuries. *J Clin Imag Sci* 2015;5:38. doi:10.4103/2156-7514.159565.

2 Mortelmans LJ, Desruelles D, Sabbe MB, Geusens EA. Axis or Harris ring in odontoid fractures, old fashioned but not obsolete. *Eur J Emerg Med* 2009;16:214–216. doi: 10.1097/MEJ.0b013e32831040d8.

3 Keller S, Bieck K, Karul M, et al. Lateralized odontoid in plain film radiography: sign of fractures? A comparison study with MDCT. *RoFo* 2015;187:801–807. doi: 10.1055/s-0035-1553237.

4 Aydin K, Cokluk C. The segments and the inferior boundaries of the odontoid process of C2 based on the magnetic resonance imaging study. *Turk Neurosurg* 2008;18:23–29.

5 Guan J, Bisson EF. Treatment of odontoid fractures in the aging population. *Neurosurg Clin N Am* 2017;28:115–123. doi: 10.1016/j.nec.2016.07.001.

(1A)

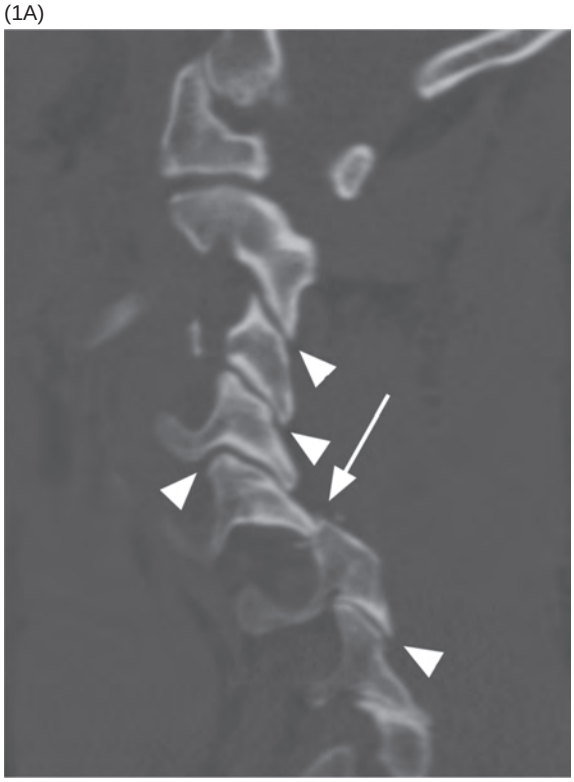

(1B)

Figure 21.1 **A)** Sagittal CT image shows dislocated locked C5 facet with adjacent small fracture fragments (arrow). Note appropriate alignment of other facet joints (arrowheads). **B)** Mediosagittal CT image demonstrates C5 anterolisthesis (arrowhead) and widening of the C5–C6 interspinous and intralaminar space (arrow).

(2A)

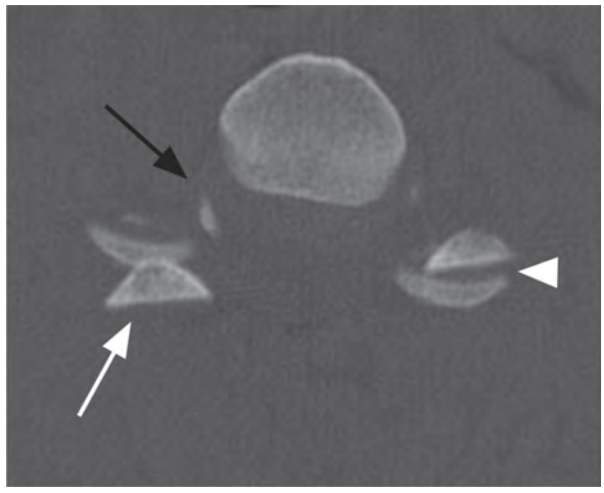

(2B)

Figure 21.2 **A)** Axial CT image in a different patient reveals the "reverse hamburger" sign on the right (white arrow) with opposing convex cortical surfaces, consistent with unilateral locked facets. Note the normal relationship of the adjacent flat articular surfaces on the left side (arrowhead), resembling a hamburger bun. There is also malalignment of the right uncovertebral joint (black arrow) with rotation and widening of the joint space. **B)** Coronal CT shows misalignment of the right C4–C5 uncovertebral joint (arrow). The uncovertebral process appears to be missing on this image. Compare to the normal contralateral (arrowhead) and bilateral uncovertebral joints at other levels.

CASE 21 Unilateral Facet Dislocation

Zoran Rumboldt

Imaging Findings

Axial CT images show unilateral "reverse hamburger" (originally "reverse hamburger bun") sign with the convex nonarticular surfaces facing each other, in contrast to the normal approximation of flat articular surfaces. Ipsilateral uncovertebral malalignment is another reliable sign on axial or coronal images. Midsagittal CT images demonstrate anterolisthesis of the superior vertebra along with widening of the interlaminar and interspinous space. More lateral CT images are the key, as they directly show the locked facets, in contrast to the normal alignment of other ipsi- and contralateral facet joints (similar to shingling on a roof). Associated small fracture fragments may also be present. Spinous processes of the involved vertebra and those above are rotated toward the side of the lock. The images should be scrutinized for fractures involving the adjacent pedicles, laminae, and articular pillars. MRI may reveal associated injuries to the ligaments, spinal cord, and vertebral artery.

Differential Diagnosis

Bilateral Facet Dislocation

Locked facets are present on both sides.

Fractured Articular Pillar (Facet Fracture)

Small fracture fragments are frequently found with unilateral facet lock; however, the fracture does not extend through the entire articular pillar.

Flexion Sprain

Widening of the interspinous space with possible mild subluxation but without facet joint dislocation.

Clinical Findings, Implications, and Treatment

These patients typically present with neck pain, sometimes associated with radiculopathy, while spinal cord injury is uncommon. The injuries are mostly stable but require prompt stabilization and treatment. Closed traction-reduction followed by anterior fusion (ACDF) or posterior instrumented fusion (with or without preoperative closed traction-reduction) is an effective treatment. Combined anterior and posterior surgical approach with fusion is commonly performed in patients with spinal cord injury. Following appropriate treatment, neurological deficits improve or resolve in a majority of affected individuals.

Additional Information

The mechanism of this injury is a combination of lateral flexion and distraction. Although facet dislocation most commonly occurs in the lower cervical region, it may affect any spinal level, all the way to the lumbosacral junction. Patients with cervical facet dislocation and spinal cord injury (SCI) tend to present with a more severe degree of initial trauma and display less potential for motor recovery, compared to SCI patients without facet dislocation. Facet dislocations without fractures have a significantly higher association with cord syndromes than do facet injuries with fractures. A rare case of unilateral facet dislocation as a preexisting lesion, possibly originating from a forceps delivery at birth, has been described, with full clinical recovery following conservative approach.

References

1 Daffner SD, Daffner RH. Computed tomography diagnosis of facet dislocations: the "hamburger bun" and "reverse hamburger bun" signs. *J Emerg Med* 2002;23:387–394.

2 Palmieri F, Cassar-Pullicino VN, Dell'Atti C, et al. Uncovertebral joint injury in cervical facet dislocation: the headphones sign. *Eur Radiol* 2006;16:1312–1315.

3 Wilson JR, Vaccaro A, Harrop JS, et al. The impact of facet dislocation on clinical outcomes after cervical spinal cord injury: results of a multicenter North American prospective cohort study. *Spine (Phila Pa 1976)* 2013;38:97–103. doi: 10.1097/BRS.0b013e31826e2b91.

4 De Jong RJ, Vreeling AW, Van Susante JL. Unilateral facet dislocation: always reduce? *Acta Orthop Belg* 2012;78:808–810.

5 Blecher R, Geftler A, Anekstein Y, Mirovsky Y. Isolated unilateral facet dislocation of the lumbosacral junction. *J Bone Joint Surg Br* 2010;92:1456–1459. doi: 10.1302/0301-620X.92B10.24718.

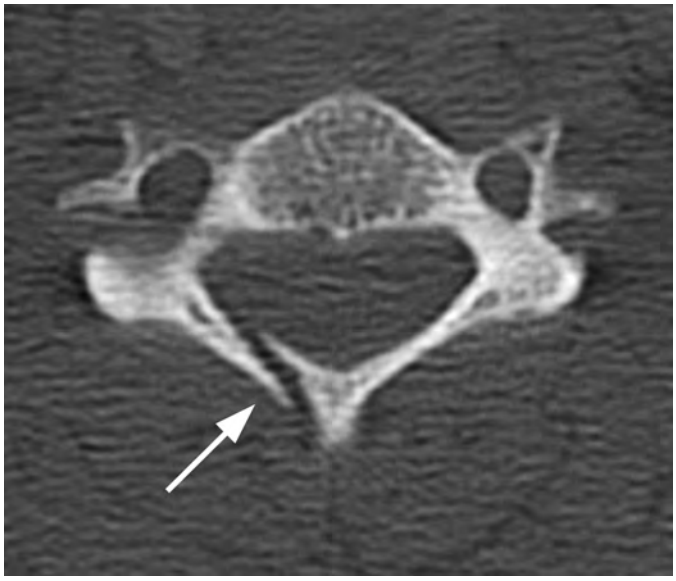

Figure 22.1 Axial CT image shows a minimally displaced oblique fracture of a cervical right lamina (arrow).

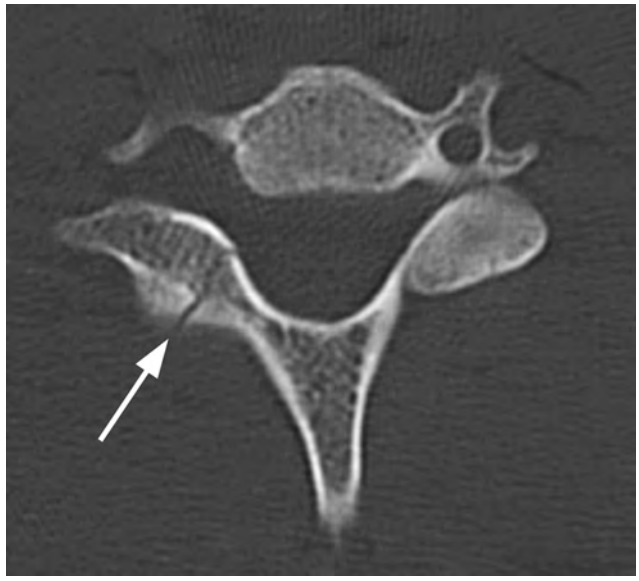

Figure 22.2 Axial CT image demostrates a nondisplaced fracture (arrow) through the anterior portion of the right C6 lamina.

(3A)

(3B)

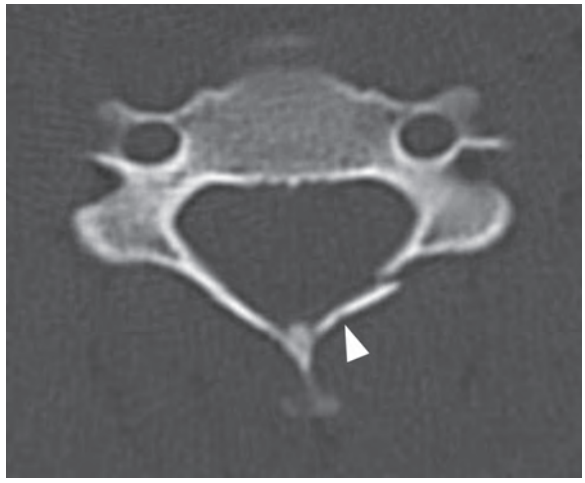

Figure 22.3 A) Sagittal CT image in a patient following cervical spine trauma reveals a fracture of the left C5 lamina (arrow). The fracture is clearly depicted, although it is partially obscured by the beam hardening streak artifact from the shoulder girdle. **B)** Axial CT image shows that there are actually two fracture lines: a complete one more anteriorly and a greenstick type more posteriorly (arrowhead). There were no additional fractures in this patient.

CASE 22 Isolated Fracture of the Lamina

Zoran Rumboldt

Imaging Findings

Radiographs show disruption of the spinolaminar line, while CT directly reveals fracture of the lamina, which is usually best seen in the axial plane. Laminae lesion may be complete or of the greenstick type (incomplete, the fracture line does not extend through the entire thickness of the bone). The fracture line may extend to the spinous process and/or contralateral lamina, articular pillar/facet joint, and transverse process/transverse foramen, which should be carefully searched for as the presence of those lesions excludes an isolated laminar fracture and is indicative of a more serious injury. Depressed fractures of the lamina may be associated with spinal cord injury.

Differential Diagnosis

Burst Fracture with Laminar Fracture

Obvious additional fracture(s) with compression of the vertebral body and retropulsion of fragment(s) into the spinal canal, frequent associated ligamentous injury.

Retroisthmic Cleft

Typically found in the lumbar spine, the defect in the lamina is of smooth appearance, sclerotic margins are usually associated with bony overgrowth.

Clinical Findings, Implications, and Treatment

Isolated fractures of the lamina have been described in all age groups, including infants. These fractures usually occur after a hyperextension injury, and the patients typically present without any neurologic compromise. Isolated fracture of the lamina caused by direct trauma to the posterior neck may, however, lead to a significant neurologic deficit, which needs to be treated surgically with posterior decompression.

Additional Information

Isolated laminar fractures, typically involving the cervical spine, are often missed on radiographs and had been considered very uncommon. However, with modern CT scanners, these lesions are now documented more frequently.

On the other hand, laminar fractures are commonly associated with burst fractures. In upper lumbar burst fractures, complete lamina fracture is an indicator of injury severity, frequently accompanied by dural tears and nerve root entrapment. Open-book laminectomy has been therefore recommended, even if the patient is neurologically intact.

"Spinolaminar breach," or disruption of the spinolaminar line, is a sign on plain films, which indicates a complex spinous process fracture with extension into the lamina and spinal canal. Misdiagnosis of a "clay shoveler's fracture" should be avoided, as spinous process fractures with spinolaminar breach may have associated posterior ligamentous injury, which carry a significant potential for delayed instability and neurological deficit.

References

1 Robles LA. Isolated cervical depressed laminar fracture in a child. Case report and review of the literature. *J Neurosurg* 2006;105(6 Suppl):496–498.

2 Hähnle UR, Nainkin L. Traumatic invagination of the fourth and fifth cervical laminae with acute hemiparesis. *J Bone Joint Surg Br* 2000;82:1148–1150.

3 Makan P. Neurologic compromise after an isolated laminar fracture of the cervical spine. *Spine (Phila Pa 1976)* 1999;24:1144–1146.

4 Matar LD, Helms CA, Richardson WJ. "Spinolaminar breach": an important sign in cervical spinous process fractures. *Skeletal Radiol* 2000;29:75–80.

5 Skiak E, Karakasli A, Harb A, et al. The effect of laminae lesion on thoracolumbar fracture reduction. *Orthop Traumatol Surg Res* 2015;101:489–494. doi: 10.1016/j.otsr.2015.02.011.

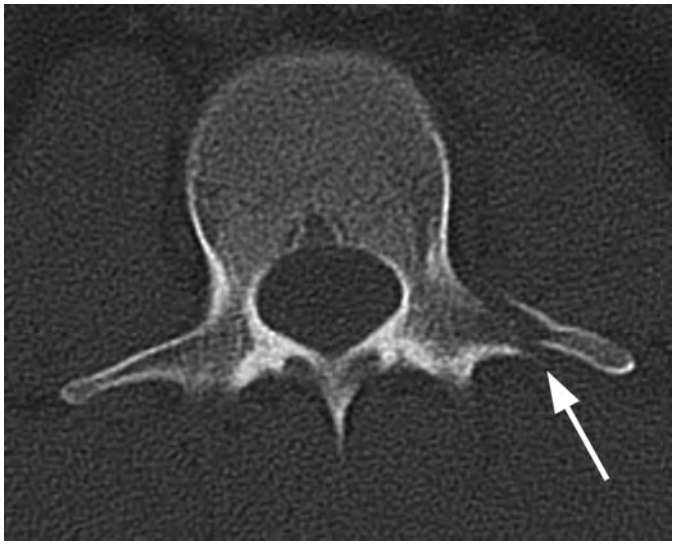

Figure 23.1 Axial CT image shows a displaced fracture (arrow) of the left transverse process of L1 vertebra. There was an additional left L2 transverse process fracture, without other spine injuries.

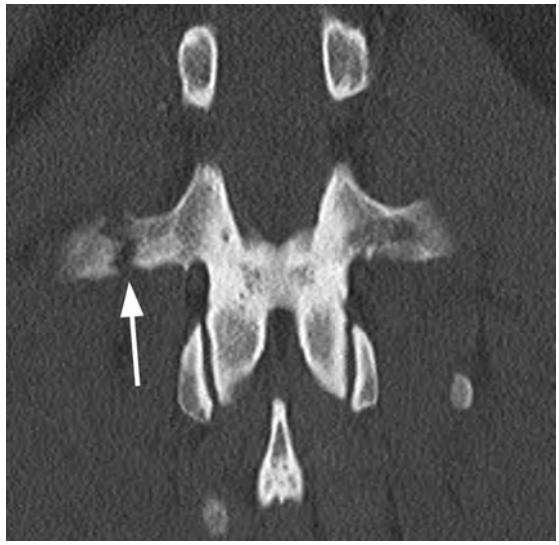

Figure 23.2 Coronal CT image in a different patient reveals a right transverse process fracture (arrow) of a lower thoracic vertebra.

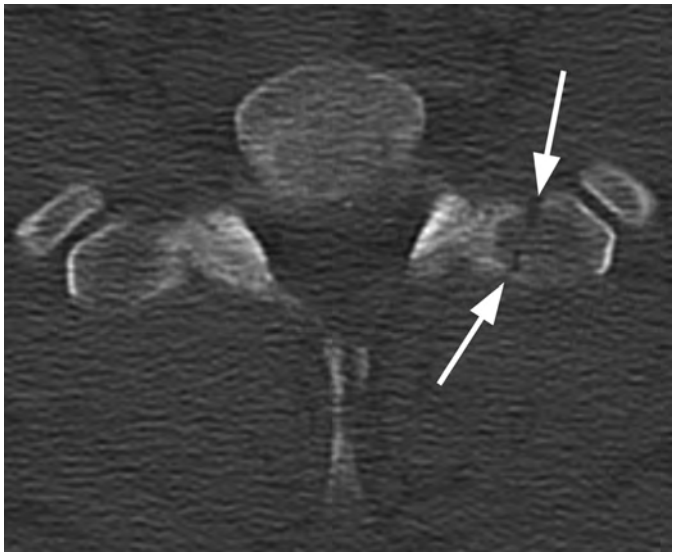

Figure 23.3 Axial CT image in a patient following MVA demostrates a nondisplaced transverse process fracture (arrow) of the first thoracic vertebra.

Figure 23.4 Coronal CT image in a different patient reveals left transverse process fractures (arrowheads) of the C7 vertebra. There were no other spine fractures. The patient, however, had additional chest injuries, including multiple rib fractures.

CASE 23 Isolated Transverse Process Fracture

Zoran Rumboldt

Imaging Findings

CT is the modality of choice for detection of these fractures, as up to 60% of lumbar transverse process fractures identified on CT will be missed on plain radiographs, primarily the nondisplaced ones. CT readily identifies these fractures, even on just axial images, as lucent lines without sclerotic margins, usually with irregular jagged edges. These injuries most frequently occur in the upper lumbar spine and are commonly multiple. Fractures of transverse processes in the thoracic and lumbar spine are clinically insignificant on their own, but they are associated with structurally unstable thoracolumbar spine fractures in 10–20% of patients. Plain radiographs miss these additional unstable thoracolumbar bony injuries in about 10% of cases. Upper thoracic and L5 fractures may be associated with rib and pelvic fractures, respectively. Also, transverse process fractures typically occur with high-energy blunt traumas, often resulting in associated injury of other organs, which should be carefully searched for.

Fracture of transverse process in the cervical spine is of special significance, as the fracture may extend into the transverse foramina, indicating possible vertebral artery injury. Cervical transverse process fractures also have a strong association with other cervical spine fractures and blunt cerebrovascular injury.

Differential Diagnosis

Secondary Ossification Center

Smooth corticated margins, at the tip of the transverse process with a somewhat rounded appearance.

Chronic Transverse Process Fracture

Sclerotic margins, with a smooth appearance instead of at least somewhat irregular edges.

Clinical Findings, Implications, and Treatment

The most common mechanism of injury is motor vehicle accident (MVA), followed by falls. MVAs appear to be more commonly the cause in pediatric patients, while falls are more frequent cause in adults. Patients with isolated transverse process fractures (not involving the transverse foramina in the cervical spine) do not present with neurological deficit.

These fractures can be treated conservatively without concern for long-term outcome sequelae such as pain, neurologic deficits, or ambulatory difficulties. Management strategies involve unrestricted movement, bracing, and orthotics.

Additional Information

Acute traumatic isolated transverse process fractures are increasingly identified in traumatized patients due to the increased routine use of CT in trauma. While theses lesions are common sequelae of trauma and considered a minor and stable fracture in the lumbar and thoracic spine, there is strong association between these fractures and other traumatic injuries. Approximately 10–50% of patients with lumbar transverse process fractures have hepatic and splenic as well as genitourinary and diaphragmatic injuries.

References

1 Patten RM, Gunberg SR, Brandenburger DK. Frequency and importance of transverse process fractures in the lumbar vertebrae at helical abdominal CT in patients with trauma. *Radiology* 2000;215:831–834.

2 Boulter JH, Lovasik BP, Baum GR, et al. Implications of isolated transverse process fractures: is spine service consultation necessary? *World Neurosurg* 2016;95:285–291. doi: 10.1016/j.wneu.2016.08.027.

3 Nagasawa DT, Bui TT, Lagman C, et al. Isolated transverse process fractures: a systematic analysis. *World Neurosurg* 2017;100:336–341. doi: 10.1016/j.wneu.2017.01.032.

4 Lombardo G, Petrone P, Prabhakaran K, Marini CP. Isolated transverse process fractures: insignificant injury or marker of complex injury pattern? *Eur J Trauma Emerg Surg* Dec 2, 2016 [Epub ahead of print]

5 Carr RB, Fink KR, Gross JA. Imaging of trauma: part 1, pseudotrauma of the spine – osseous variants that may simulate injury. *AJR Am J Roentgenol* 2012;199:1200–1206. doi: 10.2214/AJR.12.9083.

Figure 24.1 Sagittal CT image demonstrates a horizontal nondisplaced C7 spinous process fracture (arrowhead).

Figure 24.2 Midsagittal CT image shows C7 spinous process fracture with displaced distal fragment (arrowhead).

(3A)

(3B)

Figure 24.3 **A)** Sagittal CT image shows multiple spinous process fractures, which may be an indicator of more severe injuries. Anteriorly increased C5–C6 disc space and a probable fracture of the osteophyte are suggestive of hyperextension and anterior longitudinal ligament injury. Note ossification of the nuchal ligament (arrow). **B)** Axial CT image at C5 level reveals that the spinous process fracture is comminuted (arrowheads).

CASE 24 Isolated Spinous Process Fractures

Doris Dodig

Imaging Findings

Isolated fractures of the spinous process most commonly occur in the lower cervical and upper thoracic spine. A double spinous process shadow is a sign of spinous process fracture on anteroposterior radiographs, while a downward displacement of a bony fragment or a breach of the spinolaminar line can be detected on lateral x-rays. Nevertheless, a spinous process fracture can be missed on plain films, primarily nondisplaced fractures and those that are superimposed over ribs. CT is more sensitive for diagnosing bone fractures, especially small bone fragments. MRI enables precise evaluation of bone marrow and soft tissue, including ligamentous injury.

Differential Diagnosis

Pseudoarthorsis Due to a Non-Union Spinous Process Fracture

Bone fragment with well-corticated margins adjacent to the spinous process, no signs of bone marrow edema, ligamentous or paraspinal soft tissue injury on MRI.

Ossification of the Nuchal Ligament

Well-corticated oval to elongated ossicle located within the nuchal ligament in a craniocaudal orientation, posterior to the spinous processes.

Clinical Findings, Implications, and Treatment

Injury mechanism of the isolated spinous process fracture can be an avulsion due to increased shear forces of the attached ligaments and muscles, direct blow to the flexed neck or back, hyperflexion or hyprextension injury, and a stress fracture, recently more commonly recognized in weightlifters, golfers, jockeys, and other athletes. Patients typically present with neck or back pain without neurologic deficits, and severe tenderness with or without crepitation over the tips of the affected spinous processes. History of significant traumatic event may be negative, especially in cases of stress fractures; however, a typical clinical presentation should raise suspicion and prompt further imaging. Spinous process fractures are stable and do not cause any neurological damage on its own. However, multiple fractures might be an indicator of more severe injuries to the spine or surrounding tissues and organs. Isolated spinous process fractures are treated conservatively with immobilization and restriction of physical activity for 4–6 weeks. Treatment results are very good in terms of pain relief and range of motion despite a high incidence of non-union. Pseudoarthrosis develops often and is usually asymptomatic. However, if pain associated with pseudoarthrosis persists longer than 10 weeks, surgical removal of the non-united bone fragment is indicated.

Additional Information

Isolated fractures of the lower cervical and upper thoracic spine were first described in 1933 as "clay shoveler's fracture" among hard-labor workers in Australia, who tossed clay from the ditches with long-handled shovels over their shoulders. The clay sometimes stuck to the shovel, producing a sudden, unexpected opposite force to the neck and back muscles, causing an avulsion fracture at the attachment site on the spinous processes.

References

1 Lee S, Park MS, Kim YC, Kim TH. Osteoporotic thoracolumbar junctional fracture accompanied by spinous process fracture without posterior ligament injury: its clinical and radiologic significances. *Eur Spine J* 2016;25:3478–3485.

2 Han SR, Sohn MJ. Twelve contiguous spinous process fracture of cervicothoracic spine. *Korean J Spine* 2014;11:212–213.

3 Fayyazi AH, Segal L. Surgical excision of symptomatic lumbar spinous process pseudoarthrosis. *J Spinal Disord Tech* 2004;17:439–441.

(1A)

(1B)

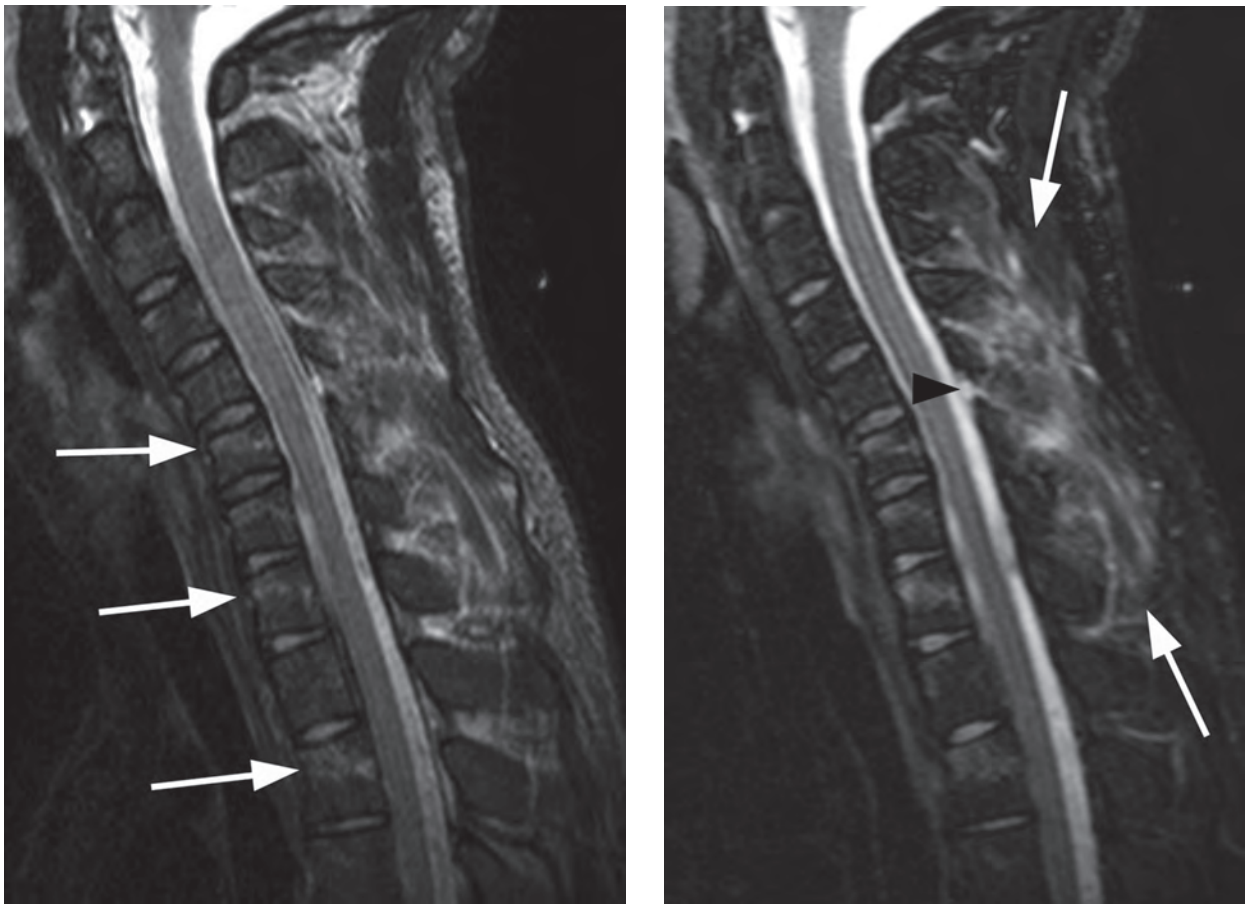

Figure 25.1 Multiple vertebral body microfractures (VBMFs) demonstrated by MRI in a patient with acute cervico-thoracic hyperflexion injury. **A)** Midsagittal T2-weighted image shows linear horizontal hyperintense bone bruises in several cervical and thoracic vertebral bodies (arrows), reflecting axial load trauma at this level. **B)** Corresponding STIR image shows the bone contusions to a better advantage and especially the hyperintense signal indicative of injury to the posterior ligaments (arrows), including disruption of C5–C6 ligamentum flavum (arrowhead).

(2A)

(2B)

(2C)

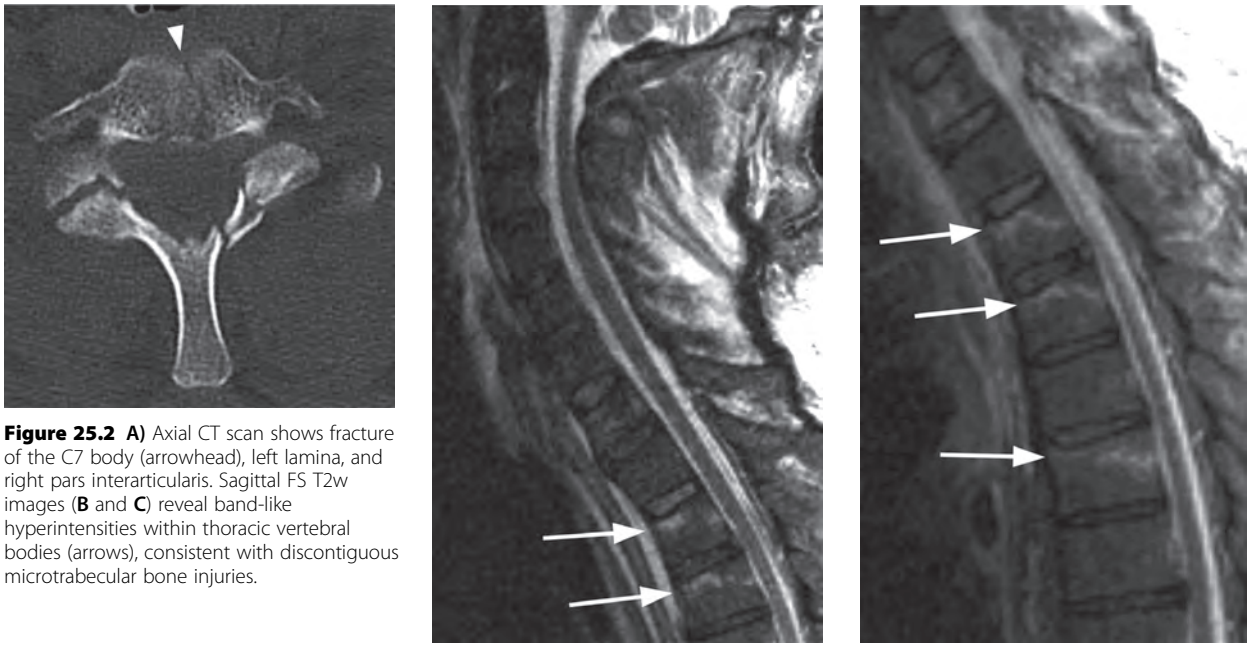

Figure 25.2 A) Axial CT scan shows fracture of the C7 body (arrowhead), left lamina, and right pars interarticularis. Sagittal FS T2w images (**B** and **C**) reveal band-like hyperintensities within thoracic vertebral bodies (arrows), consistent with discontiguous microtrabecular bone injuries.

CASE 25 Vertebral Body Microfractures / Bone Marrow Edema

Emanuele Pravatà

Imaging Findings

Occult vertebral body microfractures (VBMFs), deriving from compression injury, osteoporosis, and/or chronic stress mechanisms, may be disclosed by MRI when no vertebral height loss and/or apparent fracture lines are apparent on CT images. Increased water content of bone marrow edema within the injured vertebral bodies is best detected by T2-weighted sequences with fat suppression (short-tau-inversion-recovery – STIR or Fat Saturated – FS sequences). These microfractures (also known as vertebral bone bruises, microtrabecular bone injuries, and bone contusions) typically appear as horizontal hyperintense bands within vertebral bodies, which may or may not be parallel to the endplates. The areas of bone marrow edema may be larger, involving the entire vertebral body and even extend into the posterior elements. In patients with known spinal injury (fracture and/or dislocation), these microfractures are commonly found at other, contiguous as well as noncontiguous remote spinal levels in relation to the primary injury.

VBMFs in patients with osteoporosis may occur with no obvious trauma. While vertebral body compression fractures reliably generate bone marrow edema, this is not the case with acute fractures without compression. Absence of marrow edema can therefore lead to a false negative MRI in these cases.

Differential Diagnosis

Inflammatory

Spondylodiscitis: usually at the endplates with disk T2 hyperintensity and contrast enhancement (acute fractures may also enhance), disk and paravertebral tissue enhancement, and/or abscess formation (rim-enhancing fluid collection).

Tumor

Horizontal linear appearance is highly unusual; mass effect/cortical bone expansion, extravertebral spread, posterior vertebral wall, and joints are less frequently involved by posttraumatic edema; lytic and/or sclerotic features may be present on CT.

Clinical Findings, Implications, and Treatment

Secondary microfractures at contiguous and noncontiguous levels in patients with known traumatic spine injury generally do not require specific treatment. In patients with symptomatic vertebral body fractures, the demonstration of bone marrow edema on MRI, reflecting a recent/nonconsolidated collapse, is an important selection criterion for cement augmentation treatment.

Additional Information

Although STIR and FS T2w sequences are both sensitive to marrow edema, FS T2w images are more prone to artifacts from failure to appropriately saturate areas close to metallic hardware and at the acquisition volume borders to magnetic field inhomogeneity in general.

A higher frequency of secondary vertebral body injury is detected by MRI than with other radiographic whole spine evaluations, enabling increased confidence in the management of patients with severe spinal injury.

References

1 Provenzale J. MR imaging of spinal trauma. *Emerg Radiol* 2007;13: 289–297.

2 Qaiyum M, Tyrrell PN, McCall IW, Cassar-Pullicino VN. MRI detection of unsuspected vertebral injury in acute spinal trauma: incidence and significance. *Skeletal Radiol* 2001;30: 299–304.

3 Green RA, Saifuddin A. Whole spine MRI in the assessment of acute vertebral body trauma. *Skeletal Radiol* 2004;33:129–135.

4 Brinckman MA, Chau C, Ross JS. Marrow edema variability in acute spine fractures. *Spine J* 2015;15:454–460. doi: 10.1016/j.spinee.2014.09.032.

5 Nakatsu M, Hatabu H, Itoh H, et al. Comparison of short inversion time inversion recovery (STIR) and fat-saturated (chemsat) techniques for background fat intensity suppression in cervical and thoracic MR imaging. *J Magn Reson Imaging* 2000;11:56–60.

(1A)

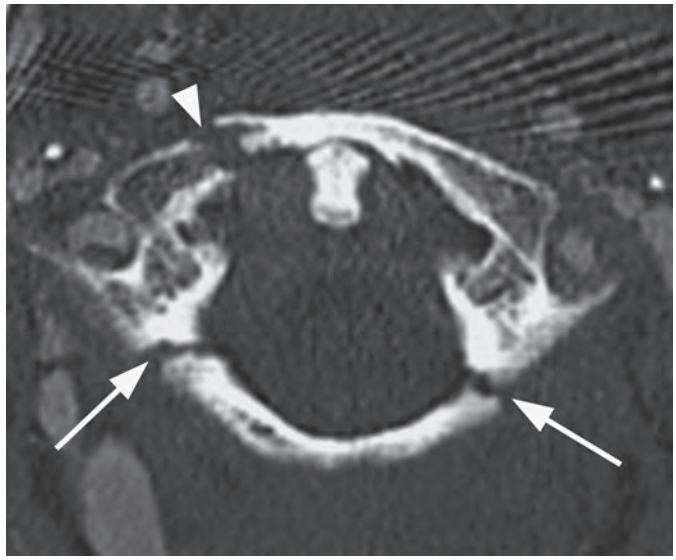

(1B)

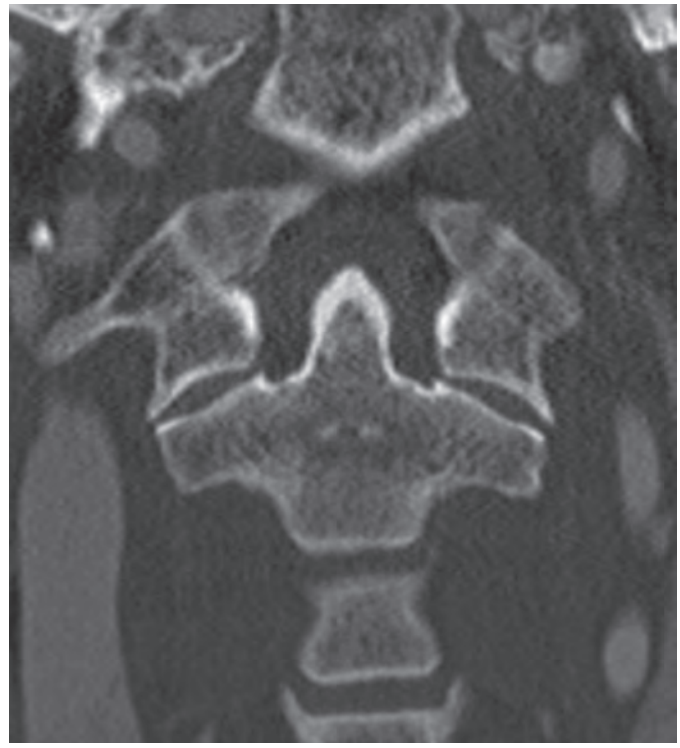

Figure 26.1 **A)** Axial CT image shows fractures of the right anterior arch (arrowhead) and bilateral posterior arches (arrows) of the atlas. Note that the atlanto-dental interval is normal, measuring <3 mm. Fractures of the posterior arches are just posterior to the lateral masses. **B)** Coronal CT shows a normal relationship between the lateral masses of C1 and C2. The atlanto-occipital joints are difficult to see because of obliquity, but the biconcave inwardly sloping wedge appearance of the C1 lateral masses is noted. This causes a centrifugal force when the atlas is loaded axially.

(2A)

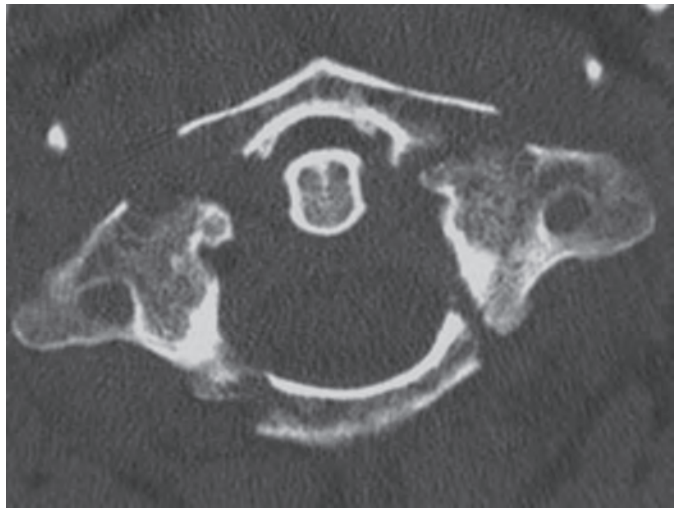

(2B)

Figure 26.2 **A)** Axial CT image demonstrates fractures of the anterior and posterior arches of C1. The atlanto-dental space is increased, measuring 5 mm. **B)** Coronal CT image shows outward displacement of the lateral masses of C1 relative to C2 (arrows) measuring 6 mm on the right and 4 mm on the left. A fracture on the right between the dens and atlas (arrowhead) is consistent with a bony avulsion of the transverse ligament from C1. An additional more superior fracture on the right adjacent to the occipital condyle is consistent with an alar ligament avulsion.

CASE 26 Jefferson Burst Fractures of the Atlas

Russel Chapin

Imaging Findings

Burst fractures of the atlas involve both the anterior and posterior arches and are considered type II within the Landells and Van Peteghem classification scheme. While all atlas fractures were classically described by Sir Geoffrey Jefferson, it is best to reserve the description Jefferson exclusively for burst injuries. These are to be distinguished from type I fractures of the atlas, which involve the anterior or posterior arch alone, or type III fractures, which involve the lateral mass of C1.

Despite primarily nonoperative treatment, the integrity of the transverse ligament is central to management of Jefferson fractures. Dickman type I injuries of the transverse ligament involve a midsubstance tear or non-bony avulsion from C1, while type II transverse ligament injuries involve avulsion of bone. On CT, an atlanto-dental interval of >3 mm or combined overhang of 7 mm of the lateral masses of C1 relative to C2 are consistent with transverse ligament disruption. The utility of these criteria has been questioned, and MRI dedicated to evaluation of the transverse ligament has been advocated.

Differential Diagnosis

Isolated Anterior or Posterior Arch Fractures or Lateral Mass Fractures of C1

Non-Fusion Variants of C1

Clinical Findings, Implications, and Treatment

More than 80% of C1 fractures are due to motor vehicle accidents or falls. Presentation is with neck pain and decreased range of motion. Neurologic injury secondary to cord compromise is uncommon with Jefferson fractures due to outward displacement of fracture fragments. However, approximately 40% of all C1 fractures are accompanied by C2 fractures, placing the patient at a greater risk for cord injury. While pain and neuropathy related to the C2 nerve are common, inferior cranial nerve injuries are not.

Stability of isolated Jefferson fractures is primarily based on the status of the transverse ligament. An atlanto-dental interval of >3 mm or lateral mass atlanto-axial combined overhang of >7 mm is consistent with transverse ligament tear and instability. Additionally, Dickman type I ligament injuries (substance tears) heal poorly compared to type II (bony avulsion) injuries. The decision to evaluate the transverse ligament directly via MRI is based on CT findings suggesting instability and the level of clinical suspicion, which incorporates the mechanism of injury. Most Jefferson fractures are treated with rigid cervical collar stabilization for 10–12 weeks with follow-up flexion-extension radiographs for instability. Unstable fractures are usually treated with halo fixation, C1–C2 posterior screw fixation, or occipital-cervical fusion. Recent studies have highlighted the morbidity of halo fixation, particularly in elderly patients, furthering the trend of C1–C2 fixation for unstable Jefferson fractures and rigid collar use for stable fractures.

Additional Information

While all fractures of C1 are associated with some degree of an axial force, the type II burst injury is due to the most direct compression from a blow to the vertex of the skull (vertical compression). On coronal images, the lateral masses of C1 are anatomically wedge-shaped sloping inward. Therefore, an axial loading injury is translated to a centrifugal force, with the bony ring failing due to distraction. Failure most typically occurs in the arches just anterior or posterior to the lateral masses. When internal fixation is considered, the indentation caused by the horizontal lateral-medial course of the vertebral artery over the posterior arch as well as the possibility of a ponticulus posticus variant must be taken into account.

References

1 Ryken TC, Aarabi B, Dhall SS, et al. Management of isolated fractures of the atlas in adults. *Neurosurgery* 2013; 72(2 Suppl):151–158. doi: 10.1227/NEU.0b013e31827 6ee55.

2 Kakarla UK, Chang SW, Theodore N, Sonntag VK. Atlas fractures. *Neurosurgery* 2010;66(3 Suppl):60–67. doi: 10.1227/01.NEU.0000366108.02499.8F.

3 Haus BM, Harris MB. Case report: nonoperative treatment of an unstable Jefferson fracture using a cervical collar. *Clin Orthop Relat Res* 2008;466:1257–1261.

4 Shatsky J, Bellabarba C, Nguyen Q, Bransford RJ. A retrospective review of C1 ring fractures – does the transverse atlantal ligament (TAL) really matter? *Spine J* 2016;16:372–379.

(1A)

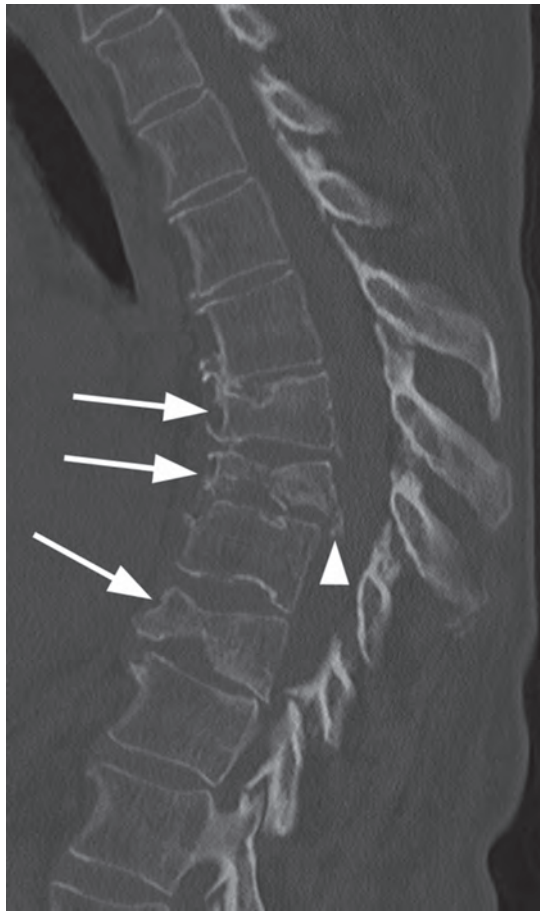

(1B)

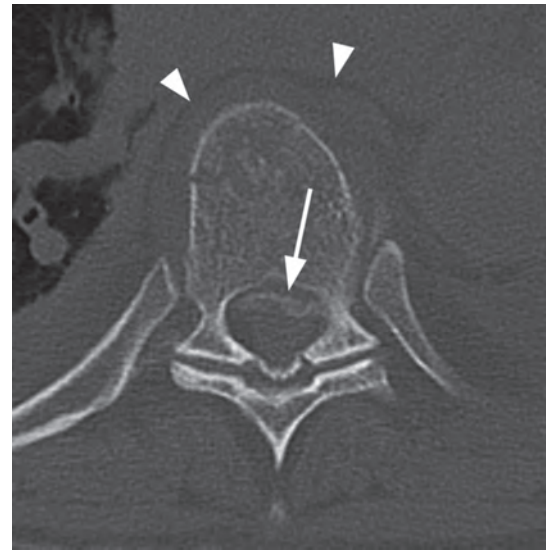

Figure 27.1 **A)** Sagittal CT image shows multiple compression fractures in the lower thoracic spine (arrows). There is retropulsion of fragments into the spinal canal with at least one of the fractures (arrowhead), consistent with a burst fracture. **B)** Axial CT through that level clearly demonstrates the fracture fragment within the spinal canal (arrow). There is also perivertebral hematoma (arrowheads).

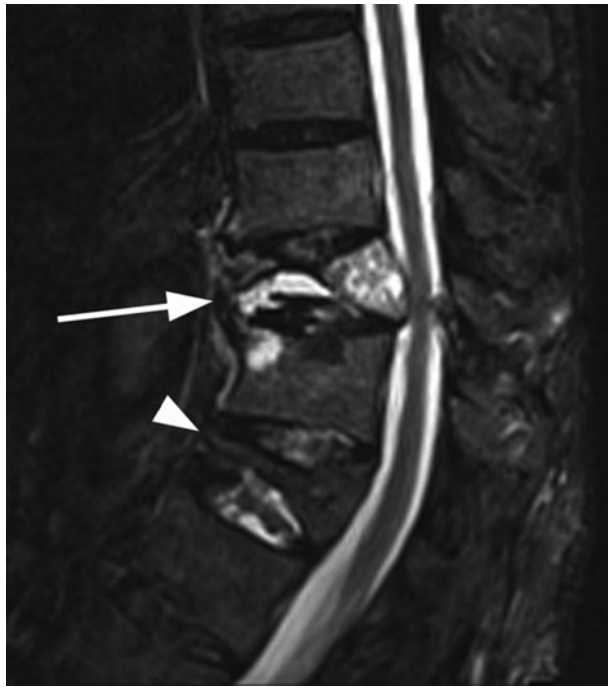

Figure 27.2 Midsagittal STIR MR image shows an acute burst fracture of T10 vertebral body (arrow) and a chronic compression of T12 (arrowhead). Possible spinal cord compression and posterior ligamentous injury.

Figure 27.3 Midsagittal T2-weighted MRI in another patient shows burst fracture of L1 vertebral body with retropulsion of the fractured superior posterior corner (arrow) into the spinal canal. The fracture is compressing the conus medullaris; intramedullary edema is present more superiorly. There is also edema in the posterior soft tissues with possible disruption of the posterior ligamentous complex.

CASE 27 Burst Fractures (Other Than Jefferson Fracture)

Hrvoje Vavro and Zoran Rumboldt

Imaging Findings

These injuries are usually found at the thoracolumbar junction – *transition zone* (T11–L1). There is loss of vertebral height, more in the anterior part; the fracture always involves posterior vertebral body cortex, so that the anterior and middle vertebral columns are always affected. There is a burst appearance of the vertebral body on axial CT, often with sagitally oriented fracture line. Retropulsion of the posterior vertebral body fragments is a characteristic finding, usually the superior posterior corner. Interpedicular widening is best seen on AP radiographs and CT images reconstructed in coronal plane. MRI demonstrates band-like marrow edema surrounding the fracture line, best seen in fat-suppressed T2-weighted images, and may also show spinal cord contusion and/or epidural hematoma.

Differential Diagnosis

Wedge Fracture, (Simple) Compression Fracture

Posterior vertebral body cortex and posterior column elements are intact, without retropulsion into the spinal canal; less than 40% loss of vertebral body height in patients with normal bone density.

Chance Fracture

Anterior wedge fracture with extension of the fracture horizontally through posterior elements or separation of facet joints and spinous processes, possibly also retropulsion of posterior cortex ("burst-Chance" fracture); this is a distraction injury.

Fracture-Dislocation

Spondylolisthesis, due to shearing or distraction, usually with MR evidence of anterior and posterior longitudinal ligament injury.

Pathologic Fracture Due to Tumor Infiltration

Usually compression fracture, rounded area of abnormal appearance on MRI, possibly epidural or paraspinal mass and involvement of other vertebrae.

Butterfly Vertebra

Well-corticated congenital vertebral malformation, no history of trauma.

Clinical Findings, Implications, and Treatment

The common mechanism of injury is fall from height on feet, resulting in excessive axial loading and driving an intervertebral disc into the adjacent vertebral body. Thoracolumbar junction is most frequently affected due to the difference in mobility of ribcage-stabilized rigid thoracic spine and relatively mobile lumbar segments. Back pain is the main presenting symptom. Retropulsion of fragments may cause spinal cord injury, and up to 30% of patients have some degree of neurologic deficit. Radiological report should include the percentage of spinal canal stenosis, assessment of kyphosis angle, and presence of interspinous widening. The *Thoracolumbar Injury Classification and Severity Score* (TLICS) takes into account three major parameters: injury morphology, integrity of the posterior ligametous complex, and neurologic status of the patient. Surgical treatment is necessary in case of progressive neurological loss, unstable fractures with complete neurological loss, or polytrauma. In case of intact neurology, the opinions differ. The usual treatment is conservative, with initial bed rest and subsequent application of extension cast or brace and early mobilization. The degree of spinal canal stenosis seems to be less important, as most of stenoses significantly regress over period of one year due to resorption of retropulsed bony fragments. The neurological deficits are thought to be a consequence of initial injury rather then later continuous cord compression. Integrity of the posterior ligamentous complex seems to be a positive predictive factor for neurological recovery.

Additional Information

Burst fracture is more severe (assigned 2 points in TLICS classification) than a simple compression fracture (1 point), the differentiating feature being fracture of the posterior vertebral body cortex with retropulsion of fragments into the spinal canal. Distraction fracture (such as Chance fracture) is even more severe (4 points) with disruption of all 3 columns.

References

1 Rajasekaran S. Thoracolumbar burst fractures without neurological deficit: the role for conservative treatment. *Eur Spine J* 2010;19(Suppl 1):40–47. doi: 10.1007/s00586-009-1122-6.

2 Heary RF, Kumar S. Decision-making in burst fractures of the thoracolumbar and lumbar spine. *Indian J Orthop* 2007;41:268–276. doi: 10.4103/0019-5413.36986.

3 Alpantaki K, Bano A, Pasku D, et al. Thoracolumbar burst fractures: a systematic review of management. *Orthopedics* 2010;33:422–429. doi: 10.3928/01477447-20100429-24.

(1A)

(1B)

Figure 28.1 **A)** Midsagittal reformatted CT image shows a dens fracture type 2 (arrowheads) with mild diastasis. **B**) Corresponding STIR MR image shows interspinous ligament edema (arrow) and a prevertebral fluid collection (arrowhead) indicating anterior longitudinal ligament injury. Note that there is no evidence of bone marrow edema with this extension injury.

Figure 28.2 Sagittal CT image shows a dislocated dens fracture type 2 with marked posterior dens displacement and encroachment of the spinal canal (arrow).

(3A)

(3B)

Figure 28.3 **A)** Midsagittal CT image shows a dens fracture type 2 with mild angulation and diastasis. **B)** Corresponding STIR image confirms the fracture, without signs of spinal cord injury. There is extensive hyperintensity of the prevertebral and interspinous soft tissues (arrowheads), consistent with ligamentous injury. No evidence of bone marrow edema.

CASE 28 Odontoid Fracture Type 2

Daniela Distefano and Alessandro Cianfoni

Imaging Findings

Odontoid fractures type 2 occur at the base of the dens between the level of the transverse ligament and the C2 vertebral body. On plain radiographs, even on good-quality anteroposterior, lateral, and open-mouth views, the findings may be subtle and lesions may be missed. Multislice CT with multiplanar reconstructions is the modality of choice to demonstrate the fracture, its orientation, and the C1–C2 relationship. Sagittal CT reconstructions are particularly helpful for treatment guidance, as they reveal the angulation of the fractured dens and its anterior or posterior displacement. Coronal and axial CT images are necessary to establish the lateral displacement of the dens from the C1 lateral masses. A thorough search for fracture fragments and associated contiguous and noncontiguous fractures should be performed, as they can change the treatment strategy. CT may depict significant soft tissue abnormalities, but MRI, with T1w and fat-suppressed T2w (STIR or fat-sat T2w) images, is the imaging modality for detection of bone marrow edema, ligamentous injuries, as well as spinal canal hematomas and spinal cord lesions.

Differential Diagnosis

Os Odontoideum

Usually round or oval, smooth and with well-corticated margins, separated from the C2 vertebral body by a wider gap than that of a generally narrow fracture; usually hypertrophic anterior arch of C1 with which it may be fused.

Non-Union of Dens Fracture

Fracture with smooth and sclerotic edges; the gap of the fracture is usually narrow.

Odontoid Fracture Type 1 / 3

The fracture involves the tip of dens above the transverse ligament / extends into the C2 vertebral body, respectively.

Clinical Findings, Implications, and Treatment

Patients with an odontoid fracture typically present with neck pain following trauma. These are the most common fractures of the geriatric cervical spine. The frequency of associated neurologic symptoms is variable and is generally associated with dens displacement. Type 2 odontoid fractures have a high non-union rate due to typical instability and micro-motion at this fracture site and the limited vascular supply at the watershed region of the dens base, which decrease the healing potential. Advanced age and osteoporosis are the two main risk factors for pseudoarthrosis. The treatment of type 2 odontoid fractures is still controversial, especially in elderly patients: nonoperative rigid immobilization generally consists of a collar or halo; operative treatment may be one of the several posterior C1–C2 fusion techniques or anterior screw fixation. It has been proposed that patients with instability and dens dislocation >5 mm should be considered candidates for surgery.

Additional Information

Odontoid type 2 fractures are the most common injuries of the dens, comprising about 60% of all dens fractures. The responsible mechanism is typically hyperextension, but it may be more complex, with multiple forces acting together producing flexion, extension, or rotation of the upper cervical spine.

Odontoid type 2 fractures, according to Anderson and d'Alonzo classification, consist of a broad range of different morphologies and associated treatment considerations: to address this limitation, Grauer et al. proposed a treatment-oriented type 2 subtype classification system consisting of type 2A, 2B, and 2C fractures: type 2A and 2B are amenable to anterior screw fixation, assuming adequate bone density; Type 2C fracture generally needs posterior atlanto-axial stabilization. Cement-augmented screw fixation has been recently proposed for treatment of elderly patients with osteoporotic fractures.

References

1 Munera F, Rivas LA, Nunez DB Jr, Quencer RM. Imaging evaluation of adult spinal injuries: emphasis on multidetector CT in cervical spine trauma. *Radiology* 2012;263:645–660.

2 Grauer JN, Shafi B, Hilbrand AS, et al. Proposal of a modified, treatment-oriented classification of odontoid fractures. *Spine* 2005;5;123–129.

3 Rizk E, Kelleher JP, Zalatimo O, et al. Nonoperative management of odontoid fractures: a review of 59 cases. *Clin Neurol Neurosurg* 2013;115:1653–1656.

4 Vaccaro AR, Kepler CK, Kopjar B, et al. Functional and quality-of-life outcomes in geriatric patients with type-II dens fracture. *J Bone Joint Surg Am* 2013;95:729–735.

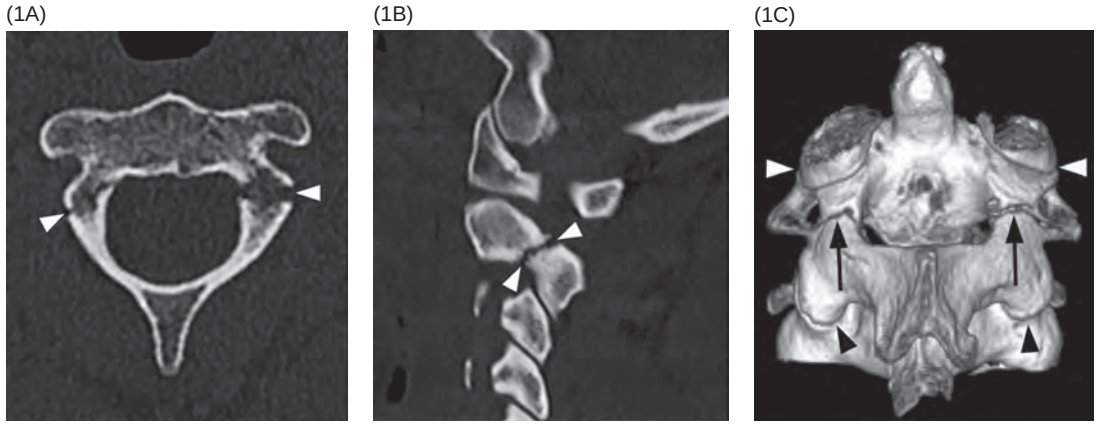

Figure 29.1 Type I hangman's fracture. **A)** Arrowheads point to a hairline (right) and minimally displaced (left) fractures of bilateral C2 pars interarticularis. **B)** Sagittally reconstructed CT image through the left pedicle shows the irregular fracture line (arrowheads). **C)** 3D volume-rendered reconstruction highlights the fractures (arrows) coursing in between the superior (white arrowheads) and inferior (black arrowheads) C2 articular masses.

Figure 29.2 Type II hangman's fracture. **A)** Sagittal CT image shows the fracture (arrow) through one of the pedicles of the axis with broadly displaced fragments. **B)** Midsagittal CT image demonstrates that the body of the axis is also displaced in flexion. There is associated widening of the intervertebral disc space (arrowhead) and interspinous space (arrow). **C)** Corresponding fat-suppressed T2w MR image reveals disc hyperintensity, indicative of severe distraction injury. Related anterior longitudinal ligament (arrowhead) and interspinous ligament injuries are also seen.

CASE 29 Hangman's Fracture

Emanuele Pravatà

Imaging Findings

Hangman's fracture (traumatic spondylolisthesis of the axis) is a bilateral fracture of the pars interarticularis of the axis, with or without concomitant body fragment displacement. The fracture, best visualized on axial and/or sagittally reconstructed CT images, may asymmetrically and variably involve the facets, pedicles, and the vertebral body. X-rays, especially in cases of fractures with undisplaced and/or asymmetrical fracture lines, have poor sensitivity. The classification proposed by Effendi and colleagues and modified by Levine and Edwards, based on radiographic findings, is used to classify the degree and type of the associated C2 fragment displacement:

- *Type I*: "Hairline" fracture with no or minimal displacement (less than 3 mm).
- *Type II*: Fracture with injured C2–C3 intervertebral disc. Translation and angulation; the trauma mechanism is flexion-distraction.
- *Type IIa*: Fracture with greater angulation and no to minimum translation; the trauma mechanism is flexion-distraction.
- *Type III*: Body displacement in flexion, with associated luxation of one or both facet joints (dislocated).

Examination with CT angiogram may show vertebral artery occlusion or dissection in up to 27% of cases, particularly with comminuted fractures and/or with involvement of the transverse foramina.

MRI may be used to assess potential injury to the intervertebral disc and/or longitudinal ligaments, as an indicator of instability. Unstable and dislocated fractures are also evaluated with MRI to investigate spinal cord injury. Fat-suppressed T2w pulse sequences, such as STIR, are best suited for these purposes.

Differential Diagnosis

Odontoid Fracture Type III (Anderson and D'Alonzo)

A fracture of the odontoid process extending into the vertebral body, does not involve the pedicles.

Congenital Spondylolysis

A very rare anomaly, symmetric and smooth edge of the pars defects with corticated rim; look for other clues of dysplastic vertebral morphology.

Clinical Findings, Implications, and Treatment

Only a minority of patients suffer neurological deficits, due to the widening of the spinal canal secondary to the isthmus separation. However, fractures with severe instability may lead to spinal cord injury. Neurological symptoms may be related to vertebral arteries injury, when present. Overall, the majority of these fractures are managed conservatively. Fractures considered stable (based on both bony fracture classification and disco-ligamentous integrity assessment) may receive nonsurgical treatment (immobilization). Surgical options include stabilization with either anterior or posterior approaches.

Additional Information

The term "hangman's fracture" (a person who hangs another, i.e., a hanger) was coined in 1965 by R. C. Schneider and colleagues, who noted similarities between hyperextension axis fractures occurring with high-energy car accidents and those seen following judicial hangings. A typical injury mechanism is that of a fall and/or hitting an obstacle with the frontal or parietal head regions, as frequently seen in car accidents where a person may hit the windscreen following an abrupt deceleration.

References

1 Levine AM, Edwards CC. The management of traumatic spondylolisthesis of the axis. *J Bone Joint Surg Am* 1985;67:217–226.

2 Effendi B, Roy D, Cornish B, et al. Fractures of the ring of the axis. A classification based on the analysis of 131 cases. *J Bone Joint Surg Br* 1981;63-B:319–327.

3 Menon KV, Taif S. Detailed description of anatomy of the fracture line in hangman's injury: a retrospective observational study on motor vehicle accident victims. *Br J Radiol* 2016;89:20150847. doi: 10.1259/bjr.20150847.

4 Schleicher P, Scholz M, Pingel A, Kandziora F. Traumatic spondylolisthesis of the axis vertebra in adults. *Global Spine J* 2015;5:346–358. doi: 10.1055/s-0035-1550343.

(1A)

(1B)

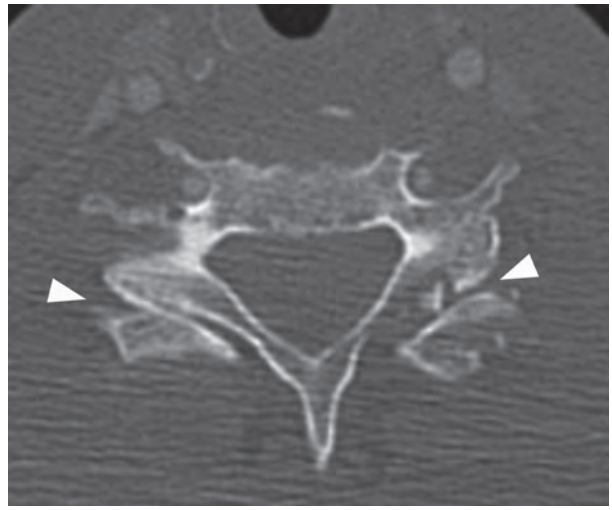

Figure 30.1 **A)** Midsagittal CT image shows anterior dislocation of C6 vertebral body with disruption of the spinolaminar line. No fracture is evident. **B**) Axial CT image reveals bilateral "reverse hamburger" sign (arrowheads) – opposing convex cortical surfaces are consistent with bilateral locked facets. There is also a fracture of the left facet joint.

(2A)

(2B)

Figure 30.2 **A)** Midsagittal T2w MRI in a different patient shows a hemorrhagic spinal cord lesion (arrow) with extensive intramedullary edema as well as disruption of the ligamentum flavum, anterior and posterior longitudinal ligaments. **B)** Sagittal CT angiography image demonstrates C6 anterolisthesis with a locked facet, absence of contrast filling of the vertebral artery proximal to dislocation, and retrograde filling of the distal part of the artery (arrow).

CASE 30 Bilateral Facet Dislocation

Hrvoje Vavro and Abhay Varma

Imaging Findings

There is anterior dislocation of the vertebral body by at least half of the AP vertebral body diameter, as well as anterior dislocation of articular masses and spinous process. The posterior ligament complex and intervertebral disc's annulus fibrosus are ruptured; the anterior longitudinal ligament is frequently also ruptured. Therefore, this is an unstable injury.

CT findings include anterior dislocation of the vertebral body by 50% or more and anterior dislocation of facets forming inverted (reverse) hamburger bun sign on axial images. Widened interspinous space indicates ligament rupture. Prevertebral soft tissue swelling is frequently present. CT angiography may show injuries of the vertebral arteries.

MR imaging additionally demonstrates ligamentous injury and often non-hemorrhagic or hemorrhagic spinal cord injury, especially in gray matter, which is more prone to damage. It may demonstrate an associated epidural hematoma as well as trauma to the vertebral artery wall and stenosis of its lumen.

Although these injuries typically occur in the cervical spine, cases of lumbar and even thoracic spine bilateral facet dislocations have been described.

Differential Diagnosis

Unilateral Facet Dislocation

Anterior vertebral dislocation is less than half of vertebral body AP diameter; also consider incomplete bilateral dislocation (facet subluxation, perched facets).

Anterior Subluxation (Hyperflexion Sprain)

Normal vertebral body shape and height, focal kyphosis, increased interspinous distance, disc height reduced anteriorly and increased posteriorly, rarely mild anterolisthesis.

Bilateral Fracture Dislocation

Look for fractures in the posterior column; if there is anterior vertebral dislocation with preserved spinolaminar line, there must be a fracture of pedicles, facets, or vertebral arch.

Clinical Findings, Implications, and Treatment

Neurological deficits are typically present, more commonly than in unilateral facet dislocation, and complete spinal cord lesions are found in more than half of the patients. In many cases there is an associated disc herniation, which can cause significant cord compression. Vertebral artery injury should always be suspected.

Cervical traction is applied to attempt closed reduction, while closely monitoring neurological status. Closed reduction is followed by anterior and/or posterior open surgical fixation, depending on morphology of injury and presence or absence of neurological deficit.

Additional Information

Bilateral facet dislocation results from hyperflexion or buckling of the spine (bending and instability under axial load). Due to distraction of the posterior elements, the joint facets "jump" over each other and become locked. Extensive soft tissue damage involving anterior longitudinal ligament, annulus fibrosus, and posterior ligamentous complex makes bilateral facet dislocation an unstable injury with a high incidence of spinal cord damage. The neurologically intact patients may have significant associated fractures that help maintain patency of the spinal canal. Delayed presentation of cervical facet dislocation has been also described in patients without neurological deficits, from a week to more than a year after the injury. With time, these neglected injuries heal with bony fusion, necessitating extensive surgical reconstruction.

References

1 Parizel PM, van der Zijden T, Gaudino S, et al. Trauma of the spine and spinal cord: imaging strategies. *Eur Spine J* 2010;19 Suppl 1: S8–S17. doi: 10.1007/s00586-009-1123-5.

2 Ivancic PC, Pearson AM, Tominaga Y, et al. Mechanism of cervical spinal cord injury during bilateral facet dislocation. *Spine (Phila Pa 1976)* 2007;32:2467–2473.

3 Zeonos GA, Agarwal N, Monaco EA 3rd, et al. Traumatic L4-5 bilateral locked facet joints. *Eur Spine J* 2016;25 Suppl 1:129–133.

4 Srivastava A, Soh RC, Ee GW, Tan SB, Tow BP. Management of the neglected and healed bilateral cervical facet dislocation. *Eur Spine J* 2014;23:1612–1616.

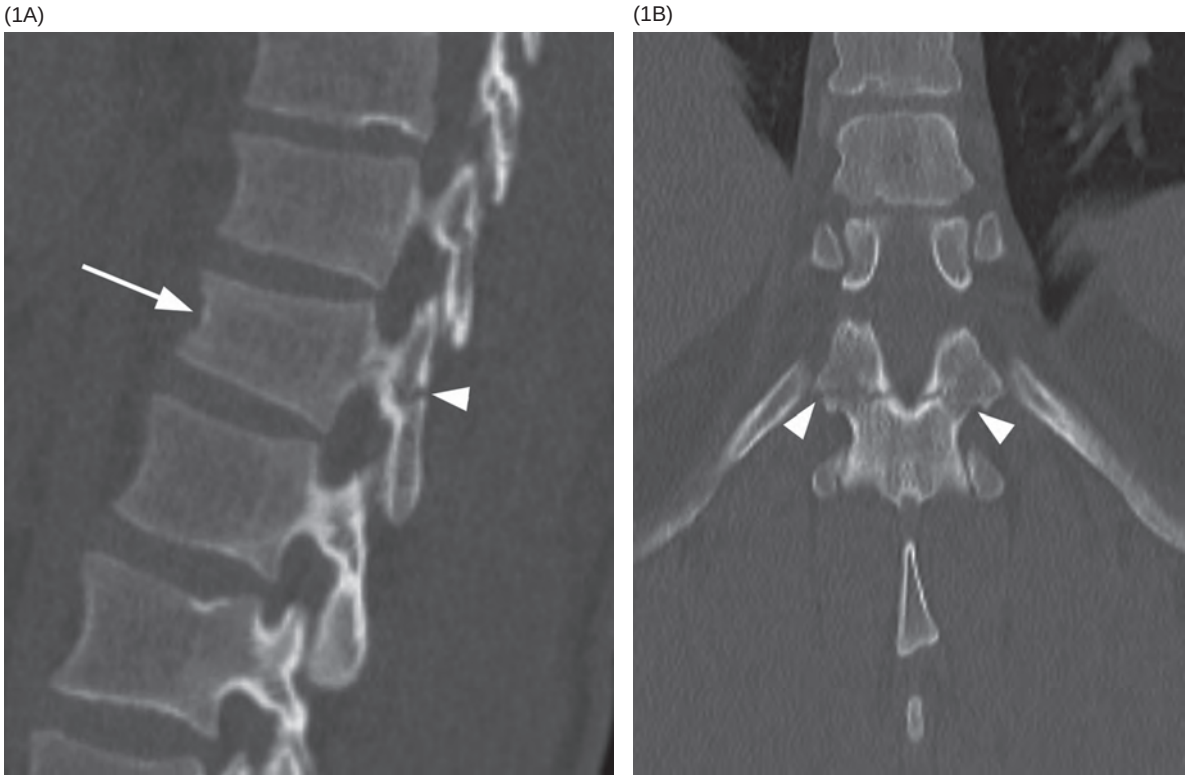

Figure 31.1 **A)** Sagittal CT image shows an apparently mild compression fracture of a lower thoracic vertebral body (arrow). The fracture, however, extends into the posterior elements (arrowheads), through the pedicle and into the lamina, consistent with a Chance-type fracture. **B)** Coronal CT image demonstrates the fracture line involving bilateral laminae (arrowhead).

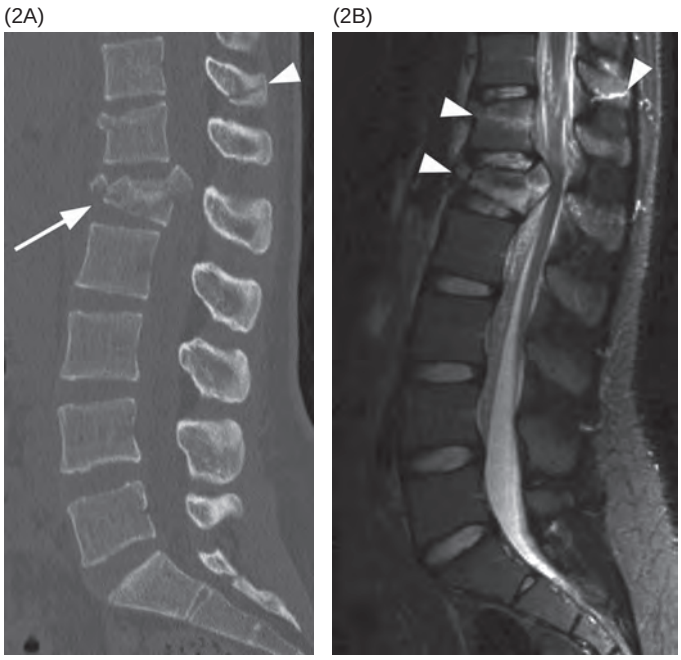

Figure 31.2 **A)** Midsagittal CT image in a different patient reveals a burst fracture (arrow) of L1 vertebral body with prominent retropulsion. There is also compression fracture of T12 superior endplate and, more importantly, a fracture through T11 spinous process (arrowhead). **B)** Corresponding STIR MR image demonstrates high signal intensity at the fractures (arrowheads). No evidence of ligamentous injury. There is also spinal cord injury and hematomas within the spinal canal.

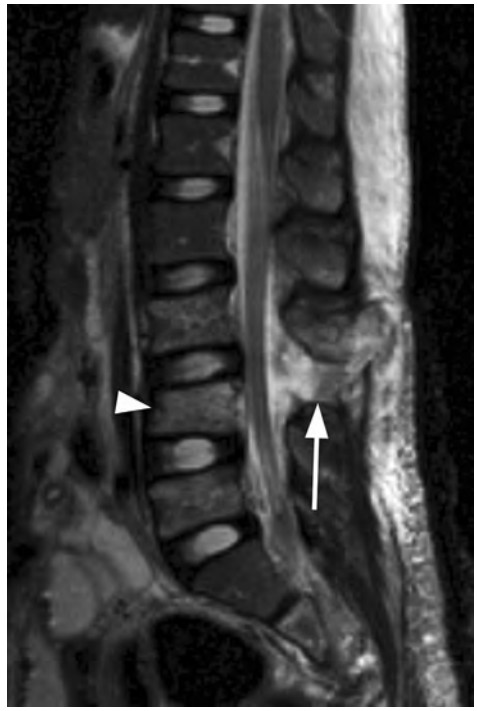

Figure 31.3 Midsagittal STIR MR image in a young child following MVA shows compression fracture of L4 vertebral body (arrow), bone marrow edema in the adjacent L3 and L5 bodies, and hyperintensity consistent with disruption of the ligamenta flava and interspinous ligaments (arrow) along with increased interspinous distance.

CASE 31 Chance-Type Fracture

Zoran Rumboldt and Hrvoje Vavro

Imaging Findings

Plain films demonstrate pedicle radiolucency, fanning of the spinous processes, and, most commonly and characteristically, "empty body" sign of the AP projection. This sign results from the vertical separation of the posterior elements displacing the spinous processes or spinous process fracture fragments off the vertebral body. A horizontal fracture through one or both pedicles may also be present. Widening of the interpedicular distance may be observed and often suggests a burst component.

Reformatted sagittal CT images demonstrate anterior wedge fracture of the vertebral body with horizontal fracture through the posterior elements or distraction of facet joints and spinous processes, accurately delineating fracture details. The horizontal orientation of the fracture is unique for Chance injury and may also be well seen on coronal CT reconstructions. MRI reveals injury of the posterior ligaments, seen as disruption of the normal hypointense bands and hyperintense signal on STIR or fat-suppressed T2-weighted images.

The term "Chance variant" is used for a pure ligamentous injury, which is analogous to bilateral interfacet dislocation, with rupture of the interspinous ligament, dislocation of the facet joints, and a horizontal disc rupture. The findings include split of the posterior elements, disc widening, and/or widening of the spinous processes and facets, with associated hyperintensity on STIR or fat-suppressed T2-weighted MRI. Horizontally oriented fractures of the posterior neural arch produce an MR imaging pattern called the sandwich sign, consisting of linear hemorrhage framed by bone marrow edema.

Differential Diagnosis

Burst Fracture

Compression of the vertebral body with retropulsion of the posterior cortex, without associated ligamentous injury. Chance-type injury is frequently combined with burst fracture of the vertebral body.

Clinical Findings, Implications, and Treatment

Chance (or Chance-type) fractures are flexion-distraction injuries most commonly occurring at the thoracolumbar junction. These injuries are unstable and frequently associated with significant intra-abdominal lesions, but usually do not present with a neurologic deficit and may be subtle on both radiographs and even axial CT images. Presence of the seat belt sign with skin bruising or avulsion across the anterior chest or abdominal wall should arouse the suspicion of the probable covert injuries; the patient should be maintained on full spinal precaution, and a CT scan should be performed.

Surgical reduction and spine fixation is the treatment of choice in patients with gross instability, significant ligamentous disruption, or multiple other injuries. If unrecognized, Chance injuries may result in progressive kyphosis with resulting pain and deformity.

Additional Information

The flexion-distraction fracture of the spine was first described by Chance in 1948. The classic mechanism of this injury is with a lap seat belt; without an additional shoulder belt, the body will fold over during a collision. This hyperflexion over the lap belt fulcrum classically produces Chance fractures; however, 40% of these injuries occur while wearing a combined shoulder and lap belt.

It seems that a majority of pediatric Chance fractures, frequently occurring in the lower lumbar spine, may be initially misdiagnosed or mistreated, with mean time to the correct diagnosis of 3 months in one series.

References

1 Bernstein MP, Mirvis SE, Shanmuganathan K. Chance-type fractures of the thoracolumbar spine: imaging analysis in 53 patients. *AJR Am J Roentgenol* 2006;187:859–868.

2 Groves CJ, Cassar-Pullicino VN, Tins BJ, et al. Chance-type flexion-distraction injuries in the thoracolumbar spine: MR imaging characteristics. *Radiology* 2005;236:601–608.

3 Suttor S, Gray R, Bridge C, Cree A. Operative treatment of chance injuries in the paediatric population. *Eur Spine J* 2013;22:510–514. doi: 10.1007/s00586-012-2582-7.

4 Andras LM, Skaggs KF, Badkoobehi H, et al. Chance fractures in the pediatric population are often misdiagnosed. *J Pediatr Orthop* 2016 Dec 23. doi: 10.1097/BPO.0000000000000925. [Epub ahead of print]

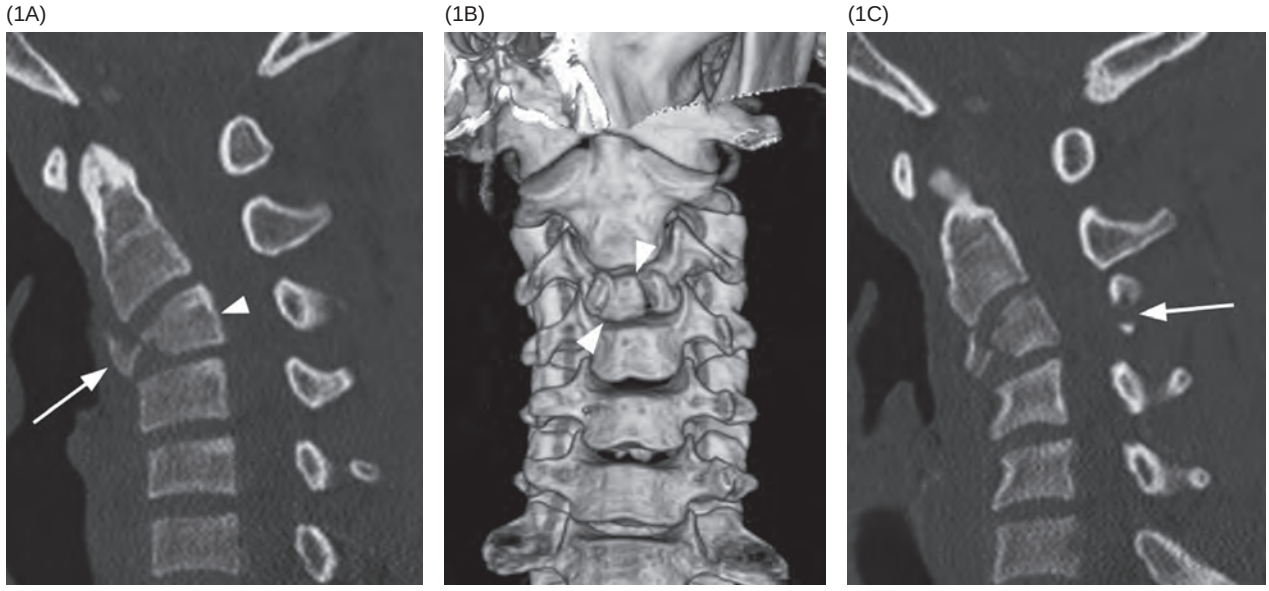

Figure 32.1 Flexion teardrop fracture of C3 vertebra. **A)** Midline sagittal reconstructed CT image shows a fracture of the C3 vertebral body with separation of the posterior fragment (arrowhead) from the triangle-shaped, anterior "teardrop" fragment (arrow). Note vertebral body height loss and wedge deformity and consequent kyphotic angulation. **B)** Frontal view of the corresponding 3D volume-rendered reconstruction shows the "teardrop" fragment as a quadrangular structure (arrowheads). **C)** A slightly off-midline sagittal CT reconstruction shows an additional fracture of the neural arch (arrow).

Figure 32.2 Flexion teardrop fracture of C6 vertebra. Midsagittal reconstructed CT image reveals the anterior "teardrop" fragment (arrow), focal kyphosis with fanning of the spinous processes (arrowhead), and a prominent posterior subluxation indicating spinal cord compression.

CASE 32 Flexion Teardrop Fracture

Emanuele Pravatà

Imaging Findings

Flexion and translation forces cause the anterior vertebral column to fail and disrupt the anterior and posterior disco-ligamentous complexes, with separation of the largest part of the vertebra from the anterior-inferior corner of its body, which remains attached to the more inferior vertebra. The resulting kyphotic deformity and, when present, posterior displacement of the upper column at the injured level carry a high risk of spinal cord injury. The fractured anterior corner is relatively small, triangle-shaped, and resembles a teardrop on lateral radiographs as well as on sagittal CT and MR images. There is frequently height loss of the fractured vertebral body. Fractures of the posterior vertebral arch and spinous process and/or anterior luxation of facet joints may also be present. Disco-ligamentous lesions can be indirectly diagnosed on lateral plain films and sagittally reconstructed CT images as a swelling of the prevertebral soft tissues and increased height of the intervertebral disc space. Fat-suppressed T2w and/or PDw MRI sequences may demonstrate hyperintensity and/or interruption of the anterior and posterior longitudinal ligaments, intervertebral disc, and interspinous ligaments.

Differential Diagnosis

Hyperextension Teardrop Fracture

Compared to hyperflexion fracture, it occurs more frequently in the upper cervical spine, there is no height loss of the fractured vertebra, and there is hyperlodosis rather than hyperkiphosis. The posterior fragment is typically not displaced into the central canal, making this injury less severe compared to the flexion teardrop fracture.

Burst Fracture

Results from a mainly axially oriented compression force affecting the whole vertebral body, but may sometimes be difficult to distinguish. In contrast to hyperflexion teardrop fracture, there is compression of the middle vertebral column, and the spinal canal may be narrowed by retropulsion of the posterior vertebral wall fragment(s).

Clinical Findings, Implications, and Treatment

This is the most severe type of unstable cervical fracture, carrying a high risk of spinal cord compression and permanent neurological deficits, depending on the degree of kyphotic angulation and dislocation of the vertebral body into the spinal canal. It occurs more frequently in young men, typically in traffic or diving accidents.

Lesions are more common at the inferior cervical levels (primarily C5 and C6). Neurological deficits occur in up to 100% of cases when the posterior fragment is dislocated into the spinal canal. These cases are treated with surgical reduction and stabilization. Anterior cervical plating has replaced halo immobilization in treatment of unstable cervical flexion teardrop fractures, minimizing treatment failures. Initial management is application of traction with cervical tongs, and minimally displaced fractures in patients without neurological deficits may be treated conservatively.

Additional Information

The antero-inferior fracture fragment can only occur with a significant posterior ligamentous disruption, and since the fragment displaces anteriorly, a significant degree of anterior ligamentous disruption also exists. The disruption of all three columns with this injury makes it an extremely unstable fracture.

References

1 Kim KS, Chen HH, Russell EJ, Rogers LF. Flexion teardrop fracture of the cervical spine: radiographic characteristics. *AJR Am J Roentgenol* 1989;152:319–326.

2 Kim HJ, Lee KY, Kim WC. Treatment outcome of cervical tear drop fracture. *Asian Spine J* 2009;3:73–79. doi: 10.4184/asj.2009.3.2.73.

3 Fisher CG, Dvorak MF, Leith J, Wing PC. Comparison of outcomes for unstable lower cervical flexion teardrop fractures managed with halo thoracic vest versus anterior corpectomy and plating. *Spine (Phila Pa 1976)* 2002;27:160–166.

4 Toh E, Nomura T, Watanabe M, Mochida J. Surgical treatment for injuries of the middle and lower cervical spine. *Int Orthop* 2006;30:54–58.

(1A)

(1B)

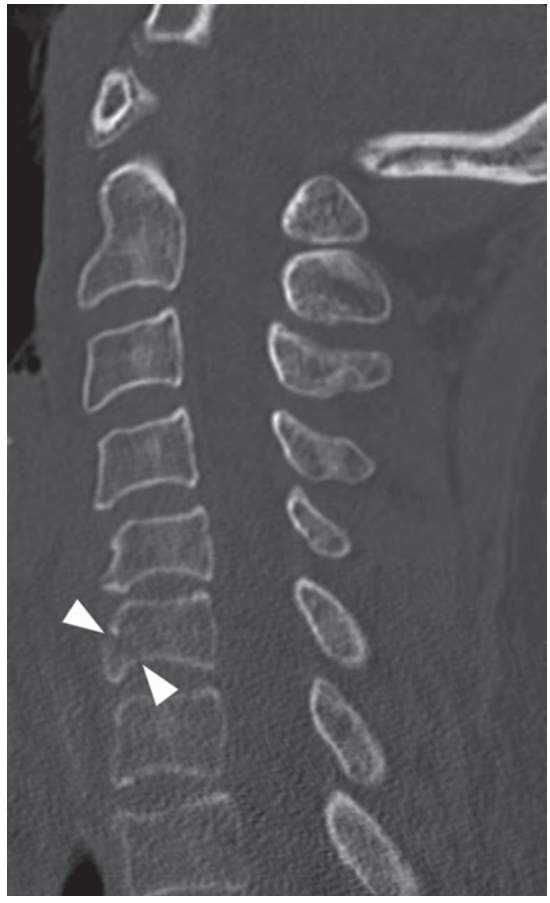

Figure 33.1 **A)** Midsagittal CT image shows an avulsion of a triangular bone fragment from the anterior inferior margin of C6 (arrow). **B)** A more lateral CT image demonstrates the fracture (arrowheads), somewhat obscured by the beam hardening artifact from shoulders, which separates the avulsed fragment from C6 body in this patient with extension teardrop injury.

(2A)

(2B)

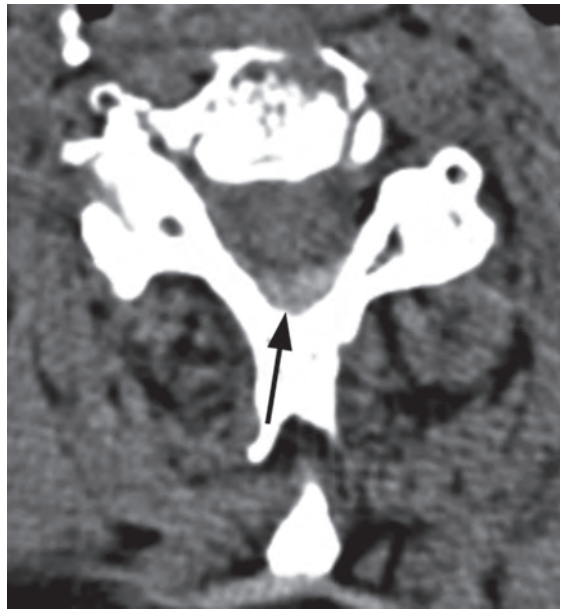

Figure 33.2 **A)** Midsagittal CT image in a different patient shows a triangular bone fragment avulsed from the anterior inferior margin of C5 (arrow). There is also a Type II dens fracture and fracture through at least one (C5) spinous process (arrowhead). **B)** Axial CT image with soft tissue algorithm and window reveals hyperdense material in the dorasal epidural space (arrow), consistent with epidural hematoma. The patient had no neurological deficits.

CASE 33 Extension Teardrop Fracture

Hrvoje Vavro and Zoran Rumboldt

Imaging Findings

These fractures occur almost exclusively in the cervical spine. There is a triangular avulsion of the anterior inferior corner of the affected vertebral body, without loss of height or displacement of the body. The vertical diameter of the fragment is equal to or larger than its width; its shape is reminiscent of a teardrop. Radiographs, CT, and MRI may also show anterior disc space widening and prevertebral tissue swelling. The bony fragment is attached to the anterior longitudinal ligament (ALL). The fibers of the ligament may be preserved, but the ligament is displaced anteriorly with the bone fragment. MRI may demonstrate spinal cord contusion and edema. This injury is often associated with other cervical spine fractures, primarily spinous process fractures, especially when it occurs at the lower cervical levels.

Differential Diagnosis

Flexion Teardrop Fracture

The most severe cervical spine fracture: loss of anterior vertebral body height due to compression, serious ligamentous injury, unstable, usually involves lower cervical spine levels.

Limbus Ossicle

A nontraumatic, well-corticated ossicle at the corner of a vertebral body caused by herniation of the nucleus pulposus of the disc through the disc endplate, similar to a Schmorl's node.

Clinical Findings, Implications, and Treatment

The patients complain of neck pain, limited range of motion, and tenderness to palpation, possibly of dysphagia. Central cord syndrome is present in up to 80% of cases, typically caused by compression injury of the spinal cord inflicted by buckled yellow ligaments at the moment of hyperextension. The injury results from pull of the ALL insertion on the anterior inferior aspect of vertebral body due to sudden extreme hyperextension of the neck, usually caused by a direct high-energy blow to the forehead or mandible. Extension teardrop fracture is stable in flexion but highly unstable in extension, as the ALL may be disrupted. In elderly patients it is most likely to occur at C2 level due to osteoporosis and degenerative fusion deformities in the lower cervical spine. In younger patients it is more common at the lower cervical levels.

Treatment is typically conservative with neck collar and restriction of activity. Surgery may only be needed in rare specific cases, such as with prolonged dysphagia or when associated with other complex fractures.

Additional Information

The bony fragment is a true avulsion, in contrast to the flexion teardrop fracture in which the fragment is produced by compression, and extension teardrop is generally considered less severe than the flexion teardrop fractures. The stability of this injury involving the axis has been a matter of debate leading to controversy regarding treatment strategies, primarily the need for stabilization. Large fragment size, displacement or angulation, disk injury, neurologic deficit, or signs of instability have been proposed as reasonable indications for surgical intervention.

References

1 Rao SK, Wasyliw C, Nunez DB Jr. Spectrum of imaging findings in hyperextension injuries of the neck. *Radiographics* 2005;25:1239–1254.

2 Utz M, Khan S, O'Connor D, Meyers S. MDCT and MRI evaluation of cervical spine trauma. *Insights Imaging* 2014;5:67–75. doi: 10.1007/s13244-013-0304-2.

3 Kim HJ, Lee KY, Kim WC. Treatment outcome of cervical tear drop fracture. *Asian Spine J* 2009;3:73–79. doi: 10.4184/asj.2009.3.2.73.

4 Watanabe M, Sakai D, Yamamoto Y, Sato M, Mochida J. Clinical features of the extension teardrop fracture of the axis: review of 13 cases. *J Neurosurg Spine* 2011;14:710–714.

5 Hu Y, Kepler CK, Albert TJ, et al. Conservative and operative treatment in extension teardrop fractures of the axis. *Clin Spine Surg* 2016; 29:E49–E54.

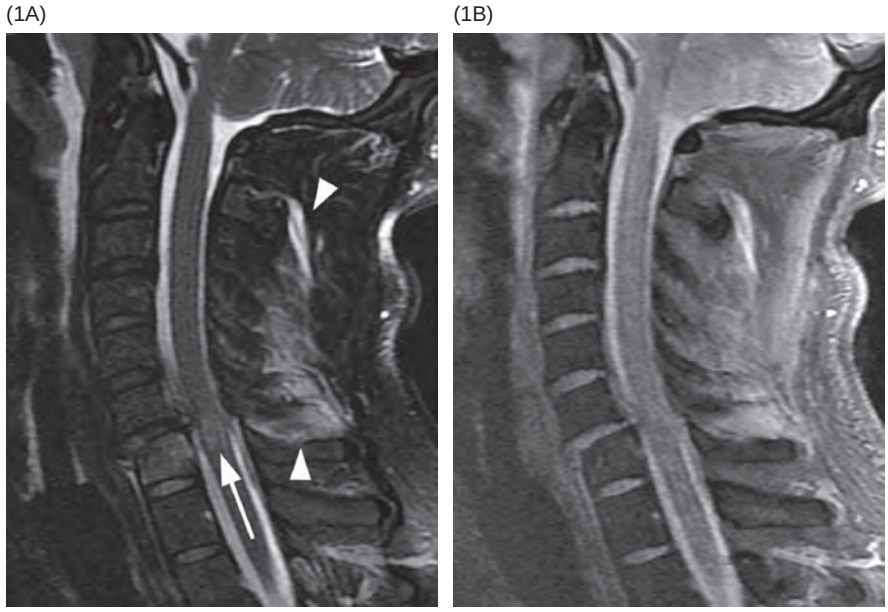

Figure 34.1 Midsagittal T2w (SE) **(A)** and T2*w (GRE) **(B)** MR images shows traumatic subluxation of C6 over C7 and traumatic C6–C7 disk herniation. There is spinal canal compromise with mild compression of the spinal cord and elevated intramedullary T2 signal consistent with edema (arrow). There are no focal areas of signal loss on the T2* images to suggest focal cord hemorrhage. Note posterior ligamentous injuries (arrowheads).

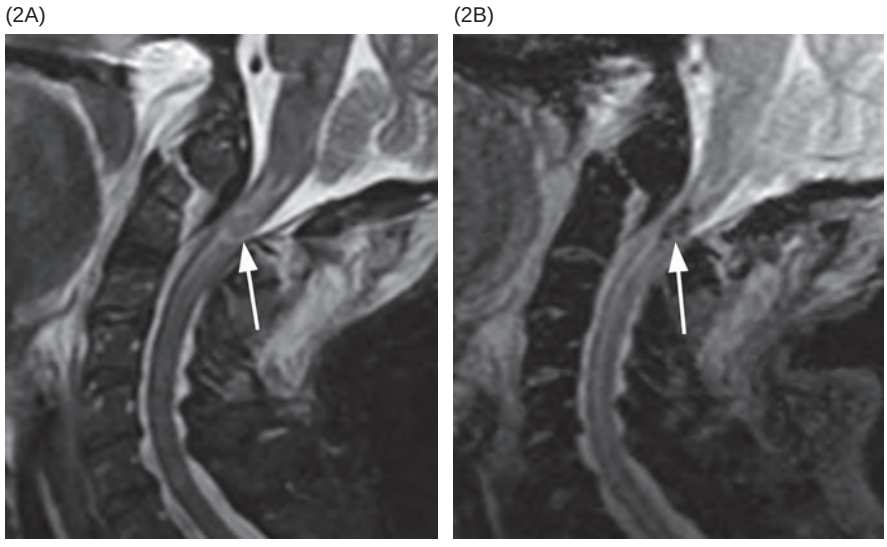

Figure 34.2 **A)** Midsagittal T2w (SE) MR image shows fracture of the odontoid. Posterior distraction of the superior fracture fragments contributes to the spinal canal stenosis and mild spinal cord compression. Areas of high and low T2 signal intensity (arrow) are consistent with hemorrhagic and non-hemorrhagic spinal cord injury, respectively. Intramedullary hemorrhage is clearly seen as an area of signal loss (arrow) on the corresponding T2*w (GRE) image **(B)**.

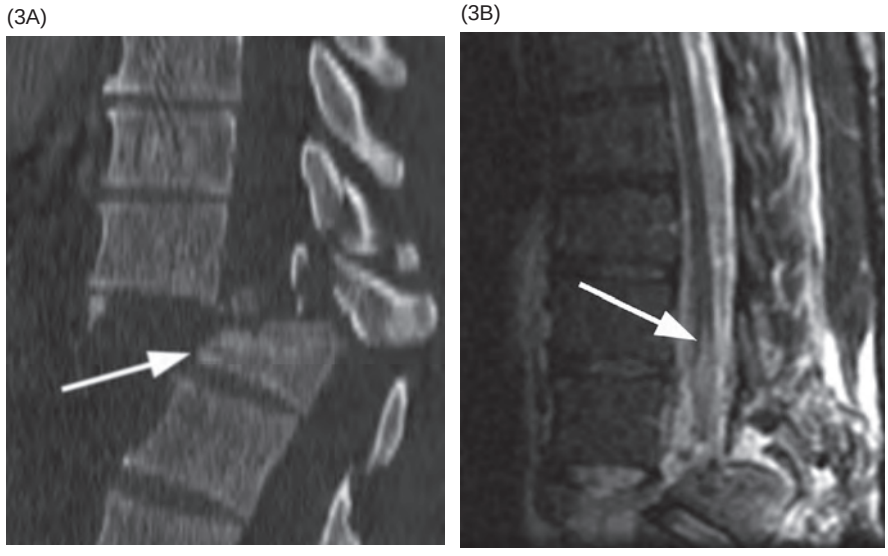

Figure 34.3 **A)** Sagittal CT image shows Chance fracture involving the superior aspect of T11 vertebral body and the posterior elements with significant posterior dislocation for the entire vertebral body width (arrow). **B)** MRI confirms spinal cord transection at the T10–11 level and intramedullary edema (arrow) extending to T9 level.

CASE 34 Spinal Cord Injury

Vikas Agarwal and Abhay Varma

Imaging Findings

Acute injuries to the spinal cord can be classified as contusions or transections. Contusions can be hemorrhagic or nonhemorrhagic. Type I injuries represent intramedullary hematoma and demonstrate heterogeneous T1 and low T2 signal with rim of higher T2 signal related to edema. Intramedullary hemorrhage is best seen on T2*w (gradient-echo or susceptibility-weighted) images as a very dark lesion/an area of signal loss. Type II injuries reflect only edema within the spinal cord and are low to isointense on T1 and T2 hyperintense. Type III injuries are a mixture of hematoma and edema and are therefore low to isointense on T1 and show heterogeneous appearance on T2-weighted images. MRI demonstrates the level of spinal cord transection.

The presence of intramedullary hemorrhage and extended segments of edema have been associated with clinically complete spinal cord injury (SCI). An important prognostic imaging characteristic, in addition to intramedullary hemorrhage and edema, is the degree of spinal cord compression.

Differential Diagnosis

Nontraumatic Compressive Myelopathy

Degenerative disease resulting in severe spinal canal stenosis with spinal cord compression and edema.

Myelitis

Hyperintense T2 signal with or without contrast enhancement; mild fusiform enlargement of spinal cord without spinal canal stenosis.

Spinal Cord Infarction

Almost exclusively involves the gray matter, primarily the anterior horns, with the characteristic "owl's eyes" appearance.

Syrinx

Cystic typically central cord lesion with longitudinal extension and variable spinal cord expansion.

Clinical Findings, Implications, and Treatment

SCI usually occurs in conjunction with bony and ligamentous traumatic lesions. Clinical findings will depend on injury location with C4–C6 being the most common level of adult spinal cord injury.

Patients with anterior cord syndrome present with variable impairment of motor function and pain and temperature sensation with relative sparing of propioception. It occurs with hyperflexion injuries, acute central disc herniation, and burst fractures with ventral cord compression.

Central cord syndrome is seen almost exclusively following cervical SCI. It is characterized by sacral sensory sparing and greater weakness in the upper limbs than in the lower limbs. This results from a lesion within the cord that afflicts the central gray matter and the surrounding fiber tracts. The peripherally located corticospinal lumbosacral fibers are spared, leading to relative preservation of lower extremity motor strength. Similarly, the laterally placed sacral spinothalamic tracts are preserved with preservation of sacral sensation. Posterior cord syndrome is uncommon.

Brown-Sequard syndrome is characterized by physiologic hemisection of the cord, producing ipsilateral motor weakness and impaired propioception with contralateral impairment of pain and temperature sensation. This syndrome usually occurs with other SCI or nerve root injury (or both) or brachial plexus injury. It is most often seen in cervical spine and less frequently in thoracic spine. This syndrome carries a favorable prognosis except when resulting from a penetrating injury.

Conus medullaris syndrome results from injury to the sacral spine segments and lumbar roots, at the T11 and T12 vertebral body levels. This part of the vertebral column is prone to injury because it lies in the transitional zone between the rigid thoracic spine and mobile lumbar spine. The patients can have a combination of upper and lower motor neuron paralysis. The deficit is usually symmetrical and involves the motor, sensory, and sphincter functions.

Cauda equina syndrome results from injury to the lumbosacral nerve roots of cauda equina in the canal from L2 vertebral body level downward. Clinical features include asymmetrical areflexic paralysis of lower extremities, sensory impairment in lumbar and sacral dermatomes, and lower motor neuron type bowel and bladder incontinence.

Type II spinal cord injuries are most common and will regress over 1–2 weeks, resulting in a more favorable prognosis. Type I and III spinal cord injuries are less common and have a poor prognosis, often without substantial neurological recovery.

Broad indications for surgical intervention following SCI include decompression of neural elements, stabilization of spine, and deformity correction. Stabilization is indicated for an "unstable" injury. Injury is considered unstable when there is progressive neurological decline, pain, or deformity of the spine under physiological loading. Surgery can range from simple decompression to instrumented fusion. Under most circumstances, some kind of stabilization would be required, as an isolated decompression can lead to persistent pain and late deformity.

(4A)

(4B)

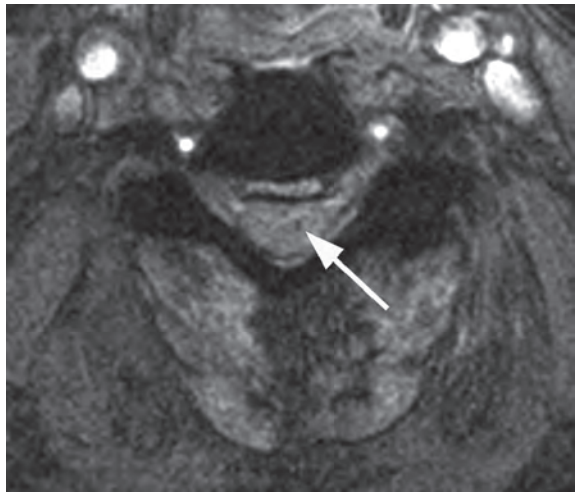

Figure 34.4 A) Midsagittal T2-weighted image in a patient following trauma shows spinal cord compression at C4–C5 level with associated intramedullary edema. **B)** Axial T2* image at lower C4 level reveals small areas of signal loss (arrow), representing hemorrhagic cord injury.

(5A)

(5B)

Figure 34.5 A) Midsagittal CT image in a different patient with bilateral C6–C7 interfacetal dislocation demonstrates spinal canal compromise. **B)** Corresponding T2* image following reduction shows hemorrhagic spinal cord injury at the level of previous dislocation.

Additional Information

Underlying degenerative disease predisposes older adults to spinal cord injury. Although more common in children, spinal cord injury can occur in the absence of bone or ligamentous injury and is referred to as SCIWORA (spinal cord injury without radiographic abnormality, the more appropriate term would be spinal cord injury without CT evidence of trauma – SCIWOCTET).

References

1 Aarabi B, Simard JM, Kufera JA, et al. Intramedullary lesion expansion on magnetic resonance imaging in patients with motor complete cervical spinal cord injury. *J Neurosurg Spine* 2012;17:243–252.

2 Bozzo A, Marcoux J, Radhakrishna M, et al. The role of magnetic resonance imaging in the management of acute spinal cord injury. *J Neurotrauma* 2011;28:1401–1411.

3 Ellingson BM, Salamon N, Holly LT. Imaging techniques in spinal cord injury. *World Neurosurg* 2014;82:1351–1358.

4 Kaiser ML, Whealon MD, Barrios C, et al. The current role of magnetic resonance imaging for diagnosing cervical spine injury in blunt trauma patients with negative computed tomography scan. *Am Surg* 2012;78:1156–1160.

5 Wilson JR, Grossman RG, Frankowski RF, et al. A clinical prediction model for long-term functional outcome after traumatic spinal cord injury based on acute clinical and imaging factors. *J Neurotrauma* 2012;29:2263–2271.

(1A)

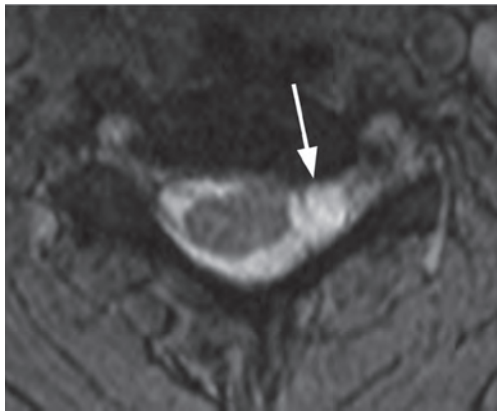

(1B)

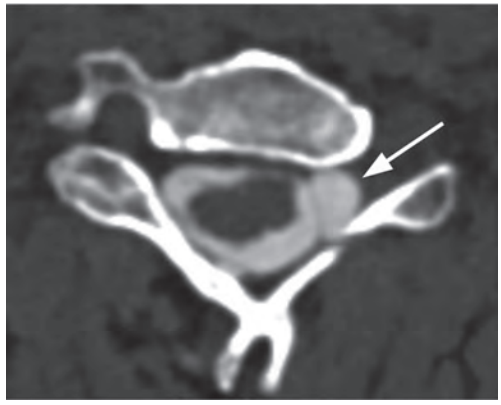

(1C)

Figure 35.1 A) Axial T2* image shows a left C5–C6 CSF collection (arrow) consistent with pseudomeningocele and deviation of the spinal cord to the right. Axial **(B)** and coronal **(C)** CT-myelogram images confirm the pseudomeningocele (arrows) and show lack of visualization of the avulsed left dorsal C6 nerve root. Note normal adjacent nerve roots (arrowheads).

(2A)

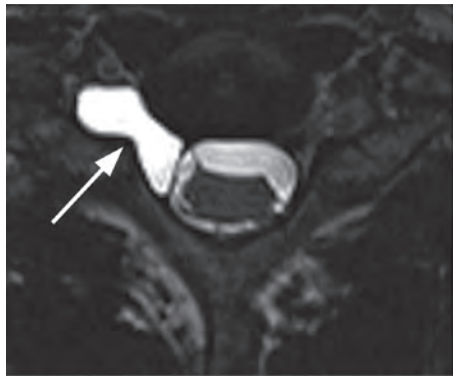

(2B)

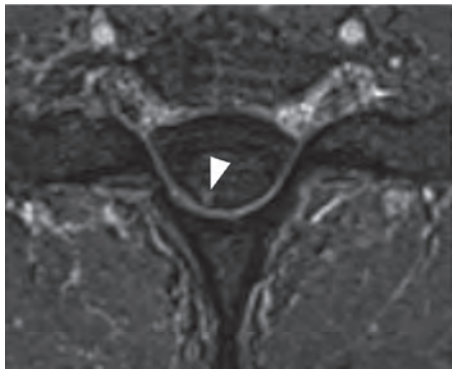

(2C)

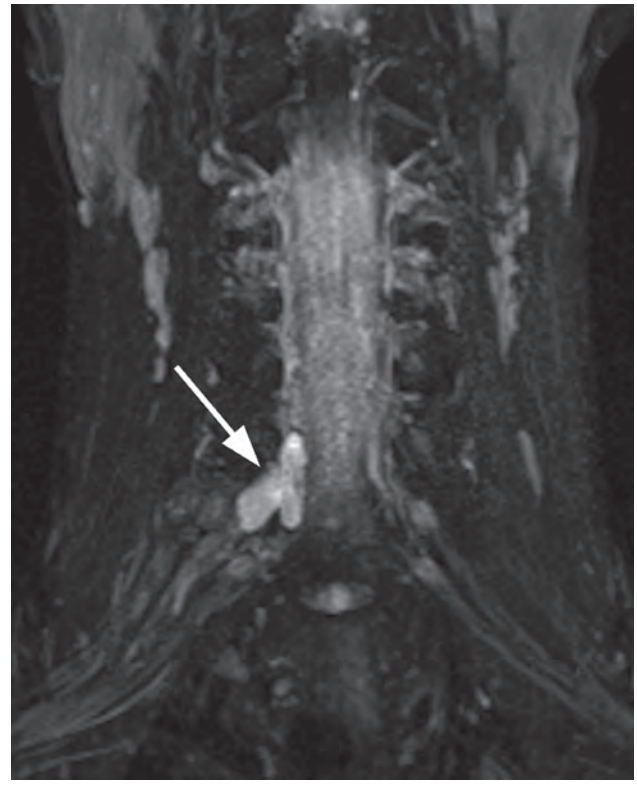

Figure 35.2 A) High-resolution axial T2w image shows a large pseudomeningocele at C6–C7 on the right (arrow) related to right C7 nerve root avulsion. **B)** Fat-saturated post-contrast axial T1w image demonstrates enhancement of the right C7 dorsal nerve root stump (arrowhead). **C)** Coronal MIP reformatted STIR image depicts the pseudomeningocele (arrow). The right brachial plexus shows subtle thickening and increased signal due to stretching injury of nerve roots.

CASE 35 Nerve Root Avulsion

Daniela Distefano and Abhay Varma

Imaging Findings

Nerve root avulsion is typically seen as a pseudomeningocele – an extra-dural CSF pouch within and/or extending to the neural foramen, sometimes with mass effect on the dural sac. The spinal cord may be displaced contralaterally. Dedicated high-resolution 3D heavily T2w MRI (MR myelography) or CT myelography are very accurate for assessment of the pseudomeningoceles. MR myelography without intrathecal contrast administration is superior to CT myelography for small meningoceles, which do not fill with contrast when there is little or no communication with the dural sac, although its spatial resolution for detailed visualization of intradural nerve roots is lower. However, visualization of rootlets in the absence of pseudomeningocele may not be helpful in detection of complete nerve root avulsion. MRI also shows contrast enhancement of the injured intradural nerve roots, suggesting functional impairment despite morphologic continuity, which is seen in approximately 20% of patients with preganglionic injuries. Furthermore, abnormal enhancement of paraspinal muscles on post-contrast fat-suppressed T1w images, consistent with acute denervation injury, is an accurate indirect sign of nerve root avulsion.

Differential Diagnosis

Spinal Extradural Arachnoid Cyst (Extradural Meningeal Cyst)

Outpouchings of the arachnoid through a congenital or acquired dural defects usually located in the mid-to-lower thoracic spine, which may protrude into the neuroforamen and remodel it. The signal within the cyst may appear T2 hyperintense compared to the CSF due to higher protein content. CT myelography is helpful in establishing communication of the cyst with the subarachnoid space.

Meningocele

CSF-filled protrusion of the dura mater and arachnoid that extends through an enlarged intervertebral foramen, most commonly seen in patients with mesenchymal disorders such as neurofibromatosis, Marfan's syndrome, and Ehlers-Danlos syndrome.

Clinical Findings, Implications, and Treatment

Nerve root avulsion, including neonatal brachial plexus palsy, results from stretch injuries. This type of injury is seen most commonly in cervical and upper thoracic region involving the brachial plexus, but is rare in the thoracolumbar region. Meticulous clinical examination, supplemented by electrodiagnostic and imaging studies, can establish the level (roots involved), extent (partial or complete), and nature (avulsion or rupture) of injury. The primary objective of imaging is to identify nerve root avulsion indicative of preganglionic injury. Treatment of nerve root injuries, usually referred to as brachial plexus injuries, may be either conservative or surgical: surgical procedures include neurolysis, nerve grafting, and nerve transfer.

Additional Information

Preganglionic nerve root avulsions are subdivided into peripheral and central: peripheral lesions occur when a traction force avulses the fibrous supporting tissues around the nerve rootlets; central mechanism of root avulsion is the result of displacement of the spinal cord, as cord bending induces avulsion of the rootlets without a rupture of the epidural sleeve. Extremely rare cases of transdural spinal cord herniation into the pseudomeningocele have been described. Postganglionic lesions involve the nerve distal to the sensory ganglion and are further classified into nerve ruptures and lesions in continuity. Differentiating preganglionic from postganglionic lesions is crucial to the management of plexus injuries. In preganglionic injuries, function of some of the denervated muscles may be restored with nerve transfers. Postganglionic lesions generally have better prognosis and can be repaired with neurolysis, nerve grafting, nerve transfer, or managed conservatively.

References

1 Yoshikawa T, Hayashi N, Yamamoto S, et al. Brachial plexus injury: clinical manifestations, conventional imaging findings and the latest imaging techniques. *Radiographics* 2006;26 suppl 1:S133–S143.

2 Tse R, Nixon JN, Iyer RS, Kuhlman-Wood KA, Ishak GE. The diagnostic value of CT myelography, MR myelography, and both in neonatal brachial plexus palsy. *AJNR Am J Neuroradiol* 2014;35:1425–1432.

3 Somashekar D, Yang LJ, Ibrahim M, Parmar HA. High-resolution MRI evaluation of neonatal brachial plexus palsy: a promising alternative to traditional CT myelography. *AJNR Am J Neuroradiol* 2014;35:1209–1213.

4 Ijiri K, Hida K, Yano S, Komiya S, Iwasaki Y. Traumatic spinal-cord herniation associated with pseudomeningocele after lower-thoracic nerve-root avulsion. *Spinal Cord* 2009;47:829–831.

5 Silbermann-Hoffman O, Teboul F. Post-traumatic brachial plexus MRI in practice. *Diagn Interv Imaging* 2013;94:925–943.

(1A)

(1B)

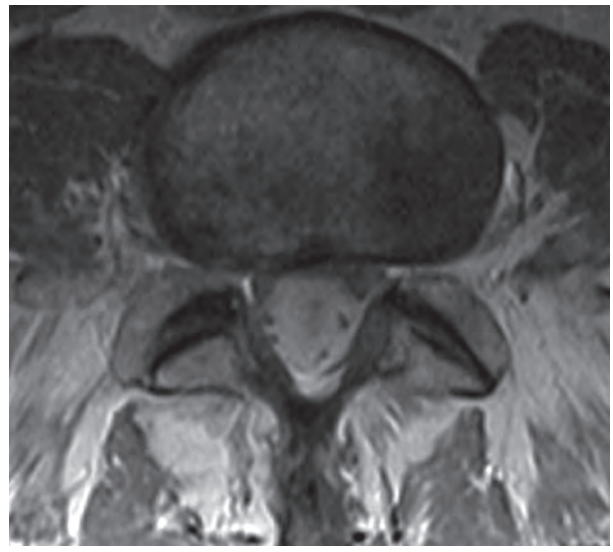

Figure 36.1 **A)** Sagittal T1-weighted MR image demonstrates high-signal intensity of the CSF (arrow), most prominent and diffuse at L5 and more inferior levels, consistent with subarachnoid hemorrhage. The nerve roots of cauda equina are seen as relatively hypointense linear structures. **B)** Axial T1-weighted image at L5–S1 level has the appearance of a T2-weighted image within the spinal canal showing dark nerve roots on the background of bright CSF.

(2A)

(2B)

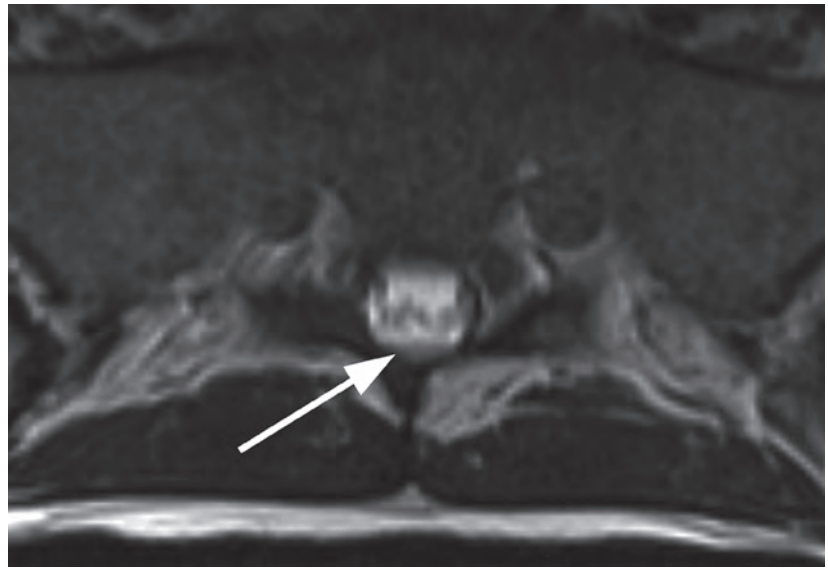

Figure 36.2 MRI in a different patient who suffered head injury with traumatic subarachnoid hemorrhage (SAH) a week earlier and then developed new pain and cauda equina symptoms. **A)** Sagittal T1-weighted reveals as a bright lesion (arrow) along the posterior aspect of the thecal sac centered at S1 level. The lesion is separated by a dark line of dura from the posterior epidural space. **B)** Axial T2-weighted image shows a small area of relatively lower signal (compared to the CSF, isointense to the cauda equina nerve roots) with layering along the posterior aspect of the dural sac (arrow) with a fluid–fluid level. The findings are consistent with a small amount of spinal SAH, which has presumably migrated from the intracranial SAH.

CASE 36 Spinal Subarachnoid Hemorrhage

Zoran Rumboldt

Imaging Findings

Spinal subarachnoid hemorrhage (SSAH) is found within the thecal sac in an intradural extramedullary location, either diffusely extending over a number of spinal levels and/or as a focal clot. The hematoma may show a fluid–fluid level, typically at the inferiormost aspect of the dural sac or at other dependent portions (thoracic spine in supine position), but may also be ventral to the spinal cord/cauda equina. Compared to the CSF, SSAH is hyperintense on T1-weighted images and usually of lower T2 signal intensity, although it may be T2 isointense and even hyperintense (in the hyperacute stage). It is rarely of very bright T1 and very dark T2 signal, presumably due to dilution with a relatively large volume of the CSF; however, a substantial amount of diffuse subarachnoid blood may lead to a misleading "T2-like" intradural appearance on T1-weighted images. The subarachnoid clot does not enhance with contrast and may displace the nerve roots of the cauda equina, frequently periferally. Larger amounts of SSAH may sometimes be seen on CT as intradural focal hyperdense masses and/or increased attenuation of the CSF.

Differential Diagnosis

Subdural Hematoma

The blod clots are separated from the CSF usually by a number of septations, giving the peripheral crescentic "Mercedes star" sign on the axial MR images; there are no fluid–fluid levels and dark signal of the dura separates these collections from the epidural fat. Spinal subdural hematoma and SAH may be coexistent.

Epidural Hematoma

The hemorrhage is outside of the thecal sac, not clearly separated and sometimes indistinguishable from the epidural fat; there are no fluid–fluid levels, the epidural clot is usually found adjacent to spinal fractures and/or ligamentous injuries.

Neoplastic, Inflammatory, or Infectious Subarachnoid Dissemination

While a focal mass is frequently present at the bottom of the thecal sac, there are usually additional nodular lesions along the cauda equina; the lesions enhance with contrast and may show postcontrast "sugarcoating," representing diffuse leptomeningeal seeding.

Clinical Findings, Implications, and Treatment

Traumatic SSAH is very rare, most commonly occurring as a complication of spinal procedures such as spinal anesthesia and lumbar puncture, often associated with blood coagulation abnormalities. Traumatic intracranial hemorrhage can cause intraspinal bleed without any direct injury to the spine – traumatic SSAH is supposed to be caused by migration of intracranial SAH, primarily with a large amount of SAH or after early ambulation. The typical presentation is delayed new pain or neurologic deficit. "Lumbar sedimentation sign" on MRI has been described in patients with nonaneurysmal SAH.

Urgent decompressive surgery is the primary treatment for SSAH when the neurological state progressively deteriorates, while conservative management is an option for selected patients with minimal neurological impairment. Syringomyelia and arachnoid cysts associated with arachnoiditis are rare complications of SSAH.

Additional Information

SSAH makes up around or less than 1% of all the cases of subarachnoid bleed. The etiology includes vascular malformations, aneurysms, spinal cord tumors, and inflammatory diseases (and Behçet's disease). Very rare cases of idiopathic spinal SAH have also been described, which could be caused by rapid changes in intrathoracic and intra-abdominal pressure.

References

1 Kim TJ, Koh EJ, Cho KT. Spinal subarachnoid hemorrhage migrated from traumatic intracranial subarachnoid hemorrhage. *Korean J Neurotrauma* 2016;12:159–162.

2 Moore JM, Jithoo R, Hwang P. Idiopathic spinal subarachnoid hemorrhage: a case report and review of the literature. *Global Spine J* 2015;5:e59–e64. doi: 10.1055/s-0035-1546416.

3 Ishizaka S, Hayashi K, Otsuka M, et al. Syringomyelia and arachnoid cysts associated with spinal arachnoiditis following subarachnoid hemorrhage. *Neurol Med Chir (Tokyo)* 2012;52:686–690.

4 Crossley RA, Raza A, Adams WM. The lumbar sedimentation sign: spinal MRI findings in patients with subarachnoid haemorrhage with no demonstrable intracranial aneurysm. *Br J Radiol* 2011;84:279–281. doi: 10.1259/bjr/68122723.

(1A)

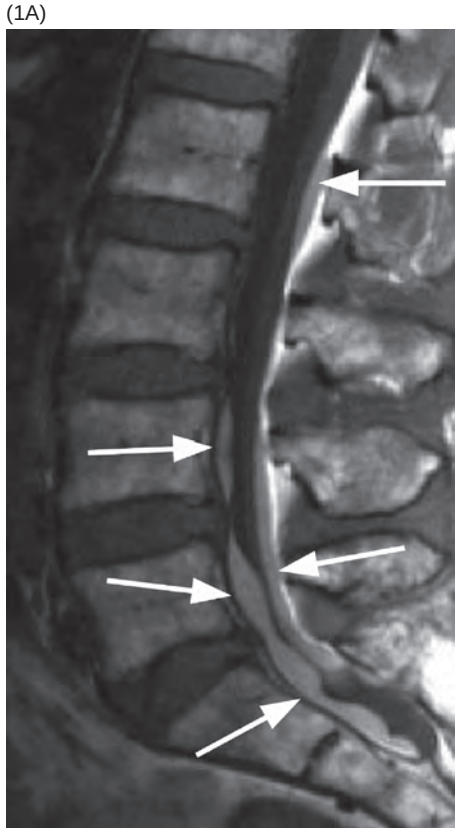

(1B)

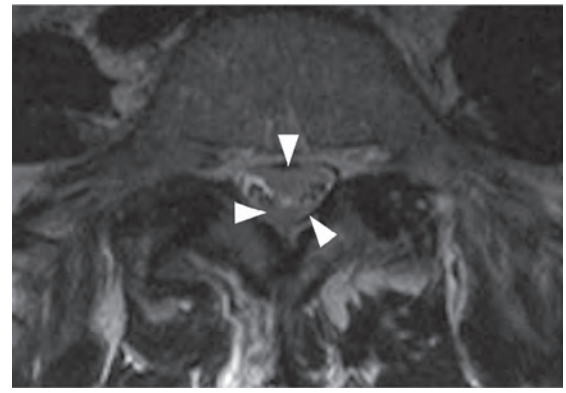

(1C)

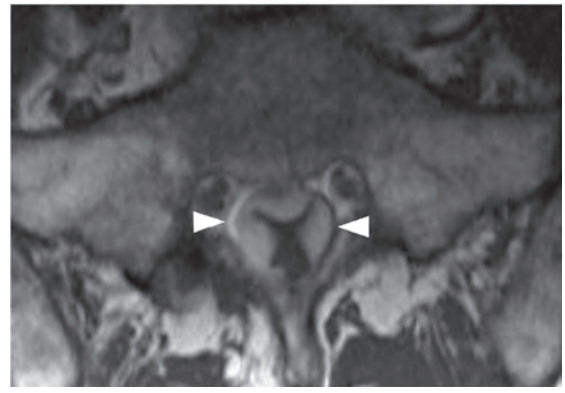

Figure 37.1 **A)** Sagittal T1w image demonstrates a hyperintense collection (arrows) in the lumbo-sacral spinal canal in this anticoagulated patient with sudden onset of back pain following minor trauma. **B)** Axial T2w image shows a hypointense collection confined to the subdural space (arrowheads), separate from the epidural fat. **C)** Axial T1w image depicts the intradural location of the hematoma and its typical multilobulated appearance, resembling an inverted Mercedes sign. Note chemical shift artifact (arrowheads).

(2A)

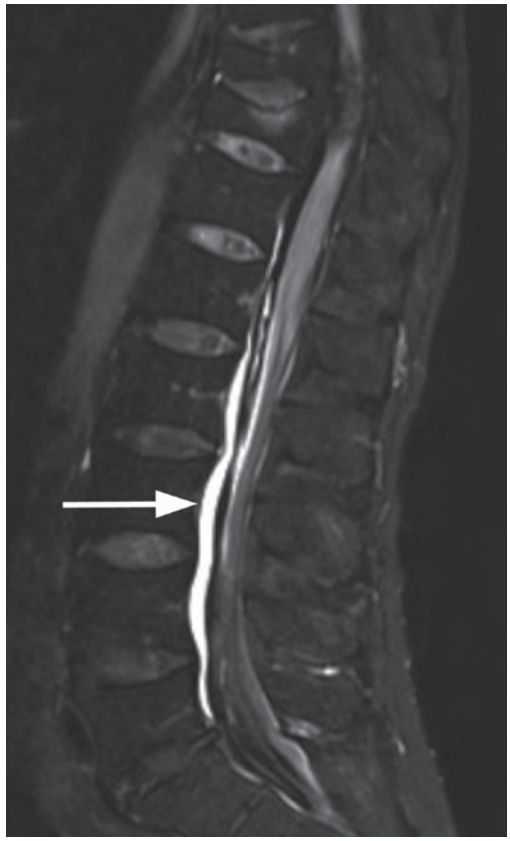

(2B)

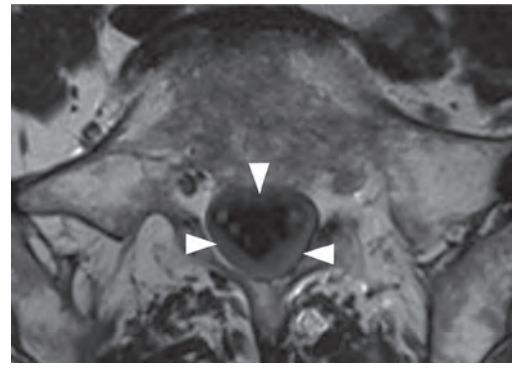

Figure 37.2 **A)** Sagittal fat-suppressed T2w image shows a stratified collection inside the spinal canal, very bright anteriorly (arrow) and dark more posteriorly and inferiorly. There are previous fractures of Th10 and Th11 vertebral bodies with mild bone marrow edema. **B)** Axial T2w image at the level of the sacrum reveals circumferential hypointense collection in the subdural space with a multilobulated appearance (arrowheads) confirming the subdural location of the hematoma. It also demonstrates diffusely hypointense CSF (resembling a T1-weighted image), confirming associated subarachnoid hemorrhage.

CASE 37 Spinal Subdural Hematoma

Daniela Distefano

Imaging Findings

Spinal subdural hematoma (SSH) has variable signal intensity on MRI: from T1 isointense to hyperintense and from hypointense to hyperintense on T2-weighted sequences. On T2*w (gradient echo) the lesions are darker, possibly with a peripheral black rim. For collections that are hyperintense on both T1w and T2w images, fat suppression may allow better delineation of the hematoma and differentiation from the epidural fat. Hematomas generally do not show significant enhancement, especially in the early stages; if present, the enhancement is linear and peripheral. To correctly localize the collection in the subdural space, it is important to visualize the epidural fat separated from the hematoma by the thin linear hypointense dura. If subdural hematomas are large enough, they show the typical multilobulated dural-based and frequently convex appearance on axial images ("Mercedes sign"), due to confinement with intradural septa. On CT, SSH may be hyperdense in the acute phase, distinct from the adjacent low-density epidural fat and silhouetted against the lower-density spinal cord and cauda equina, which it frequently compresses; there is lack of direct continuity with the adjacent osseous structures.

Differential Diagnosis

Epidural Hematoma (EDH)

Adjacent to osseous structures and not separated from the epidural fat/space.

Intradural Neoplasm

Dural tail, homogenous enhancement, low T2-signal, and calcifications are suggestive of meningioma, whereas heterogenous T2-bright enhancing mass extending across the intervertebral foramen is primarily consistent with a neural sheath tumor.

Clinical Findings, Implications, and Treatment

SSH may present with signs of spinal cord or cauda equina compression with an acute or progressive onset, which is preceded by back pain and/or radicular pain and paresthesia. The onset of symptoms may be delayed for days and even weeks after the traumatic event. Intracranial subdural hematoma or other traumatic injuries are frequently present. Back pain may also be the only symptom and SSHs may be chronic, usually following minor trauma. The necessity of surgical intervention versus conservative management should be carefully evaluated: the surgical treatment is generally performed in cases of progressive severe neurologic deficits while the conservative management is preferable in the presence of coagulopathy, with mild neurologic deficits, and when there is a rapid and progressive early improvement. SSH may be drained by lumbar puncture without surgical exploration. Emergency surgical decompression is usually the optimal treatment for a traumatic spinal subdural hematoma with acute deterioration and severe neurological deficits.

Additional Information

SSH can be caused by abnormalities of coagulation, underlying neoplasm and arteriovenous malformation, as well as invasive spinal procedures (including lumbar puncture and anesthetic procedures), more commonly than with trauma. Truly spontaneous SSH is very rare, usually occurring in the thoracic spine. One of the theories for the formation of spinal intradural hematomas suggests that they originate in the subarachnoid space and then extend subdurally.

References

1 Braun P, Kazmi K, Nogués-Meléndez P, Mas-Estellés F, Aparici-Robles F. MRI findings in spinal subdural and epidural hematoma. *Eur J Radiol* 2007;64:119–125.

2 Kreppel D, Antoniadis G, Seeling W. Spinal hematoma: a literature survey with meta-analysis of 613 patients. *Neurosurg Rev* 2003;26:1–49.

3 Küker W, Thiex R, Friese S, et al. Spinal subdural and epidural haematomas: diagnostic and therapeutic aspects in acute and subacute cases. *Acta Neurochir (Wien)* 2000;142: 777–785.

4 Post MJ, Becerra JL, Madsen PW, Puckett W, Quencer RM, Bunge RP, Sklar EM. Acute spinal subdural hematoma: MR and CT findings with pathologic correlates. *AJNR Am J Neuroradiol* 1994;15:1895–1905.

5 Abla AA, Oh MY. Spinal chronic subdural hematoma. *Neurosurg Clin N Am* 2000;11:465.

(1A)

(1B)

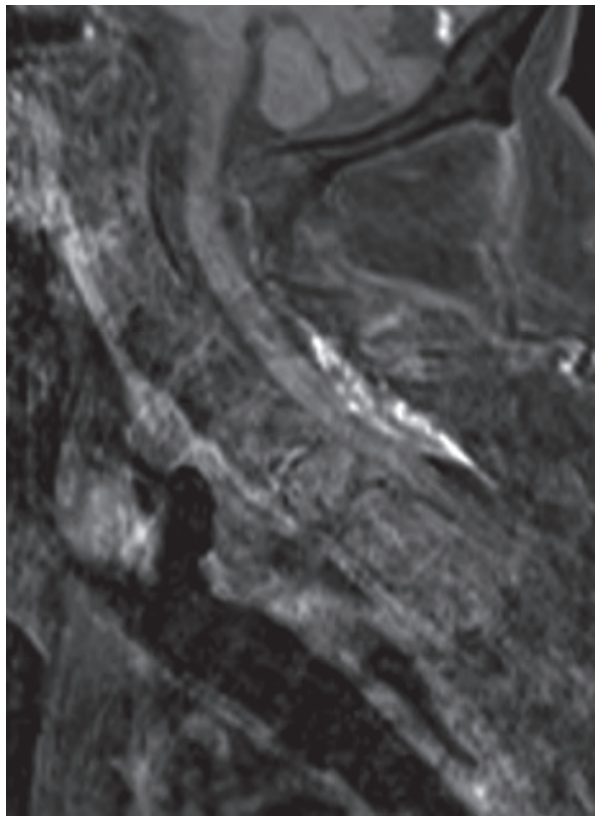

(1C)

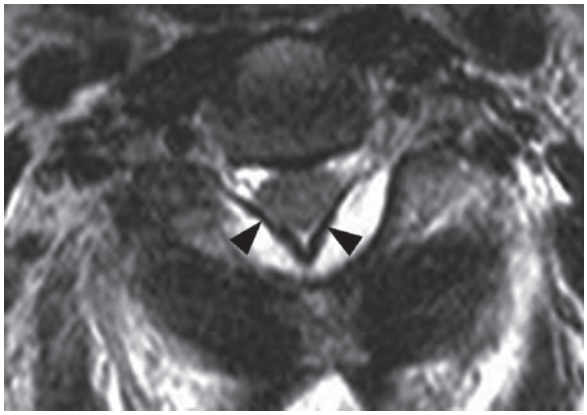

(1D)

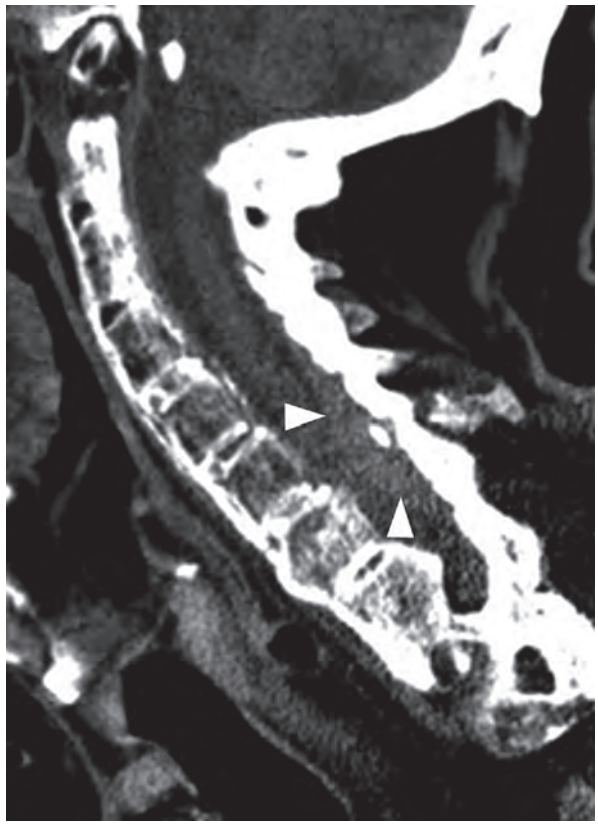

Figure 38.1 MRI of a sEDH obtained 4 days after spine trauma in a 72-year-old male with ankylosing spondylitis. **A)** Sagittal T2w MR image shows an extramedullary, markedly hypointense collection with convex margins (arrowheads) located in the dorsal aspect of the cervico-thoracic spinal canal. **B)** The corresponding T1w image with fat suppression demonstrates inhomogenous hyperintensity within the lesion, suggesting primarily methemoglobin content. **C)** Axial T2w image depicts displacement of the dura, seen as a dark rim (arrows). **D)** Sagittal-reformatted CT scan with soft tissue algorithm and window reveals the sEDH as a hyperdense mass relative to the remaining vertebral canal content, with sharply demarcated margins (arrowheads). A fractured syndesmophyte is also present.

CASE 38 Spinal Epidural Hematoma

Emanuele Pravatà

Imaging Findings

Spinal epidural hematomas (sEDHs) most commonly occur in the dorsal aspect of the cervical and thoracic spine, and usually extend over two to four vertebral segments. A ventral origin is less common due to the relatively firmer adherence of the dura to the posterior longitudinal ligament. Sagittal MR images typically show a convex collection displacing the dura into the central canal. Axial images may better reveal circumferential extension around the dural sac, and spinal cord compression, when present. The key differentiating finding is the continuity of the blood products with the epidural fat, in contrast to subdural hematomas, which are separated by the dark stripe of dura. As with other epidural masses, curtain sign is present with ventral epidural hematomas. MR signal characteristics within EDHs are variable and change over time, following blood products degradation steps. On post-contrast T1-weighted images, irregular areas of contrast enhancement may sometimes be seen, possibly reflecting active blood extravasation and/or encasement of epidural vessels and septa. T2-weighted images may demonstrate concomitant spinal cord hyperintensity, indicating edema/compression myelopathy, contusion, and/or infarction. Although MRI is the method of choice for the diagnosis, CT images with soft tissue algorithm and window may demonstrate larger sEDHs as hyperdense masses within the spinal canal.

Differential Diagnosis

Subdural Hematoma

Far less common; characteristic multilobulated appearance, separated from the epidural fat by the dark dural rim.

Epidural Abscess

Intense peripheral enhancement (sEDH may also enhance), more commonly ventral in location (look for associated discitis and/or spondylitis); no history of trauma.

Neoplasm

Masses originating from the vertebrae, enhance with contrast, commonly of an irregular shape; epidural lymphoma shows dense homogenous enhancement.

Clinical Findings, Implications, and Treatment

Symptoms include intense back pain, sensory and/or motor deficits related to the spinal cord compression level, and autonomic deficits such as acute urinary retention and/or incontinence. Paparesis, tetraparesis, or Brown-Séquard syndrome may develop within minutes, hours, or days. Lumbosacral sEDH may cause an acute cauda equina syndrome. Patients' outcome is mainly influenced by the severity of neurological deficits, presence of autonomic nervous system dysfunction, and evidence of spinal cord injury at MRI, even if the collection is promptly evacuated. Asymptomatic, clinically stable patients may not require any surgical treatment.

Additional Information

Bleeding in sEDH is generally venous in origin, as the spinal epidural space contains an extensive venous plexus, which receives tributaries from the vertebral bodies and spinal cord, and is particularly susceptible to sudden changes in pressure.

Most sEDH occur after trauma, although symptomatic cases may rarely occur as a complication of invasive spinal interventions, with multilevel lumbar procedures and/or preoperative coagulopathies being the most relevant risk factors. sEDH may occasionally occur spontaneously or in association with minor trauma, coagulopathies, and/or use of antiaggregation and anticoagulation therapy.

References

1 Chang FC, Lirng JF, Luo CB, et al. Evaluation of clinical and MR findings for the prognosis of spinal epidural haematomas. *Clin Radiol* 2005;60:762–770.

2 Boukobza M, Haddar D, Boissonet M, Merland JJ. Spinal subdural haematoma: a study of three cases. *Clin Radiol* 2001;56:475–480.

3 Kou J, Fischgrund J, Biddinger A, Herkowitz H. Risk factors for spinal epidural hematoma after spinal surgery. *Spine (Phila Pa 1976)* 2002;27:1670–1673.

4 Fukui MB, Swarnkar AS, Williams RL. Acute spontaneous spinal epidural hematomas. *AJNR Am J Neuroradiol* 1999;20:1365–1372.

(1A)

(1B)

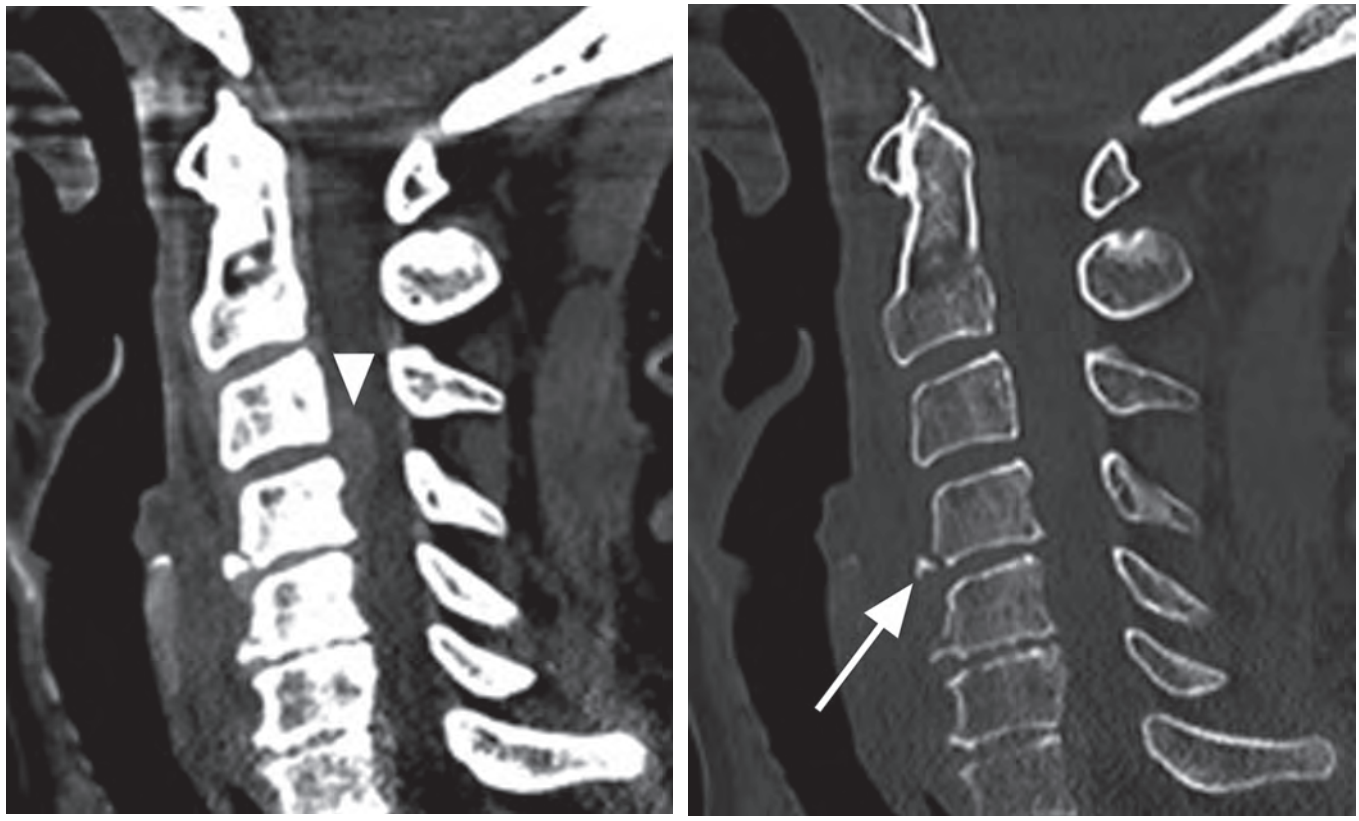

Figure 39.1 **A)** Sagittal soft tissue algorithm and window CT image demonstrates C3–C4 disc herniation (arrowhead). **B)** The associated C4 flexion teardrop fracture (arrow) is more conspicuous with the bone algorithm and window image.

(2A)

(2B)

(2C)

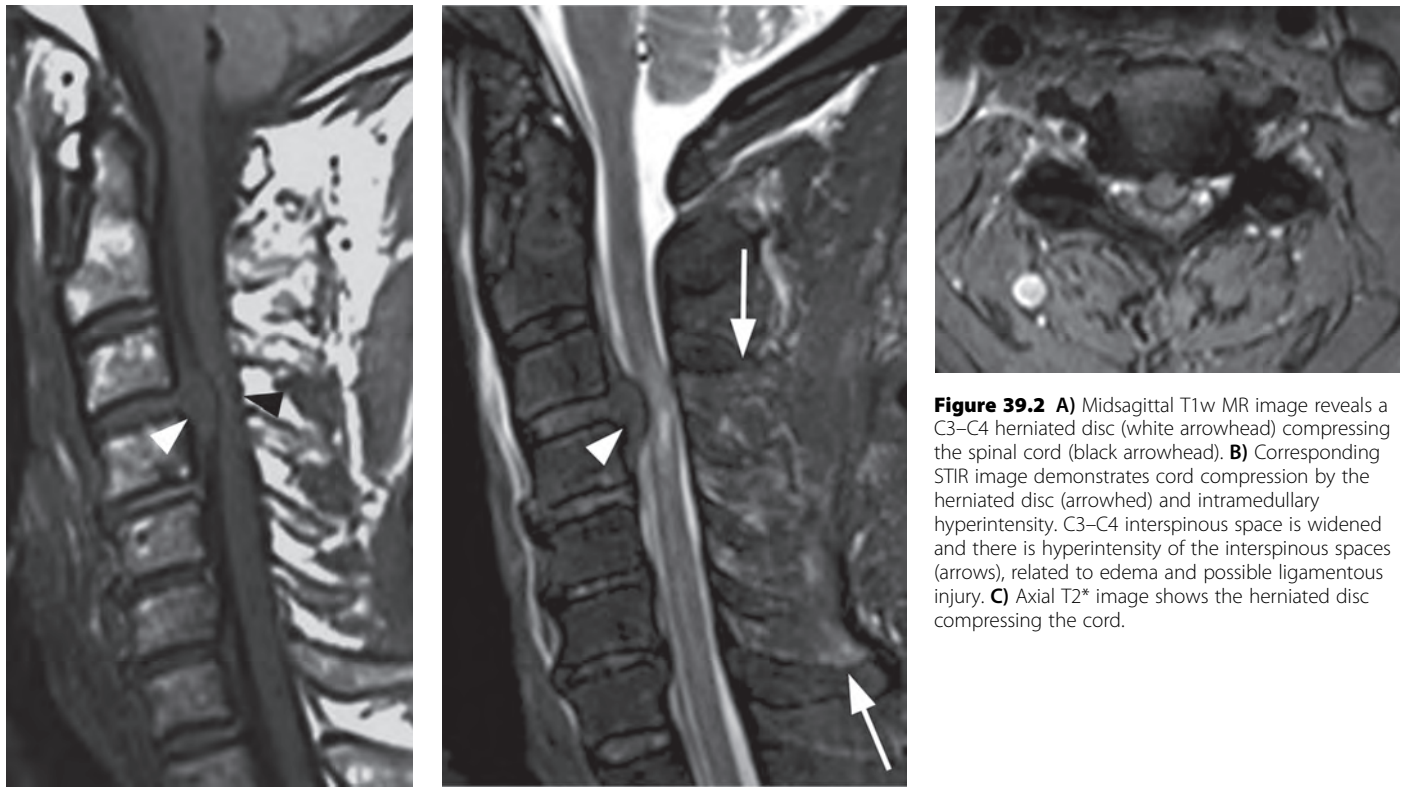

Figure 39.2 **A)** Midsagittal T1w MR image reveals a C3–C4 herniated disc (white arrowhead) compressing the spinal cord (black arrowhead). **B)** Corresponding STIR image demonstrates cord compression by the herniated disc (arrowhed) and intramedullary hyperintensity. C3–C4 interspinous space is widened and there is hyperintensity of the interspinous spaces (arrows), related to edema and possible ligamentous injury. **C)** Axial T2* image shows the herniated disc compressing the cord.

CASE 39 Traumatic Disc Herniation

Eytan Raz and Abhay Varma

Imaging Findings

Herniation is defined as a localized displacement of disc material beyond the limits of the intervertebral disc space; the disc material may be nucleus, cartilage, fragmented apophyseal bone, annulus, or any combination therein. When associated with trauma, the herniated disc is usually not desiccated and thus appears bright on T2-weighted and especially T2* gradient echo images. Traumatic disc herniations most commonly occur in the cervical spine and are almost always associated with other findings such as facet dislocation or soft tissue injury. In contrast to the degenerative lesions, which are typically found at C5–C6 and C6–C7 segments, traumatic herniations are more frequent at higher levels, primarily C3–C4. Thoracic and lumbar traumatic disc lesions are generally less frequent and with less severe consequences. While disc herniations are best evaluated with MRI, CT images with soft tissue algorithm and window will depict large cervical disc herniations (along with some other lesions), and these images should be reviewed carefully in all trauma patients. Acute traumatic disk herniation may not always be distinguished from a preexisting herniated disk on imaging studies, as degenerated discs may also show high T2 signal intensity. Alternatively, traumatic injuries may lead to (worsening) herniation of degenerated disc/disc-osteophyte complex.

Clinical Findings, Implications, and Treatment

Symptoms of a herniated disc can vary depending on the location of the herniation, and include local pain, radicular pain, radiculopathy, and myelopathy. The primary reason to consider early or immediate surgical treatment is when a patient develops radiculopathy and/or myelopathy from a herniated disc.

It has been reported that the risk of herniation increases with reduction of facet dislocation: during the reduction, the ruptured disc can extrude in the spinal canal, with neurological consequences. Diligent neurological monitoring is recommended during closed reduction of facet dislocation. Some authors recommend performing MRI prior to undertaking reduction of dislocation. Surgical management includes anterior decompression and stabilization with or without posterior stabilization.

Additional Information

Application of sudden and intense force on the discs could lead to disc herniation, at all spine levels. Examples of traumatic events that may lead to a herniated disc include a fall or sports injury that places sudden force on the upper back for thoracic herniations, and hyperflexion injuries of the neck for cervical herniations. The lumbar discs are not nearly as frequently involved as with degenerative disc changes. Traumatic disc herniations tend to occur more often in younger patients without signs of disc degeneration.

Cervical arthroplasty may yield similar improvement in clinical outcomes as the standard anterior cervical discectomy and fusion (ACDF) for a small group of selected patients with traumatic cervical disc herniation (without spinal cord injury, fracture, and instability), while preserving segmental mobility.

References

1 Fardon DF, Milette PC. Combined Task Forces of the North American Spine Society, American Society of Spine Radiology, and American Society of Neuroradiology. Nomenclature and classification of lumbar disc pathology. Recommendations of the Combined task Forces of the North American Spine Society, American Society of Spine Radiology, and American Society of Neuroradiology. *Spine (Phila Pa 1976)* 2001;26:E93–E113.

2 Maiman DJ, Barolat G, Larson SJ. Management of bilateral locked facets of the cervical spine. *Neurosurgery* 1986;18:542–547.

3 Williams AL, Haughton VM, Daniels DL, Grogan JP. Differential CT diagnosis of extruded nucleus pulposus. *Radiology* 1983;148:141–148.

4 Lurie JD, Tosteson AN, Tosteson TD, et al. Reliability of magnetic resonance imaging readings for lumbar disc herniation in the Spine Patient Outcomes Research Trial (SPORT). *Spine* 2008;33:991–998.

5 Chang HK, Huang WC, Wu JC, et al. Cervical arthroplasty for traumatic disc herniation: an age- and sex-matched comparison with anterior cervical discectomy and fusion. *BMC Musculoskelet Disord* 2015;16:228.

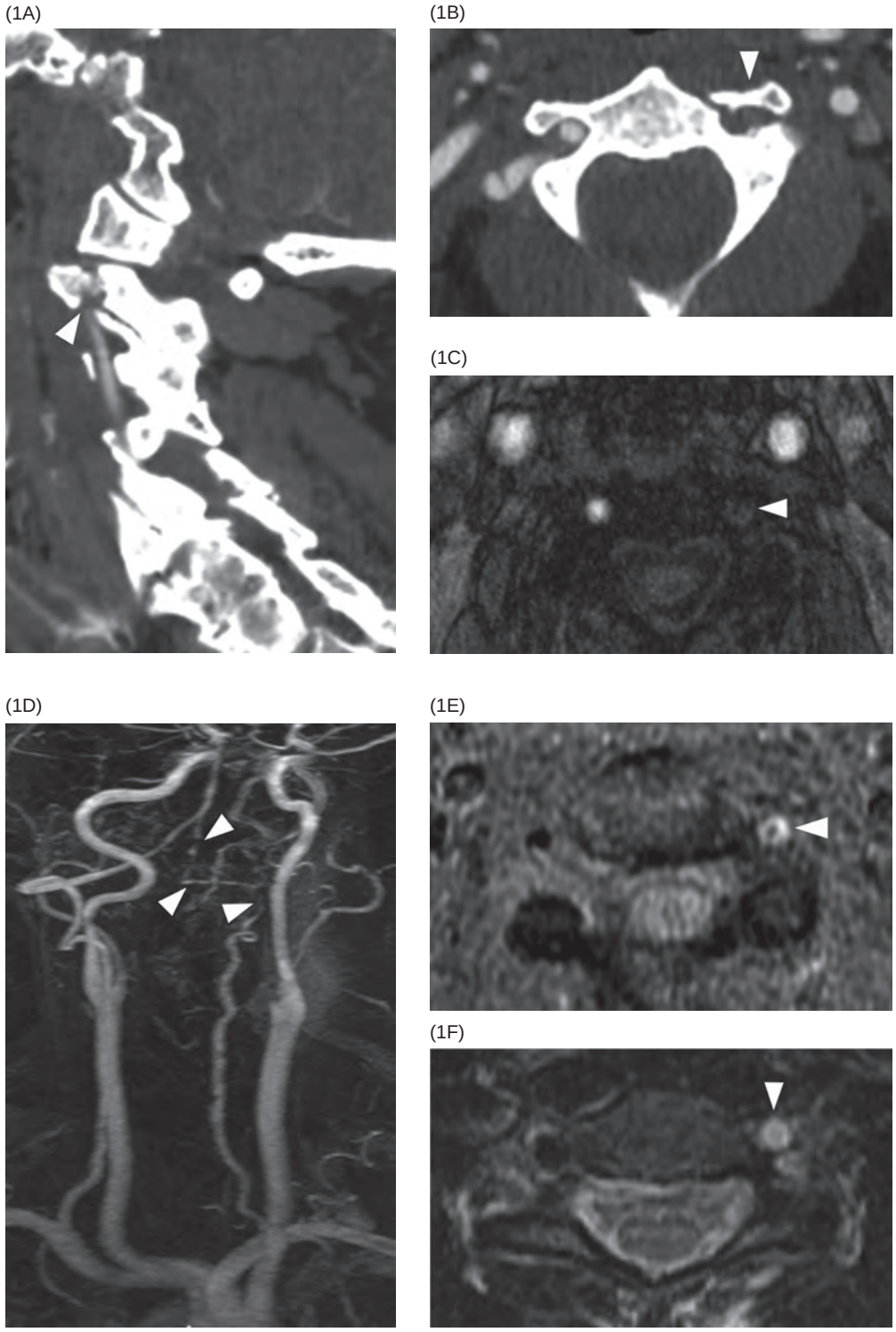

Figure 40.1 Sagittal **(A)** and axial **(B)** CTA images show abrupt occlusion of the left vertebral artery (arrowheads) related to C2 fractures. **C)** Axial MRA source image shows normal flow–related enhancement of the bilateral internal carotid arteries and right vertebral artery, while the left vertebral artery is occluded (arrowhead). **D)** Coronal oblique MIP from MRA shows irregularity of the left vertebral artery in the extra-cranial and intra-cranial segment consistent with long segment dissection (arrowheads). **E)** Axial fat-saturated T1-weighted image at the C2–3 level confirms absence of normal flow-void signal in the left vertebral artery with T1 hyperinensity related to intramural hemorrhage (arrowhead). **F)** The absence of normal flow void and hyperintensity of the thrombosed left vertebral artery (arrowhead) is clearly seen on standard axial FSE T2-weighted image.

CASE 40 Vertebral Artery Injury

Vikas Agarwal and Alessandro Cianfoni

Imaging Findings

Although conventional catheter angiography is still considered the standard of reference, CTA with multiplanar reconstructions is the preferred modality for vertebral artery evaluation in traumatized patients. Luminal irregularity with <25% stenosis is considered a grade I injury, while >25% luminal narrowing or a raised intimal flap are grade II injuries. Pseudoaneurysms are grade III injuries; complete occlusion (grade IV) and transection with free extravasation of contrast (grade V) can also be seen. Associated fractures and/or dislocations are almost always present. MRI has the advantage of early recognition of cerebral ischemia and can be performed in conjunction with the cervical spine exam. Standard FSE T2-weighted axial images will frequently show absence of normal flow void and hyperintensity related to intramural hemorrhage within the affected vessel, which may be even better seen with fat-saturated T1-weighted axial images, but they may be degraded by artifacts and the perivertebral venous plexus might at times be misinterpreted as mural hematoma. Conventional catheter angiography will show luminal changes (aneurysmal dilatation, stenosis) and/or occlusion.

Arterial dissection is a lesion of the arterial wall, which affects the vessel lumen. Catheter angiography offers the best display of the luminal changes but does not give information on the vessel wall. MRI offers the best information on the arterial wall and depicts gross narrowing of the lumen. CTA is more accurate than MRI for luminal changes and less accurate for mural hematoma depiction, seen as an eccentric soft tissue density thickening the vessel wall.

Differential Diagnosis

Extra-Cranial Atherosclerosis

Multiple vessels with irregular stenosis, intimal plaque.

Fibromuscular Dysplasia

Multiple focal strictures with a "string of beads" appearance or long segment stenosis.

Vasculitis

Irregular stenosis affecting multiple vessels of varying sizes.

Clinical Findings, Implications, and Treatment

The majority of patients with vertebral artery injury are asymptomatic. In symptomatic patients, clinical findings related to vertebrobasilar ischemia will be seen including vertigo and nystagmus, dysphagia and dysarthria, diplopia or blurred vision, and altered consciousness. Symptoms usually manifest in the first 24 hours after injury; however, the interval between injury and neurological symptoms may be delayed up to 3 months. Nondominant unilateral vertebral artery injuries rarely result in neurologic deficits. Patients with bilateral or dominant vertebral artery injury have high morbidity and mortality rates. Treatment strategies are geared toward maintenance of flow of the unaffected vertebral artery and prevention of thrombus propagation in the injured vessel. Therefore, early stabilization of the spine is paramount. Anticoagulation or antiplatelet agents can be considered for treatment of symptomatic patients and used for asymptomatic ones, always weighted against the relative risk of bleeding.

Additional Information

Fixation within the transverse foramen makes the V2 segment (usually from C6 to C2) more vulnerable to injury caused by cervical spine trauma and is therefore most frequently involved. The role of endovascular therapy in patients with vertebral artery injury has yet to be defined, but stenting is sometimes considered to preserve or restore flow in injured dominant vertebral arteries.

References

1 Biffl WL, Moore EE, Elliott JP, et al. The devastating potential of blunt vertebral arterial injury injuries. *Ann Surg* 2000;231:672–681.

2 Burlew CC, Biffl WL, Moore EE, et al. Blunt cerebrovascular injuries: redefining screening criteria in the era of noninvasive diagnosis. *J Trauma Acute Care Surg* 2012;72:330–335.

3 Harrigan MR, Hadley MN, Dhall SS, et al. Management of vertebral artery injuries following non-penetrating cervical trauma. In: Guidelines for the management of acute cervical spine and spinal cord injuries. *Neurosurgery* 2013;72(Suppl 2):234–243.

4 Provenzale JM, Sarikaya B. Comparison of test performance characteristics of MRI, MR angiography, and CT angiography in the diagnosis of carotid and vertebral artery dissection: a review of the medical literature. *AJR Am J Roentgenol* 2009;193:1167–1174.

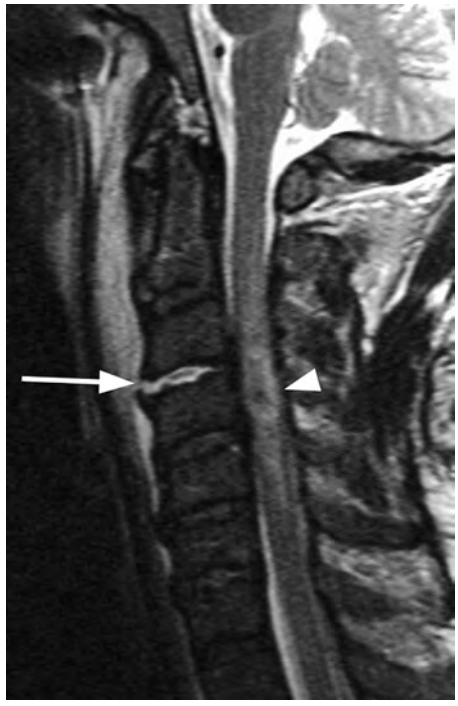

Figure 41.1 Midsagittal STIR image demonstrates disruption of the anterior longitudinal ligament (ALL, arrow) in this patient with hyperextension injury. Note prevertebral edema/hematoma and hemorrhagic contusion of the spinal cord (arrowhead).

Figure 41.2 Midsagittal STIR image shows disruption of both ALL (arrow) and ligamentum flavum (LF, arrowheads) at C5–C6.

Figure 41.3 Sagittal STIR image reveals facet joint capsule injury at C6–C7 (arrowhead) and possibly adjacent levels.

(4A)

(4B)

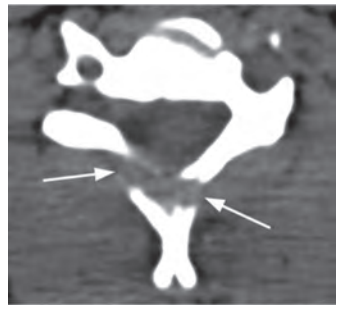

(4C)

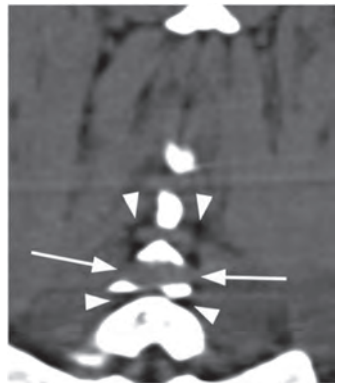

Figure 41.4 **A)** Midsagittal STIR image reveals disrupted LF (arrows) and injury of the posterior soft tissues (arrowheads) in this patient with C6 spinous process fracture. **B)** Axial and **C)** coronal CT images reveal loss of the paraspinal fat pads around the fractured spinous process (arrows). Note normal fat pads at adjacent levels (arrowheads).

Figure 41.5 Midsagittal STIR image in a patient with Chance-type injury reveals injury to T12–L1 LF (arrowheads), supraspinous ligament (arrow), and the entire posterior ligamentous complex.

CASE 41 Ligamentous Injury

Doris Dodig and Zoran Rumboldt

Imaging Findings

Signs of ligamentous injury on MRI are a focal discontinuity and high T2 signal of the hypointense fibrous band. While T2 hyperintensity, best seen on T2-weighted images with fat suppression (STIR or fat-saturated T2w), is the most sensitive sign, disruption of the hypointense ligament (primarily on T1-weighted, but also other images) is the most specific and very reliable.

Anterior longitudinal ligament (ALL) is the most commonly affected soft tissue structure in hyperextension injury, almost exclusively occurring in the cervical spine, followed by the disc and posterior longitudinal ligament (PLL). ALL injury is inferred on radiography and CT with thickening of the prevertebral soft tissues, widening of the anterior disc space, triangular avulsion of the antero-superior vertebral body corner, and spondylolisthesis.

Ligamenta flava (LF), facet capsules, interspinous ligament, and supraspinous ligament (SSL) form the posterior ligamentous complex (PLC), which is affected with flexion and distraction injuries, especially common in the thoracic and lumbar spine. The most reliable indirect signs of PLC injury on radiographs and CT images are increased distance between the spinous processes, focal kyphosis, and diastasis of facet joints. Obliteration of the paraspinal fat pad on CT has been recently described as a sign of PLC injury with a high specificity and positive predictive value. Ultrasound has a high accuracy for PLC injuries in thoracolumbar spine and may be considered when MRI is unavailable or contraindicated, or when the findings are inconclusive.

Differential Diagnosis

Traumatic Disc Herniation

Intact ALL or PLL are continuous hypointense bands detached from vertebral bodies by the herniated disc that typically shows high T2 signal.

Nonspecific Hyperintense Soft Tissue Areas on STIR

Clinical Findings, Implications, and Treatment

MRI is performed in patients with acute spine trauma for two reasons: evaluation of spinal cord and ligamentous integrity in symptomatic patients with negative CT and/or radiographs and management guidance, which includes preoperative planning in patients with unstable cervical fractures on other imaging studies, and decision whether surgery is needed in patients with thoracolumbar injuries.

The radiological findings of ligamentous injury in the cervical spine may be subtle and yet associated with severe neurologic deficit, particularly central cord syndrome with extension injuries and anterior cord syndrome with hyperflexion, as ligaments are essential for maintaining spinal stability. They are also important for surgical planning, especially if cervical posterior fusion is considered – unnoticed injuries of the ALL, PLL, and disk place the patient at risk for progressive spinal cord compression during the posterior approach surgery. Integrity of the SSL and FL appear to be crucial for PLC stability, and their disruption on MRI has been found to have the best accuracy for unstable PLC injury.

Additional Information

In patients with spinal cord injury without CT evidence of trauma (SCIWOCTET, instead of the old term SCIWORA), which occurs in children but also in adults, disruption of the LF or ALL, in addition to the cord lesion length, appear to be negative outcome predictors indicating lack of neurological improvement.

The hyperflexion sprain injuries with high T2 signal of the posterior soft tissues and bone marrow contusions, which are detected only on MRI, are of indeterminate clinical significance, and it remains unclear if any treatment is required in these patients.

References

1 Dundamadappa SK, Cauley KA. MR imaging of acute cervical spinal ligamentous and soft tissue trauma. *Emerg Radiol* 2012;19:277–286.

2 Benedetti P, Fahr LM, Kuhns LR, et al. MR imaging findings in spinal ligamentous injury. *AJR* 2000;175:661–665.

3 Molière S, Zaragori-Benedetti C, Ehlinger M, et al. Evaluation of paraspinal fat pad as an indicator of posterior ligamentous complex injury in cervical spine trauma. *Radiology* 2017;282:790–797.

4 Gabriel AC, Angel JP, Juan JG, et al. Diagnostic accuracy of ultrasound for detecting posterior ligamentous complex injuries of the thoracic and lumbar spine: a systematic review and meta-analysis. *J Craniovertebr Junction Spine* 2013;4:25–31.

5 Pizones J, Sánchez-Mariscal F, Zúñiga L, Álvarez P, Izquiredo E. Prospective analysis of magnetic resonance imaging accuracy in diagnosing traumatic injuries of the posterior ligamentous complex of thoracolumbar spine. *Spine (Phila Pa 1976)* 2013;38:745–751.

6 Martinez-Perez R, Munarriz PM, Paredes I, Cotrina J, Lagares A. Cervical spinal cord injury without computed tomography evidence of trauma (SCIWOCTET) in adults: MRI prognostic factors. *World Neurosurg* 2017;99:192–199.

(1A)

(1B)

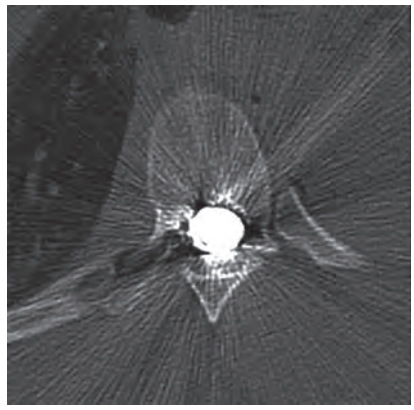

(1C)

Figure 42.1 Sagittal **(A)** and axial **(B, C)** CT images of a gunshot wound (GSW) to the thoracic spine – the bullet is within the spinal canal, with more inferiorly located smaller fragments (arrow). The findings are indicative of spinal cord transection.

(2A)

(2B)

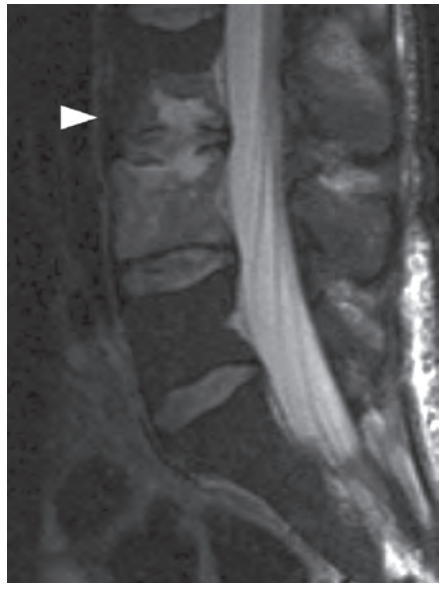

Figure 42.2 **A)** Sagittal CT image in a different patient with a GSW demonstrates tiny metallic fragments lodged within the anterior aspect of L4 vertebral body and associated cortical defect (arrow). **B)** Corresponding STIR MR image shows that the injury is more extensive and involves the adjacent L3–L4 intervertebral disc and L3 vertebral body (arrowhead).

CASE 42 Penetrating Injuries of the Spine

Zoran Rumboldt and Abhay Varma

Imaging Findings

Penetrating trauma may be either missile (most typically gun-related) or non-missile (most typically knife-related). Gunshot wounds (GSW) and other metallic foreign bodies are readily identified on radiographs and CT images. CT also shows associated fractures and dislocations, while MRI is needed for evaluation of spinal cord (and other soft tissue) injuries. MRI detects contusions and hematomas resulting from direct penetration and indirect concussion effects as well as cord compression, but may not be performed for safety reasons if metallic foreign bodies are present. Air bubbles, bone fragments, and small metallic fragments may give rise to susceptibility artifacts on MRI, obscuring the anatomy and/or mimicking lesions. Due to their density and radiologic properties, wood and glass are typically overlooked on radiographs but well depicted on CT and MRI.

Differential Diagnosis

Surgical Hardware

Characteristic shape and imaging appearance of these objects, such as screws, rods, wires, vascular clips, etc.

Foreign Bodies from Remote Injuries

The presence of these foreign bodies is frequently known; typically an incidental finding not associated with acute traumatic injury.

Clinical Findings, Implications, and Treatment

The goals of treatment are to ensure spine stability, minimize the extent of neurologic deficit, and prevent further loss of function. Penetrating injuries of the spinal cord have a higher morbidity and mortality compared to blunt injuries secondary to associated visceral injuries, of neck, chest and abdomen. There is an increased risk of mechanical instability in patients with cervical GSW-induced spinal cord injury. Not all civilian spinal gunshot injuries require surgical intervention. Canal compromise (by bone, bullet fragment, or hematoma) with incomplete deficit, cauda equina injury, mechanical instability, infection, and persistent external CSF fistula are the main indications for surgery.

Additional Information

GSW to the spine accounts for 13–17% of all gunshot injuries and occurs predominantly in the thoracic region in civilian practice. Penetrating injury is the cause of about half of all spinal cord injuries in urban centers. The rate of complete spinal cord injury in cervical GSW is about 70%, similar to the rate of incomplete injury with lumbosacral injuries. The extent of injury depends on ballistics, the degree of transection and contusion of the cord, the degree of concussive blast injury, compression of the cord by hematoma or displaced bone fragments, disruption of the vasculature, and the mechanical stability of the involved segment. GSW without direct cord injury may lead to complete paraplegia, likely due to the emission of kinetic energy by the missile to the surrounding tissue. Blast injuries and high-velocity GSW to the spine encountered by military surgeons tend to be more destructive and more readily require exploration.

Penetrating spinal injuries due to knives or other sharp objects are much less common. The lower cervical and thoracic regions are most commonly affected due to assaults from behind; the patients frequently present with Brown-Séquard-type syndrome (ipsilateral motor and proprioception loss and contralateral pain and temperature loss).

References

1 Rosenfeld JV, Bell RS, Armonda R. Current concepts in penetrating and blast injury to the central nervous system. *World J Surg* 2015;39:1352–1362. doi: 10.1007/s00268-014-2874-7.

2 Brywczynski JJ, Barrett TW, Lyon JA, Cotton BA. Management of penetrating neck injury in the emergency department: a structured literature review. *Emerg Med J* 2008;25:711–715. doi: 10.1136/emj.2008.058792.

3 Moyed S, Shanmuganathan K, Mirvis SE, et al. MR imaging of penetrating spinal trauma. *AJR Am J Roentgenol* 1999;173:1387–1391.

SECTION **4**

Thoracolumbar Trauma Classification

Cases

(1A)

(1B)

Figure 43.1 A) Sagittal CT image shows L1 burst fracture with significant height loss and large fracture fragment within the spinal canal (arrowhead), as well as a mild compression fracture involving the superior T12 endplate without significant retropulsion (arrow). **B)** Corresponding STIR MR image reveals bone marrow edema of T11 and L2 vertebral bodies (arrowheads), consistent with bone contusions (microfractures). There is indeterminate disruption of the posterior ligamentous complex (PLC, arrow) and severe spinal canal stenosis with compression of the lower thoracic spinal cord/conus medullaris, which has abnormal signal consistent with hemorrhagic and nonhemorrhagic cord injury. TLICS imaging score 2 + 2 + 2 (or 3 for cord injury) = 6 (or 7), directed to surgical management.

(2A)

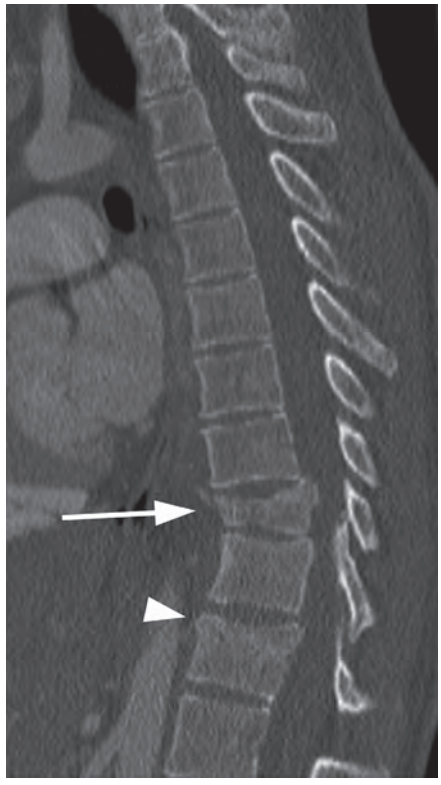

(2B)

Figure 43.2 A) Sagittal CT image demonstrates T10 burst fracture (arrow) with significant height loss, wedging (resulting in mild kyphotic deformity), and displacement of the posterior vertebral body into the spinal canal. There is a more subtle compression fracture inlvoing the superior endplate of T12 (arrowhead) without significant retropulsion. **B)** Corresponding MR STIR image confirms the CT findings. Additional vertebral body bone contusions (arrowheads) are noted, but no evidence for PLC injury. Although there is mild canal stenosis at T10 level, there is no frank spinal cord compression or abnormal intramedullary signal. TLICS imaging score 2 + 0 = 2, nonsurgical treatment as the patient was neurologically intact.

CASE 43 TLICS Scoring and Compression/Burst Injury

Vikas Agarwal and Russel Chapin

The thoracolumbar injury classification system (TLICS) identifies three major injury characteristics to describe thoracolumbar spine injuries: (1) injury morphology; (2) posterior ligamentous complex (PLC) integrity; and (3) neurological status. Within each category, there are subgroups with a numeric value assigned to each injury pattern, which are then totaled to provide a comprehensive score.

In addition, minor injury characteristics such as injury level, confounding variables (such as ankylosing spondylitis), multiple injuries, and chest wall injuries are also identified. Each major characteristic is assigned a numerical score, weighted by severity of injury, which is then summated to yield the injury severity score.

Imaging Findings

Two of the three major categories are assessed on the imaging studies: injury morphology, and PLC integrity.

Imaging Morphology: Compression injuries result from axial loading and are the most common. TLICS assigns one point for a compression fracture with visible loss of height or disruption of the vertebral endplate. An additional point is assigned if there is involvement of the posterior vertebral body with retropulsion (burst fracture). Translational/rotational injuries are the second subcategory. Rotation of the spinous processes, unilateral or bilateral facet fracture-dislocation, and vertebral subluxation can be seen. Because torsional and/or shear forces cause significant ligamentous and/or osseous damage and instability, TLICS assigns three points to this morphology. The third subcategory is related to distraction injuries and is assigned four points, identified as dissociation through the anterior/posterior ligaments and/or osseous elements.

Posterior Ligamentous Complex (PLC): The PLC can be evaluated using radiographs, CT, or MRI. On radiographs or CT, the PLC is considered disrupted if there is splaying of the spinous processes, avulsion fracture of the superior/inferior aspects of contiguous spinous processes, widening of the facet joints, naked facets, perched/dislocated facets, or vertebral body translation/rotation. MRI with fluid-sensitive sequences (STIR and fat-saturated T2w) allows for direct PLC visualization. The signs of injury are disruption of the normally dark T1/T2 stripe on sagittal images, fluid within facet capsules, or interspinous edema. Disruption of the ligamentous dark band on T1-weighted images is the most reliable and specific. If the PLC is intact, the TLICS assigns zero points. Indeterminate disruption is given two points and complete disruption is assigned three points.

Clinical Findings, Implications, and Treatment

Neurologic Status: There are five categories of neurologic injury: intact (zero points), nerve root injury (two points), complete spinal cord injury (two points), incomplete spinal cord injury (three points), and cauda equina syndrome (three points). Although evaluation requires thorough neurological examination, MR imaging can help identify the presence of nerve root and spinal cord injury.

The total TLICS score is calculated by adding the assigned points in the three categories. Patients with 0–3 points are considered nonoperative candidates. Patients with $\geq$5 points are directed to surgical management. Patients with a total score of 4 are considered indeterminate, and treatment may be surgical and/or nonsurgical, depending on clinical and functional status, including comorbidities and other traumatic injuries.

Additional Information

AO Spine System is another contemporary classification of the thoracolumbar trauma, which also focuses on the injury morphology but is used primarily to describe injuries and does not account for the patients' neurological status.

References

1 Lee JY, Vaccaro AR, Lim MR, et al. Thoracolumbar injury classification and severity score: a new paradigm for the treatment of thoracolumbar spine trauma. *J Orthop Sci* 2005;10:671–675.

2 Khurana B, Sheehan SE, Sodickson A, et al. Traumatic thoracolumbar spine injuries: what the spine surgeon wants to know. *Radiographics* 2013;33: 2031–2046.

3 Gupta R, Mittal P, Sandhu P, et al. Correlation of qualitative and quantitative MRI parameters with neurologic status: a prospective study on patients with spinal trauma. *J Clin Diag Res* 2014;8:RC13–RC17.

4 Pizones J, Sanchez-Mariscal F, Zuniga L, et al. Prospective analysis of magnetic resonance imaging accuracy in diagnosing traumatic injuries of the posterior ligamentous complex of the thoracolumbar spine. *Spine* 2013;38:745–751.

5 Schroeder GD, Harrop JS, Vaccaro AR. Thoracolumbar trauma classification. *Neurosurg Clin N Am* 2017;28:23–29.

(1A)

(1B)

Figure 44.1 **A)** Sagittal CT image of the lumbar spine in a 32-year-old patient after a tree fell on him. There is 30% anteriorlisthesis of L2 on L3, which measured 11 mm on the right and 15 mm on the left. **B)** On a coronal CT image there is rightward listhesis of L2 measuring 10 mm. Facet fracture dislocation was present bilaterally. While suggested by the provided coronal image, counterclockwise rotation of L2 relative to L3 was more apparent on sequential axial images. Imaging findings are consistent with a translation and rotation injury. Patient presented with near-complete motor and sensory loss in the legs and cauda equina symptoms. After posterior decompression and fusion, the patient gradually regained near-full strength with minimal intermittent bladder dysfunction.

(2A)

(2B)

Figure 44.2 **A)** Midsagittal CT image in a 34-year-old patient after a fall from a ladder shows a compression fracture of T11 vertebral body with a burst component. There is 6 mm of anteriolisthesis of T10. Fracture through the spinous processes is noted at T9 and T10 without splaying. Spinous process fractures are equivalent to PLC injury, but there is no evidence of a distraction mechanism. **B)** Sagittal CT image demonstrates a jumped facet with a small fracture fragment. The patient experienced mild senory loss in the bilateral lower extremities, had a combined TLICS of 10 (3 fracture morphology + 4 PLC integrity + 3 neurologic status), and underwent posterior decompression and fusion.

CASE 44 TLICS Translation or Rotation Injury

Russel Chapin and Zoran Rumboldt

Imaging Findings

In order to maximize standardization in the treatment and prognosis of thoracolumbar spine injuries, the morphology of injuries described by TLICS (thoracolumbar injury classification and severity score) is based on objective radiographic findings. In the presence of more than one injury morphology, the morphology yielding the higher score is used. Translation/rotation injuries within the TLICS scheme are most typified by unilateral or bilateral facet dislocations with or without facet fractures. Burst or compression fractures with anterolisthesis should be scored as translation/rotation injuries. Translation injuries with significant widening of the anterior disc space from hyperextension and anterior ligament disruption or significant kyphosis from posterior ligamentous disruption are scored as disctraction type injuries under TLICS.

Table 44.1 Scoring based on injury morphology according to the thoracolumbar injury classification and severity score (TLICS).

Injury Morphology	Points
Compression	1
Burst	2
Translation or Rotation	3
Distraction	4

Clinical Findings, Implications, and Treatment

While thoracolumbar fractures may be seen in elderly and osteoporotic patients after minor trauma, listhesis is almost always secondary to an MVC or fall from height. Because of the mechanism, these patients generally undergo contrast-enhanced whole body CT to assess for thoracic aortic or solid organ injury and vertebral or pelvic fracture. If traumatic listhesis is detected on radiographs, CT is indicated for further evaluation. MRI is performed to evaluate for spinal canal compromise, spinal cord lesion, and integrity of the posterior ligamentous complex (PLC). A thorough neurologic exam with attention to evidence of nerve root or spinal cord injury and cauda equina syndrome is mandatory. Injury morphology, PLC integrity, and clinical neurologic status determine the TLICS.

Patients with a TLICS of 3 or less are generally treated nonoperatively, while a score of 5 or more is usually managed surgically. Dislocated facets and translational injuries are almost invariably accompanied by PLC injury, therefore these patients will essentially all have a TLICS of 5+ and undergo surgery. Progressive cord compromise is a strong indication for nonconservative management.

Additional Information

Prior spine injury classification systems have inferred a mechanism (e.g., flexion) based on imaging findings. The Denis 3-column model emphasizes the integrity of anatomic structures and is widely recognized. However, the Denis model has shown only fair to good reproducibility and does not provide significant prognostic or therapeutic information. The TLICS has shown good intra- and inter-reader reproducibilty for scoring injuries and approximately 90% agreement for operative vs. nonoperative treatment. Recently proposed AOSpine Classification and Injury Severity System has been found to have an even better interrater and intrarater reliability for identifying fracture morphology, compared to the TLICS. Further studies are needed to evaluate the reliability and clinical significance of the classification systems.

References

1 Vaccaro AR, Lehman RA Jr, Hurlbert RJ, et al. A new classification of thoracolumbar injuries: the importance of injury morphology, the integrity of the posterior ligamentous complex, and neurologic status. *Spine (Phila Pa 1976)* 2005;30:2325–2333.

2 Khurana B, Sheehan SE, Sodickson A, Bono CM, Harris MB. Traumatic thoracolumbar spine injuries: what the spine surgeon wants to know. *Radiographics* 2013;33:2031–2046. doi: 10.1148/rg.337135018.

3 Patel AA, Vaccaro AR. Thoracolumbar spine trauma classification. *J Am Acad Orthop Surg* 2010;18:63–71.

4 Lewkonia P, Paolucci EO, Thomas K. Reliability of the thoracolumbar injury classification and severity score and comparison with the Denis classification for injury to the thoracic and lumbar spine. *Spine (Phila Pa 1976)* 2012;37:2161–2167. doi: 10.1097/BRS.0b013e3182601469.

5 Kaul R, Chhabra HS, Vaccaro AR, et al. Reliability of AOSpine thoracolumbar spine injury classification system and Thoracolumbar Injury Classification and Severity Score (TLICS) for thoracolumbar spine injuries: results of a multicentre study. *Eur Spine J* 2017;26:1470–1476. doi: 10.1007/s00586-016-4663-5.

Figure 45.1 Sagittal CT image shows a fracture of L1 with anterior compression and preserved posterior cortex of the vertebral body. There is mild anteriorlisthesis of L1, which would upstage this to a translation injury. However, there is clear posterior interspinous splaying (arrowhead), making this a distraction type injury (TLICS morphology score of 4). As there is at least suspected posterior ligamentous complex (PLC) disruption, the imaging score is at least 6 – the patient was treated surgically.

(2A)

(2B)

(2C)

Figure 45.2 **A)** CT was performed on a 53-year-old male after MVC with back pain and no neurologic deficit. Sagittal CT image shows anterior widening of the disc space between T8 and T9 (arrow) consistent with a distraction injury. The posterior disc space at T8–T9 is more subtly widened compared to the level above and below. **B)** Sagittal T2w MRI shows disruption of the anterior longitudinal ligament, disc, and, more subtle, posterior longitudinal ligament. There is also disruption of ligamentum flavum (arrow). Using the Denis 3-column concept, all three columns are disrupted. **C)** Corresponding STIR image is degraded by poor signal to noise. There is high signal in the interspinous space (arrow), which would be indeterminate for PLC disruption. However, with the clear evidence of ligamentum flavum disrpution on the accompanying T2w image, PLC injury is definitive in this patient. TLICS imaging score is 7.

CASE 45 TLICS Distraction Injury

Russel Chapin

Imaging Findings

According to the TLICS, in the presence of more than one injury morphology, the morphology yielding the higher score is used. In the setting of vertebral body compression, interspinous widening or facet joint uncovering should be considered evidence of distraction and yield an injury morphology score of 4. Similarly, injuries with significant widening of the anterior disc space from hyperextension and anterior ligament disruption should be assigned a morphology score of 4.

Table 45.1 Scoring based on injury morphology according to the thoracolumbar injury classification and severity score (TLICS).

Injury Morphology	Points
Compression	1
Burst	2
Translation or Rotation	3
Distraction	4

Clinical Findings, Implications, and Treatment

In the setting of compression (flexion) injury, disruption of the facets or other elements of the posterior ligamentous complex (PLC) suggests possible distraction morphology. In this respect, there is considerable overlap between the morphology and PLC integrity domains of TLICS. Determination of PLC integrity is based on both clinical and imaging findings. Palpation of a widened interspinous gap is consistent with a clinical diagnosis of PLC disruption. A patient classified as having a distraction-type mechanism will frequently have a suspected (score 2) or definite (score 3) PLC disruption. The exception would be a patient with an anterior distraction injury. Therefore, patients classified with distraction injuries will frequently have a TLIC score of 6 or 7 prior to consideration of neurologic status. A TLIC score of 4 may be treated surgically or nonsurgically while a score of 5+ is directed to surgical management. Other clinical features such as intracranial injury, hemodynamic status, significant solid organ injury, or worsening spinal cord or nerve root findings obviously play an overarching role in this decision-making process.

Additional Information

Maximizing the reliability and reproducibilty of thoracolumbar injury description and treatment is a central tenet to the development of the TLICS. The most difficult and significant problem in describing injury morphology is whether high-grade compression (flexion) injuries are classified as compression (2 points) or distraction (4 points). While not overwhelming, the consensus from the spine trauma study group is that compression injuries with disruption of the PLC should be scored as distraction type. Unfortunately, determination of PLC status is the least consistent domain of TLICS. A survey of the Spine Trauma Study Group found that most members rely on CT rather than MRI for determining PLC integrity.

References

1 Patel AA, Vaccaro AR. Thoracolumbar spine trauma classification. *J Am Acad Orthop Surg* 2010;18:63–71.

2 Lewkonia P, Paolucci EO, Thomas K. Reliability of the thoracolumbar injury classification and severity score and comparison with the Denis classification for injury to the thoracic and lumbar spine. *Spine (Phila Pa 1976)* 2012;37:2161–2167. doi: 10.1097/BRS.0b013e3182601469.

3 Schweitzer KM, Vaccaro AR, Harrop JS, et al. Interrater reliability of identifying indicators of posterior ligamentous complex disruption when plain films are indeterminate in thoracolumbar injuries. *J Orthop Sci* 2007;12:437–442.

4 van Middendorp JJ, Patel AA, Schuetz M, Joaquim AF. The precision, accuracy and validity of detecting posterior ligamentous complex injuries of the thoracic and lumbar spine: a critical appraisal of the literature. *Eur Spine J* 2013;22:461–474. doi: 10.1007/s00586-012-2602-7.

5 Joaquim AF, Ghizoni E, Tedeschi H, Batista UC, Patel AA. Clinical results of patients with thoracolumbar spine trauma treated according to the Thoracolumbar Injury Classification and Severity Score. *J Neurosurg Spine* 2014;20:562–567. doi: 10.3171/2014.2.SPINE121114.

SECTION **5**

Specifics of Pediatric Spinal Trauma

Cases

Figure 46.1 Lateral view radiograph in an 18-month-old girl shows oval to slightly triangular shape of the cervical vertebral bodies and buckling of the prevertebral soft tissues (*) due to neck flexion. There is pseudosubluxation of C2 – the spinolaminar line is drawn, and posterior arch of the C2 falls on the line. Normal atlanto-dental measurement of 2.6 mm (under 5 mm).

Figure 46.2 Midsagittal reformatted CT image of the cervical spine in a 5-year-old child demonstrates mild anterior wedging of the vertebral bodies, most notably C3 (arrow), representing a normal variant in preteen children.

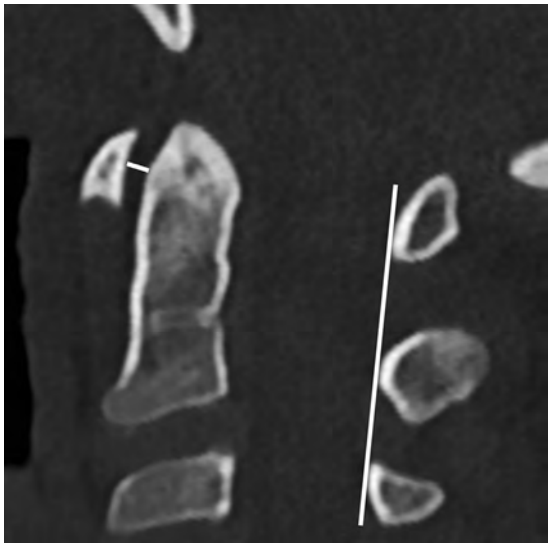

Figure 46.3 Midsagittal cervical spine CT image in a 7-year-old girl with drawn atlanto-dental and posterior spinolaminar white lines. Note subdental synchondrosis.

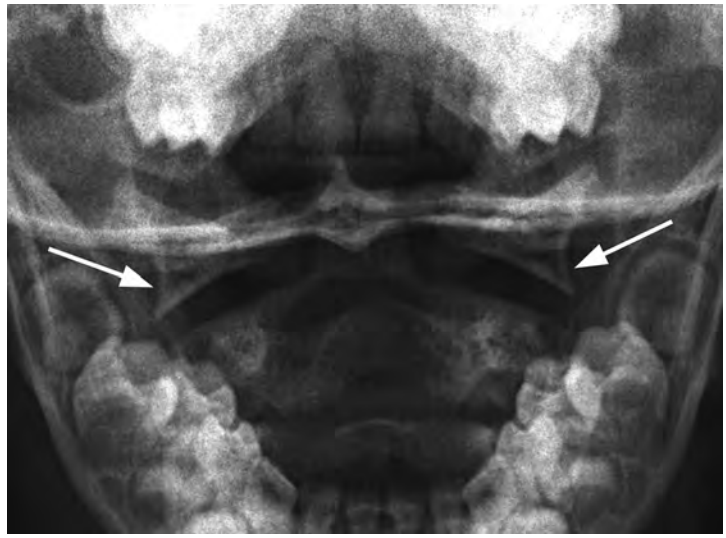

Figure 46.4 Open-mouth view radiograph in a 4-year-old boy shows lateral offset of the C1 lateral masses (arrows) compared with the C2 lateral masses, a normal finding.

CASE 46 Pediatric Cervical Spine Measurements and Pitfalls

Alisa Sumkin and Giulio Zuccoli

Imaging Findings

The craniovertebral junction ossification centers should be understood in order to prevent their misinterpretation as fractures. A normal *physis* can be identified by the presence of its smooth borders with subchondral sclerotic lines. C1: Anterior arch fuses at 7 years while the neural arches fuse posteriorly at approximately 3 years. C2: Ossification center at the odontoid apex, the *os terminalis* or *os odointoideum*, normally fuses by 12 years. The body of C2 fuses with the odontoid by 3–6 years. This fusion line is called the subdental synchondrosis and can be seen up until 11 years and even later. The neural arches fuse posteriorly by 2–3 years and the odontoid fuses at 3–6 years.

The shape of the normal vertebral body in infancy is oval on lateral view radiographs, sagittal CT reformats, and sagittal MRI. The vertebral bodies may later have anterior wedging, especially at the C3 level, which is normal in children up to 7 years of age.

Examine the prevertebral/retropharyngeal space swelling in conjunction with the other findings. The normal prevertebral space should not be greater than 6 mm at the level of C3; however, marked buckling of the soft tissues occurs with neck flexion and in expiration. In order to avoid interpretation errors, the radiographs should be obtained with neck extended and in inspiration, the patient awake in the standing or seated position, if possible. This will allow visualization of the patient's definite cervical lordosis, which can be falsely underestimated in a supine position. If the image is taken supine, lift the patient's shoulders from the table, because the relatively larger head of a child can diminish the lordosis. Additionally, the x-ray beam should be completely perpendicular to the region of interest in order to decrease pitfalls.

Measurements

Atlanto-Dental Interval: Distance between the anterior aspect of the dens and the posterior cortex of the anterior C1 ring should be less than 5 mm. If greater than 5 mm, ligamentous abnormalities need to be excluded by MRI to depict bone edema and/or ligamentous injury.

"Pseudo-Jefferson Fracture": Lateral offset of the C1 lateral masses compared to the lateral masses of the axis of up to 6 mm is normal in children (due to discrepancy in growth rates). The atlanto-dental interval should be normal with this pseudospread of atlas.

Pseudosubluxation: Physiologic motion of C2 on C3 in flexion with anterior displacement of C2 measures up to 4 mm in children under 8 years of age. Pseudosubluxation may be differentiated from true subluxation by the posterior spinolaminar line, which connects the anterior cortices of the posterior C1 and C3 arches (Swischuk line). With true subluxation, the posterior C2 arch does not fall within 2 mm from the Swischuk line.

Constitutional Variants: Occipitalization (assimilation) of the atlas is the osseous fusion of the atlas and the occiput. Basilar invagination is when the tip of the odontoid is at or above the foramen magnum.

Clinical Findings, Implications, and Treatment

There are many normal variants of the pediatric cervical spine, which can be easily confused with traumatic injuries. The most common presenting symptoms of true cervical spine injury are neck pain, occipital pain, and acute torticollis. If physical examination is unremarkable, unstable cervical spine injury can reliably be excluded in children $\leq$5 years old.

Additional Information

Atlanto-axial instability (AAI) is present in 10–30% of individuals with Down syndrome. AAI is an increase in the atlanto-dental interval or a decrease in the neural canal width. These patients are usually asymptomatic; however, if the neural canal width is less than 14 mm or the atlanto-dens interval is greater than 4.5 mm on a lateral radiograph, cervical spine MRI should be obtained. If the patient has symptomatic atlanto-axial instability, initial examination should include both a lateral radiograph and an MRI.

References

1 Hosalkar HS, Sankar WN. Congenital osseous anomalies of the upper cervical spine. *J Bone Joint Surg Am* 2008;90:337–348.

2 Brockmeyer D. Down syndrome and craniovertebral instability. Topic review and treatment recommendations. *Pediatr Neurosurg* 1999;31:71–77.

3 Ghanem I, El Hage S, Rachkidi R, et al. Pediatric cervical spine instability. *J Child Orthop* 2008; 2:71–84.

4 Lustrin ES, Karakas SP, Ortiz AO, et al. Pediatric cervical spine: normal anatomy, variants, and trauma. *Radiographics* 2003;23:539–560.

5 Alam Khan T, Jamil Khattak Y, Awais M, et al. Utility of complete trauma series radiographs in alert pediatric patients presenting to emergency department of a tertiary care hospital. *Eur J Trauma Emerg Surg* 2015; 41:279–285.

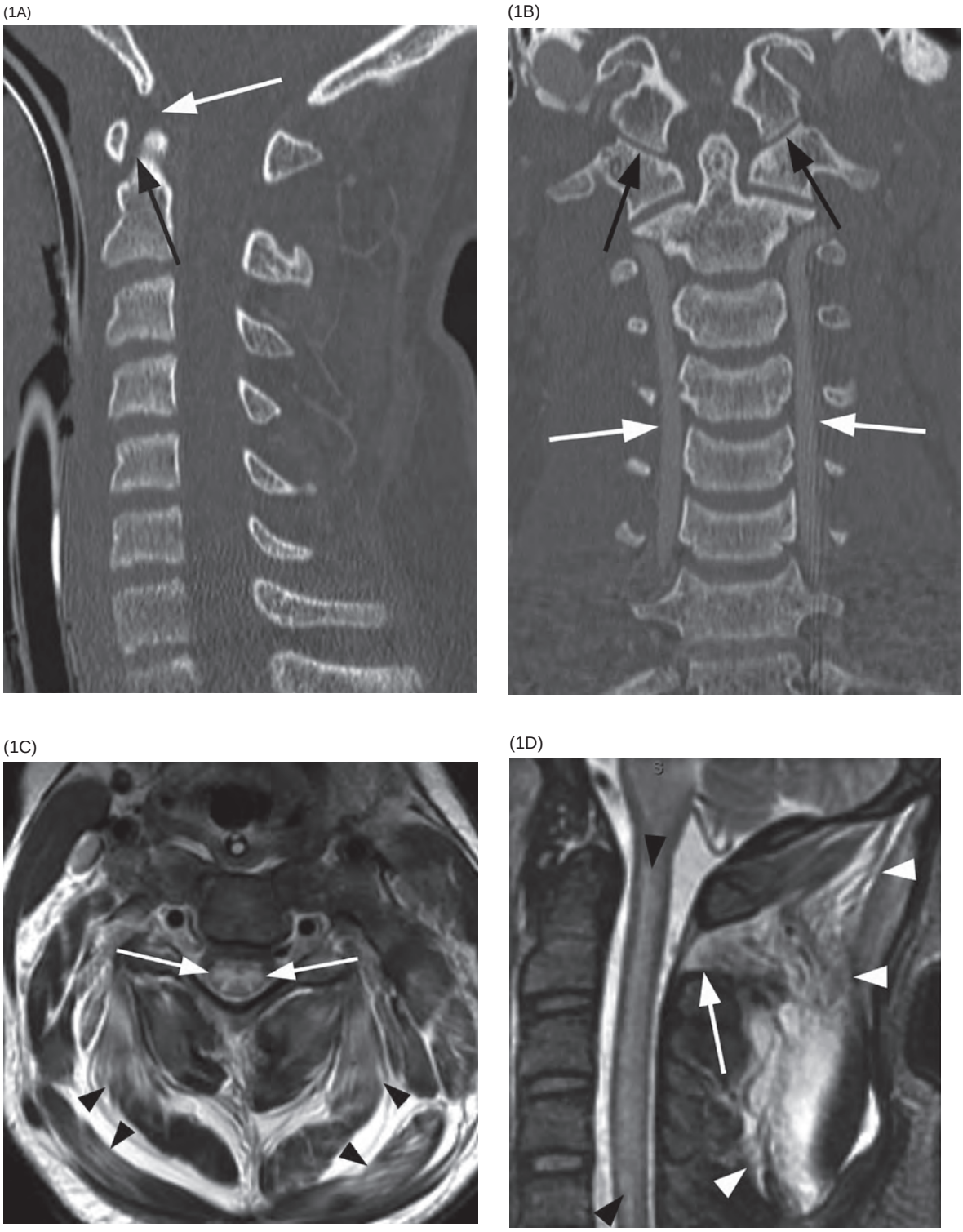

Figure 47.1 **A)** Midsagittal reformatted CT image (CT angiogram) shows a normal alignment of the cervical spine. There is no compression deformity or acute fracture. The basion-dental interval (white arrow) and atlanto-dental interval (black arrow) are normal. **B)** Coronal CT image demonstrates a normal atlanto-occiptal interval (black arrows). The vertebral arteries (white arrows) are normal in course and caliber. **C)** Axial T2w MR image shows symmetric cord edema (arrows). There is diffuse myofascial injury with involvement of the paraspinous musculature (arrowheads). **D)** Sagittal STIR MR image demonstrates extensive cervical spinal cord edema. There is posterior ligamentous injury at the craniocervical junction with involvement of the posterior atlanto-axial ligament (arrow) and nuchal ligament (arrowheads).

CASE 47 Spinal Cord Injury without Radiographic Abnormalities in Children

Orrie Close and Giulio Zuccoli

Imaging Findings

Spinal cord injury without radiographic abnormalities (SCIWORA), as the name would imply, is a syndrome by which patients present with objective signs of myelopathy without plain radiographic or CT abnormalities. Spinal cord injury without CT evidence of trauma (SCIWOCTET) is the same entity in adults with preexisting central canal stenosis and degenerative changes of the cervical spine. Pediatric SCIWORA primarily affects the cervical spine, resulting in cord contusion and axonal injury. STIR is probably the most sensitive MR sequence for depicting soft tissue, ligamentous, and muscular injury and therefore should be performed in all cases of spinal trauma. An acute cord contusion (edema), resulting from either transient subluxation or distraction injury, will appear iso to hypointense on T1WI and hyperintense on T2WI. It is estimated that as many as 35% of patients will have no MR abnormalities, and therefore follow-up imaging is needed to capture the delayed presentation of cord edema. Repeat MRI is typically performed at 1 week and again at 3–6 weeks to evaluate for syrinx, as the incidence of posttraumatic syrinx formation is estimated at 3.5%.

Differential Diagnosis

Spinal Cord Infarct

Typically bilateral anterior gray matter involvement with characteristic symmetric T2 hyperintense lesions ("owl's eyes"), very bright on DWI (enteroviral infection may look the same); etiologies include trauma (including surgery, especially of the aorta), vasculitis, venous thrombosis, and embolic phenomenon (including fibrocartilaginous emboli); usually no evidence for ligamentous spine injury.

Demyelinating Diseases

Central T2 hyperintense lesion extending three or more vertebral segments with variable post-contrast enhancement pattern; commonly post-infectious or part of the neuro-immune continuum, which includes neuromyelitis optica and acute disseminated encephalomyelitis (ADEM); although the intramedullary lesions may have similar appearance to SCIWORA on imaging, there are no ligamentous injuries.

Clinical Findings, Implications, and Treatment

The presentation of these patients is variable and may range from transient neurological symptoms to complete spinal cord injury. The clinical features of SCIWORA are typically apparent by 48 hours following a traumatic event. Those with minor injuries may demonstrate transient numbness, paresthesias, or paresis. Severe injury can result in one of four neurological syndromes: central cord syndrome, complete cord syndrome, partial cord syndrome, and Brown-Séquard syndrome. SCIWORA patients with minor injuries are treated with external immobilization for up to 12 weeks and requested to avoid high-risk activities for up to 6 months.

Additional Information

The mechanism of injury in SCIWORA is related to hyperextension and flexion, which results in transient vertebral dislocation or distraction. This condition commonly occurs in children less than 8 years of age as a result of increased laxity and elasticity of the developing cervical spine. Extreme extension/flexion can disrupt vertebral and anterior spinal arteries, leading to cord ischemia and/or infarct. Hypermobility of the vertebral column with respect to the cord leads to distraction and transection type injuries. Congenital cervicospinal anomalies may further predispose children to development of SCIWORA and related syndromes.

References

1 Egloff AM, Kadom N, Vezina G, Bulas D. Pediatric cervical spine trauma imaging: a practical approach. *Pediatr Radiol* 2009;39:447–456.

2 Shah LM, Zollinger LV. Congenital craniocervical anomalies pose a vulnerability to spinal cord injury without radiographic abnormality (SCIWORA). *Emerg Radiol* 2011;18:353–356.

3 Buldini B, Amigoni A, Faggin R, Laverda AM. Spinal cord injury without radiographic abnormalities. *Eur J Pediatr* 2006;165:108–111.

4 Rozzelle CJ, Arabi B, Dhall SS, et al. Spinal cord injury without radiographic abnormality (SCIWORA). *Neurosurgery* 2013;72:227–233.

5 Como JJ, Samia H, Nemunaitis GA, et al. The misapplication of the term spinal cord injury without radiographic abnormality (SCIWORA) in adults. *J Trauma Acure Care Surg* 2012; 73:1261–1266.

(1A)

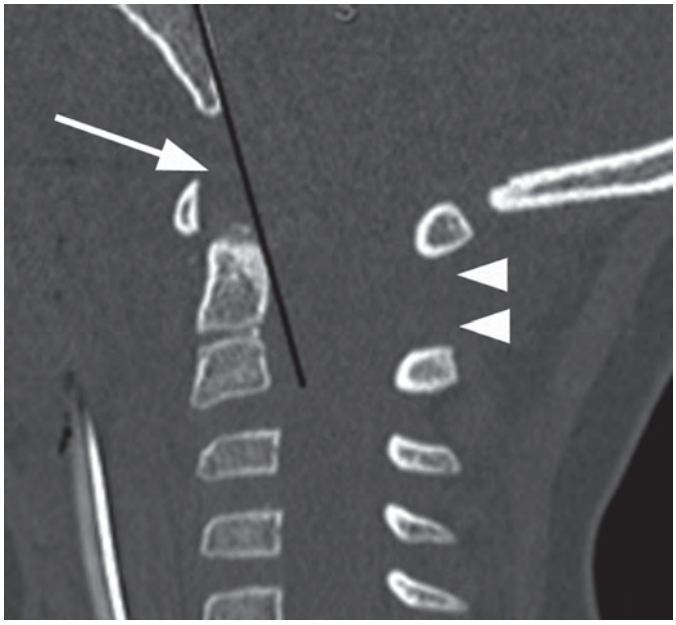

(1B)

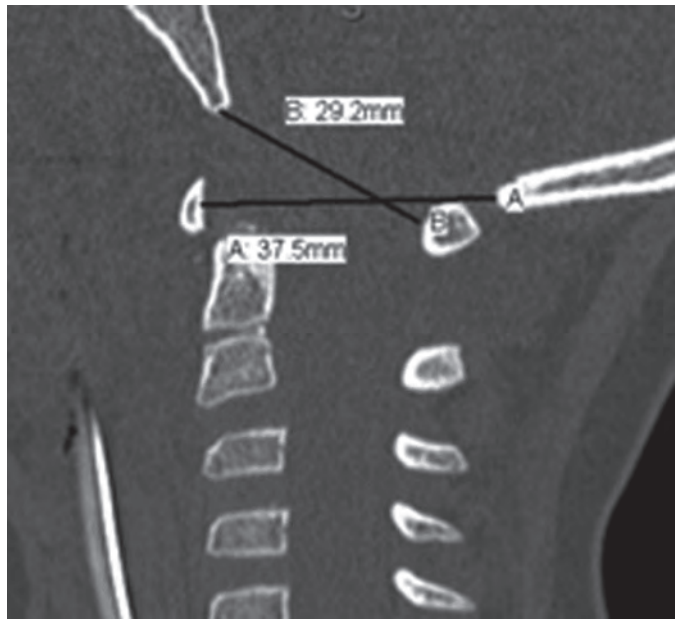

Figure 48.1 **A)** In this 3-year-old patient post motor vehicle collision, the Wackenheim line (black line) fails to pass through the odontoid process on this midsagittal CT image, suggestive of atlanto-occipital distraction. The image also shows increased dens-basion interval (arrow) and atlanto-axial instability (arrowheads). **B)** A calculated Powers ratio in the same patient was normal (29 mm/37 mm = ~0.8, less than the normal value of 0.9), indicating the importance of using several techniques in evaluation of AOD.

(2A)

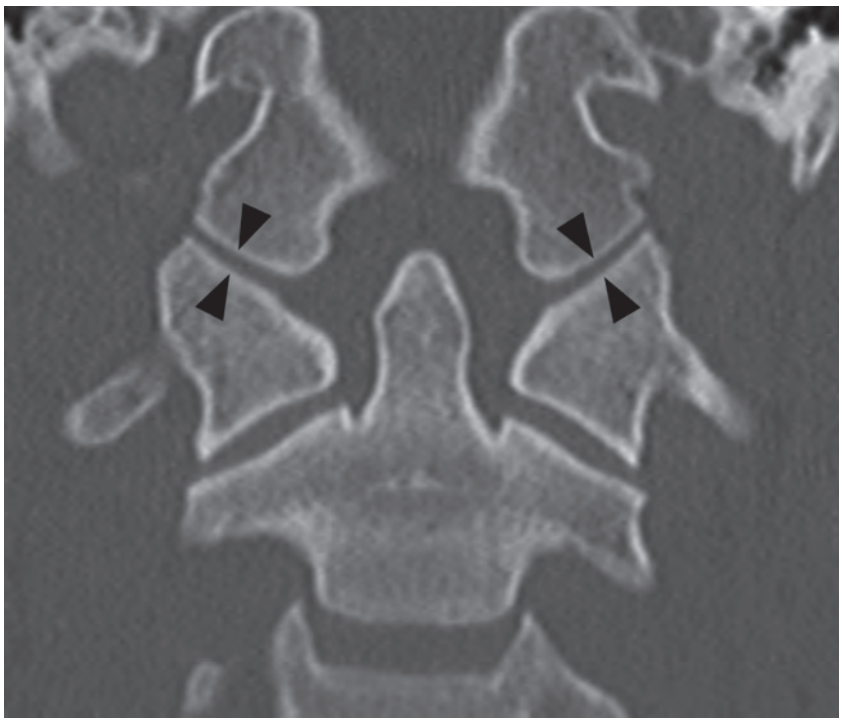

(2B)

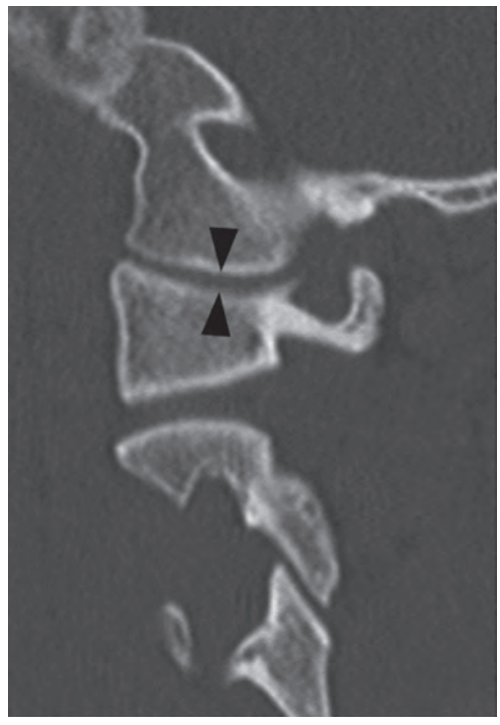

Figure 48.2 **A)** Coronal and **B)** sagittal CT images demonstrating condyle to C1 interval (CCI) measurements (arrowheads).

CASE 48 Atlanto-Occipital Dislocation

Michael Paul Yannes and Zoran Rumboldt

Imaging Findings

Intracranial hemorrhage, facial trauma, and fractures of the occipital condyles, atlas, and axis should all raise the suspicion for atlanto-occipital dislocation (AOD, craniocervical dissociation), and subarachnoid hemorrhage at the craniocervical junction may be the most common association.

A multitude of craniometric measures have been proposed in the diagnosis of AOD, and no single measurement is considered paramount (Table 48.1). The oldest one is the dens-basion interval – the distance between the basion and the tip of the odontoid should be less than 12 mm in a pediatric patient with unossified physes, and less than 10 mm in a mature individual; this may be unreliable due to variability in ossification. Wackenheim clivus line is drawn from the posterior aspect of the clivus toward the odontoid process; AOD is suspected if the line does not intersect the posterior one-third of the odontoid process. With Powers ratio, the basion-posterior atlas arch distance is divided by the distance from the opisthion to the anterior arch – it should be less than 1 or 0.9. Condyle to C1 interval (CCI) may be particularly sensitive – it measures the distance between the occipital condyle and the superior articular facet of the atlas; in a recent study CCI $\geq$ 4 mm was diagnostic for AOD in children with sensitivity and specificity of 100%. Additional measurement methods include basion-axial interval and X-lines of Lee.

Table 48.1 List of commonly used atlanto-occipital measurements with normal CT values.

Normal Atlanto-Occipital Measurements in the Pediatric Population	
Occipital Condyles to Atlas Interval (CCI)	<4 mm (<2 mm in adults)
Powers Ratio	<1 (or 0.9)
Basion Tip to Odontoid	<12 mm if unossified physes; <10 mm if ossified physes

Differential Diagnosis

Other Traumatic Injuries

Occipital condyle, C1 (Jefferson), and C2 (hangman) fractures can all predispose, be associated with, or be mistaken for AOD.

Congenital Abnormalities

Predispose to AOD, including Morquio syndrome and neurofibromatosis; the most important is Down syndrome, as these patients frequently have ligamentous laxity – there is no consensus regarding a higher threshold for radiographic measurement and diagnosis of AOD.

Clinical Findings, Implications, and Treatment

MVC is the prevailing mechanism of injury, and patients commonly present with cardiopulmonary arrest, spinal cord injury, and cranial nerve deficits. Once considered rare and almost invariably fatal, improvements in diagnosis and management have made AOD a more prevalent and survivable injury, which is likely due to improvements in field resuscitation, cervical immobilization, rapid transport, as well as evolution of emergency medicine and advances in radiological imaging. Prompt diagnosis is crucial, and surgical stabilization with posterior internal fixation (occipito-cervical fusion) is the recommended treatment. About a third of the patients die and a quarter have a complete neurological recovery.

Additional Information

As recognition of ligamentous instability is critical and craniometric measurements appear unreliable, MRI may be the diagnostic modality of choice for suspected AOD, which has been recently stratified into two grades: Grade 1 injuries with normal CT and moderately abnormal MRI findings (high signal of the ligaments) can be treated conservatively; Grade 2 is managed surgically and defined by at least one abnormal CT measurement and/or grossly abnormal MRI of the atlanto-occipital joints, tectorial membrane, alar, or cruciate ligaments. The main ligaments that maintain the stability of craniocervical junction are the anterior (a continuation of the anterior longitudinal ligament), posterior, and lateral atlanto-occipital ligaments, cruciate ligaments, and the articular capsule; tectorial membrane (a continuation of the posterior longitudinal ligament) and paired alar ligaments that connect the tip of the dens and the lateral masses of atlas to the occipital condyles.

AOD is considered both more common and more survivable in the pediatric population, which is thought to be related to relatively more horizontal facet joints, flatter and more anteriorly wedged vertebral bodies, and increased ligamentous laxity in young children.

References

1 Baez T, Brown J. Traumatic atlanto-occipital dislocation in children – a case-based update on clinical characteristics, management and outcome. *Childs Nerv Syst* 2017;33:27–33.

2 Riascos R, Bonfante E, Coates C, et al. Imaging of atlanto-occipital and atlanto-axial traumatic injuries: what the radiologist needs to know. *Radiographics* 2015;35:2121–2134.

3 Kasliwal MK, Fontes RB, Traynelis VC. Occipitocervical dislocation – incidence, evaluation, and treatment. *Curr Rev Musculoskelet Med* 2016;9:247–254.

4 Roy AK, Miller BA, Holland CM, et al. Magnetic resonance imaging of traumatic injury to the craniovertebral junction: a case-based review. *Neurosurg Focus* 2015;38:E3.

(1A)

(1B)

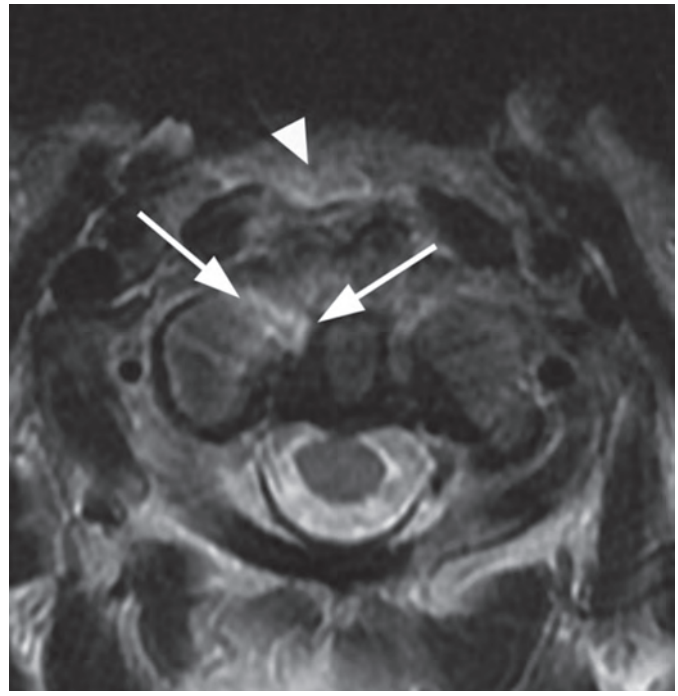

Figure 49.1 **A)** Midsagittal CT image demonstrates an increased atlas-to-dens interval of 7.8 mm in this adolescent. This distance is normally less than 5 mm in children, and 3.5 mm in adults. **B)** Subsequent axial T2-weighted MR image reveals increased signal in the alar ligament (arrows), consistent with edema and indicative of ligamentous injury. The superior extent of a prevertebral hematoma is also identified (arrowhead).

(2A)

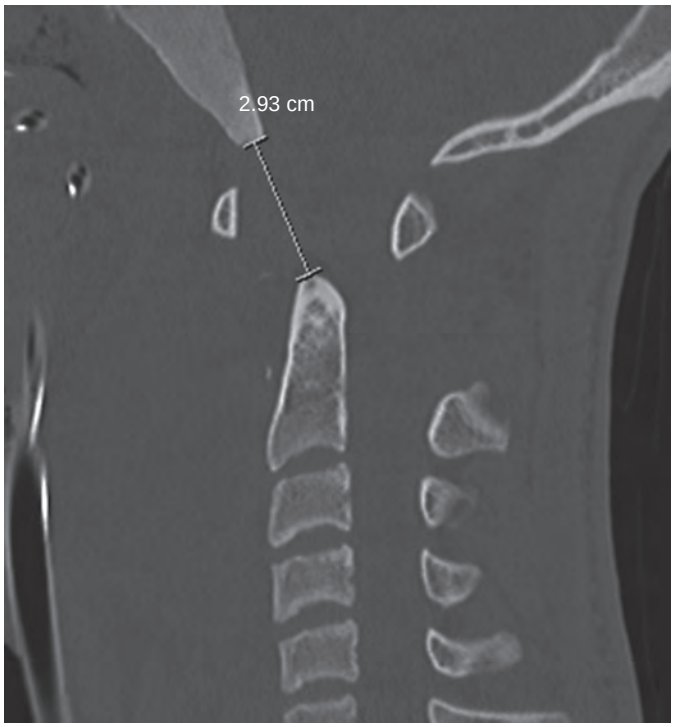

(2B)

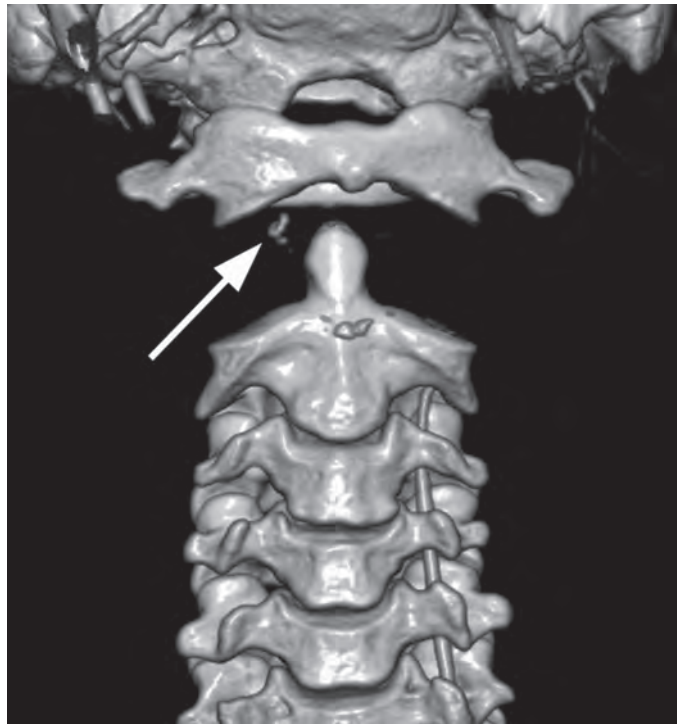

Figure 49.2 **A)** Midsagittal CT image shows substantially increased dens-basion interval, measuring 29 mm (12 mm is the upper limit of normal) with normal relationship of the atlas to the occiput, consistent with severe atlanto-axial distraction. There is also anterior translation of the atlas. Note enlarged prevertebral space due to a large hematoma, as well as incidental fibrous dysplasia of the clivus. **B)** Volume rendering of CT angiogram clearly demonstrates the separation of the C2 vertebra from the atlas. There is a small avulsion fracture (arrow). Note occlusion of both vertebral arteries.

CASE 49 Atlanto-Axial Dislocation

Michael Paul Yannes and Giulio Zuccoli

Imaging Findings

AAD encompasses a spectrum of injuries, ranging from disruption of a single ligament to subluxation to frank dislocation. Unlike the diagnosis of atlanto-occipital dislocation (AOD), there is broad consensus regarding the radiological diagnosis of atlanto-axial instability (AAI). The atlanto-dental interval (ADI, the distance between the anterior cortex of the dens and the posterior cortex of the anterior atlas ring) is the key measurement and it should be less than 5 mm in children (3.5 mm in adults); any increase in this distance indicates ligamentous injury of the atlanto-axial articulation. Additionally, dens-basion interval (the distance between the basion and the tip of the odontoid) of more than 12 mm (less than 10 mm in a mature individual) indicates atlanto-axial distraction (AAD) injury in patients without AOD (with normal atlanto-occipital measurements).

In patients who are predisposed to AAI, the space available for the spinal cord (SAC) is considered to be a more reliable measurement: the distance from the posterior aspect of the odontoid to either the foramen magnum or the posterior ring of the atlas is measured, and values of less than 13 mm indicate spinal cord compression.

Differential Diagnosis

Other Traumatic Injuries of the Cranio-Cervical Junction

Fractures of the occipital condyles, C1 (Jefferson) fracture, and axis (hangman) fractures; AAD also often occurs in conjunction with these fractures.

Basilar Invagination

No history of trauma, frequently associated additional abnormalities such as platybasia, atlas occipitalization, Chiari malformation.

Disease States That Predispose Patients to AAD

Rheumatoid arthritis, Grisel syndrome, muccopolysaccharidoses, Klippel-Feil syndrome, and multiple others; Down syndrome is the most important – SAC and especially C1/C4 SAC ratio has been found to be substantially smaller in patients requiring surgery.

Clinical Findings, Implications, and Treatment

The mechanism of injury leading to AAD is similar to that of atlanto-occipital dislocation and other cervical spine injuries. Management of AAI ultimately depends on degree of neurological impairment. In asymptomatic individuals, treatment can consist of rigid immobilization in a cervicothoracic orthosis. For neurologically symptomatic patients, atlanto-axial arthrodesis by posterior surgical fusion is the treatment of choice. C1–C2 pedicle screw internal fixation may be the preferred method for treating AAI.

Additional Information

The transverse ligament (the horizontal limb of the cruciate ligament) is the primary stabilizer of the atlanto-axial joint, effectively limiting anterior translation and flexion, in addition to its stabilizing effect with respect to the atlanto-occipital articulation. Furthermore, the alar ligaments, with their attachment at the tip of the odontoid process, are also major stabilizers of the atlanto-axial articulation.

AADs may be classified based on the direction and plane of the dislocation into anteroposterior, central, rotatory, and mixed. Rotatory atlanto-axial subluxation is discussed in a separate chapter.

References

1 Riascos R, Bonfante E, Coates C, et al. Imaging of atlanto-occipital and atlanto-axial traumatic injuries: what the radiologist needs to know. *Radiographics* 2015;35: 2121–2134.

2 Jain VK. Atlantoaxial dislocation. *Neurol India* 2012;60:9–17.

3 Zheng Y, Hao D, Wang B, et al. Clinical outcome of posterior C1–C2 pedicle screw fixation and fusion for atlantoaxial instability: a retrospective study of 86 patients. *J Clin Neurosci* 2016;32:47–50.

4 Roy AK, Miller BA, Holland CM, et al. Magnetic resonance imaging of traumatic injury to the craniovertebral junction: a case-based review. *Neurosurg Focus* 2015;38:E3.

5 Nakamura N, Inaba Y, Aota Y, et al. New radiological parameters for the assessment of atlantoaxial instability in children with Down syndrome: the normal values and the risk of spinal cord injury. *Bone Joint J* 2016; 98-B:1704–1710.

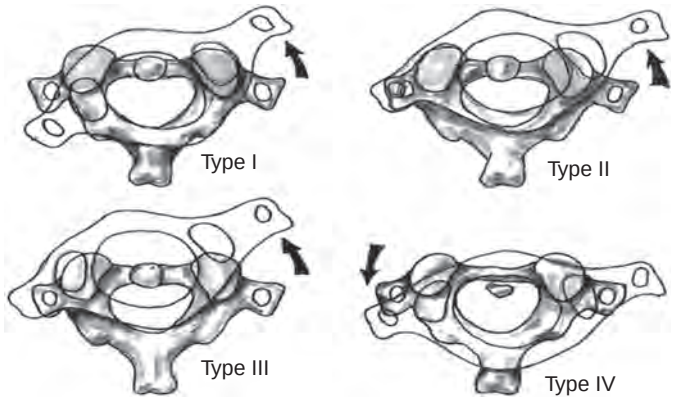

Figure 50.1 Fielding and Hawkins classification of C1–C2 rotatory subluxation.

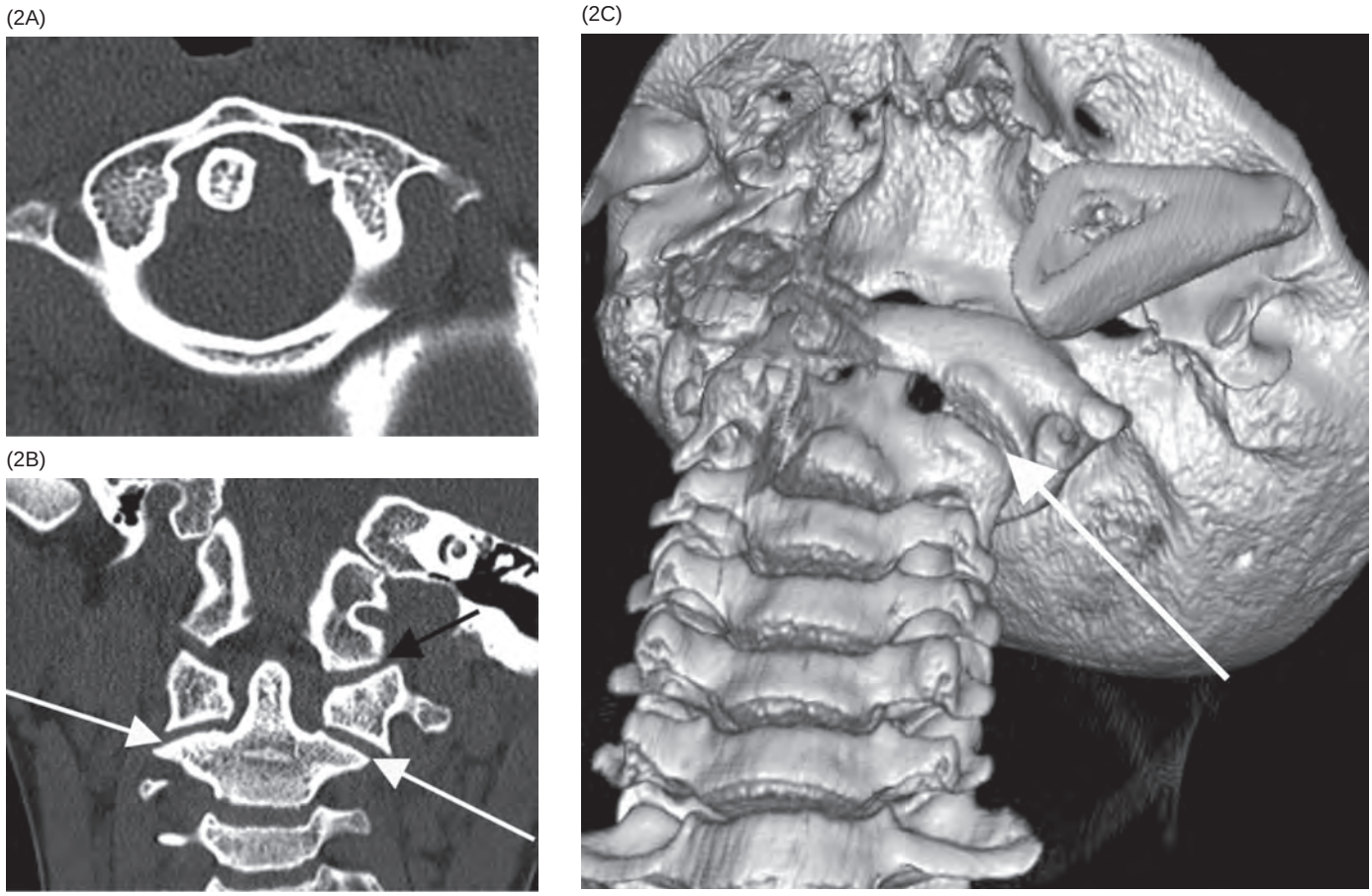

Figure 50.2 Type 1 rotatory subluxation. **A)** On axial CT image there is minimal displacement of the atlas with respect to the axis. **B)** Coronal reconstruction CT shows asymmetry of the atlanto-axial (white arrows) and atlanto-occipital (black arrow) joints. **C)** 3D reconstruction of the CT data demonstrates subluxation of the atlas with respect to the axis (arrow).

CASE 50 Atlanto-Axial Rotatory Subluxation

Giulio Zuccoli and Alessandro Cianfoni

Imaging Findings

Atlanto-axial rotatory subluxation (AARS) and its more serious variant, atlanto-axial rotatory fixation (AARF), refer to a persistent rotational deformity of the C1–C2 complex. The anterior facet of C1 becomes locked on the facet of C2, resulting in impaired rotation at the joint.

Fielding and Hawkins first provided a classification scheme for C1–C2 rotatory dislocation in 1977, and this classification scheme is still widely used today. Type 1 refers to a rotatory fixation within the normal range of movement of the atlas and axis, without anterior dislocation of the atlas. Type 2 is a rotatory fixation with an anterior shift of the atlas by up to 5 mm. Type 3 is defined as rotatory fixation with anterior displacement of the C1 by more than 5 mm. Type 4 refers to rotatory fixation with posterior displacement of the atlas.

Radiographs are typically not used in patients with suspected AARS, secondary to frequent rotated neck positioning and restricted movements. CT is the modality of choice, and thick axial MIPs that include both atlas and axis on a single image can be very helpful. Dynamic CT, preferably in a neutral position followed by maximum rotation to both sides, with 3D reconstruction is the best imaging technique for identification and evaluation of these disorders.

Clinical Findings, Implications, and Treatment

AARS is a spectrum of disorders from muscle spasm to a fixed mechanical block. The most common presentation is a child with painful torticollis, which becomes more painful when attempts at rotational correction are made. The head is often laterally flexed, resulting in the characteristic "cock-robin" appearance. Falls are a common injury mechanism, and presentation is often delayed. Most atlanto-axial rotatory displacements resolve spontaneously. For rotatory displacement/subluxation lasting less than 1 month in duration, a combination of cervical traction, immobilization, muscle relaxants, and analgesics is usually indicated. When conservative therapy fails, the deformity recurs, or there are associated neurological symptoms, posterior C1–C2 fusion can be performed. The treatment varies across institutions, and optimal management has yet to be identified.

Infection or other inflammatory diseases should be considered as an underlying precipitating cause. In patients with suspected Grisel syndrome, the treatment is purely medical.

Additional Information

The exact etiology of AARS is not understood, and it can occur even after relatively minor trauma. Conditions that predispose children to ligamentous laxity, including Marfan syndrome, Down syndrome, and Morquio syndrome, increase the risk of AARS/AARF. Furthermore, a well-known entity, Grisel's syndrome, is characterized by spontaneous atlanto-axial subluxation with inflammation of adjacent neck tissues following an upper respiratory infection. Finally, prior head and neck surgery is a risk factor, likely secondary to a combination of inflammation, general anesthesia, and muscle relaxants.

Studies in children and adults have demonstrated that a CT scan showing wide but incomplete rotational facet displacement is not sufficient to define subluxation, and there is a risk of overdiagnosis and overtreatment. AARS is a doubtful phenomenon and may not be associated with acute acquired torticollis in children. There is a huge overlap with findings in normal control subjects, and the symptoms usually resolve spontaneously, so the imaging studies may therefore not be necessary. This does not apply to the patients who cannot rotate the neck in the opposite direction due to a locked facet joint.

References

1 Fielding JW, Hawkins RJ. Atlanto-axial rotatory fixation. (Fixed rotatory subluxation of the atlanto-axial joint). *J Bone Joint Surg Am* 1977;59:37–44.

2 Riascos R, Bonfante E, Coates C, et al. Imaging of atlanto-occipital and atlanto-axial traumatic injuries: what the radiologist needs to know. *Radiographics* 2015;35:2121–2134.

3 Powell EC, Leonard JR, Olsen CS, et al. Atlantoaxial rotatory subluxation in children. *Pediatr Emerg Care* 2017;33:86–91.

4 Hicazi A, Acaroglu E, Alanay A, et al. Atlanto-axial rotator fixation-subluxation revisited: a computed tomographic analysis of acute torticollis in pediatric patients. *Spine (Phila Pa 1976)* 2002;15:2771–2775.

5 Mönckeberg JE, Tomé CV, Matías A, et al. CT scan of atlantoaxial rotator instability in asymptomatic adult subjects: a basis for better understanding C1-C2 rotatory fixation and subluxation. *Spine (Phila Pa 1976)* 2009;20:34:1292–1295.

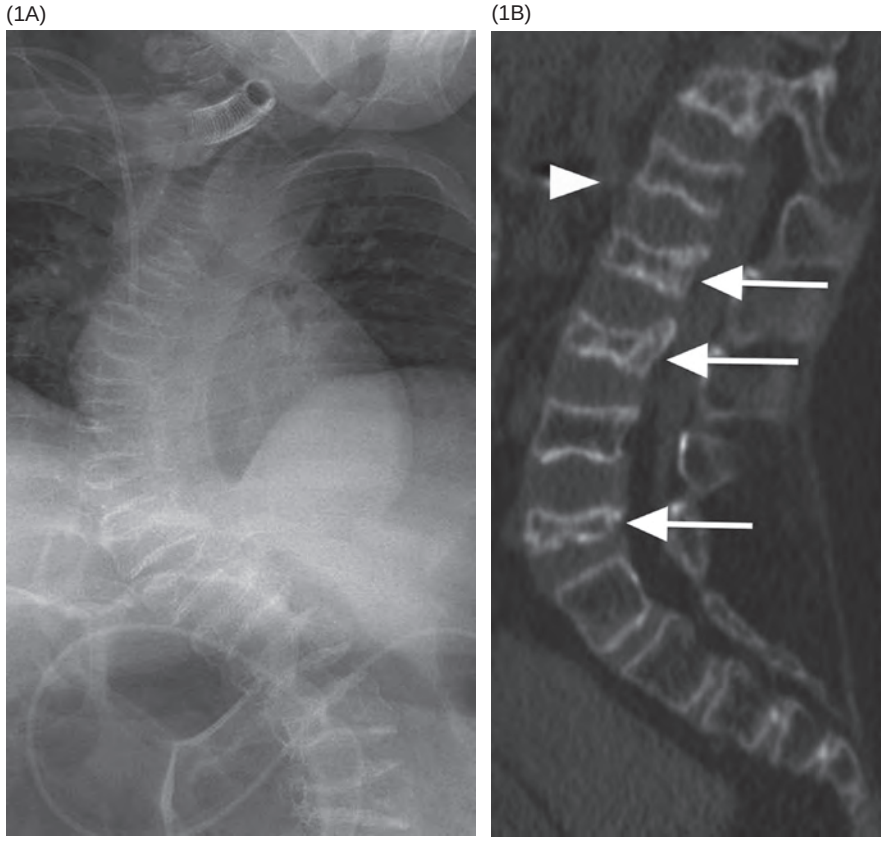

Figure 51.1 A) Chest radiograph demonstrates severe scoliosis in a patient with osteogenesis imperfecta (OI). **B)** Reformatted sagittal CT image of the lumbar spine shows multiple vertebral compression deformities (arrows). Note also a biconcave vertebral body (arrowhead).

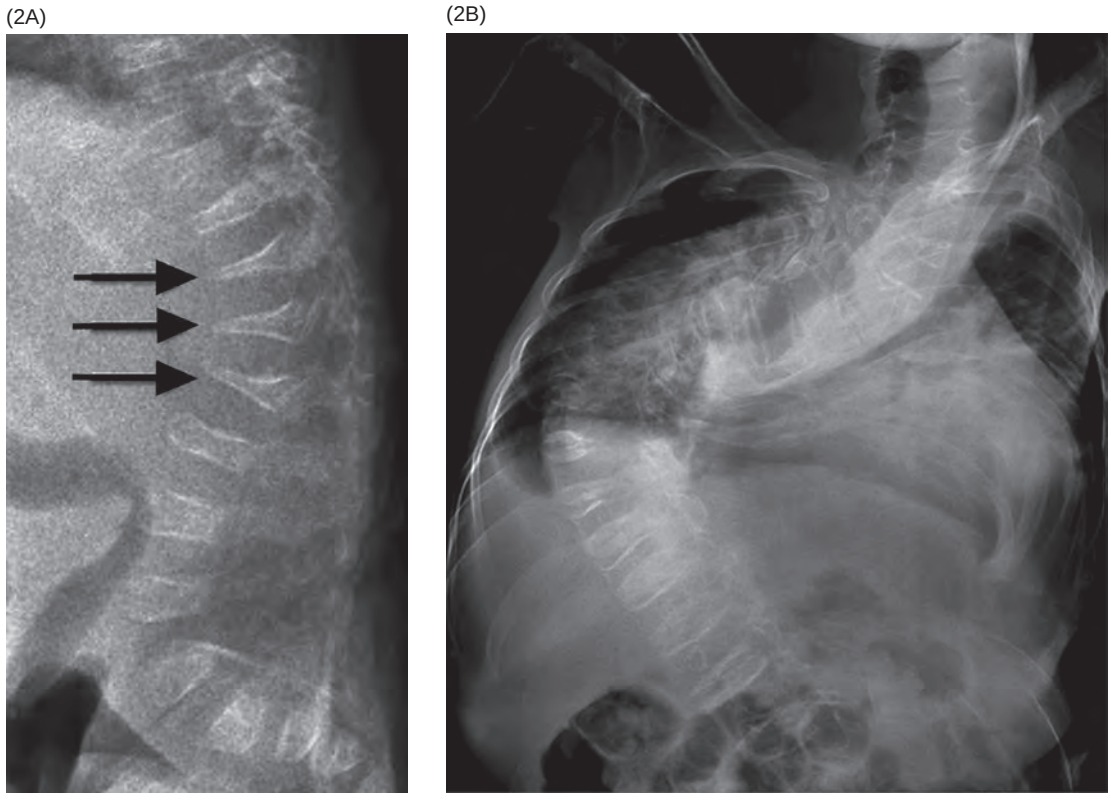

Figure 51.2 A) Lateral view of the lumbar spine demonstrates severe wedge-shaped compression deformities (arrows) in a patient with type II OI. **B)** Radiograph of the chest and abdomen shows a prominent focal dextroscoliosis of the thoracolumbar spine.

CASE 51 Osteogenesis Imperfecta

Orrie Close and Giulio Zuccoli

Imaging Findings

Osteogenesis imperfecta (OI, "brittle bone disease") may present in a highly variable fashion, from long bone fractures to profound skeletal disfigurement. The craniospinal manifestations include craniocervical junction abnormalities, endplate deformities, vertebral height loss, kyphosciolosis, and lumbosacral spondylolisthesis. Basilar impression and/or invagination can lead to aqueductal stenosis, hydrocephalus, brainstem displacement, spinal cord edema, and syrinx. Vertebral body endplate changes include sclerosis and cupping (biconcave vertebrae). Ligamentous laxity may result in spondylolisthesis in up to 5% of patients. OI should be considered in the differential diagnosis of severe compression and burst fractures, especially when following a minor trauma.

Differential Diagnosis

Non-Accidental Trauma

Shaking-type trauma with vertebral compression deformities and spondylolisthesis.

Osteoporosis (Various Etiologies)

Cortical thinning, codfish vertebrae, vertebral compression fractures.

Bruck Syndrome

Recessive disorder featuring congenital contractures and early childhood fractures.

Clinical Findings, Implications, and Treatment

The clinical features of OI vary with respect to the Sillence classification. Type I (mild) disease often manifests late in teenage years with nondeforming features such as insufficiency fractures, blue sclerae, dentinogenesis imperfecta, and deafness. The inheritance pattern is autosomal dominant with variable penetrance. A decline in the incidence of insufficiency fractures occurs with completion of ossification. Type II disease has autosomal recessive inheritance pattern and is most often fatal in utero or soon after birth, commonly diagnosed prenatally with demineralized calvarium, multiple fractures, and shortened long bones. The hallmarks of type III (severe) disease are early childhood fractures, short stature, micrognathia, blue-gray sclerae, dental anomalies, and progressive scoliosis. Two-thirds of patients will develop basilar invagination; however, only 30% will be symptomatic. Early clinical symptoms of basilar invagination include trigeminal neuralgia and facial numbness. Type IV (moderate) disease is characterized by occasional fractures, absence of wormian bones, normal sclerae, deafness, and mild progressive scoliosis. Individuals with type I and IV disease often have a normal lifespan, whereas type II and III have high childhood mortality.

Bisphosphonates are considered the mainstay therapy for most forms of OI. The approach to basilar invagination remains controversial: treatment options include dorsal decompression, ventral decompression with dorsal occipitocervical fixation, external orthosis, and traction. A lateral cervical radiograph before 6 years of age is recommended for surveillance of craniocervical junction. Compression deformities may be treated with immobilization and/or vertebroplasty.

Additional Information

OI represents a heterogeneous group of inheritable genetic diseases of type I collagen, which is present in bones, joints, dermis, tendons, ligaments, sclerae, and dentin. Mutations of collagen-encoding genes lead to either a reduction in quality (OI types II–IV) or quantity of type I (OI type I) pro-collagen. There are currently four main types (types I–IV) of OI caused by mutations in COL1A1 and COL1A2. An additional four (types V–VIII) types of OI have been described, each with unique gene defects.

References

1 Khandanpour N, Connolly DAJ, Raghavan A, et al. Craniospinal abnormalities and neurologic complications of osteogenesis imperfecta: imaging overview. *Radiographics* 2012;32:2101–2112.

2 Renaud A, Aucourt J, Weill J, et al. Radiographic features of osteogenesis imperfecta. *Insights Imaging* 2013;4:417–429.

3 Van Dijk FS, Sillence DO. Osteogenesis imperfecta: clinical diagnosis, nomenclature and severity assessment. *Am J Med Genet A* 2014;164:1470–1481.

4 Wallace MJ, Kruse RW, Shah SA. The spine in patients with osteogenesis imperfecta. *J Am Acad Orthop Surg* 2017;25:100–109.

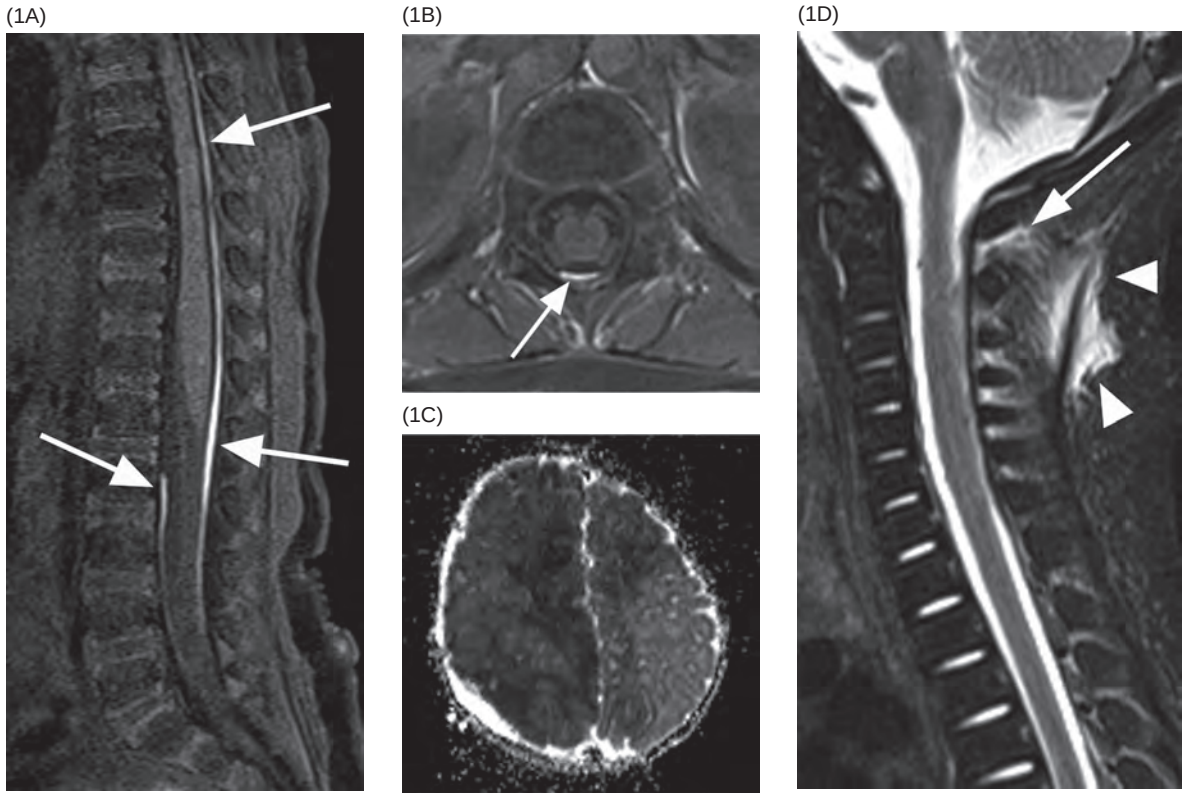

Figure 52.1 Midsagittal **(A)** and axial **(B)** T1-weighted MR images with fat saturation in a 6-month-old girl show subdural hematomas (arrows) in thoracolumbar spine. **C)** Axial ADC map of the brain reveals large bilateral dark areas, consistent with acute infarcts. **D)** Midsagittal STIR image shows injuries to the posterior atlanto-axial (arrow) and nuchal ligaments (arrowheads).

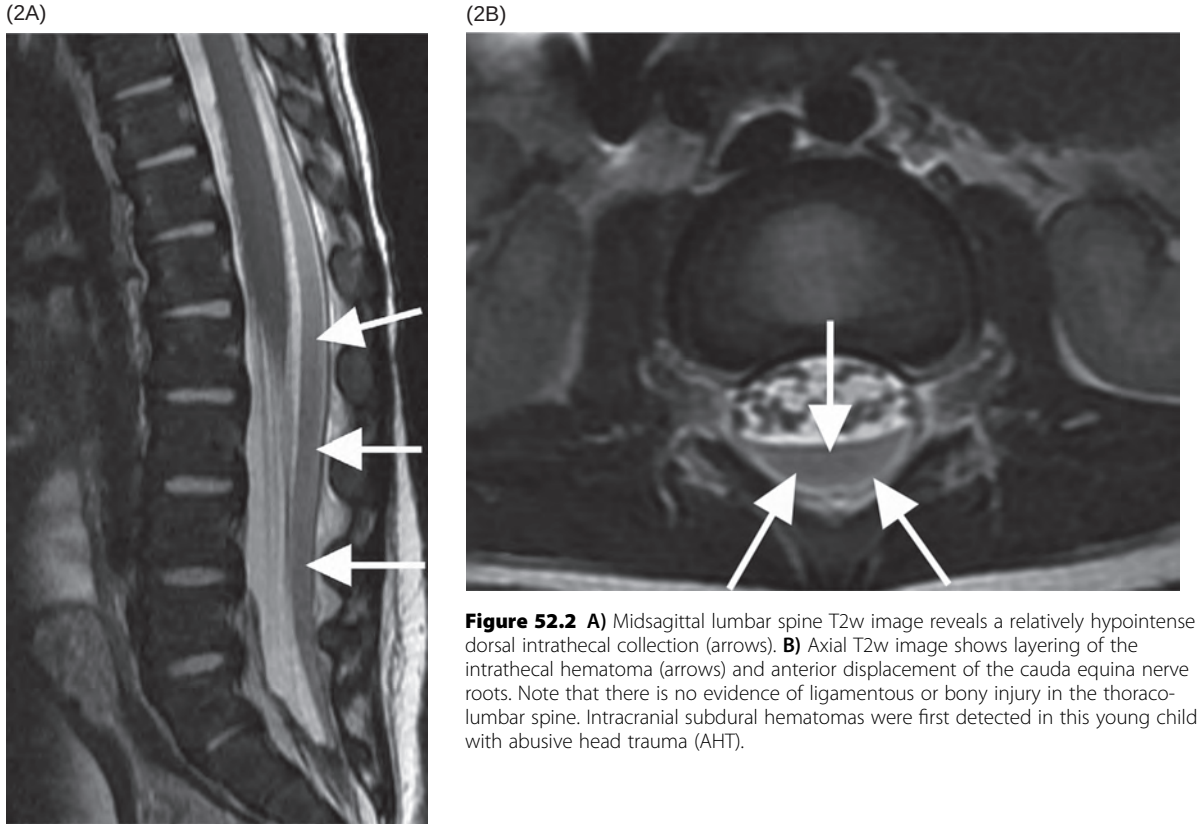

Figure 52.2 **A)** Midsagittal lumbar spine T2w image reveals a relatively hypointense dorsal intrathecal collection (arrows). **B)** Axial T2w image shows layering of the intrathecal hematoma (arrows) and anterior displacement of the cauda equina nerve roots. Note that there is no evidence of ligamentous or bony injury in the thoraco-lumbar spine. Intracranial subdural hematomas were first detected in this young child with abusive head trauma (AHT).

CASE 52 Abusive Spinal Injury

Orrie Close and Zoran Rumboldt

Imaging Findings

The initial skeletal survey is mandatory for detecting vertebral compression injuries and spinous process fractures. Spinal imaging has been a neglected part of abusive head trauma (AHT), and MRI is needed to identify ligamentous, vascular, and spinal cord injuries. T1-weighted images are the most sensitive for detection of subdural and subarachnoid hemorrhage, which is hyperintense relative to the adjacent CSF. Subdural hematomas may be found at cervical spine and/or thoracolumbar junction. STIR images are the most sensitive for ligamentous and soft tissue injury showing hyperintensity of edema and disruption of ligaments. The imaging characteristics of the abusive spine injury are difficult to differentiate from other forms of trauma. However, several clinical and radiographic findings are helpful in making the correct diagnosis: injuries to the posterior ligamentous complex of the cervical spine (primarily the nuchal, atlanto-occipital, and atlanto-axial) are more frequent and often found together with hypoxic-ischemic brain injury, while thoracolumbar subdural hematomas are also more frequent and not associated with ligamentous injury.

Differential Diagnosis

Osteogenesis Imperfecta

Early childhood vertebral compression deformities and progressive kyphoscoliosis.

Accidental Injury

Osseous, ligamentous, and soft tissue injuries in patients with an appropriate clinical history and severity of injury.

Epidural/Subdural Abscess

Rim-enhancing collection demonstrating hyperintense T2 and DWI signal, frequently of ellipsoid shape.

Clinical Findings, Implications, and Treatment

A high level of suspicion for spinal injuries is needed in child abuse, as they may be overlooked due to coexistent brain injury. Vertebral deformity and focal neurological deficits are the common presenting features. Ligamentous injuries often occur in the absence of fractures, and therefore MRI can define the extent of lesions. Spinal subdural hematomas resulting in cord compression warrant emergent neurosurgical evaluation, whereas small subdural hematomas will resolve spontaneously. Isolated ligamentous injuries are managed with rest and immobilization.

Additional Information

In 1946, Caffey was the first to describe the radiological association between multiple long bone fractures and chronic subdural hematomas in cases of child abuse. Two proposed mechanisms for the development of spinal subdural hematoma include inferior tracking of intracranial subdural or direct vascular injury. Several factors predispose infants to hyperextension and flexion injuries. First, the infant's head is disproportionally large relative to the support structures of the cervical spine, which is where the majority of spinal hematomas occur. Second, the fulcrum of the pediatric cervical spine is centered at the C2–C3 level, in contrast to C5–C6 in adults. Lastly, the spine is hypermobile due to ligamentous laxity, underdeveloped spinous processes, and horizontally oriented facet joints. The high correlation between the imaging findings of occipitocervical ligamentous injuries and brain ischemia in AHT is suggesting that upper spinal cord injury leads to disordered breathing, resulting in hypoxic-ischemic encephalopathy.

References

1 Choudhary AK, Ishak R, Zacharia TT, Dias MS. Imaging of spinal injury in abusive head trauma: a retrospective study. *Pediatr Radiol* 2014;44:1130–1140.

2 Fernando S, Obaldo RE, Walsh IR, Lowe LH. Neuroimaging of nonaccidental head trauma: pitfalls and controversies. *Pediatr Radiol* 2008;38:827–838.

3 Kadom N, Khademian Z, Vezina G, et al. Usefulness of MRI in detection of cervical spine and brain injuries in the evaluation of abusive head trauma. *Pediatr Radiol* 2104;44:839–848.

4 Knox J, Schneider J, Wimberly RL, Riccio AI. Characteristics of spinal injuries secondary to nonaccidental trauma. *Pediatr Orthop* 2014;34:376–381.

5 Choudhary AK, Bradford RK, Dias MS, Moore GJ, Boal D. Spinal subdural hemorrhage in abusive head trauma: a retrospective study. *Radiology* 2012;262:216–223.

SECTION **6**

Trauma to Compromised Spine

Cases

(1A)

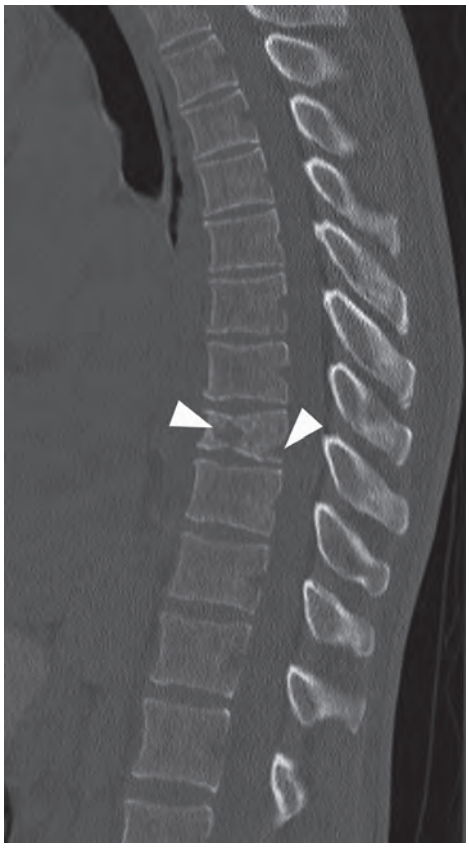

(1B)

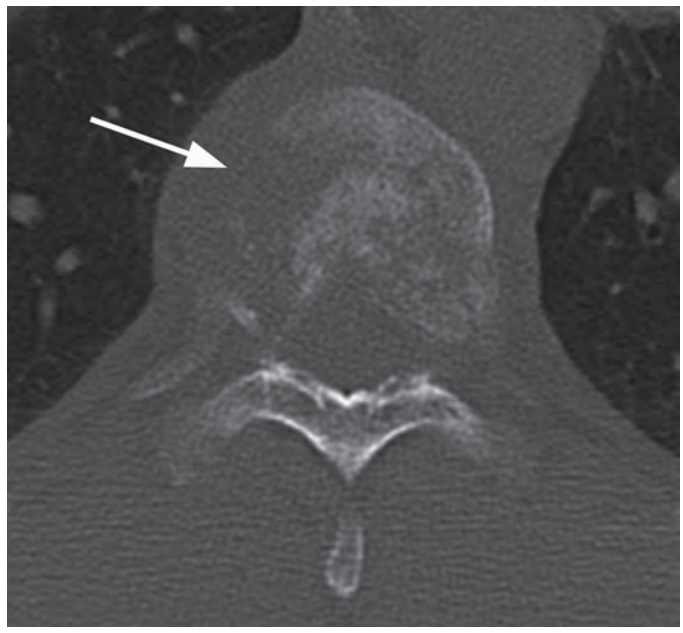

Figure 53.1 A) Midsagittal CT image demonstrates a lower thoracic vertebral body compression fracture following minor trauma. Note that the fractured body does not appear as sclerotic as expected; there are also internal lucent areas (arrowheads). **B)** Axial CT through the fractured vertebra shows the altered trabecular texture with permeative lytic changes, more extensive on the right side (arrow).

(2A)

(2B)

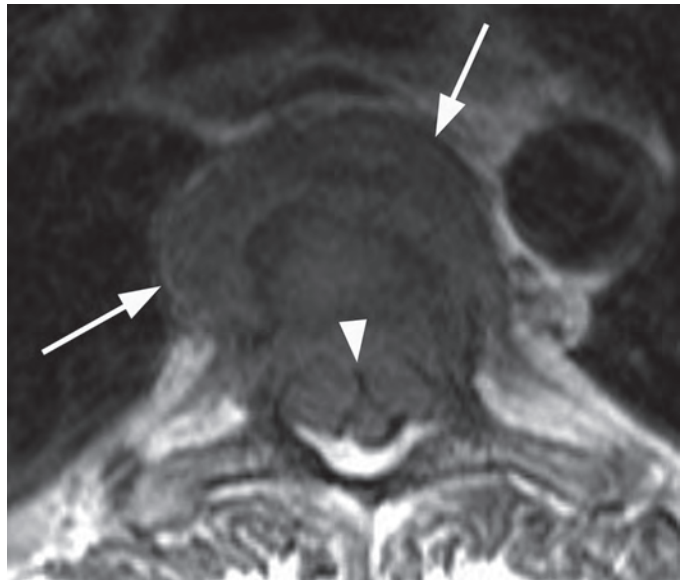

Figure 53.2 A) Midsagittal T1w image shows compression deformity of thoracic vertebral body with substanial loss of height and loss of normal marrow signal intensity. Note the extension of tissue into the prevertebral and anterior epidural space (arrowheads). **B)** Axial T1w image confirms the prevertebral (arrows) and anterior epidural tissue, with a characteristic curtain sign (arrowhead).

CASE 53 Malignant Compression Fractures

Alessandro Cianfoni

Imaging Findings

Malignant vertebral fractures are almost invariably characterized by a compression deformity. As with benign compression fractures, the vertebral body appears defomed, with a wedge, lateral wedge, biconcave, or crush deformity. MRI and CT are sensitive and accurate, and have complementary diagnostic roles. The posterior wall of the vertebral body can have a dorsally convex appearance, so-called bulging posterior wall, especially well seen on sagittal MR images. The normal signal of the bone marrow is replaced by hypointensity on T1w (darker than the disc) and hyperintensity on fat-suppressed T2w or STIR images, as well as enhancement, best seen on fat-suppressed post-contrast T1w sequences. These signal changes reflect a variable combination of neoplastic tissue infiltration, bone marrow edema, and hemorrhage. Non-fat-suppressed T2w and post-contrast T1w images without fat saturation may be completely unrevealing.

Sclerotic changes appear hypointense on T1w and T2w images, with mild, absent, or peripheral enhancement on fat-suppressed post-contrast T1w scans. The signal abnormalities can involve the vertebral body and posterior elements partially or entirely, often in a heterogeneous manner. Extra-osseous enhancing soft tissue, in continuity with the signal abnormalities within the bone, is characteristically seen in the epidural space and perivertebral regions. The anterior epidural enhancing neoplastic tissue frequently gives the "curtain sign" due to preserved median ligament. CT detects lytic lesions involving the trabecular and cortical osseous structures, with a diffuse permeative or focal pattern. Mixed pattern of lytic and sclerotic changes can also be present. In some cases there is diffuse osteopenia only, and in others no osseous structural changes are seen on CT while MRI can still be markedly abnormal. Abnormal MRI signal and CT osseous abnormalities can be present at multiple sites and levels.

Bright DWI signal, absence of signal drop on in-phase/out-of-phase imaging (both at least in part due to hypercellularity), and hyperperfusion on dynamic contrast-enhanced T1w images are frequently seen. MRI is able to detect the presence and severity of central canal and foraminal compromise, spinal cord and nerve roots compression, and signs of myelopathy, due to a variable combination of vertebral column deformity, osseous fragments' encroachment, and epidural soft tissue component. Bone scan shows increased radiotracer uptake due to osteoblastic reaction adjacent to a lytic or sclerotic lesion, or prompted by a pathological fracture. Bone scans can be completely negative in multiple myeloma lesions due to lack of osteoblastic activation. PET (PET-CT) detects high levels of metabolic activity at the sites of malignant fractures due to presence of active neoplastic tissue.

In neoplastic spine involvement, CT and MRI, in a complementary way, detect lesions at risk of impending collapse: lytic lesions involving a large portion of the vertebral body (>30%), especially at the anterior third or the central region in the axial plane, are at greater risk of compression fracture.

Differential Diagnosis

Benign Fractures

Traumatic and osteoporotic fractures may at times be indistinguishable from malignant fractures; abnormal signal extending from the vertebral body into the pedicles, by some authors reported as a sign of malignant fractures, can be encountered in benign fractures as well; DWI, in phase/out-of phase imaging, and dynamic contrast enhancement have been reported as useful, but are not commonly used in clinical routine, and the findings and interpretation are not always unequivocal.

Band-like bone marrow edema, bone marrow sparing, fluid cleft within the fracture (fluid-like hyperintensity within the collapsed body on STIR images), and presence of healed fractures at other levels are all suggestive of a benign fracture.

Vertebral Venous Malformation (Hemangioma)

In fragility fractures due to benign vertebral hemangioma, wide intertrabecular vascular spaces might mimic lytic lesions on CT, and the typical T1 hyperintensity of hemangioma may be replaced by hypointensity due to edema associated with the recent fracture; T2 hyperintense, contrast-enhancing extra-osseous soft tissue can be seen in aggressive vertebral hemangiomas.

A diagnostic clue is the presence of coarse thickened sclerotic trabeculae interdispersed in the cancellous bone.

Spondylo-Discitis (Discitis-Osteomyelitis)

Vertebral body collapse can complicate spondylo-discitis; infectious process can be suggested by edematous changes and contrast enhancement involving the disc space and the subchondral region of adjacent vertebral body/bodies.

A very specific finding is the presence of peripherally enhancing perivertebral collections (abscess/inflammatory mass).

Clinical Findings, Implications, and Treatment

In contrast to benign osteoporotic fractures, the "crush and crumble" that very rarely cause spinal cord compression, malignant vertebral lesions due to the presence of intra and/or extra-osseous soft tissue components "crush and squeeze" so that neurological impairment is much more common. Different sets of criteria have been suggested to predict the risk of impending collapse, usually combining clinical and imaging

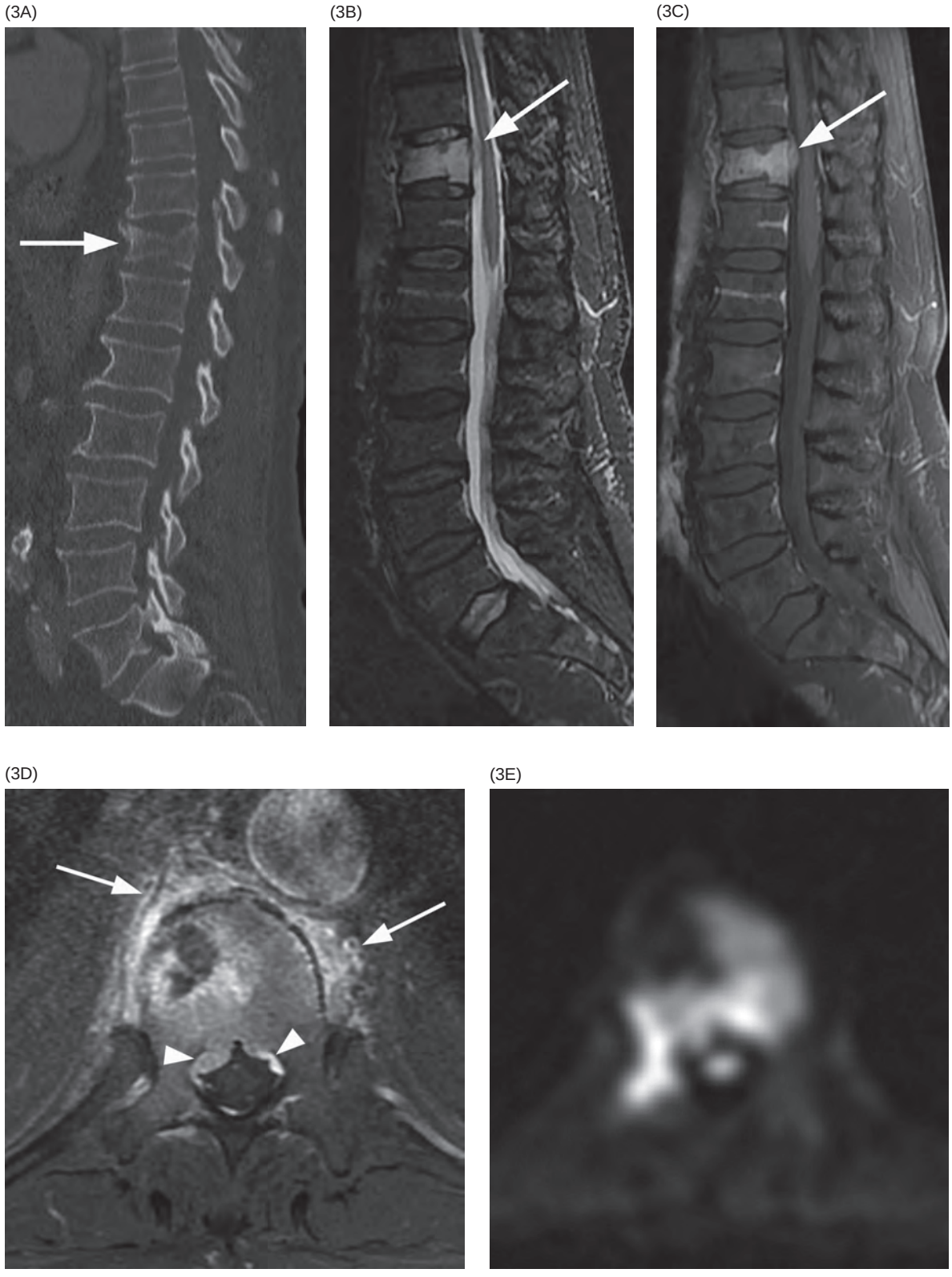

Figure 53.3 **A)** Sagittal reformatted CT of thoracolumbar spine shows a mild compression fracture of T11 body (arrow) in this non-osteopenic patient. Corresponding STIR (**B**) and post-contrast fat-suppressed T1-weighted **(C)** images demonstrate high signal and enhancement within the vertebral body, a nondistinctive finding, but also reveal enhancing epidural tissue (arrows), which is confirmed (arrowheads) on post-contrast fat-suppressed axial T1-weighted image **(D)**. Note also the irregular perivertebral enhancing tissue (arrows). **E)** Corresponding DWI shows very bright signal within the vertebral body and right pedicle lesion, which is commonly seen in malignant fractures. Final diagnosis was lung cancer metastasis.

data. The treatment goal of a malignant vertebral fracture can be radical resection, pain palliation, and/or decompression and/or stabilization. Malignant fractures or lesions at risk of collapse can be treated with many different approaches or combination thereof, including radiation, cement augmentation, decompressive laminectomy, posterior fixation, or 360-degree approaches requiring corpectomy or spondylectomy with posterior stabilization.

Additional Information

A percutaneous image-guided (fluoroscopy or CT) bone core-biopsy is often performed to differentiate a malignant fracture from a benign one, or to assess tumor type. Even in patients with a known malignancy, a vertebral fracture can have a benign etiology, for example due to osteoporosis from frequently implemented corticosteroid treatment. On the other hand, a fracture with benign imaging characteristics can still have a malignant cause, as in multiple myelomas presenting with diffuse osteopenia instead of multifocal discrete lytic lesions.

In addition to metastatic neoplasms and multiple myeloma, so-called pathological compression fractures may also be secondary to primary bone lesions, most commonly giant cell tumor, but also aneurysmal bone cyst and other etiologies.

References

1 Cho WI, Chang UK. Comparison of MR imaging and FDG-PET/CT in the differential diagnosis of benign and malignant vertebral compression fractures. *J Neurosurg Spine* 2011;14:177–183.

2 Ishiyama M, Fuwa S, Numaguchi Y, Kobayashi N, Saida Y. Pedicle involvement on MR imaging is common in osteoporotic compression fractures. *AJNR Am J Neuroradiol* 2010;31:668–673.

3 Thawait SK, Marcus MA, Morrison WB, Klufas RA, Eng J, Carrino JA. Research synthesis: what is the diagnostic performance of magnetic resonance imaging to discriminate benign from malignant vertebral compression fractures? Systematic review and meta-analysis. *Spine (Phila Pa 1976)* 2012;37: E736–E744.

4 Thawait SK, Kim J, Klufas RA, Morrison WB, Flanders AE, Carrino JA, Ohno-Machado L. Comparison of four prediction models to discriminate benign from malignant vertebral compression fractures according to MRI feature analysis. *AJR Am J Roentgenol* 2013;200:493–502.

5 Abdel-Wanis ME, Solyman MT, Hasan NM. Sensitivity, specificity and accuracy of magnetic resonance imaging for differentiating vertebral compression fractures caused by malignancy, osteoporosis, and infections. *J Orthop Surg (Hong Kong)* 2011;19:145–150.

(1A)

(1B)

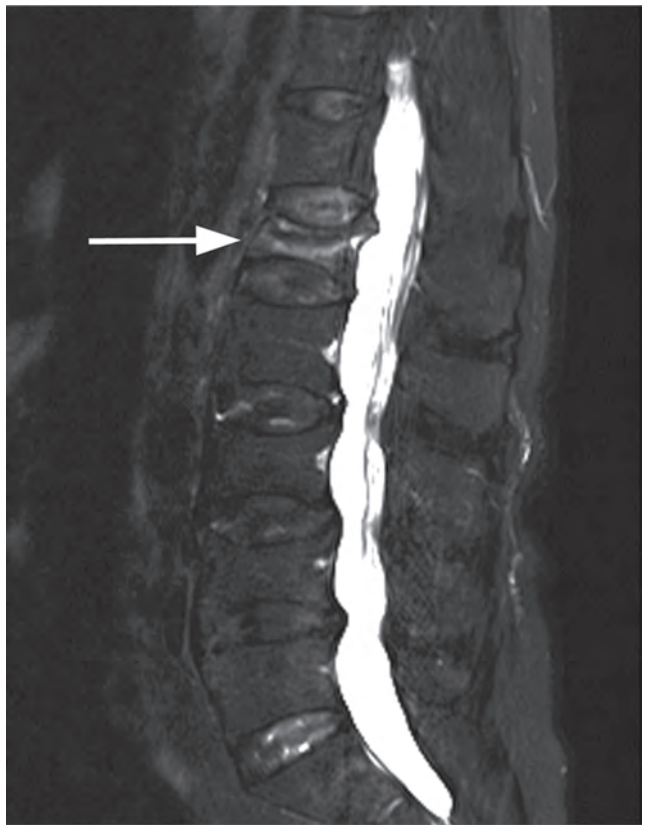

Figure 54.1 **A)** Sagittal lumbar spine CT shows compression fractures at multiple levels with wedging and biconcave shape, superior endplate being more commonly involved. The posterior wall is preserved, except for the typical retropulsion of the L1 superior posterior corner (arrow). The age of fractures cannot be determined on CT. **B)** Corresponding STIR MR image depicts band-like hyperintensity (arrow) of trabecular edema in L1 vertebral body, indicating a more recent or unhealed fracture.

(2A)

(2B)

Figure 54.2 **A)** Sagittal STIR image shows two adjacent mid-thoracic compression fractures: the more cranial one displays normal marrow signal (arrowhead), consistent with a chronic healed fracture, while the more caudal deformity has high signal intensity (arrow) of bone marrow edema, consistent with a recent vertebral body collapse. **B)** Sagittal post-contrast fat-suppressed T1-weighted image shows avid enhancement (arrow) at the recent benign compression fracture.

CASE 54 Benign Compression Fractures

Alessandro Cianfoni

Imaging Findings

Vertebral body compression fractures show variable degrees and morphologies of compression deformities. The vertebral body can appear wedged, with the base at the frequently preserved posterior wall, and the superior endplate is more frequently involved than the inferior one; alternatively, the vertebral body can have a biconcave appearance, the "fish-vertebra" or "cod-fish" deformity, or, when the central compression is particularly prominent, the vertebra has a "butterfly" or "papillon" morphology on coronal images. The compression deformity is in principle an impacted fracture, frequently caused by a low-energy trauma with an axial force, or even spontaneous, but it is in a continuum with burst fractures, so that some degree of fragmentation of the superior endplate or the entire vertebral body, with some mild outward displacement of the fracture fragments, may be present. In fact, a typical feature of benign compression fractures is the retropulsion of the postero-superior vertebral body corner, possibly encroaching on the central canal, but the posterior wall is otherwise straight and not convex and bulging. The degree of vertebral body collapse varies from mild to severe, from "crush vertebra" to "vertebra plana." In severe cases, there are linear fractures through the pedicles, which are very rarely displaced in the coronal plane at the junction with the posterior wall.

Kyphosis can be seen at the fracture level, especially when multiple adjacent levels are affected. An asymmetrical compression deformity in the coronal plane (lateral wedge) can be observed, especially when scoliosis is present. Plain films, although commonly utilized to screen for compression fractures, are not very accurate when the compression deformity is mild or asymmetric, with a central compression deformity predominance, located in the areas with poor visibility (as in the upper thoracic spine), or with scoliosis so that the incident x-ray beam is not parallel to the endplates. Cross-sectional imaging with multiplanar views is the best imaging method to differentiate various features of compression fractures, especially if an invasive or minimally invasive treatment is planned. CT and MR have complementary roles, especially in the differential diagnosis of benign versus malignant fracture. CT can show diffuse osteopenic changes and/or variable mixed sclerotic changes due to trabecular compaction and callus formation. Lytic alterations should not be present in benign fractures. MR findings are variable, depending on the age and healing stage of the fracture. MR is also useful in differentiating benign from malignant compression fractures. A typical feature of fractures in severely osteoporotic patients is the presence of an intravertebral osteonecrotic cleft, also known as Kummel's disease. The cleft, usually linear or band-like, can be located along an endplate or centrally within the vertebral body, and is filled with fluid (with characteristic CSF-like hyperintensity on STIR images) and/or blood and/or gas. Vertebral clefts do not allow the fracture to heal and make it mobile, so that the degree of compression deformity increases with axial load (i.e., on orthostatic plain films) and changes with movements, even with breathing, as commonly seen under fluoroscopy. Furthermore, the cleft can be mistaken for a malignant lytic lesion on CT, but its linear or discoid morphology, the absence of associated soft tissue lesion, and the common presence of air should direct toward benign etiology.

Acute versus Chronic

Differentiating acute, subacute, or nonhealed versus chronic and healed fractures can be challenging if not impossible on plain films and CT. MR is much more specific, showing normal bone marrow signal in chronic healed fractures, similar to that of the adjacent nondeformed levels, and signs of bone marrow edema with low T1 signal and hyperintensity on STIR or T2w images with fat saturation. Edematous changes can be distributed along the fractured disc-endplate, in a band-like area along the subchondral bone, or involve the entire vertebral body. Edema can extend into the pedicles, and this does not necessarily imply pedicular fracture. Edema can also extend to the perivertebral soft tissues in the acute phase. Thickening of the ventral epidural space can be due to epidural hematoma or more frequently to congested epidural ventral venous plexus. These osseous edematous changes usually show dense post-contrast enhancement, which is not a discriminating finding between benign and malignant or infectious conditions. In the setting of spinal trauma, MRI has higher sensitivity than does CT for the diagnosis of subtle compression fractures at multiple vertebral levels, revealing bone marrow edema along impacted disc-endplates even in the absence of frank compression deformities.

When MRI is not feasible (i.e., in patients with a pacemaker), bone scan can reveal increased accumulation of radiotracer at the sites of increased osteoblastic activity, suggesting an ongoing healing osseous process, compatible with a recent rather than old fracture.

Differential Diagnosis

Burst Fracture

Caused by greater forces, a greater degree of fragmentation of the vertebral body, and outward displacement of fracture fragments, the posterior wall is retropulsed not only at its superior aspect; perivertebral ad epidural hematoma is frequently associated; ligamentous and spinal cord injury may be present.

Malignant Compression Fracture

Not always distinguishable on imaging, the posterior wall may have a bulging appearance, contrast enhancement may be

(3A)

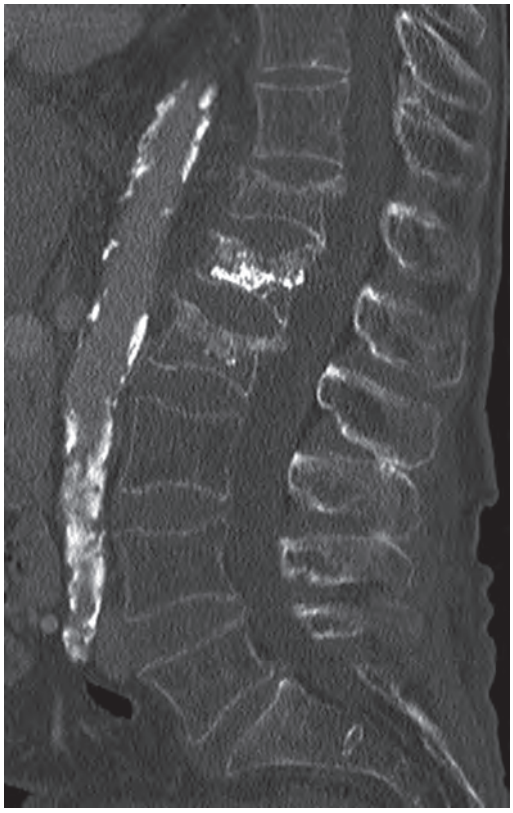

(3B)

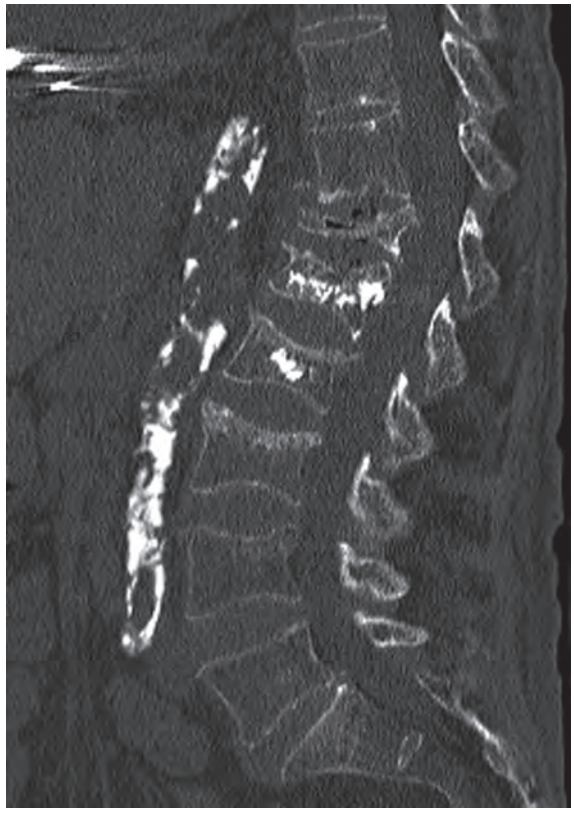

Figure 54.3 **A)** Sagittal reformatted CT of the lumbar spine shows compression fractures of L1 and L2 vertebral bodies, treated with cement augmentation, and mild compression deformity of T12, treated conservatively. **B)** Follow-up CT 4 weeks later shows marked progression of the T12 vertebral collapse, now with vertebra plana appearance (arrow) and intravertebral gas cleft. There is also new compression of the L3 superior endplate (arrowhead). Although stable regarding neurological compromise potential, compression fractures tend to progress to a more severe deformity.

Figure 54.4 Sagittal STIR image shows a hyperintense T12 area (arrow), representing a fluid-filled osteonecrotic cleft, which is characteristic for benign fractures.

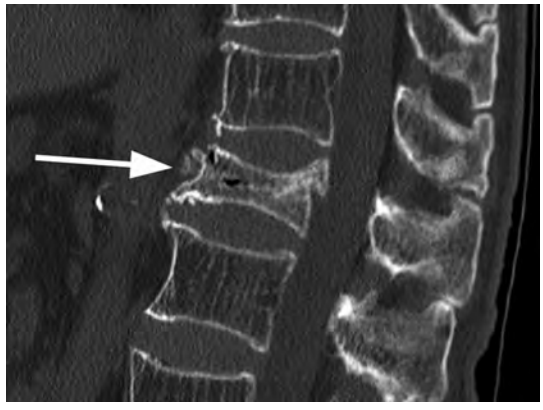

Figure 54.5 Sagittal CT in a different patient shows the classic appearance of the cleft (arrow) filled with gas and fluid within L1 fracture. Note the fracture of the superior posterior corner.

heterogeneous, with solid enhancing tissue extending beyond osseous borders; lytic lesions may be visible on CT, frequently hyperintense on DWI MRI, increased SUV on PET; additional lesions may be present; biopsy may be necessary.

Degenerative Subchondral Changes (Modic's Type I Reactive Endplate Changes)

Abnormal band-like low T1 and high T2 signal of marrow edema in the subchondral bone on both sides of a degenerated disc, usually without compression deformity, with contrast enhancement.

Clinical Findings, Implications, and Treatment

Compression fractures are the biomechanical result of hyperflexion or axial loading forces and are classified, in their typical form, as type A1 (simple compression fracture) in the AO classification system, but in reality they lie in a continuum and may share features with A2, A3, and A4 (complete burst fracture) fracture types. They are encountered much more frequently at the thoracic and lumbar levels than in the cervical spine, and in spinal trauma they can be present at multiple levels in addition to more severe traumatic injuries at adjacent or distant levels. Compression deformities of mild degree can be treated conservatively, in some practices with a corset or, to allow early mobilization and pain relief, with percutaneous cement vertebral augmentation (vertebroplasty or kyphoplasty). When there is a high degree of deformity, focal kyphosis, and/or evidence of ligamentous disruption on MRI, surgical stabilization is considered. In osteoporotic patients these fractures can be spontaneous or caused by minor trauma, asymptomatic and incidentally discovered at imaging studies, or extremely painful, requiring bed rest and opioid analgesics, compromising pulmonary function, and ultimately impacting mortality in elderly individuals. In these patients, and in those with less severe but persistent pain despite conservative treatment, minimally invasive cement augmentation, which can be performed under local anesthesia, is commonly considered, despite the ongoing debate in literature regarding efficacy, to allow prompt pain relief and early mobilization.

Additional Information

Presence of vertebral body edema on MRI in trauma setting, even in the absence of compression deformity, might alter surgical management of a more severely injured adjacent vertebral level: surgeons would rather avoid using an injured vertebral body as a stabilizing level for insertion of bipedicular screws in a posterior stabilization procedure.

In osteoporotic patients, a compression fracture occurring spontaneously or following minor trauma should be considered stable, even with a high degree of collapse, posterior wall retropulsion, and pedicular fracture. Stability, however, does not prevent these fractures from progression with time and load; progressive vertebral body collapse at follow-up imaging is usually not complicated with neurological impairment. Another common feature of these compression fractures is involvement of multiple adjacent levels, especially at sites of biomechanical stress, at different time points, spontaneously or after cement augmentation treatment. Spontaneous vertebral fractures are indicative of underlying osteoporosis, regardless of bone density scan's results.

References

1 Klazen CA, Lohle PN, de Vries J, Jansen FH, et al. Vertebroplasty versus conservative treatment in acute osteoporotic vertebral compression fractures (Vertos II): an open-label randomised trial. *Lancet* 2010;376: 1085–1092.

2 Brinckman MA, Chau C, Ross JS. Marrow edema variability in acute spine fractures. *Spine J* 2015;15:454–460. doi: 10.1016/ jspinee.2014.09.032.

3 Gerdhem P. Osteoporosis and fragility fractures: vertebral fractures. *Best Pract Res Clin Rheumatol* 2013;27:743–755.

4 McKiernan F, Faciszewski T. Intravertebral clefts in osteoporotic vertebral compression fractures. *Arthritis Rheum* 2003;48:1414–1419.

5 Kanchiku T, Taguchi T, Kawai S. Magnetic resonance imaging diagnosis and new classification of the osteoporotic vertebral fracture. *J Orthop Sci* 2003;8:463–466.

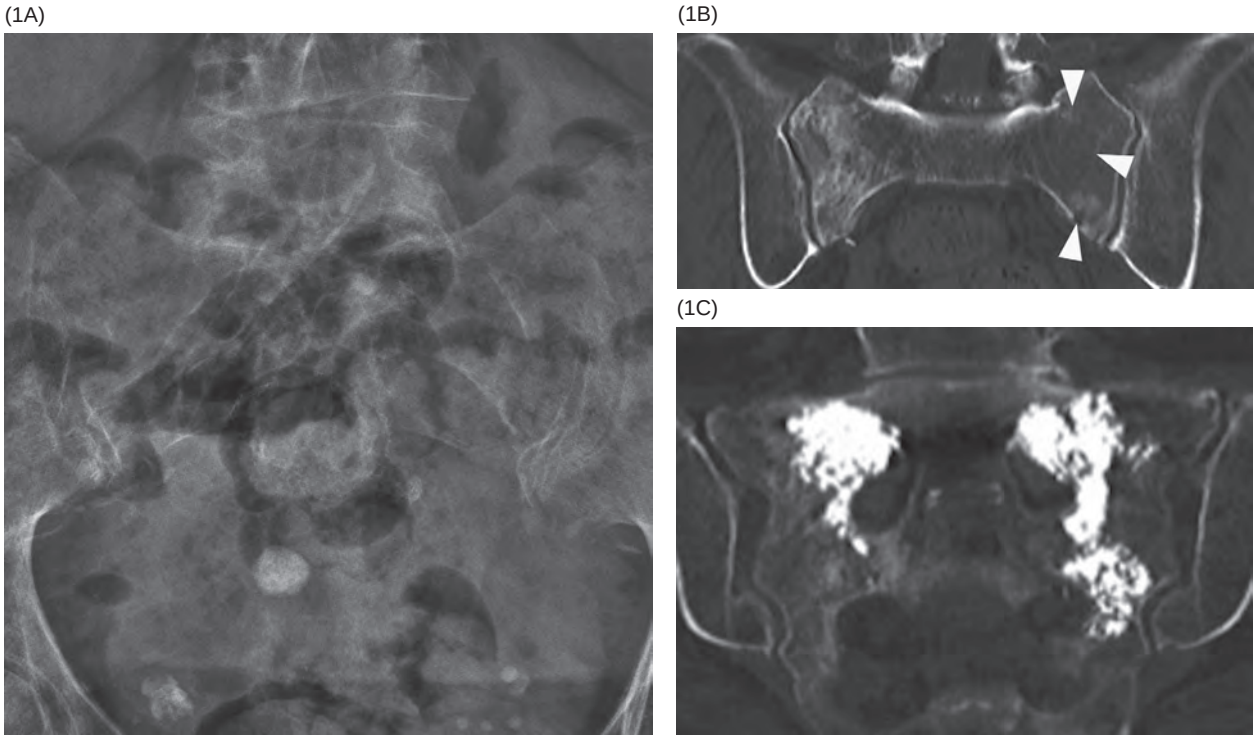

Figure 55.1 **A)** AP view radiograph shows no clear evidence of sacral fractures due to superimposed bowel gas and fecal material in a patient with osteoporosis and severe bilateral pelvic pain. **B)** Coronal reformatted CT image shows diffuse sclerosis of the right sacral ala parallel to the sacroiliac joint, suggesting a chronic sacral fracture; vertical linear radiolucent fractures are evident on the opposite side (arrowheads). **C)** The patient was treated with sacroplasty, as showed on this coronal CT image, with substantial pain relief.

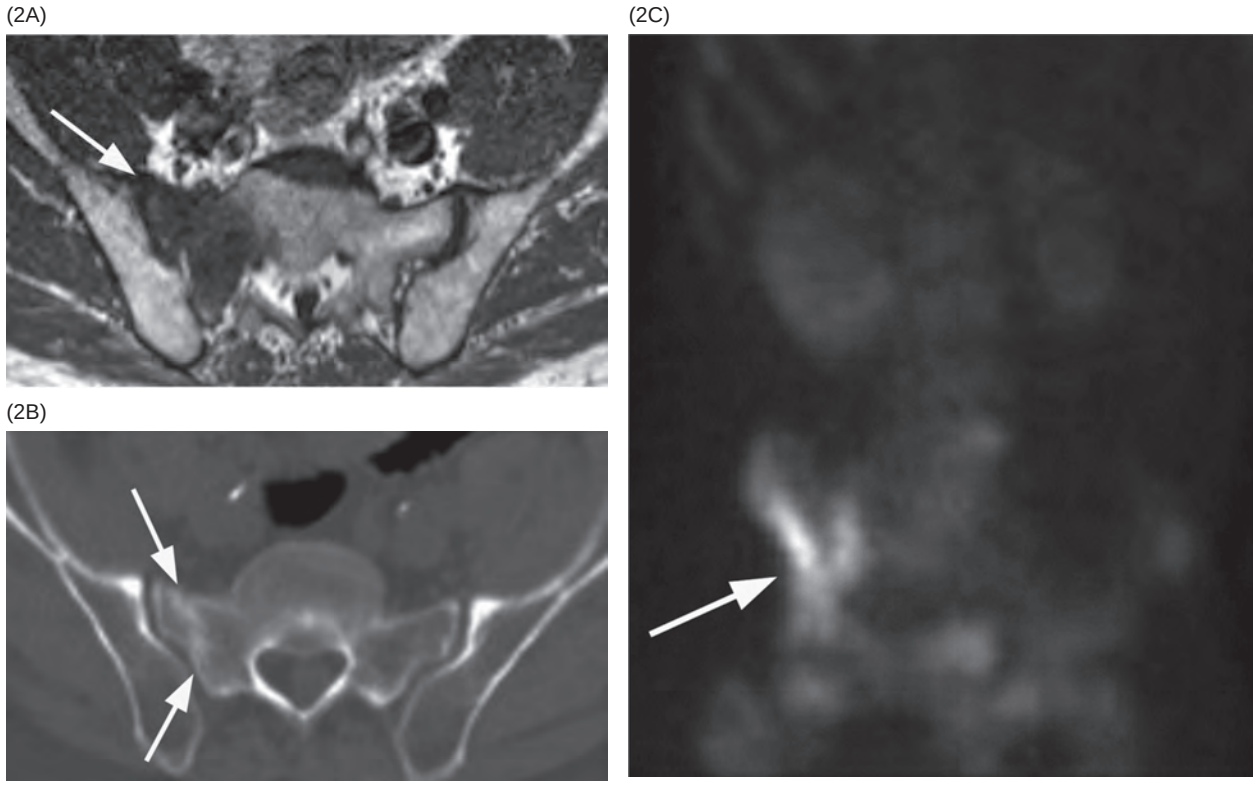

Figure 55.2 **A)** In this patient with pelvic pain axial T1w image shows diffuse hypointensity (arrow) in the right sacral ala, consistent with bone marrow edema. **B**) Axial CT image demonstrates a sclerotic fracture line (arrows) in the right sacral ala parallel to the sacro-iliac joint. **C**) Technetium 99m (Tc-99m) bone scan confirms the fracture as an increased uptake in the right sacral ala with involvement of the ipsilateral sacroiliac joint (arrow).

CASE 55 Sacral Stress (Insufficiency) Fractures

Daniela Distefano

Imaging Findings

Sacral stress fractures (SSF) may be seen on radiographs as vertical sclerotic bands, fracture lines, or cortical disruptions. The diagnosis may be difficult due to high prevalence of osteopenia, bowel gas, or fecal material. SSF present as sclerotic bands, linear fractures lines, or a combination thereof within the sacral ala on CT, adjacent and parallel to the sacroiliac joints. Coronal images show the full extent of the fractures. It is important to search for bony fragments, cortical breaks, and involvement of neural foramina. Nuclear medicine bone scan is very sensitive for SSF: bilateral increased uptake in the upper sacrum is the classic "Honda" sign, pathognomonic of SSF in the appropriate clinical setting. SSF, however, can also be unilateral. MRI shows bone marrow edema as bands of low T1 signal and hyperintensity on T2-weighted images with fat suppression (preferably STIR) with a sensitivity at or near 100%. A hypointense fracture line is usually evident within marrow edema. Contrast enhancement is commonly seen in recent or nonhealed fractures, similar to benign compression fractures of vertebral bodies.

Differential Diagnosis

Metastatic Disease

Osteolytic or sclerotic lesions with cortical disruption and often expansion; multiple additional lesions are frequently present.

Osteomyelitis

Lytic destructive lesion, extensive soft tissue changes; epidural rim-enhancing collections suggestive of abscess; osseous sequestra with chronic infection.

Inflammatory Sacroiliitis

Sclerosis with erosions on CT, possible ankylosis; subchondral bone marrow edema $>$ 1 cm along the articular surfaces on MRI.

Osteoarthritis or Degenerative SI Joints Disease

Joint space narrowing, sclerosis, and osteophytosis.

Osteitis Condensans Ilii

Triangular area of subchondral sclerosis at the antero-inferior iliac side of the joint, without erosions or joint space narrowing.

Paget Disease

Lytic, mixed lytic-sclerotic, or sclerotic patterns, depending on the stage of disease activity.

Clinical Findings, Implications, and Treatment

Severe, intractable diffuse low back or pelvic pain coupled with a significant reduction in mobility is the typical presentation. SSF should always be considered in low back and pelvic pain, particularly in elderly patients without a history of trauma. Neurological symptoms are rare. Osteoporosis, prolonged corticosteroid treatment, radiation therapy, rheumatoid arthritis, Paget's disease, osteomalacia, long-standing bed rest, and metabolic bone diseases are common underlying causes. SSF may rarely occur in young women during the last trimester of pregnancy or a few weeks after delivery. Conservative management has been the standard of care of SSF; however, sacroplasty has emerged as an effective minimally invasive alternative, preventing complications due to prolonged bed rest, such as venous thrombosis, muscular atrophy, pneumonia, and bone demineralization.

Additional Information

The terms "insufficiency" and "stress" fracture are frequently used interchangeably. Insufficiency fractures are actually a subgroup of stress fractures: fatigue fractures are caused by abnormal stress applied to normal bone; insufficiency fractures occur when an abnormally weakened bone is subjected to physiologic stresses. SSF are often seen with other pelvic insufficiency fractures, most commonly the pubic bone and then ilium. SSF are thought to be underreported due to general lack of awareness of this condition and nonspecific symptoms.

References

1 Lyders EM, Whitlow CT, Baker MD, Morris PP. Imaging and treatment of sacral insufficiency fractures. *Am J Neuroradiol* 2010;31:201–210.

2 Longhino V, Bonora C, Sansone V. The management of sacral stress fractures: current concepts. *Clin Cases Miner Bone Metab* 2011;8:19–23.

3 Kortman K, Ortiz O, Miller T, et al. Multicenter study to assess the efficacy and safety of sacroplasty in patients with osteoporotic sacral insufficiency fractures or pathologic sacral lesions. *J Neurointerv Surg* 2013;5:461–466.

4 Deschamps Perdomo A, Tomé-Bermejo F, Piñera AR, Alvarez L. Misdiagnosis of sacral stress fracture: an underestimated cause of low back pain in pregnancy? *Am J Case Rep* 2015;16:60–64.

(1A)

(1B)

Figure 56.1 A) A 60-year-old male presenting with pain after a fall. There is a very subtle horizontal fracture at the anterior inferior aspect of the C6 vertebral body (arrowhead) adjacent to the C6–C7 disc. Posterior element fractures are seen in the spinous processes of C6 and C7 (arrows). This is a 3-column injury. **B)** A 2-month follow-up CT was performed on the same patient after rigid collar stabilization. Horizontal fracture line is more apparent in the C6 vertebral body (arrowhead) and the spinous processes (arrows) with minimal evidence for bony healing.

(2A)

(2B)

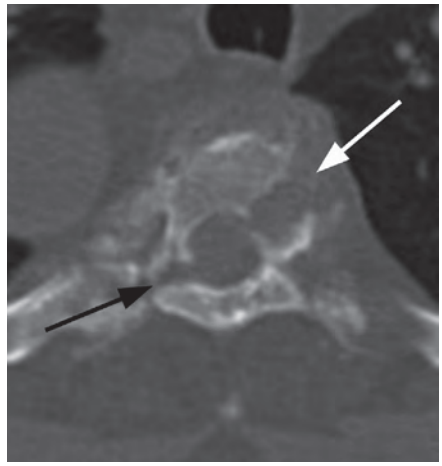

Figure 56.2 A) Sagittal MRI in a 72-year-old male presenting with increasing pain 1 month after a fall. There is a well-defined wide area of very high T2 signal (arrows) extending in an oblique fashion through the T6 vertebral body, reaching the disc level anterior-superiorly and extending through the ossified ligamentum flavum. Anterior vertebral body fusion is subtle on this MR image. **B)** The fracture is also running in an oblique fashion through the vertebral body and posterior elements (arrows) in the axial plane, as seen on this body CT image.

Figure 56.3 Sagittal CT shows anterior flowing paravertebral calcifications typical of DISH. There is a subtle fracture line (arrowhead) across the fused C5–C6 level. Clinical findings and MRI were consistent with a central cord injury, typical of a hyperextension mechanism.

CASE 56 Fractures of the Ankylosed Spine

Russel Chapin

Imaging Findings

Vertebral fractures in ankylosing spondylitis (AS) are difficult to diagnose initially due to a mild injury mechanism, lack of vertebral compression, and significant osteopenia. However, involvement of all three columns, particularly with failure of the osseous constraints of the posterior ligamentous complex, is present in a large majority of patients. Fractures in AS patients are more likely to occur through the disk than the vertebral body itself; the disc is thought to represent the weakest link in the ankylosed spine. The fractures are frequently extending in an oblique fashion in both sagittal and axial planes. Fractures in patients with diffuse idiopathic skeletal hyperostosis (DISH) also may occur after minor injury and be difficult to visualize. In patients with possible cervical spine injury, AS or DISH are considered high-risk criteria (similar to altered mental status or a high mechanism MVC) always necessitating CT imaging rather than radiographs. For imaging of lumbar spine pain, AS is considered a "red flag" favoring the use of MRI or CT over radiography.

Differential Diagnosis

Other causes of ankylosis, including degenerative spine changes

Other seronegative spondyloarthropathies including psoriatic and enteropathic arthropathy

Incomplete bridging of an osteophyte or disc annular calcification

Clinical Findings, Implications, and Treatment

The majority of fractures in patients with AS present after a history of minor trauma such as fall from standing or sitting and may be found with no history of injury at all. Because of daily back pain due to baseline AS, a delayed presentation with pseudoarthrosis or neurologic deficit is relatively common. Cervical spine fractures are only moderately more common than thoracic or lumbar fractures.

A literature review by Westerveld et al. reported 400 cases of fracture in patients with AS or DISH. In these cases, extension (75%) and flexion (15%) type mechanisms were overwhelmingly common, while compression type injuries were rare. In AS or DISH patients, 50–66% of fractures presented with a neurologic deficit, and mortality was 15–30% at 1 year. Potentially most important is that a significant percentage (14%) of patients developed a secondary neurologic deficits due to instability and, frequently, inadequate immobilization. Given the association of pulmonary fibrosis and cardiac valvular disease with AS and advanced age of many patients with DISH, comorbidities are a major part of treatment planning. Despite the high rate of unstable injuries, 30–45% of patients in the Caron and Westerveld reports were treated nonsurgically. However, due to advances in surgical techniques and improved perioperative management, there is a strong trend toward earlier operative treatment with long segment posterior fixation. Percutaneous stabilization of fractures may be preferred, as it is associated with lower complication rate and shorter operative times.

The incidence of epidural hematoma after fracture in AS or DISH is increased, and posterior decompression is added as indicated. If treated conservatively with rigid bracing, vigilance for instability and pseudoarthrosis should be high. Complications from halo fixation are more common in AS and elderly patients.

Additional Information

AS has a prevalence of approximately 0.5% and typically occurs in males <30 years of age. The lifetime fracture risk in AS is 4 times that of the general population. Diffuse idiopathic skeletal hyperostosis (DISH) is a noninflammatory ankylosing disease of older patients affecting primarily the thoracic spine with a higher prevalence than AS. DISH also increases the risk for spinal fracture and instability, though not to the degree that AS does.

References

1 Westerveld LA, Verlaan JJ, Oner FC. Spinal fractures in patients with ankylosing spinal disorders: a systematic review of the literature on treatment, neurological status and complications. *Eur Spine J* 2009;18:145–156.

2 Caron T, Bransford R, Nguyen Q, et al. Spine fractures in patients with ankylosing spinal disorders. *Spine* 2010;35:E458–E464.

3 Moussallem CD, McCutheon BA, Clarke MJ, et al. Perioperative complications in open versus percutaneous treatment of spinal fractures in patients with ankylosed spine. *J Clin Neurosci* 2016;30:88–92.

4 Lu ML, Tsai TT, Lai PL, et al. A retrospective study of treating thoracolumbar spine fractures in ankylosing spondylitis. *Eur J Orthop Surg Traumatol* 2014;24 Suppl 1:S117–S123. doi: 10.1007/s00590-013-1375-y.

Index